Second Series *December, 1927* *Vol. 30, No. 6*

THE

PHYSICAL REVIEW

DIFFRACTION OF ELECTRONS BY A CRYSTAL OF NICKEL

By C. Davisson and L. H. Germer

Abstract

The intensity of scattering of a homogeneous beam of electrons of adjustable speed incident upon a single crystal of nickel has been measured as a function of direction. The crystal is cut parallel to a set of its {111}-planes and bombardment is at normal incidence. The distribution in latitude and azimuth has been determined for such scattered electrons as have lost little or none of their incident energy.

Electron beams resulting from diffraction by a nickel crystal.—Electrons of the above class are scattered in all directions at all speeds of bombardment, but at and near critical speeds sets of three or of six sharply defined beams of electrons issue from the crystal in its principal azimuths. Thirty such sets of beams have been observed for bombarding potentials below 370 volts. Six of these sets are due to scattering by adsorbed gas; they are not found when the crystal is thoroughly degassed. Of the twenty-four sets due to scattering by the gas-free crystal, twenty are associated with twenty sets of Laue beams that would issue from the crystal within the range of observation if the incident beam were a beam of heterogeneous x-rays, three that occur near grazing are accounted for as diffraction beams due to scattering from a single {111}-layer of nickel atoms, and one set of low intensity has not been accounted for. *Missing beams* number eight. These are beams whose occurrence is required by the correlations mentioned above, but which have not been found. The intensities expected for these beams are all low.

The spacing factor concerned in electron diffraction by a nickel crystal.—The electron beams associated with Laue beams do not coincide with these beams in position, but occur as if the crystal were contracted normally to its surface. The spacing factor describing this contraction varies from 0.7 for electrons of lowest speed to 0.9 for electrons whose speed corresponds to a potential difference of 370 volts.

Equivalent wave-lengths of the electron beams may be calculated from the diffraction data in the usual way. These turn out to be in acceptable agreement with the values of h/mv of the undulatory mechanics.

Diffraction beams due to adsorbed gas are observed except when the crystal has been thoroughly cleaned by heating. Six sets of beams of this class have been found; three of these appear only when the crystal is heavily coated with gas; the other three only when the amount of adsorbed gas is slight. The structure of the gas film giving rise to the latter beams has been deduced.

THE investigation reported in this paper was begun as the result of an accident which occurred in this laboratory in April 1925. At that time we were continuing an investigation, first reported in 1921,[1] of the distribution-in-angle of electrons scattered by a target of ordinary (poly-

[1] Davisson & Kunsman, Science **64**, 522, (1921).

crystalline) nickel. During the course of this work a liquid-air bottle exploded at a time when the target was at a high temperature; the experimental tube was broken, and the target heavily oxidized by the inrushing air. The oxide was eventually reduced and a layer of the target removed by vaporization, but only after prolonged heating at various high temperatures in hydrogen and in vacuum.

When the experiments were continued it was found that the distribution-in-angle of the scattered electrons had been completely changed. Specimen curves exhibiting this alteration are shown in Fig. 1. These curves are all for a bombarding potential of 75 volts. The electron beam is incident on the target from the right, and the intensities of scattering in different directions are proportional to the vectors from the point of bombardment to the curves. The upper curves (for different angles of incidence) are characteristic of the target prior to the accident. They are of the type

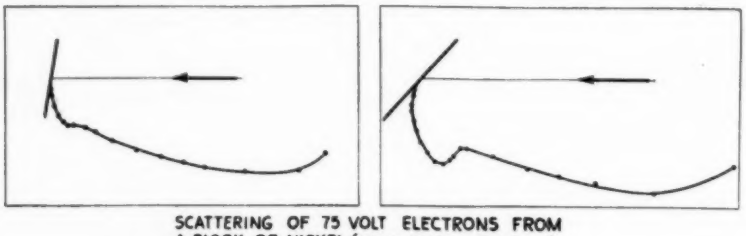

SCATTERING OF 75 VOLT ELECTRONS FROM A BLOCK OF NICKEL (MANY SMALL CRYSTALS)

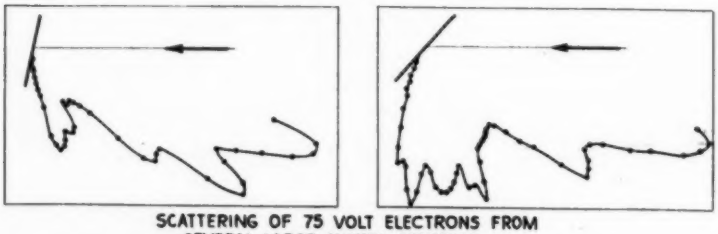

SCATTERING OF 75 VOLT ELECTRONS FROM SEVERAL LARGE NICKEL CRYSTALS

Fig. 1. Scattering curves from nickel before and after crystal growth had occurred.

described in the note in "Science" in 1921, and are similar to curves that have been obtained for nickel in four or five other experiments. The lower curves—obtained after the accident—were the first of their sort to be observed. This marked alteration in the scattering pattern was traced to a re-crystallization of the target that occurred during the prolonged heating. Before the accident and in previous experiments we had been bombarding many small crystals, but in the tests subsequent to the accident we were bombarding only a few large ones. The actual number was of the order of ten.

It seemed probable from these results that the intensity of scattering from a single crystal would exhibit a marked dependence on crystal direction, and we set about at once preparing experiments for an investigation of this dependence. We must admit that the results obtained in these experiments have proved to be quite at variance with our expectations. It seemed to us likely that strong beams would be found issuing from the crystal along what

may be termed its transparent directions—the directions in which the atoms in the lattice are arranged along the smallest number of lines per unit area. Strong beams are indeed found issuing from the crystal, but only when the speed of bombardment lies near one or another of a series of critical values, and then in directions quite unrelated to crystal transparency.

The most striking characteristic of these beams is a one to one correspondence, presently to be described, which the strongest of them bear to the Laue beams that would be found issuing from the same crystal if the incident beam were a beam of x-rays. Certain others appear to be analogues, not of Laue beams, but of optical diffraction beams from plane reflection gratings—the lines of these gratings being lines or rows of atoms in the surface of the crystal. Because of these similarities between the scattering of electrons by the crystal and the scattering of waves by three- and two-dimensional gratings a description of the occurrence and behavior of the electron diffraction beams in terms of the scattering of an equivalent wave radiation by the atoms of the crystal, and its subsequent interference, is not only possible, but most simple and natural. This involves the association of a wave-length with the incident electron beam, and this wave-length turns out to be in acceptable agreement with the value h/mv of the undulatory mechanics, Planck's action constant divided by the momentum of the electron.

That evidence for the wave nature of particle mechanics would be found in the reaction between a beam of electrons and a single crystal was predicted by Elsasser[2] two years ago—shortly after the appearance of L. de Broglie's original papers on wave mechanics. Elsasser believed, in fact, that evidence of this sort was already at hand in curves, published from these Laboratories,[3] showing the distribution-in-angle of electrons scattered by a target of polycrystalline platinum. We should like to agree with Elsasser in his interpretation of these curves, but are unable to do so. The maxima in the scattering curves for platinum are of the type of the single maximum in the curves for nickel shown in the upper half of Fig. 1, and are, we believe, unrelated to crystal structure.

Preliminary announcement of the main results contained in this paper was made in "Nature" for April 16, 1927. In the present article we give a more complete account of the experiments and additional data.

The Apparatus

The essential parts of the special apparatus, Fig. 2, used in these experiments are the "electron gun" G, the target T and the double Faraday box collector C. The electrons constituting the primary beam are emitted thermally from the tungsten ribbon F, and are projected from the gun into a field-free enclosure containing the target and collector; the outer walls of the gun, the target, the outer box of the collector and the box enclosing these parts are held always at the same potential. The beam of electrons

[2] W. Elsasser, Naturwiss. **13**, 711 (1925).
[3] Davisson & Kunsman, Phys. Rev. **22**, 242 (1923).

meets the target at normal incidence. High speed electrons scattered within the small solid angle defined by the collector opening enter the inner box of the collector, and from thence pass through a sensitive galvanometer. Electrons leaving the target with speeds appreciably less than the speed of the incident electrons are excluded from the collector by a retarding

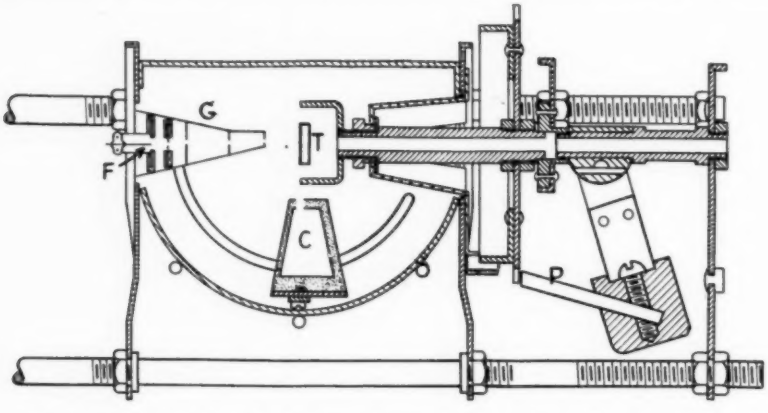

Fig. 2. Cross-sectional view of the experimental apparatus—glass bulb not shown.

potential between the inner and outer boxes. The angle between the axis of the incident beam and the line joining the bombarded area with the opening in the collector can be varied from 20 to 90 degrees. Also the target can be rotated about an axis that coincides with the axis of the incident beam. It is thus possible to measure the intensity of scattering in any direction in

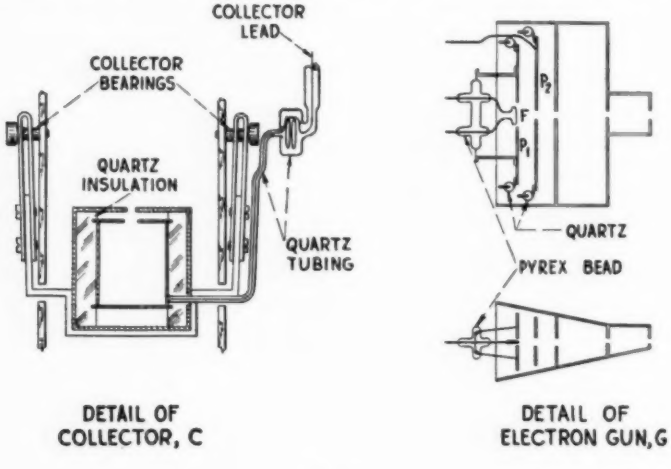

Fig. 3.

front of the target with the exception of directions lying within 20 degrees of the incident beam.

Details of the "electron gun" are shown in Fig. 3. The tungsten ribbon F lies in a rectangular opening in a nickel plate P_1. The purpose of this plate is to assist in concentrating the emission from the filament onto an opening

in the parallel plate P_2. This is accomplished by making the potential of P_1 slightly more negative than that of the filament. The potential of P_2 relative to that of the filament is adjusted ordinarily to a rather high positive value.

The opening in P_2 is circular and slightly more than 1 mm in diameter. Some of the electrons passing through this opening continue on through apertures in a series of three plates that are at the same potential as the outer walls of the gun. It is the difference between this potential and that of the filament which determines the speed of the emergent beam. The first two of these apertures are 8 mm apart and are 1 mm in diameter; the diameter of the third is slightly greater. The geometry of these parts is such as to insure a well defined emergent beam relatively free from low speed secondary electrons. The gun was tested in a preliminary experiment, and was found to give a homogeneous beam. The distance from the end of the gun to the target is 7 mm.

The two parts of the collector (Fig. 3) are insulated from one another by blocks of clear quartz. The openings in the outer and inner boxes are circular,

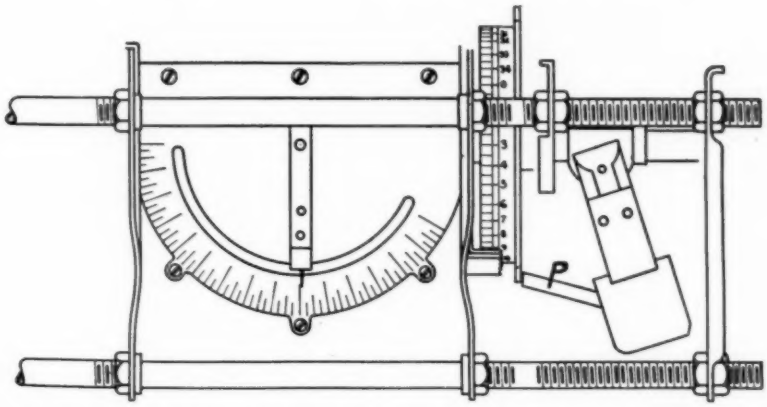

Fig. 4. Outside view of the experimental apparatus—glass bulb not shown—0.7 actual size.

their diameters being 1.0 mm and 2.0 mm respectively. These openings were made as near as possible to the side of the box adjacent to the gun in order to reduce to a minimum the unexplored region about the incident beam. The collector is suspended by arms from bearings outside the enclosing box (Fig. 4), and is free to rotate about a horizontal axis through the bombarded area and normal to the incident beam. The angular position of the collector is varied by rotating the whole tube, which is sealed from the pumps, about this axis. The lead to the inner box must be especially shielded from stray currents; it is enclosed in small quartz tubing from the point at which it leaves the outer box to the seal at which it leaves the tube. The distance from the bombarded area to the opening in the outer box is 11 mm.

The target is a block of nickel $8\times5\times3$ mm cut from a bar in which crystal growth had been induced by straining and annealing. The orientations of the largest crystals in the bar were determined by an examination of the optical reflections from crystal facets that had been developed by

etching. A cut was then made through one of the crystals approximately parallel to a set of its {111}-planes. One of the surfaces so exposed was polished, etched, examined and corrected, and became eventually the face of the target.

No particular care was taken in preparing the target to avoid straining or damaging the crystal. The cutting was done with a jeweler's saw; holes were drilled through the ends of the block, and nickel wires were passed through these to serve as supports. After this rather rough usage the target was heated in an auxiliary tube to near its melting point without its showing any indication of recrystallization.

The effect of etching a nickel crystal, either chemically or by vaporization, is to develop its surface into sets of facets parallel to its principal planes. Those parallel to the {111}-planes are developed most readily, but we have also observed others parallel to the {110}-planes.[4] Four sets of the predominant {111}-facets are, in general, exposed on a plane surface. If one of these is parallel to the general plane of the surface, as in the case of our

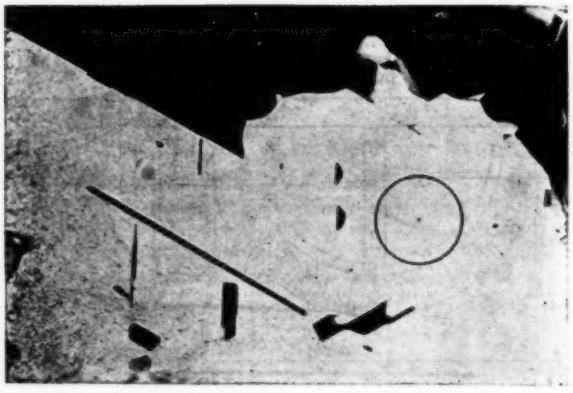

Fig. 5. Microphotograph of the nickel target.

target, the other sets have normals lying 20 degrees above the general plane of the surface and equally spaced in azimuth about the normal to the first set.

A microphotograph of the face of the target is shown in Fig. 5. The illumination is at normal incidence, and the large crystal shows white on account of the strong reflection from the {111}-facets lying in its surface. That these facets make up nearly the whole of the surface seems probable from the fact that in the visual examination of the crystal the reflections from the lateral facets were very weak. This conclusion may not, however, be stated without reservation, as the weakness of these reflections may indicate merely that some dimension of the individual facets is small compared with optical wave-lengths. The regions appearing black in the photograph are made up of crystals having no facets parallel to the surface. Those included in the large crystal and others adjacent to it are twinned with the main structure. The area selected for bombardment is shown enclosed in a circle.

[4] See also Potter and Sucksmith, Nature **119**, 924 (1927), who found {100}-facets.

The target was mounted in a holder from which it was insulated, and the holder was fixed to the end of a hollow shaft mounted in bearings. A small tungsten filament mounted back of the target (not shown in Fig. 2) supplies electrons for heating the target by bombardment. Leads from the target and from this filament pass out through the hollow shaft and are connected through platinum brush contacts to other leads which are carried through seals in the tube.

The mechanism for rotating the target is shown in Figs. 2 and 4. When the tube is rotated counter-clockwise about the collector axis, to bring the collector into range in front of the target, the molybdenum plunger p (attached to a heavy pendulum) passes through an opening in a toothed wheel (attached to the shaft) and engages with a milled edge of a strip of molybdenum that is attached to the frame. The wheel and the target are then locked to the frame. When the tube is rotated clockwise until the main or longitudinal axis of the tube has passed slightly beyond the horizontal, the plunger disengages from the milled edge but still remains within the opening in the toothed wheel. The pendulum has a second degree of freedom (it revolves about a fixed hollow shaft coaxial with the shaft carrying the target) so that, by rotating the tube about its main axis, the pendulum and engaged wheel are rotated relative to the frame. The range of this rotation is only 20° or 30°, but by rotating the tube slightly further in the clockwise direction about the collector axis the plunger is disengaged from the wheel, and can be moved, by rotation again about the main axis, to a different opening in the toothed wheel. By these operations the target can be worked through any angle. Its azimuth is read from a scale ruled on the wheel. This scale and that for reading the position of the collector are shown in Fig. 4. The bearings throughout the tube, with the exception of one nickel on nickel bearing, are either molybdenum on molybdenum, or molybdenum on nickel.

Preparation of the Tube

The metal parts of the tube were preheated to 1000°C in a vacuum oven, and were then assembled and sealed into the bulb with the least possible delay. The bulb is of Pyrex and has sealed to it two auxiliary tubes, one containing cocoanut charcoal, and the other a misch metal vaporizer. This latter consists of a small pellet of misch metal attached to a molybdenum plate anode which may be bombarded from a nearby tungsten filament. The thermal contact between the pellet and the plate is reduced by the interposition of a narrow strip of molybdenum, so that the misch metal may be vaporized only by raising the plate to a very high temperature. The misch metal is vaporized when the pumping is nearly completed, and various of its constituents form solid compounds with the residual gas, thus improving and maintaining the vacuum.

During the pumping, which lasted several days, the tube itself and the tubing connecting it with the pumps were baked for hours at a time at 500°C, and the side tube containing charcoal was baked at an even higher temperature—about 550°C. This baking was alternated with heating by bom-

bardment of such of the metal parts as could be reached from the filaments. The target in particular was heated several times to a temperature at which it vaporized freely. The tube was sealed from the pumps with the target at a high temperature, and the charcoal at 400 or 500°C and cooling. The pressure in the tube at the time was 2 or 3×10^{-6} mm of mercury. As soon as the tube containing charcoal had cooled sufficiently it was immersed in liquid air. No means were provided for measuring the pressure of the gas in the tube after sealing from the pumps, but from experience with similar tubes in which such measurements could be made we judge that its equilibrium value was 10^{-8} mm of mercury or less. The pumping equipment consisted of a three stage Gaede diffusion pump backed by a two stage oil pump.

The Crystal

It is important to have a clear picture of the arrangement of atoms presented to the incident beam by the crystal. The nickel crystal is of the

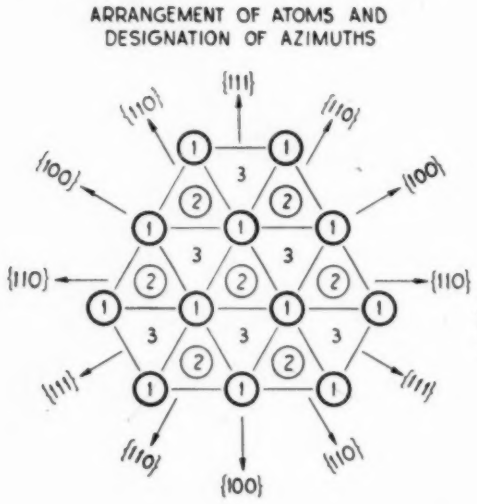

Fig. 6.

face-centered cubic type. The {111}-plane is the plane of densest packing, and in this plane the atoms have a triangular arrangement. Looking directly downward onto a crystal cut to this plane (Fig. 6) one sees the atoms of the second plane below the centers of alternate triangles of the first plane, and the atoms of the third plane below the centers of the remaining triangles. The atoms of the fourth plane are below those of the first. The lines joining any second-layer atom with the three nearest first-layer atoms are {110}-directions in the crystal, and the lines joining it with the three next-nearest surface atoms are the orthogonal {100}-directions. It will be convenient to refer to the azimuths of these latter directions as {100}-azimuths. The azimuths of the {110}-directions are also those of the three lateral {111}-directions, already referred to, and we shall designate these as {111}-azimuths. We need also a designation for the azimuths that bisect the dihedral angles between adjacent members of the two sets already specified. There are six such azimuths and they will be referred to as {110}-azimuths.

It follows from the trigonal symmetry of the crystal that if the intensity of scattering exhibits a dependence on azimuth as we pass from a {100}-azimuth to a next adjacent {111}-azimuth (60°), the same dependence must be exhibited in the reverse order as we continue on through 60° to the next following {100}-azimuth. Dependence upon azimuth must be an even function of period $2\pi/3$.

Distribution of Speeds among Scattered Electrons

The electrons leaving the target in any given direction appear always to have speeds that are distributed in one of two ways, depending upon whether the direction lies within or outside a diffraction beam. In the latter

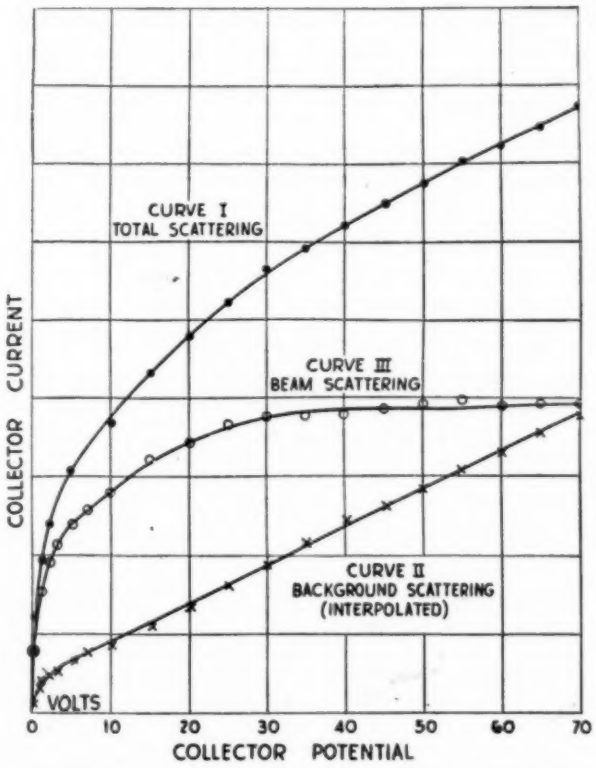

Fig. 7. Current to collector as a function of collector potential—bombarding potential 160 volts.

case—that of the electrons making up the "background" scattering—there is always a definite group having the speed of those in the incident beam. Below this speed there is in general a range over which the distribution in energy is very nearly uniform; and below this a range, ending with zero speed, in which the representation increases rapidly with decreasing energy.

These characteristics are inferred from the relation between collector current and the potential of the collector relative to that of the filament. The lower portion of a typical curve exhibiting this relation for the "background" scattering is shown in Fig. 7 (Curve II). The ordinate of a curve

of this sort is not, of course, an actual measure of the number of electrons entering the outer box with sufficient energy to reach the inner box. On account of the distortion of the field about the openings the probability that an electron entering the outer box with just sufficient energy to reach the walls of the inner box will actually do so is vanishingly small; the saturation current due to electrons of a given speed is attained only when the potential of the inner box is somewhat higher than that corresponding to their speed. The rounding off of the current-voltage curve at the top of the initial rise is due to some extent to this cause.

For this reason the group of high speed, or full speed, electrons is more nearly homogeneous than would be inferred from the current-voltage curve if no account were taken of this distortion. It seems probable, in fact, that the distortion accounts almost completely for the rounding off of the curve, and that the group is as nearly homogeneous as is permitted by the drop in potential along the filament and the initial speeds of the emitted electrons. This view is strongly supported by the observations of Becker,[5] Brown and Whiddington,[6] Sharman,[7] and Brinsmade[8] on the magnetic spectrum of electrons scattered by metals, and by similar curves obtained by Farnsworth.[9]

Within a diffraction-beam the distribution-in-speed is somewhat different. There is again a definite group of full speed electrons, but speeds just inferior to the maximum have much greater representation than among the background electrons. This is inferred from curve III in Fig. 7 which is representative of the current-voltage relation for electrons of this class. We shall return in a later section to a further consideration of the curves in this figure.

In studying the distribution in direction of the scattered electrons measurements have been confined, as nearly as possible, to the group of full speed electrons. The potential of the collector is set just high enough to admit all of this group. The ratio of collector to bombarding current is then of the order 10^{-4}, so that, by using bombarding currents of the order 10^{-6} ampere, collector currents are obtained that are easily measurable with a sensitive galvanometer. The total integrated current of full speed scattered electrons is from a tenth to a twentieth as great as the current of the incident beam.

Distribution of Directions among Full Speed Scattered Electrons

The current of full speed electrons entering the collector is proportional to the current incident upon the target and is otherwise a function of the bombarding potential and of the latitude and azimuth of the collector. Three simple types of measurement are thus possible in each of which two of the independent variables are held constant and the third is varied. When bombarding potential and azimuth are fixed and exploration is made in

[5] J. A. Becker, Phys. Rev. **23**, 664 (1924).
[6] D. Brown and R. Whiddington, Nature **119**, 427 (1927).
[7] C. F. Sharman, Proc. Camb. Phil. Soc. **23**, 523 (1927).
[8] J. B. Brinsmade, Phys. Rev. **30**, 494 (1927).
[9] H. E. Farnsworth, Phys. Rev. **25**, 41 (1925).

latitude a dependence of current upon angle is observed which is generally of the form shown in Fig. 8; the current of scattered electrons is zero in the plane of the target and increases regularly to a highest value at the limit of observations—colatitude 20°. This type of dependence upon angle is essentially the same as is observed when the target is of ordinary nickel—made up of many small crystals.

When bombarding potential and latitude angle are fixed and exploration is made in azimuth a variation of collector current is always observed, and this exhibits always the three-fold symmetry required by the symmetry of the crystal. The curves show in general two sets of maxima—a set of three in the $\{111\}$-azimuths, and a set of three of different intensity in the $\{100\}$-azimuths. These crests and troughs in the azimuth curves are usually not pronounced.

In the third method of observation the position of the collector is fixed in one of the principal azimuths at one after another of a series of colatitude

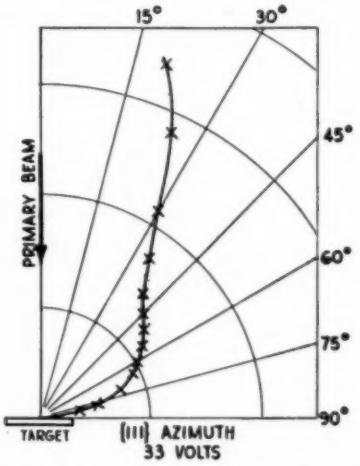

Fig. 8. Typical colatitude scattering curve for the single nickel crystal.

angles, and at each such setting the current to the collector is observed as a function of bombarding potential. It would be desirable in making observations of this sort to keep constant the current in the incident beam but, as there is no ready means of doing this, the current to the plate P_2 (Fig. 3) is kept constant instead. Beginning at colatitude 20° a series of such observations is made, over a predetermined voltage range, at 5° intervals to colatitude 80° or 85°. A portion of a set of curves constructed from such data is shown in Fig. 9.

The general trend of a single one of these curves is not significant as it is determined in part by variation with voltage of the bombarding current. The relative displacements among them, however, are significant as they indicate departures from the simple type of colatitude curve shown in Fig. 8. From the curves in Fig. 9 we see, for example, that the colatitude curves for bombarding potentials near 55 volts are characterized by exceptional intensities at colatitude angles near 50°. The data for constructing colatitude

curves for particular bombarding potentials are taken directly from such curves as those of Fig. 9, or the features in these latter curves are used as

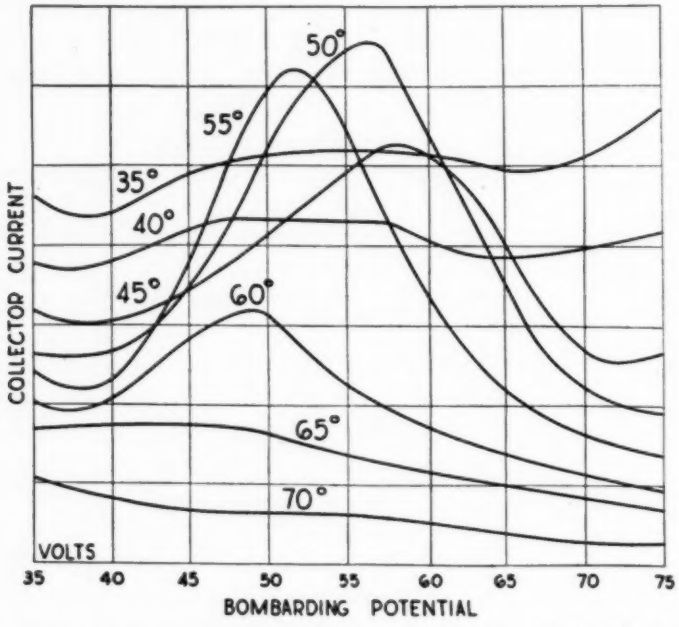

Fig. 9. Curves of collector current vs. bombarding potential—showing the development of the "54 volt beam." Azimuth {111}.

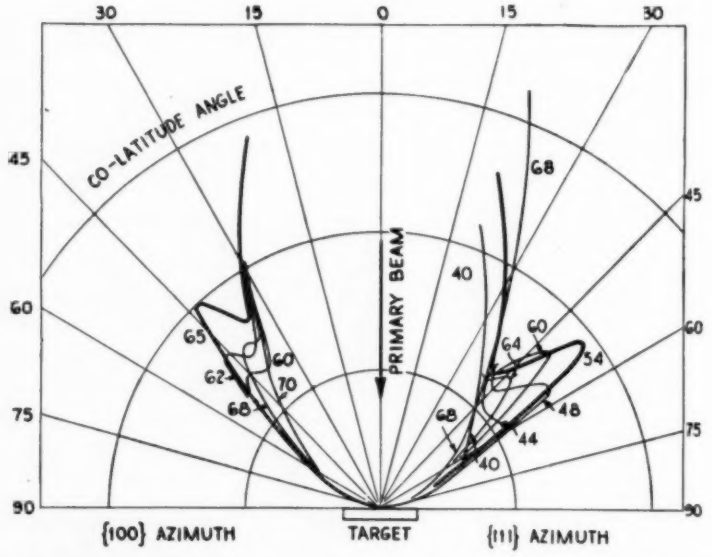

Fig. 10. Scattering curves showing the occurrence of the "54 volt" electron beam and the "65 volt" electron beam. (On each scattering curve is indicated the bombarding potential in volts.)

a guide to voltage-colatitude ranges requiring special study. This method has been employed in exploring the principal azimuths in the range from

15 to 350 volts, and two other azimuths, to be specified later, over the range from 200 to 300 volts. Every feature of the sort shown in Fig. 9 has been investigated.

The unusual and significant feature revealed by the curves of Fig. 9 is exhibited again in the set of colatitude curves on the right in Fig. 10. We see a slight hump at 60° in the colatitude curve for 40 volts, and observe that as the bombarding potential is increased this hump develops into a strong spur which reaches a maximum development at 54 volts in colatitude

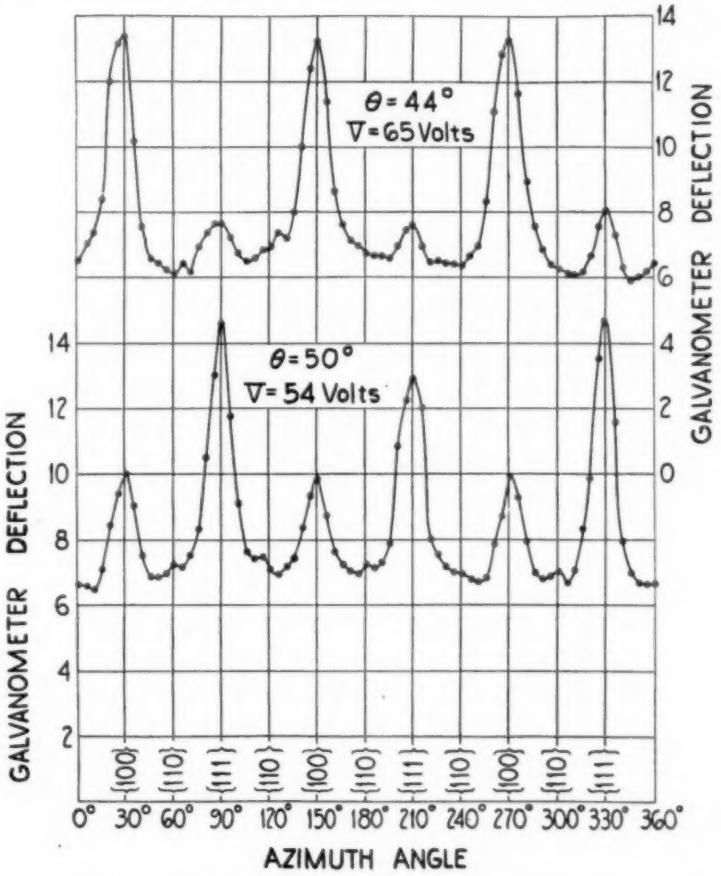

Fig. 11. Azimuth scattering curves through the "54-volt" electron beam and through the "65-volt" electron beam.

50°, then decreases in intensity and finally disappears at about 66 volts in colatitude 40°.

A section in azimuth through the center of this spur in its maximum development is shown in the lower curve of Fig. 11. The spur is sharp in azimuth as well as in latitude and is one of a set of three spurs as the symmetry of the crystal requires. The smaller peaks in the {100}-azimuth are sections of a similar set of spurs that attains its maximum development at 65 volts in colatitude 44°. A complete set of colatitude curves

for one of these spurs is shown on the left in Fig. 10. The upper curve in Fig. 11 is an azimuth curve through the peaks of these 65 volt spurs. The small peaks in the $\{111\}$-azimuth are the remnants of the "54 volt" spurs.

The colatitude angles at which the various spurs of a single set are strongest are found not to have exactly the same values. This is due apparently to imperfect alignment of the normal to the crystal planes and the axis of rotation of the target. In each of several sets that have been studied these angles are expressed by the formula $\theta=\theta_0+\Delta\theta\cos(\phi-\phi_0)$, where θ_0 is a constant for a given set and is taken to represent the colatitude angle at which all spurs in the set would be strongest if the alignment were perfect, and $\Delta\theta$ and ϕ_0 are constants that have the same values for all sets, 2° and 1° respectively. This is taken to mean that the axis of rotation is displaced about one degree from the normal to the crystal planes into azimuth 181°. The correction $2\cos(\phi-1°)$ degrees has been applied to all observed values of the colatitude angle θ.

The voltages at which the different spurs of a given set are strongest probably show a like variation. The differences are slight, however, and no attempt has been made to apply a voltage correction.

If we regard the spur as a feature superposed on the simple scattering curve the position of its maximum is falsified to some extent by the variation with angle of the background against which it appears. The method of correcting for this effect is indicated by the curves in Fig. 12. The end portions of the observed curve are joined by a curve of the known form of the simple relation (see e.g., Fig. 8), and the difference of these curves is plotted as the graph of the spur. The position of the maximum of this difference curve is taken as the true value of θ.

The Width of the Spur

From the difference curve in Fig. 12 we see that the spur has an apparent angular width of about 25°. What width is to be expected if the spur is due to a beam of electrons which is as sharply defined as the primary beam? This latter beam is defined by circular apertures 1 mm in diameter, and if we assume that the beam is a cylinder of this diameter, an equally sharp beam scattered at colatitude θ would extend over a colatitude arc of $(1\times\cos\theta)$ mm. The circular opening in the outer box is 1 mm in diameter, and its distance from the axis of rotation is 11 mm, so that the least possible value for the apparent colatitude width is $(1+\cos\theta)/11$ radians, or $5.2(1+\cos\theta)$ degrees. For the spur under consideration $\theta=50°$, and the calculated width is 8.5°.

The width in azimuth of the same spur is seen from the lower curve of Fig. 11 to be about 30°. The least value for this width is given by $5.2(2)/\sin\theta$ which for $\theta=50°$ amounts to 13.5°. Thus both in colatitude and in azimuth the observed width of the beam is more than double the least possible value.

It is to be expected, of course, that the observed values will be somewhat greater than those calculated, since it is hardly likely that the primary beam is as sharply defined as has been assumed; it is probably divergent as well as somewhat nonhomogeneous. There is no way, however, of investigating

these matters. The most that can be said with certainty is that the spur is due to a beam of electrons whose definition is comparable in sharpness with that of the incident beam.

Distribution of Speeds among Electrons Constituting the Diffraction Beams

Assuming that the sharply defined beam is a distinct feature superposed upon the general background scattering, it is natural to inquire in what way

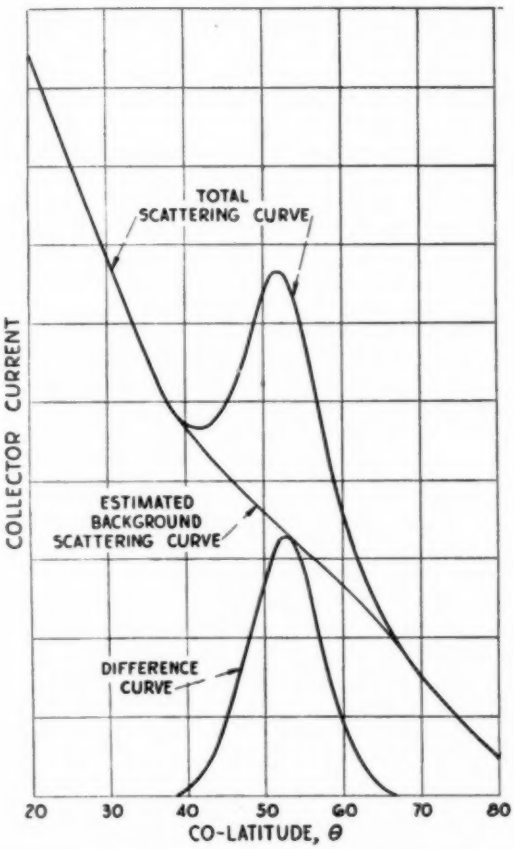

Fig. 12. Scattering curve of the "54 volt" beam, showing the method of determining the position of the maximum. (Angles not corrected for the tilt of the target).

the electrons constituting the whole of the superposed scattering are distributed in speed. Is the complete superposed scattering made up of full speed electrons only, or is it made up in part of electrons of lower speeds? This point has been investigated in several different ways. The fact seems to be that in addition to the group of full speed electrons observed in the distribution-in-direction measurements the complete superposed scattering includes also other electrons that have lost energy in various amounts up to about one quarter of their incident energy; it seems to include no electrons that have lost more than this amount.

These characteristics are inferred from the experimental results exhibited in Fig. 7. The upper curve was obtained with the collector in the center of a beam in the {100}-azimuth which is strongest at 160 volts. Two other curves (not shown) were then obtained with the position of the collector unaltered, but with the bombarding potential changed to 120 volts in one case, and to 200 volts in the other. The spur does not appear at either of these voltages, so that the current-voltage curves for these voltages are for "background" electrons only. These curves are not very different, so that a similar curve for 160 volts may be interpolated with considerable certainty. Curve II of Fig. 7 is this interpolated curve representing the current-voltage relation for "background" electrons only at 160 volts.

Curve III has been obtained by subtracting II from I, and consequently represents the current-voltage curve that would be obtained if the "background" scattering could be eliminated. We infer from the form of this curve that the electrons making up the whole of the superposed scattering are distributed in energy as described in the previous paragraph. The distribution is that which might be expected among the emergent electrons if a homogeneous beam were incident upon an extremely thin plate—a plate only one or two atoms in thickness.

Although the matters here considered require much more study than they have so far received, it is fairly clear that the superposed scattering is made up of beams of full speed and nearly full speed electrons that approximate the incident beam in sharpness, and that these beams appear only at and near certain critical bombarding potentials.

Positions and Voltages of Electron Beams

The work of investigating these beams and searching out new ones has progressed in several distinct stages. To begin with an exploration was made through the principal azimuths in the range 15 to 200 volts. Thirteen sets of beams were found, and these were described in our note to "Nature." The exploration was then extended to 350 volts, and eight additional sets were found. Up to this time the target had been heated last while the tube was still on the pumps.

After completing the exploration to 350 volts the target was strongly heated, and allowed to cool again to room temperature. The effect of this treatment was to increase generally the intensities of the beams without altering either the voltages at which they occurred or their positions. Three sets of beams only were exceptions to this rule, and these were the particular three sets which in our note in "Nature" we regarded as anomalous; the intensities of these were decreased.

These alterations in intensity resulted, we believe, from removal of gas from the surface of the target. In further tests it was found that immediately after bombardment, while the target is still hot, the beams are all weak; that they then increase in intensity as the target cools and that later, presumably as gas collects again on the surface, their intensities decrease. This final decrease in intensity was rather rapid after the first heat treatments, but after ten or a dozen heatings it was much slower—the intensities of the

beams remaining for hours near their maximum values. This was the behavior of the normal beams. The three sets of anomalous beams were progressively weakened, and finally disappeared.

The alteration brought about in the "54 volt" beam by this degassing of the target is shown in Fig. 13. Curve *A* is reproduced from Fig. 10 and shows the beam in its maximum development in the earlier tests. Curve *B* is for the same beam from the cleaned target. The intensity has been increased between four and five fold, while the intensity of the background scattering has been decreased. For beams of higher voltage the increase in intensity was in general less marked, but even for beams above 300 volts intensities were at least doubled. *The ratio of full speed electrons scattered into any one of the most intense sets of beams to the total number scattered in all directions is about two-tenths.*

A further effect of cleaning the target has been to cause the appearance of certain new beams in the range below 200 volts. These beams are of peculiar interest. They are exceptionally sensitive to gas, and were entirely absent at the time the earlier observations were made.

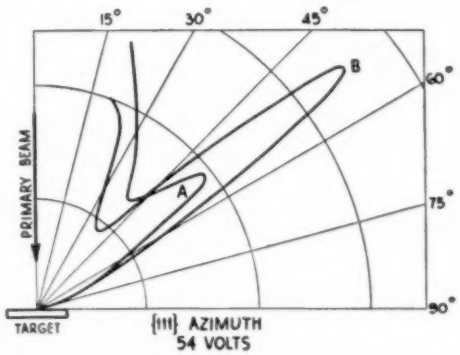

Fig. 13. The "54 volt" beam before and after heating the crystal by electron bombardment. *A*. Original condition as in Fig. 10. *B*. After heating the crystal.

We have found altogether thirty sets of beams, including those due to gas. Most of these are analogues of Laue beams, and the data for beams of this class are listed in Table I. The intensities in column 5 are estimated for a constant electron current bombarding the target, and for the target surface as free as possible from gas. In a few cases redetermined constants for the beams of Table I are somewhat different from those given in the note in "Nature." The beams not listed in Table I will be considered individually.

It would be possible to follow, with the beams listed in Table I, the procedure employed in our note in "Nature" (to point out a correspondence between the electron beams and the Laue beams that would issue from the same crystal if the incident beam were a beam of x-rays); then, with this suggestion of the wave nature of the phenomenon, to show that wave-lengths may be associated in a simple and natural way with the electron beams, and finally to compute these wave-lengths and show that they are in accord with the requirements of the undulatory mechanics. It is prefer-

able, however, to start at once with the idea that a stream of electrons of speed v is in some way equivalent to a beam of radiation of wave-length h/mv, and to show to what extent the observations can be accounted for on this hypothesis. We assume that this radiation is scattered and absorbed by the atoms of the crystal and that, just as in the case of x-rays, strong diffraction beams result from coincidence in phase of all of the radiation scattered in some particular direction.

TABLE I

Space lattice electron beams

Azi.	Bombarding Potential V	Equivalent Wave-length $\lambda=(150/V)^{1/2}$	Colatitude θ	Beam Intensity (Arbitrary Scale)	Beam Int. / Background Int.
{111}	54 volts	1.67 A	50°	1.0	7.0
	106	1.19	28	0.4	1.4
	174	0.928	22	2.0	1.3
	181	0.910	55	0.7	1.0
	248	0.778	44	1.0	2.6
	258	0.762	<20	4.5	1.8
	343	0.661	34	3.0	1.5
	347	0.657	62	0.07	0.3
{100}	65	1.52	44	1.0	7.0
	126	1.09	28	2.0	3.8
	160	0.968	60	0.8	5.7
	190	0.889	20	2.0	1.3
	230	0.807	46	0.4	1.2
	292	0.716	<20	7.0	2.0
	310	0.695	70	0.15	0.8
	312	0.693	37	1.5	1.2
	370	0.636	57	0.15	0.4
{110}	143	1.024	56	0.2	0.9
	170	0.940	46	0.1	0.5
	188	0.893	43	0.3	1.0
	248	0.778	34	0.45	0.6

In considering the conditions under which such beams will occur it will be convenient to regard the crystal as built up of {111}-planes of atoms parallel to the principal facets, and to picture the radiation scattered by the crystal as made up of the contributions from all such planes. This viewpoint has a distinct advantage, in the present case, over regarding diffraction beams as built up of contributions regularly reflected from the Bragg atom-planes. The amplitude of the radiation proceeding in a given direction from the crystal is then to be regarded as the sum of the amplitudes (with due regard to phase) of the increments of radiation proceeding in the same direction from all such {111}-planes of atoms—or more precisely, the fractions of such increments that actually escape from the crystal.

If we imagine a system of Cartesian coordinates with its origin at the center of a surface atom, its positive z-axis extending outward from the facet, and its positive x-axis lying in one of the {110}-azimuths of the crystal, then atom centers occur at the points

$$x=(M+N+P)s/2$$
$$y=3^{1/2}(M-N+P/3)s/2$$
$$z=-2^{1/2}Ps/3$$

where $s(=a/2^{1/2})$ represents the least distance between atoms in a $\{111\}$-plane (the side of the elementary triangle), M and N are any integers, and P is zero or any positive integer.

If a beam of plane waves is incident upon any one of these atom planes along a line whose direction cosines are l_1, m_1, n_1, it may be shown that the radiation scattered by the individual atoms will be in phase along the directions

$$l_2=l_1+(p+r)\lambda/s$$
$$m_2=n_1+(p-r)\lambda/3^{1/2}s$$
$$n_2=\pm(1-l_2^2-m_2^2)^{1/2}$$

where λ represents the wave-length of the radiation, and p and r are any integers. If the waves meet the layer at normal incidence, as in our experiments, then $l_1=m_1=0$, $n_1=-1$, and

$$l_2=(p+r)\lambda/s$$
$$m_2=(p-r)\lambda/3^{1/2}s$$
$$n_2=\pm(1-l_2^2-m_2^2)^{1/2}$$

It may be shown that these are just the directions in which diffraction beams are to be expected if the plane of atoms is regarded as equivalent to a great number of line gratings. All of the atoms in the plane may be regarded as arranged on lines parallel to the line joining any two of them, and every such set of lines functions as a line grating. Diffraction beams due to each such grating occur in the plane normal to its lines, and satisfy the ordinary plane grating formula, $n\lambda=d\sin\theta$.

The grating constant d has its greatest value for the three plane gratings the lines of which are parallel to the sides of the elementary triangle. For these $d=d_1=3^{1/2}s/2$, and $n\lambda=(3^{1/2}s/2)\sin\theta$. The beams due to these gratings occur symmetrically in the $\{111\}$ and $\{100\}$-azimuths.

The longest wave-length that can give rise to a diffraction beam is found by setting $n=1$ and $\sin\theta=1$ in the grating formula in which d has its greatest value, i.e., it is the wave-length $3^{1/2}s/2$. When waves of this length are incident normally on the plane of atoms first order diffraction beams should appear at grazing emergence in the $\{111\}$ and $\{100\}$-azimuths—six beams in all. When the wave-length is decreased these beams should split into two sets of six beams each—one set moving upward toward the incident beam, and the other set moving downward. We are concerned with the upward moving set only. When the wave-length has been decreased to $3^{1/2}s/4$ second order beams should appear at grazing, and these should follow the course of the first order beams with still further decrease in the wave-length. In the meantime, however, six first order beams from the three gratings of second largest spacing $(d=d_2=s/2)$ should have appeared at grazing in the $\{110\}$-azimuths. And as the wave-length is shortened beams should appear in still other azimuths.

These are the diffraction beams to be expected from a single layer of atoms. In general, when the incident beam is being scattered simultaneously from a large number of such layers the diffraction beams from the different layers must emerge from the crystal out of phase with one another, and the amplitude of the resultant beam must be much smaller than that which a single layer should produce.

There are two conditions, however, under which the amplitude of a given set of beams may be as great as, or greater than, that due to a single layer. One of these is the well known case of the Laue beams in which the scattered waves contributed to a particular beam from the consecutive atom layers are in phase and reenforce one another by constructive interference; the other is the case in which the reduction in intensity of the radiation on passing through a single layer of atoms—due to scattering and absorption—is so great that no appreciable radiation emerges from the interior of the crystal to interfere with that scattered by the first layer. The resultant scattering in this case will be approximately that from a single layer of atoms. This condition will be most closely approached near grazing, since in this region the paths in the crystal over which radiation from the second and lower layers must escape are greatly lengthened. The new electron beams discovered below 200 volts after the crystal was thoroughly degassed appear to be of this latter type. We shall begin our discussion of the data with an examination of these "plane grating" beams.

The value of the spacing s for nickel is 2.48A, so that $d_1 = 3^{1/2}s/2 = 2.15$A, and first order beams should appear at grazing emergence in the $\{111\}$ and $\{100\}$-azimuths when $\lambda(=h/mv)$ has this value. Rewriting de Broglie's formula for λ in terms of the kinetic energy V of the electrons expressed in equivalent volts, we have:

$$\lambda(\text{in Angstrom units}) = (150/V)^{1/2}$$

From this we calculate that the electron wave-length will have its critical value when $V = 32.5$ volts.

The new beams in the $\{100\}$ and $\{111\}$-azimuths are shown in Figs. 14 and 15 in which current to the collector is plotted against bombarding potential for various colatitude angles. In both azimuths beams appear at grazing ($\theta = 90°$) at or very near the calculated voltage, and then move upward toward the incident beam as the voltage is increased. The low intensities of the beams near grazing are attributed to the general roughness of the surface and to absorption of the radiation scattered by the first layer by the atoms of the same layer. The final disappearance of these beams at about 30° above the surface is accounted for by interference between the radiation scattered by the first layer and that escaping from below. Over this range we expect wave-length and angular position of the beam to be related through the plane grating formula $\lambda = d_1 \sin\theta$, or voltage and position through the equivalent relation $V^{1/2} \sin\theta = (32.5)^{1/2} = 5.70$. That the observations are in accord with this requirement is shown by the values calculated from Figs. 14 and 15 and recorded in Table II.

TABLE II

Occurrence of "plane grating" electron beams.

θ	Azimuth $-\{100\}$ V	$V^{1/2}\sin\theta$	Azimuth $-\{111\}$ V	$V^{1/2}\sin\theta$	Azimuth $-\{110\}$ V	$V^{1/2}\sin\theta$
85	32.0	5.64	32.5	5.68	97.5	9.83
80	33.0	5.66	34.0	5.75	100.0	9.85
75	35.0	5.72	35.0	5.72	103.5	9.83
70	36.0	5.64	36.5	5.68	108.0	9.77
65	38.5	5.63	35.0	5.37	112.5	9.62
60	42.5	5.65				

The difference in intensity between the beams shown in Figs. 14 and 15 is due apparently to a real dependence of intensity upon azimuth; the beams in the three $\{100\}$-azimuths are all more intense than the beams in the $\{111\}$-azimuths. We naturally try to account for this difference (which could not occur if the scattering were from a single atom layer) by supposing that although the extinction of the radiation in the metal is sufficiently great to leave first layer scattering predominant, it is not sufficiently great, even

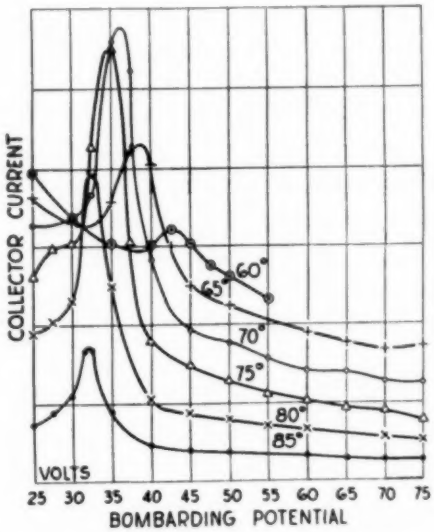

Fig. 14. Collector current vs. bombarding potential showing plane grating beams near grazing in $\{100\}$-azimuth.

near grazing, to suppress completely the escape of radiation from lower layers. The phase difference between first and second layer beams is not the same in the two azimuths, and as a consequence an intensity difference results. Whether the observed difference is in the sense to be expected will be considered later.

It was expected that second order beams corresponding to the ones just described would be found at grazing for $V=4\times 32.5=130$ volts. These appear, however, to be entirely missing. We cannot account for this.

On the other hand the anticipated first order beams in the {110}-azimuths resulting from the atomic line gratings of second widest spacing are duly found. One of these beams is shown in Fig. 16. The grating constant is $s/2$,

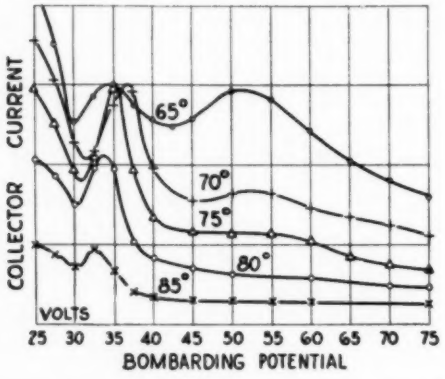

Fig. 15. Collector current vs. bombarding potential showing plane grating beams near grazing in {111}-azimuth.[10]

or $1/3^{1/2}$ as great as that of the former gratings, so that the beam should appear at grazing for $V=3\times 32.5=97.5$ volts. The beam appears quite accurately at this voltage. It also conforms over the range through which

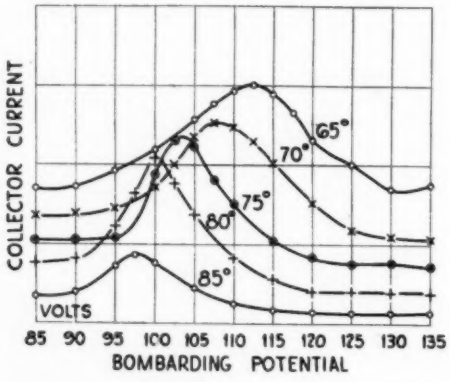

Fig. 16. Collector current vs. bombarding potential showing plane grating beams near grazing in {110}-azimuth.

it can be followed to its appropriate grating formula, $\lambda=d_2 \sin\theta$, or $V^{1/2}\sin\theta = (97.5)^{1/2}=9.88$. Values of $V^{1/2}\sin\theta$ taken from Fig. 16 are given in the last section of Table II.

These beams, as has been mentioned, are extremely sensitive to the presence of gas on the surface of the target. They fall off in intensity as the

[10] In Fig. 15 the maxima near 50 volts in the curves for 65 and 70 degrees are due to the "54 volt" beam in early stages of its development. The curves in Fig. 15 should be compared with those in Fig. 9. The latter are for the target covered with gas; the "plane grating" beam is altogether lacking here, and the "54 volt" beam shows much more weakly than in the curves in Fig. 15. The rapid rise of the current in all colatitudes below 30 volts in Fig. 15 is not significant. It is due to a rapid increase of current in the incident beam which resulted, under the conditions of these measurements, from a focussing action within the electron gun.

gas collects, and disappear when the amount of gas on the surface is insufficient to affect more than slightly the intensity of beams occurring at higher voltages and smaller colatitude angles.

This behavior is consistent with the view already proposed that near grazing the intensity of scattering is determined almost entirely by the atoms in the topmost layer. When the crystal is clean this is a layer of regularly arranged nickel atoms which gives rise to the plane grating beams—when gas has collected on the surface it is a layer of gas atoms or molecules which may or may not give rise to diffraction effects of its own, but which, in either case, serves to absorb the radiation from the first layer of nickel atoms.

We thought that since the radiation in the grazing beams is scattered mostly by top layer atoms, the electrons in these beams would be more nearly homogeneous (made up more completely of full speed electrons) than those in beams at higher voltages and lower colatitude angles—beams more dependent for their intensities upon radiation scattered from atoms in lower layers. This appears, however, not to be the case. Current-voltage curves similar to those in Fig. 7 have been constructed for the grazing beams, and these indicate a distribution of speeds quite like that inferred from Curve III of Fig. 7.

We have looked also for the first order grazing beams from the plane gratings of third largest spacing, but have failed to find them. There should be twelve such beams (six in each of two new azimuths) appearing at 227 volts. It is to be expected, of course, that the higher voltage beams of this type will be weak on account of a less rapid extinction of the equivalent radiation in the metal. Here, as elsewhere, it appears a dependable procedure to infer characteristics of the equivalent radiation from known properties of electrons; if high speed electrons are less rapidly absorbed than low speed electrons, we may infer that short wave equivalent radiation is less rapidly absorbed than long.

We have looked (also without success) for other beams of this type grazing the inclined $\{111\}$-facets. The calculated positions of most of these beams fall so close to intense space lattice beams that it seems unlikely they could be found, even if present. On the other hand a careful exploration for one particular beam of this sort, the predicted position of which is not too close to any space lattice beam, was a complete failure.

Space Lattice Beams

The diffraction pattern for radiation of a given wave-length scattered by a single atom layer is made up, as has already been described, of the plane grating beams from all of the gratings that can be constructed from lines of atoms in the layer. The beams occur in planes normal to the lines of these gratings, and satisfy the plane grating formula $n\lambda = d \sin \theta$, where d represents the constant of the particular grating considered. This relation is represented graphically by the straight lines in Fig. 17, in which wave-length λ is plotted against $\sin \theta$, for beams occurring in the principal azimuths. For a given value of λ the positions of the beams in the various orders may be read off from these lines.

We consider now what diffraction effects are to be expected when the incident waves are scattered not by a single layer of atoms, but by a number of such layers piled one above the other. We see that if the various atom layers are similarly oriented, the lines in Fig. 17 represent the wave-length angle relation for the diffraction beams from each layer in the pile, and that, therefore, they must represent the same relation for the beams issuing from

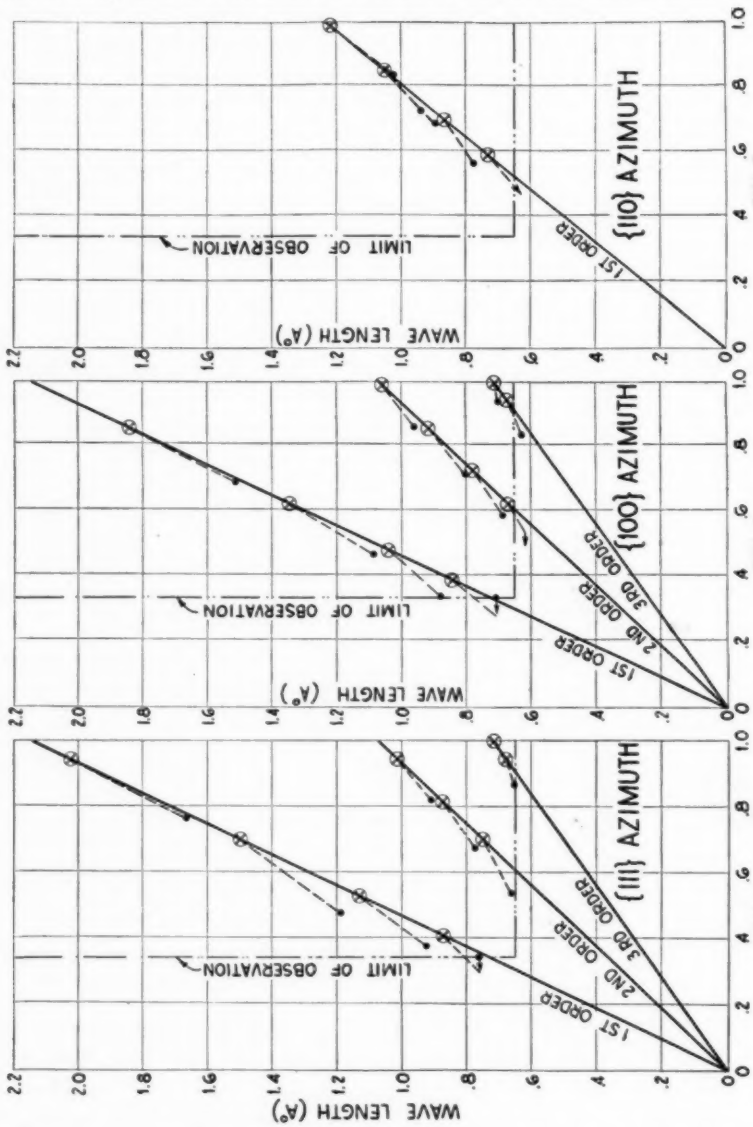

Fig. 17. Plots of the grating formulas in the three prinipal azimuths. Positions of theoretical x-ray beams are indicated by crossed circles and positions of actual electron beams by dots.

the pile of layers; the sum of the superposed beams is still the same set of beams. As far, therefore, as the positions of the beams are concerned the diffraction of waves by a pile of parallel and similarly oriented atom layers is the same as by a single layer.[11]

[11] It is assumed in this paragraph that the atom plane is large enough to be highly resolving and that we are not interested in discrepancies of the order of the width of its diffraction beams.

There is, however, a great difference in the intensities of the beams in the two cases. In the case of scattering from a single layer the intensity of a given beam would be found ordinarily not to change greatly as the wave-length and position of the beam are varied. In the case of scattering from a pile of such layers, however, the intensity of the emergent beam is greatly affected by interference among the beams from the individual layers. If a great number of layers contribute individual beams of about the same intensity, as is the case in x-ray scattering, the intensity of the resultant beam will ordinarily be quite low. When, however, the beams from the individual layers emerge from the crystal in phase the intensity of the resultant beam passes through a strong maximum. The wave-lengths for which this occurs depend upon the way in which the atom layers are piled up—that is, upon the separation between successive layers and upon the lateral shift from one layer to the next. If the wave-length of the radiation within the crystal is not the same as outside this also will have an effect upon the occurrence of intensity maxima.

The purpose of setting forth these rather elementary matters at such great length is to bring out clearly that the intense space lattice beams are always also plane grating beams. If the wave-length and position of such a beam is represented by a point in Fig. 17 the point must fall somewhere on one of the plane grating lines.

If the incident beam in the present experiments were a beam of heterogeneous x-rays an array of Laue diffraction beams would issue from the crystal. The wave-lengths and positions of all such beams in the three principal azimuths within the range of our observations ($\theta > 20°$, $\lambda > 0.63$A) are indicated in these figures by crossed cycles.

The plane grating lines for azimuths $\{111\}$ and $\{100\}$ are, of course, the same, but the occurrence of Laue beams in these azimuths is different. The wave-lengths that give rise to diffraction beams in the $\{111\}$-azimuth are not the same, except in such orders as are exactly divisible by three, as those that give rise to beams in the $\{100\}$-azimuth. And the same statement, *mutatis mutandis*, may be made, of course, in regard to the angles at which beams occur in the two azimuths. When the wave-lengths or angles of the beams of any order, not exactly divisible by three, are ordered according to magnitude the members belonging to one azimuth occur alternately with those belonging to the other. These characteristics result from the fact that to superpose the atoms of one layer upon those of an adjacent layer involves a displacement normal to the grating lines equal to $(2n+2/3)$ times the grating space—n representing any integer. If the odd fraction were one-half or zero, as in the $\{110\}$-azimuth, these differences would not occur.

In this same figure we have indicated by dots the wave-lengths and positions of all sets of electron beams listed in Table I. The first thing to be noted about the dots is that they fall generally along the basic plane grating lines, and to this extent satisfy the fundamental requirement that a space grating beam shall be first of all a plane grating beam. It will be noted also that they occur along these lines at about the same intervals as the

crossed circles, and further that in the {111} and {100}-azimuths they exhibit the alternate occurrence characteristic of the crossed circles.

While the dots representing the sets of electron beams fall generally along the plane grating lines, one cannot fail to note that they actually fall off these lines—and systematically; they are above or to the left of the lines as one cares to view them. At the time of writing our note to "Nature" we believed that these departures could be accounted for by imperfections in the geometry of the apparatus. At present, with more data at our disposal, we are less certain that this is true. The fault of this explanation is that if the displacements of the dots from the lines result from imperfect alignment, angular displacement should be a function of angular position, and this condition seems not very well satisfied. The results of these investigations do not, however, rule out mechanical imperfection as the principal cause of these displacements, and for the present we shall assume it to be the only cause. We shall assume, that is, that the wave-lengths or voltages of the beams are correct but that the dots should be shifted to the right onto the lines. These shifts correspond to corrections in angle ranging from zero to about four degrees. We hope to remove the uncertainty here involved by measurements with a new tube now being constructed.

As the dots occur at about the same intervals along the lines as the crossed circles it is possible to associate each dot with a particular crossed circle—each set of electron beams, that is, with a particular set of x-ray beams, and consequently with a particular set of Bragg atom planes in the crystal. The associations which seem most natural are indicated by dotted lines in the figure. In the {110}-azimuth the association is imperfect as it appears that both the 0.893A and the 0.940A electron beams should be associated with the same x-ray beam. We have associated the stronger of these with the x-ray beam, and left the extremely weak electron beam at 0.940A without an apparent x-ray analogue. Also there is apparently a third order electron beam missing in the {111}-azimuth. We should expect this beam to be extremely weak.

We consider next the difference in position between each crossed circle and the location upon the line to which the associated dot is shifted as explained above. The positions of the lines are determined by the arrangement of atoms in a single plane and the scale factor of the structure, while the positions of the crossed circles are determined by the separation between successive planes and the lateral shift from one plane to the next. If the separation were decreased the crossed circles would all be moved downward along their lines; if it were increased they would be moved upward. Merely as a matter of description, therefore, we may say that a given dot when shifted occupies the position that its associated crossed circle would occupy if the separations between atom planes were decreased by a certain factor. This factor β may be calculated from the formula

$$\beta=\frac{\tan(\theta'/2)}{\tan(\theta_z/2)}$$

Here θ_x represents the colatitude angle of the Laue x-ray beam and θ' that of the associated electron beam after having been corrected to make the beam satisfy the grating formula exactly.

This factor β is found to be neither constant nor very regular in its behavior, but to increase generally with the speed of the electrons. The relation between the factor β and the bombarding potential is represented by the lower set of points in Fig. 18. There is a vague suggestion here that β approaches unity as a limiting value. If this is actually the case, it means, of course, that at sufficiently high voltages (short wave-lengths) there is no difference between the occurrence of x-ray and electron diffraction beams. This approach of the electron beam to the associated x-ray beam with

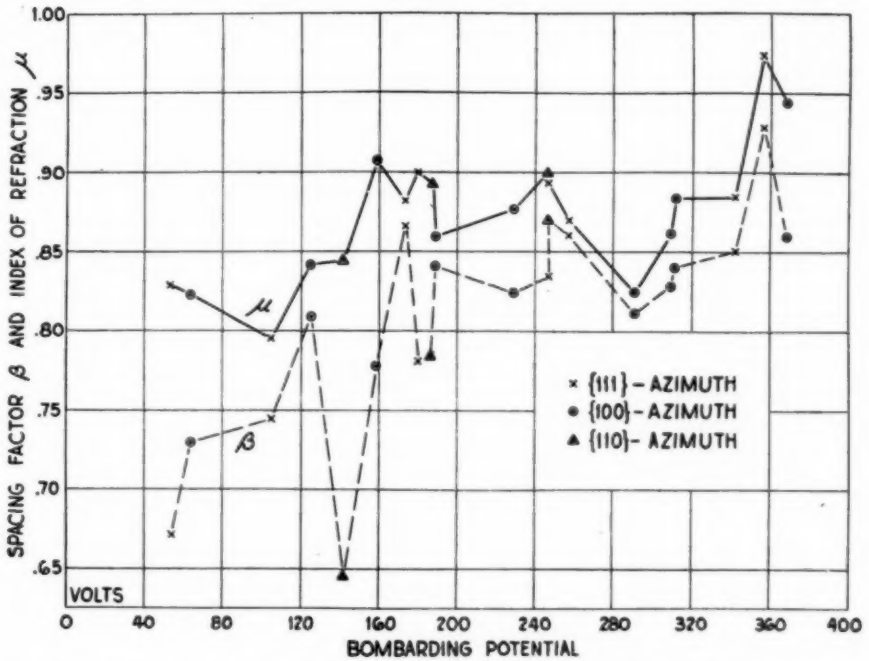

Fig. 18. Lower set of points—Spacing factor β vs. bombarding potential; Upper set of points—Index of Refraction μ vs. bombarding potential.

increasing voltage is shown very clearly by the series of three dots (Fig. 17) representing the first three orders of the beam whose first order is the 54 volt beam in the $\{111\}$-azimuth ($\lambda = 1.67$A). The first, second and third order beams occur at $\theta = 50°$, 55° and 62° respectively, while the corresponding x-ray beam occurs in each case at $\theta = 70°$ ($\sin\theta = 0.94$).

It has been suggested by Eckart[12] that this β factor may be interpreted as an index of refraction of the nickel crystal for the equivalent radiation. If the index of refraction of a crystal for radiation of a given wave-length is other than unity, diffraction will indeed occur as if the spacing between crystal planes were altered by a certain factor. This factor is not, however,

[12] Eckart, Proc. Nat. Acad. Sci. **13**, 460 (1927).

equal to the index of refraction. For the case in which we are interested, that of normal incidence, and emergence from the same surface, the quantity appearing in the measurements as "spacing" factor β is given by

$$\mu=\frac{\beta}{\cos^2\psi+\beta^2\sin^2\psi}$$

where ψ is the angle between the set of Bragg atom planes associated with the diffraction beam and the surface of the crystal. Values of μ calculated from this formula are represented by the upper set of points in Fig. 18. There is no greater regularity in the points representing μ than in those representing β.

There is the question, of course, as to whether the association of x-ray and electron beams indicated in Fig. 17 is the correct one. We might, for example, associate each dot in this figure with the next lower crossed circle instead of with the next higher, and there is at least one consideration favoring this procedure; the indices of refraction would then be slightly greater than unity for low speed electrons, and would approach unity for electrons of high speed. Such a dependence could be correlated with the increase in speed (decrease in wave-length) which an electron experiences on passing into a metal. In fact, we might naturally expect the index of refraction to be given by $\mu=[(V+\phi)/V]^{1/2}$, where ϕ represents the voltage equivalent of the work function of the metal.

The principal consideration opposed to this association is the absence of electron beams to be associated in the various orders with the x-ray beams of greatest wave-length. The absence of some of these might be accounted for by total reflection of the diffraction beam at the surface of the crystal. It seems unlikely, however, that the absence of analogues in three orders of the x-ray beams at $\theta=70°(\sin\theta=0.94)$ in the $\{111\}$-azimuth could be accounted for in this way. The absence of an electron beam to be associated with the first order x-ray beam of greatest wave-length in the $\{100\}$-azimuth would seem decisively against this alternative association were it not that the strong grazing beam in this azimuth (Fig. 14) may, in fact, be this analogue. This matter of association should, we think, be regarded as still an open question to be decided by further and more precise measurements. For the present, however, we shall adhere to the associations of Fig. 17.

Missing Beams

When electron and x-ray beams are associated as in Fig. 17 there is only one x-ray beam in the three principal azimuths for which an electron beam analogue predicted within the range of our observations has not been found. This is the third order beam in the $\{111\}$-azimuth already mentioned. There are, however, three Laue beams in range in two new azimuths, one of wave-length 0.78A at $\theta=74°$ in the $\{331\}$-azimuth, and two of wave-lengths 0.81A and 0.76A at $\theta=86°$ and $\theta=68°$ in the $\{210\}$-azimuth. The first of these azimuths[13] lies 11° from the $\{110\}$-azimuth toward the nearest $\{111\}$-

[13] We have consistently designated each azimuth by the Miller indices of the densest plane of atoms the normal of which lies in the azimuth and in or above the surface of the crystal.

azimuth, and the second lies an equal interval on the opposite side of the {110}-azimuth. A thorough but fruitless search has been made for the electron beam companions of these three Laue beams.

The total number of x-ray beams for which electron beam companions are expected within the range of our observations is twenty-four, and for twenty of these the electron beam companions have been found. The four sets of missing electron beams are all beams whose intensities we should expect to be low. They are all short wave-length beams lying not far above the plane of the target.

Third Order Beams in the {111} and {100}-Azimuths

The differences which have been noted between the occurrence of x-ray diffraction beams in the {111} and {100}-azimuths do not extend, as has been mentioned, to orders that are exactly divisible by three; the wave-lengths and positions computed for the third order x-ray beams in one of these azimuths are identical with those computed for the third order beams in the other. Differences in intensity between corresponding beams might possibly result from a dependence of the scattering power of a single atom upon crystal direction, but, so far as we are aware, differences of this sort are not found in x-ray data.

It seemed reasonable to expect, therefore, that the third order electron beams in the {111}-azimuth would be found identical in voltage, position, and possibly also in intensity, with beams of the same order in the {100}-azimuth. This agreement, however, is not observed. Two pairs of beams are available for observation, and the beams of each pair have constants that are different. The data are given below in Table III.

Table III

Third order electron beams.

{111}-azimuth				{100}-azimuth			
x-ray companion	θ	V	Int.	x-ray companion	θ	V	Int.
{55$\bar{1}$}	—	—	0.00	{711}	70°	310	0.15
{551}	60°	347	0.07	{822}	57	370	0.15

Resolving Power of the Crystal

It has been remarked (Fig. 10) that the space lattice beams are not sharply defined in voltage. The "54 volt" beam, for example, appears when the bombarding potential is about 40 volts and is still prominent in the curve for $V=64$ volts. In terms of equivalent wave-lengths the beam has appreciable intensity over a range $\Delta\lambda$ which is about one quarter as great as the equivalent wave-length of the beam at its maximum intensity. The corresponding ratios for beams of higher voltage are generally less, but even for beams for which V is greater than 300 volts values of $\Delta\lambda/\lambda$ are found as great as 0.07. We naturally conclude that as an optical instrument the crystal has low resolving power.

It might appear that this low resolving power is readily accounted for by the fewness of the atom planes contributing effectually to the scattering. In accounting for the "plane grating" beams we have already had occasion to assume that the extinction of the equivalent radiation in the metal is extremely rapid, and it may appear that no further assumption will be required to account for the low resolving power observed in the space lattice beams. It must be realized, however, that the resolving power of a space lattice is dependent not only upon the number of its atom planes, but also upon the number of grating lines in each plane, and that to ascribe the low resolving powers in the present case solely to the slight penetration of the radiation into the metal is to assume that the number of grating lines in each of the atom planes making up the lattice is relatively great—great compared with the number of effective planes. If the width of the lattice were the same as the width of the bombarded area this assumption would, of course, be amply justified. There are, however, at least two reasons for regarding the diffracting system not as a single lattice, but as a collection of very many extremely small lattices, similarly oriented but otherwise unrelated. A large part of the radiation proceeds, it would seem, from lattices not more than five or ten atom lines in width.

The first reason for ascribing this small width to the unit lattice is that on no other assumption have we been able to account for the great width of such peaks as those shown in Figs. 9, 14, 15 and 16. The width of these peaks is due in part, of course, to the width of the diffraction beam and to that of the collector opening, but these geometrical considerations are quite insufficient for the purpose. The curves referred to seem to show clearly that the resolving power of the topmost atom layer is quite low, and that consequently most of the radiation from this layer comes from independent gratings containing only a few atom lines each.

The second reason has to do with the relation between the voltage and the angular position of a space lattice beam in the various stages of its development. We have seen (Table II) that as a "plane grating" beam rises from the surface of the crystal the product $V^{1/2} \sin \theta$ remains constant. At one time we expected that the same relation would be found to obtain within a space lattice beam—that as the voltage was increased the beam would in all cases move upward to keep $V^{1/2} \sin \theta$ constant. This relation does in fact hold reasonably well for the "54 volt" beam. It holds less well, however, for the "65 volt" beam shown in Fig. 10, and fails entirely for most beams occurring at higher voltage. In many cases the total angular displacement during the growth and decay of the beam is not more than one-tenth that required by the plane grating formula. It may be shown, however, that the plane grating formula ($V^{1/2} \sin \theta = \text{constant}$) will describe the motion of the beam if the lattice is sufficiently wide, but that it will fail to do so otherwise. If the number of lines in the plane grating is not great compared with the number of atom planes, the plane grating relation will not obtain (except at the maximum of a beam—when the scattering from successive layers is exactly in phase) and departures from it will be in the direction of those that we have observed.

There are thus these two reasons for thinking that most of the scattered radiation proceeds from lattices not more than five or ten grating lines in width, and that the low resolving power of the plane gratings that make up the representative lattice is partly responsible for the low resolving power apparent in the space lattice beams.[14] It seems probable that the independent lattices are to be identified with the individual facets of the principal set—those parallel to the general plane of the target.

If the resolving power of the crystal were determined solely by the rate of extinction of the radiation in the metal, it would be possible to make use of the intensity-voltage relation within a given beam to calculate a coefficient of extinction of the metal for radiation of the wave-length of the beam, as suggested by Eckart (loc. cit.), or to estimate the number of atom planes effective in the scattering, as suggested by Patterson.[15] It may even be possible under the actual conditions of the scattering to evaluate these constants by making use also of the observed relation between the angular position of the beam and voltage. But the data which we have at present seem to us too inaccurate to make such calculations worth while. We hope to obtain data sufficiently precise for this purpose in the near future.

We have, however, calculated a rate of extinction from the data obtained for the "54 volt" beam with the surface of the target free from gas (not from the data of Fig. 10). As has already been mentioned, the product $V^{1/2} \sin \theta$ is very nearly constant in this beam, which means that its intensity-voltage relation is determined almost entirely by the rate of extinction. As the result of this calculation we have obtained the value 0.4 for the fraction by which the intensity of a beam of 54 volt equivalent radiation is reduced when such a beam passes normally through a single $\{111\}$-layer of nickel atoms. In terms of electrons this means presumably that when a 54 volt electron is incident normally upon such a layer the probability of its passing through without appreciable deflection or loss of energy is 0.6.[16]

Intensities of "Plane Grating" Beams

We return now to a further consideration of the intensity difference between the first order "plane grating" beams in the $\{100\}$ and $\{111\}$-azimuths (Figs. 14 and 15). If these were truly plane grating beams no difference of intensity should be observed. We have already pointed out, however, that it is only in the limit, as θ approaches $\pi/2$, that these beams are due to scattering from a single atom layer. They are actually space lattice beams, and their occurrence and behavior are described by the same mathematical formulas that describe the Laue type of beam. The intensity of a "plane grating" beam depends upon the efficiency with which a single

[14] It was shown in an earlier section that the apparent angular width of a space lattice beam (voltage constant) has more than double its least possible value as calculated from the dimensions of the apparatus. It seems probable from the present considerations that a considerable part of this additional width is to be ascribed to the low resolving power of the crystal.

[15] A. L. Patterson, Nature **120**, 46, (1927).

[16] This question of resolving power has been considered recently by F. Zwicky (Proc. Nat. Acad. Sci. **13**, 519 (1927)) in terms of the wave mechanics as formulated by Schroedinger and Born.

atom scatters the radiation incident upon it, and upon the rate of extinction of the radiation in the crystal. Such beams are not found when x-rays are scattered by a crystal because in this case both of these quantities are small.

The problem of finding which of the two beams under consideration should be the stronger resolves itself into finding in which azimuth the first order diffraction beams from successive atom layers are more nearly in phase near grazing emergence; the beam in this azimuth will be the more intense. These phase differences between beams from successive atom layers are readily deduced from the geometry of the lattice. Thus it may be shown that if the diffraction occurs as though the crystal were contracted normally to its surface to a fraction β of its normal spacing, this phase difference in the $\{111\}$-azimuth will be given by

$$\alpha_{111}=\frac{4\pi n}{3}\left[\beta 2^{1/2}\frac{1+\cos\theta}{\sin\theta}+1\right],$$

and in the $\{100\}$-azimuth by

$$\alpha_{100}=\frac{4\pi n}{3}\left[\beta 2^{1/2}\frac{1+\cos\theta}{\sin\theta}-1\right]$$

where n represents the order of the beam. Phase differences for $\theta=75°$ and for various values of β have been computed from these formulas, and are given in Table IV.

TABLE IV

First order phase differences for $\theta=75°$

Spacing Factor β	0.5	0.6	0.7	0.8
$(\text{Phase Diff})_{111}$	$2\pi+1.8$	$2\pi+2.5$	$4\pi-3.0$	$4\pi-2.2$
$(\text{Phase Diff})_{100}$	-0.3	0.4	1.2	2.0

From the results shown in Fig. 18 we expect that at 35 volts, the bombarding potential for these beams, the value of β will lie near 0.7. The phase difference in the $\{111\}$-azimuth is, therefore, about 3.0 radians and that in the $\{100\}$-azimuth about 1.2 radians. The beam in the $\{100\}$-azimuth should therefore be the stronger, and this is what is actually observed.

THE TEMPERATURE EFFECT

It has been mentioned already that immediately after bombardment, while the target is still at a high temperature, the intensities of all beams, as far as observed, are low, and that as the target cools the intensities rise again to their normal values for room temperature. The behavior is illustrated by the curves in Fig. 19 in which the intensities of the beams at ($V=54$ volts, $\theta=50°$) and ($V=343$ volts, $\theta=34°$) in the $\{111\}$-azimuth are plotted against time. The temperature of the target at zero time was perhaps 1000°K. The data for these curves were taken during the same run—observations on one beam being alternated with those on the other.

This temperature effect has not yet been studied in detail. There seems no reason for doubting, however, that it is the analogue of the Debye temperature effect observed in the diffraction of x-rays. This view is supported by the evidence of the curves in Fig. 19 that the higher voltage (shorter wavelength) beam is the more sensitive to temperature.

Beams Due to Adsorbed Gas

The "plane grating" beams and space lattice beams for which data have been given in previous sections are the only beams observed when the target is, as we believe, free from gas. When the target is not free from gas still other beams appear. Three sets of these have already been mentioned as the ones referred to in our note to "Nature" as anomalous; one set occurs in each of the three principal azimuths, and all attain their maximum intensity at or close to $\theta = 58°$, $V = 110$ volts. These beams appear to depend for their existence upon the presence of a considerable amount of gas on the surface of the target; they were most intense before the first bombardment of the target, and were not found when the amount of adsorbed gas was known

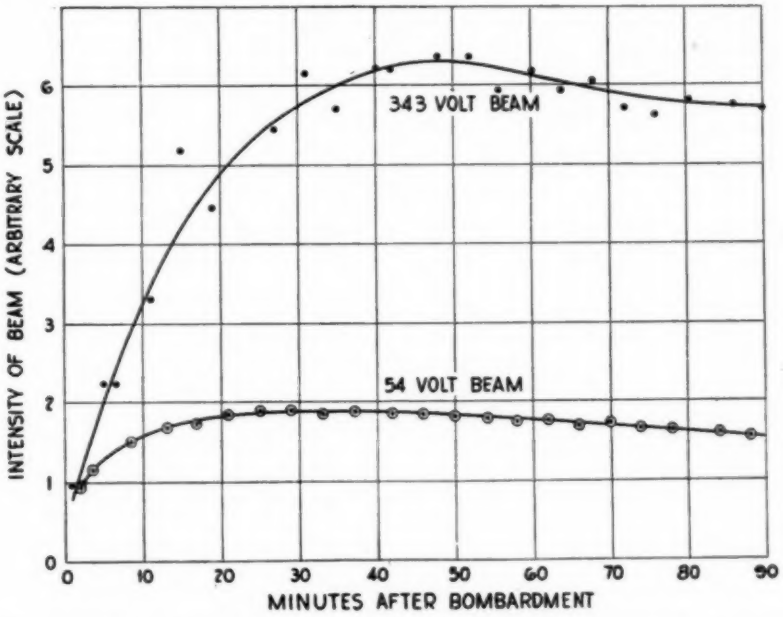

Fig. 19. Intensities of 54 volt beam and 343 volt beam vs. time, immediately after heating the target crystal.

to be slight. It should be possible to infer from the characteristics of these beams something about the arrangement of atoms to which they are due. It is clear, for example, that the arrangement is determined in part by the underlying nickel, since the beams occur in the principal azimuths of the nickel structure. We have been unable, however, to carry the deduction beyond this point.

With certain other beams due to gas we have been more successful. These constitute a family attaining greatest intensity when the quantity of adsorbed gas has a certain critical value. Various members of this family were observed first as beams of unusual behavior that appeared in places in which no beams were expected, and disappeared or changed in intensity for no apparent reason. Thus a beam was occasionally found in the $\{110\}$-azimuth at $\theta = 75°$, $V = 25$ volts. No such beam could result from scattering

by the nickel crystal unless our entire theory is fallacious; the first order grazing beam for this azimuth appears at $V=97.5$ volts, and no diffraction beam is possible for any lower voltage.

A correlation was eventually established between the intensity of this 25 volt beam and that of the normal grazing beam in the same azimuth. It was found that the 25 volt beam was strongest when the intensity of the grazing beam had been reduced by adsorbed gas to about one-fifth of its maximum value, and that when the grazing beam was at its maximum intensity the 25 volt beam was not to be found. Furthermore the 25 volt beam was not found when the surface was so contaminated that the normal grazing beam was absent; nor was it present when the 110 volt "anomalous" beams could be found.

It was noticed also that the voltage of this beam is almost exactly one quarter the voltage of the normal first order beam occupying the same position. The equivalent wave-length is thus twice that of the corresponding

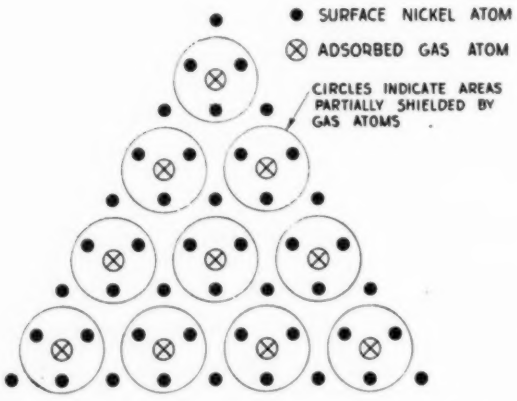

Fig. 20. Arrangement of gas atoms on the surface, and the topmost layer of nickel atoms.

first order beam, and the beam could be accounted for as radiation scattered by a layer of gas atoms of the same structure and orientation as the nickel atoms, but of twice the scale factor. Such a layer can be imagined built onto the surface layer of nickel atoms as indicated in Fig. 20. The first order diffraction beams from such a layer agree in wave-length and position with "one-half order beams" from the underlying lattice of nickel atoms, and as these latter have zero intensity the resultant beams should be those due to the single layer of gas atoms only. The beams should, therefore, move continuously upward as the voltage is increased without marked change in intensity. What is observed is not quite so simple; the beam can indeed be followed continuously from $\theta=85°$, $V=24$ volts up to $\theta=30°$, $V=98$ volts, but its intensity passes through broad maxima at $\theta=75°$, $V=25$ volts, and at $\theta=45°$, $V=50$ volts.

A possible explanation of this behavior may be pointed out. It will be noticed (Fig. 20) that the nickel atoms in the surface are of two sorts—those that are adjacent to gas atoms and those that are not. One-fourth of the

nickel atoms are of this latter class, and they together form a layer of the same structure, orientation and scale factor as the gas atoms. If the two classes of nickel atoms scatter radiation in different amounts—if, for example, the gas atoms shield the adjacent nickel atoms more effectually than the non-adjacent—then, of course, the layer of nickel atoms as a whole will give rise to a differential diffraction beam capable of interference with that due to the gas layer, and broad maxima of the sort observed will result.

It was anticipated, of course, that beams of the same nature would be found in the $\{111\}$ and $\{100\}$-azimuths. These should appear at grazing at $V=32.5/4=8.1$ volts and should move upward with increasing voltage—reaching $\theta=20°$ at $V=70$ volts. Observations cannot be made for bombarding potentials as low as 8 volts. The beams have been picked up, however, in both azimuths at $\theta=60°$, $V=12$ volts, and have been followed upward to $\theta=25°$, $V=45$ volts. Broad maxima occur at $\theta=35°$, $V=25$ volts, and at $\theta=55°$, $V=13$ volts in the $\{100\}$-azimuth; and in the $\{111\}$-azimuth a broad maximum occurs at $\theta=55°$, $V=14$ volts, and another is indicated in the neighborhood of $\theta=25°$, $V=45$ volts. It should be possible from these data to calculate the separation, or at any rate the apparent separation, of the gas layer from the crystal—but this has not yet been attempted.

We have further observed that these beams cannot be made to appear when the temperature of the target is somewhat above that of the room; glowing the filament back of the target raises the temperature of the target sufficiently to eliminate them entirely, although under these conditions gas still collects on the target, and reduces the intensities of the grazing beams. The explanation of this behavior may be that the melting point of the two dimensional gas crystal is not far above room temperature. We have not yet observed whether the beams disappear sharply at a critical temperature.

Further Experiments with Gas

In a final series of experiments the effect was studied of introducing large amounts of gas into the tube. The liquid air was removed from the charcoal tube, and the behaviors of the "54 volt" beam and of one of the anomalous "110 volt" beams were observed as the charcoal was heated. The latter of these beams had not been observed for several weeks—not since its disappearance during the first heatings of the target.

The initial effect of increasing the gas pressure was to decrease the intensity of the "54 volt" beam. Its intensity was, however, greater than that represented by curve *A* in Fig. 13 until the charcoal temperature reached 350°C. At about this time the anomalous beam made its appearance. Maintaining the charcoal at 350°C the 54 volt beam decreased rapidly in intensity, vanishing entirely within a few minutes. In the meantime the intensity of the anomalous beam increased, reaching a maximum at about the time the 54 volt beam vanished, after which it too decreased and finally vanished. The gas pressure within the apparatus, as shown by ionization measurements, was perhaps 10^{-4} mm Hg at this time.

Heating was discontinued and liquid air was replaced on the charcoal. This caused the pressure to return to a very low value, but it did not bring

back either the 54 volt beam or the anomalous beam. Heating the target by electron bombardment did, however, bring back the 54 volt beam to about its maximum intensity (curve *B*, Fig. 13). At this time the anomalous beam was found to be absent. The 54 volt beam did not maintain its initial intensity but decreased rapidly, indicating that the vacuum condition of the tube as a whole had been greatly impaired by heating the charcoal. No further tests were made.

Summary of Electron Beams

Thirty sets of electron beams in all have been observed for bombarding potentials below 370 volts. Eleven of these occur in the {111}-azimuth, twelve in the {100}-azimuth and seven in the {110}-azimuth.

Twenty of the sets have been associated with twenty sets of Laue beams that would issue from the same crystal if the incident beam were x-rays.

Three sets are accounted for as "plane grating" beams which result from a preponderance of top layer scattering at angles near grazing emergence.

Six sets are attributed to scattering by adsorbed gas on the surface of the crystal, and the structure of the gas film giving rise to three of these beams has been inferred.

Some explanation has thus been given for twenty-nine of the thirty sets of beams. The remaining set occurs at $\theta = 46°$ in the {110}-azimuth for $V = 170$ volts, and is quite weak.

The explanations used in accounting for the observed beams require the occurrence of still other beams that have not been observed. The total of these missing beams is at least eight; four space lattice beams (one third order beam in the {111}-azimuth, one first order beam in the {210}-azimuth and two first order beams in the {331}-azimuth); and four "plane grating" beams (first order {210} and {331}-azimuths, and second order {111} and {100}-azimuths).

Discrepancies have also been noted between the characteristics of the third order space lattice beams in the {111}-azimuth and those of their companions in the {100}-azimuth.

The possibility of carrying through these investigations to their present stage has depended very largely upon the cooperation we have received from a number of our colleagues here in the laboratory. We are particularly indebted to Drs. H. D. Arnold and W. Wilson for the encouragement they have given us and for the benefit of their criticisms. We have had the benefit also, in technical matters, of discussions with Drs. L. W. McKeehan, K. K. Darrow and R. M. Bozorth.

We are indebted to Mr. H. T. Reeve for producing for us single nickel crystals of appropriate size—to Mr. C. J. Calbick for assistance in making the observations and for contributing not a little to their interpretation—and to Mr. G. E. Reitter for the great care with which he constructed the special apparatus and for his many contributions to its design.

Bell Telephone Laboratories, Inc.,
New York, N. Y.
August 27, 1927.

X-RAY K ABSORPTION IN ELEMENTS W(74) TO U(92), AND K SCREENING NUMBERS

By J. E. Mack and J. M. Cork

Abstract

Values are recorded for the *K* absorption edges of elements 74, 76 to 83 inclusive, 90, and 92. Absorption is noted due apparently to the material of the slit but not to the passage of rays through the wedges formed by the jaws of the slit. An attempt is made to determine Sommerfeld's screening numbers for the *K* shell from empirical data, on the assumption that the first term screening number is a linear function of the atomic number. Since this assumption leads to negative values for the "relativistic" screening number, it is conluded that Sommerfeld's term formula does not account for all the curvature of the lines in the Moseley diagram.

I. Absorption Edge Values

THE *K* absorption edges of nearly all the elements studied in this investigation have already been measured by de Broglie,[1] Siegbahn and Jönsson,[2] and Duane, Shimizu, Fricke, and Stenstrom.[3] Since these values are somewhat in disagreement, it was considered useful to carry out this investigation, employing a spectrograph previously used in the measurement of emission wave-lengths.[4]

X-rays were allowed to fall on the crystal on each side of the axis in succession, giving an absorption edge toward each end of the photographic plate; so that the distance between edges, together with the distance between the slit and the plate, gave the angle of deviation without reference to any other point on the plate. In the case of a few plates reference was made to the tungsten $K\alpha$ line, whose position (208.62 x-units) was assumed known. An ordinary 200,000 volt Coolidge tube with tungsten filament and target was used. The tube was run at about 170,000 volts (or somewhat less for the lower atomic numbers) and 4 milliamperes. The exposures varied from 40 to 100 milliampere hours, depending upon the screen thickness.

The samples studied were in the form of sheets of the element, except in the cases of Hg (80), where the sample consisted of a drop pressed between two pieces of glass; Th (90), where the element was powdered; and U (92), where the powdered acetate was used. The total thickness of the sample varied from about 0.1 mm for some sheets to about 1 mm for the powders. The samples were placed between the slits, or between the second slit and the plate. In some cases two elements (not of successive atomic number)

[1] M. de Broglie, J. de Physique p. 161 (May–June 1916).

[2] Siegbahn and Jönsson, Phys. Zeits. **20**, 251 (1919).

[3] Duane and Shimizu, Phys. Rev. **14**, 522 (1918); Duane, Fricke, and Stenstrom, Nat. Acad. Sci. Proc. **6**, 607 (1920).

[4] J. M. Cork, Phys. Rev. **25**, 197 (1925); and Stephenson and Cork, Phys. Rev. **27**, 138 (1926).

were photographed simultaneously. All the spectra were of the first order. Exposures and measurements were made at approximately a uniform temperature of 22°C.

For finite slit width an edge on a plate is not sharp; the change in blackening takes place throughout a region, if there is no overexposure. In this investigation the measurements were made to the center of this region. For the spectrograph used, this gave directly the distance between the ideal edges.

The order of magnitude of the probable error in λ is estimated to be $\pm.00010$A; giving for ν/R, from ± 3 for W (74) to ± 8 for U (92), and for $(\nu/R)^{1/2}$, from ± 0.02 for W (74) to ± 0.05 for U (92).

Table I gives the values obtained for the wave-lengths of the absorption edges, together with the frequencies ν/R and their square roots. The wave-lengths recorded by the other investigators are reprinted for convenience. All the values recorded were obtained photographically except those of Duane and his collaborators, who used the ionization method. Their wave-length values, moreover, are averages from several orders, so that they must be slightly increased in order to be comparable with all the other values, which are for first order only and are not corrected for refraction in the crystal.

TABLE I

K absorption edges. Constants used: log $2D=0.78235$[8] for calcite at 22°; log $R=0.040353$.

Z	λ(Angstroms) de B[1] (phot.)	S., J.[2] (phot.)	D. F. S. S.[3] (ion.)	present (phot.)	ν/R present	$(\nu/R)^{1/2}$ present
74 W			.1781	.17822	5113	71.51
76 Os			.1683	.16755	5439	73.75
77 Ir				.16209	5622	74.98
78 Pt	.152	.1578	.1581	.15770	5778	76.02
79 Au	.149	.1524	.1534	.15320	5948	77.12
80 Hg	.146	.1479	.1491	.14893	6119	78.22
81 Tl	.142	.1427	.1448	.14441	6310	79.44
82 Pb	.138	.1385	.1410	.14049	6486	80.54
83 Bi	.133	.1346	.1372	.13678	6678	81.62
90 Th		.1127	.1131	.11270	8085	89.92
92 U		.1048	.1075	.10658	8550	92.46

II. Absorption Due to Slit Material

On almost every plate there appeared absorption edges characteristic of the material of the slit faces in the second (i.e., the fine) slit. Thus for lead slits the K edge of lead was obtained and in fact the radiation was so much reduced on the short wave-length side of the edge that it was found difficult to obtain the K edge of the next heavier element, bismuth. In this case platinum faced slits were employed. Other materials used on the slit faces were tungsten and tantalum, each of which gave its characteristic edge. The effect was not observable for long wave-length x-rays in such cases as with the iron slits in the Siegbahn vacuum spectrograph.

[8] Siegbahn, "The Spectroscopy of X-Rays" (1925) § 19.

An obvious hypothesis for the explanation of this phenomenon would be that the penetration of the short wave-length x-rays into the material of the wedges forming the jaws of the slit, makes the slit effectively wider for these rays. In order to eliminate the effect, then, new slits were made of thick lead plates, with faces parallel and shaped at such an angle as to reduce to a negligible amount the possible penetration of rays falling on the photographic plate in the neighborhood of the lead edge. But the effect was not materially diminished.

If the above penetration hypothesis were correct, the absorption edge due to the material of the slit would appear on the plate displaced toward long wave-lengths with respect to an edge due to a sheet of material traversed by all the x-rays passing through the slit. Moreover, for a slit .15 mm thick, the additional transmission would be such a small part of the total that only a slight decrease in blackening would be expected on the short wave-length side of the edge.

Faced by the dilemma offered by the occurrence of absorption due to the material of the jaws of the slit but apparently not to penetration of this material by the rays, we must consider a second possibility: namely, that for this short wave-length radiation the jaws of the slit possess an effective range of absorption extending somewhat beyond their boundaries. While on its face improbable, it is not inconceivable that such an effect might occur due to a possible appreciable cross-section possessed by the quanta of hard x-rays. Such a property might play a part in other phenomena, such as the reduction of intensity of x-rays at angles close to grazing angles of emergence from the target face of an x-ray tube.

III. The K Screening Numbers

The investigations of Sommerfeld and Wentzel[6,7] have shown that the x-ray term values may be represented by the following infinite series in powers of α, where $\alpha = 2\pi e^2/hc$:

$$\frac{\nu}{R} = \frac{[Z-s(Z,n,k_1)]^2}{n^2} + \alpha^2 \frac{[Z-d(n,k_1)]^4}{n^4}\left(\frac{n}{k_2} - \frac{3}{4}\right) + \cdots \qquad (1)$$

$$+ \alpha^{2p}[Z-d]^{2(p+1)} f_{2p}(n,k_2) + \cdots\cdots .$$

Here Z denotes the atomic number, n the total quantum number (equal to 1 for the K shell, 2 for the L shell, etc.) and k_1, k_2 the two quantum numbers characteristic of the sublevels of a shell. An irregular or screening doublet is formed by two levels with the same n and the same k_2 but different k_1, and a regular or relativistic doublet by two levels with the same n and the same k_1 but different k_2. The first-term screening number s and the relativistic screening number d are functions which must be obtained empirically. In general, one may determine s and d for all the levels within a shell by making use of certain regularities[6] in the doublet differences. In the K shell,

[6] Sommerfeld and Wentzel, Zeits. f. Physik **7**, 86 (1921).

[7] Wentzel, Zeits. f. Physik **16**, 46 (1923).

however, there are of course no doublets, and it may easily be seen that for the observed K terms (i.e., K absorption edges) of any number of elements, the number of unknowns, $s(Z)$ and d, is always greater by one than the number of available Eqs. (1).

In an attempt to overcome this difficulty, the following graphical method suggested by Dr. O. Laporte is used here: For several arbitrary values of d as a parameter, s is plotted as a function of Z; and *that value of d is considered most probable, for which s(Z) is most nearly linear with Z, at least for the higher values of Z.* The validity of the remainder of this discussion rests upon this single assumption. Its plausibility is made clear by a glance at the curves $s(Z)$ for the other shells, as plotted in Sommerfeld's book.[8]

The s-values of successively deeper shells ($\cdots M$, L) become more nearly linear with Z as the outer disturbing effect of the addition of electrons

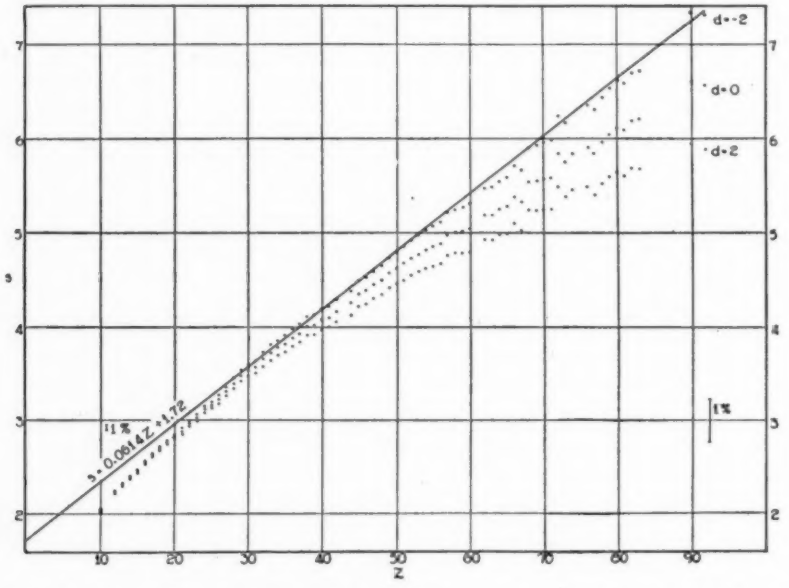

Fig. 1. The first-term K screening number s plotted against atomic number Z for the parametric values $d=-2, 0, 2$, assigned to the relativistic K screening number d.

belonging to different sub-groups diminishes; for instance, only a slight change of slope is noticed in the two curves for the L shell in the neighborhood of the rare earths. Sommerfeld inserts the K screening number as a dotted straight line.

Surface influences might be expected to cause the curve for the K shell to depart appreciably from linearity for the lowest values of Z and even for values somewhat higher than that (10 Ne) at which the L shell becomes complete.

Because of the slow convergence of Eq. (1) for the K shell ($n=k_1=k_2=1$), especially for high values of Z, it is convenient to sum the series from the

[8] Sommerfeld, "Atombau und Spektrallinien," 4. Aufl., fig. 95.

second term on, remembering that Eq. (1) was derived from Sommerfeld's relativistic term formula for hydrogen-like orbits, which in our case becomes

$$\frac{\nu}{R}=\frac{2}{\alpha^2}[1-(1-\alpha^2 Z_{eff}^2)^{1/2}]. \tag{2}$$

Here Z_{eff} stands for $Z-s$ in the first member, and for $Z-d$ in all higher members of the series expansion (1). Therefore Eq. (1) becomes

$$\frac{\nu}{R}=\frac{2}{\alpha^2}\{1-[1-\alpha^2(Z-d)^2]^{1/2}\}-(Z-d)^2+[Z-s(Z)]^2. \tag{3}$$

Now knowing ν experimentally for any element, we may insert a value for the parameter d and solve for s. The frequency ν, corrected to eliminate Sommerfeld's relativistic correction terms, has been called the "reduced frequency": $\nu_{red}=R(Z-s)^2$.

The figure shows the family of Z, s curves for $d=-2$, 0, 2. Intervals indicating the change in ordinate due to an arbitrary change of one percent in term value, are marked at abscissas 10 and 92 to show the increased sensitivity of s to small relative errors in ν, as Z increases.

The term values for $Z<74$ in the figure are from Siegbahn[9] except for the later determinations for 10 Ne (by critical potential),[10] 14 Si,[11] 28 Ni,[12] 30 Zn,[12] 36 Kr,[13] 54 X,[13] and 68 Zr.[14]

The best value for d, as the figure shows, is approximately $d=-2$, which gives for $Z>26$, $s=0.0614Z+1.72$ within about the limits of experimental error.

If we limit ourselves to easily interpretable, i.e., positive values of d, we are forced to be content with a curve somewhat downward. Thus it is to be concluded that Sommerfeld's "relativity correction" does not account for all the curvature in the Moseley diagram for the K term wherein $(\nu/R)^{1/2}$ is plotted against Z. In order that the correction account for the curvature, it would be necessary that $(\nu_{red})^{1/2}$, and consequently s, be linear with respect to Z.

Though we have conventionally used a value with six digits[5] for the calcite grating distance D, it may be noted that the probable error of 0.03 percent in D[15] may lead to uncertainty not only in the values of the energy levels themselves, but also in the shapes of such curves as are drawn in the figure. This is true especially when the energy values plotted extend over a wide relative range. A change of 0.03 percent in D would, however, have only about the same effect on the shape of our curve as a change on the order of 0.04 in d. In the present case, then, the uncertainty in D may be neglected.

[9] Siegbahn, "The Spectroscopy of X-Rays" § 26.
[10] Holweck, Comptes rendus, **182,** 53 (1926).
[11] Lindh, Zeits. f. Physik **31,** 210 (1925).
[12] Walter, Zeits. f. Physik **30,** 350 (1924).
[13] M. de Broglie and Lepape, Comptes rendus **176,** 1611 (1923).
[14] Martin, Roy. Soc. Victoria Proc. **35,** 2 p. 164 (1923).
[15] A. H. Compton, Beets, and DeFoe, Phys. Rev. **25,** 625 (1925).

Although recent theoretical investigations have developed expressions somewhat different from Eq. (1) for term values, the newer viewpoint has been embodied, up to the present, in no formula as satisfactory as (1), so far as agreement with observation is concerned. For this reason (1) has been used in the present discussion, as an empirical formula. Its accuracy, indeed, has been confirmed by the deduction by Heisenberg and Jordan[16] on the basis of the matrix mechanics, of an expression for the energy contributed by the spin and the relativistic variation of the mass of the electron. This deduction, which neglects higher order terms, yields in the case of x-ray terms a quantity which agrees exactly with the second term on the right hand side of Eq. (1), provided the factor Z^4 in the Heisenberg-Jordan expression be replaced by Z_{eff}^4; that is, provided the same screening be assumed to affect both the contribution due to the mass variation and that due to the spin.

DEPARTMENT OF PHYSICS,
UNIVERSITY OF MICHIGAN,
AUGUST 31, 1927.

[16] Heisenberg and Jordan, Zeits. f. Physik **37**, 263 (1926).

THE M-SERIES X-RAY ABSORPTION SPECTRA OF OSMIUM, IRIDIUM, AND PLATINUM

By R. A. Rogers

Abstract

Using a metal x-ray tube and vacuum spectrometer of the Siegbahn type, the absorption spectra of osmium (76), iridium (77), and platinum (78) have been investigated from 3.5A to 7A. Spectrograms have been obtained showing five discontinuities for osmium at 6.194A (M_1), 5.975A (M_2), 5.027A (M_3), 4.412A (M_4), and 4.037A (M_5); four for iridium at 5.961A (M_1), 5.754A (M_2), 4.851A (M_3), and 4.270A (M_4); four for platinum at 5.736A (M_1), 5.541A (M_2), 4.674A (M_3), and 3.738A (M_5). Discontinuities corresponding to an M_5 level for iridium and an M_4 level for platinum were not obtained. The results are shown to be consistent with those of other investigators for tungsten and bismuth. Comparison between experimental values of $(\nu/R)^{1/2}$ and those computed by Bohr and Coster and Sommerfeld reveals some disagreement, the probable cause for which is discussed. Two types of absorption discontinuities were found on the spectrograms—"limits" separating regions of unequal darkening and "white line" absorption. Although, for each element, the same absorbing screen was used throughout, the first two discontinuities, corresponding to M_1 and M_2, for each element appeared as "limits" while the discontinuities M_3, M_4, and M_5 appeared as "white lines." Photometric curves are shown in support of this conclusion. Attention is called to the bearing of the phenomenon on the theory of "white lines." No evidence was found of a component on the short wave-length side of M_3 as was reported by Zumstein for tungsten.

Introduction

THE extension of our knowledge of absorption limits to include the elements osmium, iridium, and platinum is especially important, aside from its value as a contribution to the field of atomic structure, in view of the disagreement with computed values of the experimentally determined limits for tungsten and of the possibility of an additional unpredicted limit, M'_3, both of which were reported by Zumstein.[1]

Osmium, iridium, and platinum were chosen principally for the following reasons: (1) their proximity to tungsten in the periodic table, (2) the need of experimental data for elements between tungsten and bismuth, and (3) the slight experimental advantages over elements of less atomic number on account of shorter wave-lengths.

It was proposed to obtain spectrograms showing as many as possible of the M-series absorption limits, to determine their variation in wave-length from predicted values, and to investigate for all limits, particularly M_3, the presence of any components near the principal discontinuity.

Experimental

A vacuum spectrograph of the Siegbahn type was used in the investigation. This apparatus, with a few improvements, was the same as that employed

[1] R. V. Zumstein, Phys. Rev. **25**, 747 (1925).

by Zumstein[1] in his investigation of tungsten. The voltage on the tube was always kept sufficiently low to exclude the possibility of any second order radiation obscuring the detail of the first order. The range of voltage supplied by the transformer was between 2000 and 5000 volts. No rectifying device was necessary as the tube was self-rectifying at these low voltages. The filament was a 15 mil tungsten wire placed about 3 mm from the copper target.

The slit was covered by a very thin membrane upon which was deposited a thin coat of carbon obtained from a kerosene flame. The membrane was made from a solution of celluloid in amyl acetate. A single droplet when allowed to fall on the surface of water formed a film from two to four inches in diameter. This was lifted and dried on a circular wire frame, then mounted over the slit with an ordinary household cement. This type of window was much thinner than the collodion and lampblack window used by Zumstein. The time of exposure for the continuous spectrum was thereby reduced from twelve hours to approximately one hour. Extreme care was required in operating the tube to prevent destruction of the window.

The absorption screens were made by dissolving compounds of the elements under investigation, soluble in ether, in a mixture of flexible collodion and ether, and then pouring on to a glass plate to dry. During exposures the screen was mounted midway between the slit and the crystal.

Absorption screens containing the pure powdered metals held in suspension in a collodion film did not give the absorption discontinuities. The explanation is apparently the following. There is an optimum thickness for the best photographic impression of the absorption limit. This optimum must be fairly general over the screen and cannot be imitated by relatively thick absorbing particles separated by spaces having no absorber. Neither of these areas give the absorption limit and hence both would not. In short, the optimum thickness is not a mean thickness but a uniform one.

The power input of the tube was approximately 1 kva. The width of the slit was 0.2 mm. The crystal used was gypsum (optical selenite). Exposures for only the continuous spectrum and emission lines required from one to three hours. For absorption photographs, continuous exposures of from one to two days were required. Imperial Eclipse Tropical plates were used throughout.

All measurements of absorption limits were made with reference to two or more known emission lines. The wave-lengths of the reference lines were taken from Siegbahn's "Spectroscopy of X-Rays."[2]

Distances on the plates were measured by a low power micrometer comparator focused on the long wave-length edge of both emission lines and absorption limits. A simple interpolation formula was used in computing the wave-length. Lack of sharpness of the edges rendered a more complicated method of determination impractical.

[2] Siegbahn, Spectroscopy of X-rays, English translation, 1925, Tables 7, 14, and 15, pages 105–125.

Results

Spectrograms were obtained showing five absorption discontinuities for osmium, four for iridium, and four for platinum. These results are given in Tables I, II, and III. The columns therein are respectively as follows:

TABLE I

Osmium M-series absorption spectrum.

Limit	Plate	Screen	Reference Lines	Wave-length	Mean
M_1	1	OsO_4	W$M\alpha$, W$M\beta$, P$K\alpha$	6.194A	
M_1	2	"	P$K\alpha$, P$K\beta$, Hg$M\alpha$	6.193	
M_1	3	"	P$K\alpha$, P$K\beta$	6.195	6.194A
M_1	4	"	P$K\alpha$, P$K\beta$, Hg$M\alpha$	6.195	
M_1	5	"	P$K\alpha$, P$K\beta$, Hg$M\alpha$	6.193	
M_2	1	"	W$M\alpha$, P$K\alpha$, W$M\beta$	5.972	
M_2	2	"	P$K\alpha$, P$K\beta$, Hg$M\alpha$	5.976	5.975
M_2	3	"	P$K\alpha$, P$K\beta$, Hg$M\alpha$	5.976	
M_2	4	"	P$K\alpha$, P$K\beta$, Hg$M\alpha$	5.977	
M_3	1	"	Pb$M\alpha$, Pb$M\beta$, SK_A	5.027	
M_3	2	"	SK_A	5.025	
M_3	3	"	Pb$M\beta$, SK_A	5.029	
M_3	4	"	Pb$M\beta$, SK_A	5.028	5.027
M_3	5	"	Bi$M\alpha$, Bi$M\beta$, SK_A		
			Bi$M\gamma$, S$K\alpha$	5.026	
M_3	6	"	S$K\alpha$, Pb$M\alpha$, Pb$M\beta$, Bi$M\alpha$	5.026	
M_3	7	"	Pb$M\alpha$, Pb$M\beta$, Bi$M\alpha$,		
			Bi$M\beta$, Cl$K\alpha$, SK_A	5.027	
M_4	1	"	Ag$L\alpha$, Ag$L\beta$	4.412	
M_4	2	"	Ag$L\alpha$, Ag$L\beta$	4.411	4.412
M_4	3	"	Ag$L\alpha$, Ag$L\beta$	4.414	
M_5	1	"	Ag$L\alpha$, Ag$L\beta$	4.035	
M_5	2	"	Ag$L\alpha$, Ag$L\beta$	4.039	4.037
M_5	3	"	Ag$L\alpha$, Ag$L\beta$	4.038	

TABLE II

Iridium M-series absorption spectrum.

Limit	Plate	Screen	Reference Lines	Wave-length	Mean
M_1	1	$IrCl_3$	P$K\alpha$, P$K\beta$	5.965A	
M_1	2	"	P$K\alpha$, P$K\beta$, Hg$M\alpha$	5.961	5.961A
M_1	3	"	P$K\alpha$, Hg$M\alpha$	5.958	
M_2	1	"	P$K\alpha$, P$K\beta$	5.750	
M_2	2	"	P$K\alpha$, P$K\beta$, Hg$M\alpha$	5.753	5.754
M_2	3	"	P$K\alpha$, Hg$M\alpha$	5.760	
M_3	1	"	S$K\alpha$, Pb$M\alpha$, Pb$M\beta$, Cl$K\alpha$	4.849	
M_3	2	"	S$K\alpha$, Pb$M\alpha$, Pb$M\beta$, SK_A, ClK_α	4.850	
M_3	3	"	S$K\alpha$, Pb$M\alpha$, Bi$M\alpha$, Pb$M\beta$, SK_A	4.851	4.851
M_3	4	"	Pb$M\alpha$, Bi$M\alpha$, Pb$M\beta$, Bi$M\beta$, SK_A	4.853	
M_4	1	"	Cd$L\alpha$, Cd$L\beta$	4.275	4.270
M_4	2	"	Cd$L\alpha$, Cd$L\beta$	4.265	

TABLE III

Platinum M-series absorption spectrum.

Limit	Plate	Screen	Reference Lines	Wave-length	Mean
M_1	1	$PtCl_4$	P$K\alpha$, Hg$M\alpha$, P$K\beta$	5.738A	
M_1	2	"	P$K\alpha$, Hg$M\alpha$	5.738	5.736A
M_1	3	"	P$K\alpha$, P$K\beta$, Hg$M\alpha$	5.733	
M_1	4	"	P$K\alpha$, P$K\beta$, Hg$M\alpha$	5.734	
M_2	1	"	P$K\alpha$, Hg$M\alpha$	5.544	
M_2	2	"	P$K\alpha$, P$K\beta$, Hg$M\alpha$	5.534	5.541
M_2	3	"	P$K\alpha$, P$K\beta$, Hg$M\alpha$	5.545	
M_3	1	"	Bi$M\alpha$, SK_A, Bi$M\beta$, Bi$M\gamma$	4.673	
M_3	2	"	Bi$M\alpha$, Bi$M\beta$, Bi$M\gamma$, SK_A	4.674	
M_3	3	"	Bi$M\alpha$, Pb$M\beta$, Bi$M\gamma$, Bi$M\beta$, Cl$K\alpha$	4.675	4.674
M_3	4	"	Bi$M\alpha$, Bi$M\beta$, Pb$M\beta$, SK_A, Bi$M\gamma$, ClK_A	4.676	
M_5	1	"	Ag$L\alpha$, Ag$L\beta$	3.738	3.738
M_5	2	"	Ag$L\alpha$, Ag$L\beta$	3.739	

first, the symbols of the discontinuities, M_1, M_2, M_3, M_4, and M_5 in the order of decreasing wave-length; second, the plate number; third, the compound used in preparing the absorption screen; fourth, the reference lines used in measuring the wave-length of each absorption limit; fifth, the average results for each plate, obtained from repeated measurements, of the wave-length of the absorption limit; sixth, the mean value for each discontinuity of the wave-length of all the plates measured.

The wave-lengths of all reference lines used in the computations are contained in the following table:

TABLE IV

Wave-lengths of reference lines.

W$M\alpha$	6.973A	Pb$M\alpha$	5.2751A	S$K\alpha$	5.3613A
W$M\beta$	6.745	Pb$M\beta$	5.0648	Cl$K\alpha$	4.7182
P$K\alpha$	6.1417	SK_A	4.988	Ag$L\alpha$	4.1456
P$K\beta$	5.789	Bi$M\alpha$	5.1072	Ag$L\beta$	3.9266
Hg$M\alpha$	5.649	Bi$M\beta$	4.8993	Cd$L\alpha$	3.9478
Hg$M\beta$	5.439	Bi$M\gamma$	4.5238	Cd$L\beta$	3.7300

DISCUSSION OF RESULTS

The limitations of the accuracy of the experimental results were determined by the accuracy of the wave-lengths of the emission lines used for reference, by the distance on the plate over which interpolation was made, but mainly by the accuracy with which one is able to focus the cross-hair of the comparator on the edge of the absorption discontinuity.

The first of these may be summarily dismissed since only well established and precisely measured emission lines were used as reference. In the event of any revision of the reference lines, adjustment of the wave-length of the absorption discontinuities can easily be made.

An attempt was always made to choose such lines for reference as would keep the distances on the plate over which interpolation was made well within one centimeter. A check on the inaccuracies due to this cause was made on emission lines. They were found to be insignificant compared to the following source of inaccuracy.

In those cases where the absorption discontinuities were fairly weak or not extremely sharp, some difficulty was experienced in focusing the cross-hair exactly on the edge of the discontinuity. Repeated measurements over many plates on known emission lines and absorption edges together with the agreement obtained from repeated measurements on the absorption discontinuities of the present investigation determined the possible accuracy (0.005A) which is claimed for the results. This represents accuracy to approximately one-tenth of one percent.

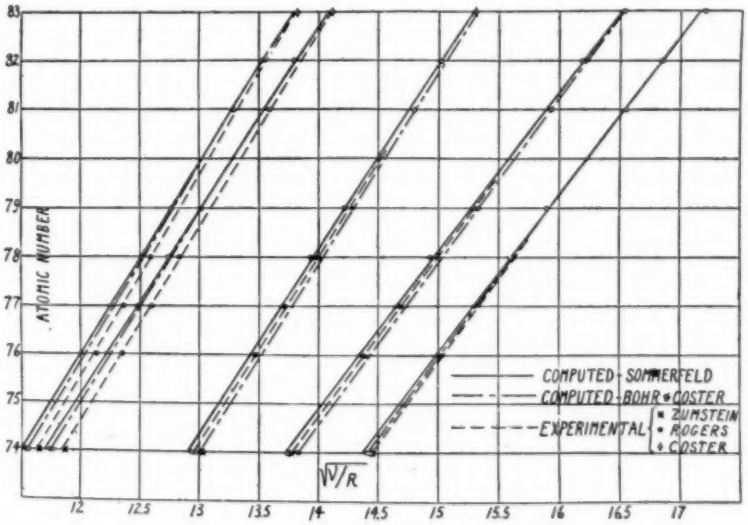

Fig. 1. Relation between the present experimental results and those for tungsten and bismuth.

It is recognized that chemical combination may have some influence on the value of the absorption discontinuities. The valences of the elements in the compounds used in the absorbing screens were: osmium eight, iridium three, and platinum four. To be sure, there is a possibility of reduction of the compounds by the x-ray beam. Investigation of possible chemical effects on the *M* levels in one of these elements is under investigation at the present time in this laboratory.

In Fig. 1 above are shown graphically the relation of the present experimental results to the corresponding measurements for tungsten[1] and for bismuth[3]; also their relation to the computed values for the *M* levels as given by Bohr and Coster[4] and Sommerfeld.[5]

[3] D. Coster, Phys. Rev. **19**, 22 (1922).
[4] N. Bohr and D. Coster, Zeits. f. Physik **12**, 347 (1923).
[5] A. Sommerfeld, Atombau etc., 4th Edition, p. 304–305.

With atomic number as ordinates and $(\nu/R)^{1/2}$ as abscissas, the maximum deviation from a linear relationship between the various experimental results was approximately five volts. One may therefore conclude that the linear relation in this region is thereby established. This shows excellent agreement between the present results and those of the other investigators whose values are shown on the curve above, and adds credence to the belief in the reliability of the experimental determinations.

In making comparison of the experimental values of $(\nu/R)^{1/2}$ with the computed values, it must be recalled that the computations of Bohr and Coster[4] and of Sommerfeld[5] necessarily assume one or more absorption discontinuities whence, by the principle of combination of emission lines and absorption discontinuities, other levels are calculated. For the elements here represented the L_1 level has, with one exception, been used as the absorption limit on which the computations are based. The literature is not clear as to the specific measurements used by Bohr and Coster and Sommerfeld in making the computations. However, it has generally been possible, by reversing the computation process, to identify the emission lines and absorption limits, their wave-lengths, and observer. For bismuth, the M_1, M_2, and M_3 values contained in both tables are Coster's experimental values. From them the values for M_4 and M_5 of bismuth have been computed.

A very small error in the wave-length of the L_1 limit produces a relatively large error in the computed M levels. Assuming the same percent of error in the L_1 measurements as has been allowed for the M levels, the error thereby introduced in the computed M levels is between four and five times that in the direct experimental measurements. Furthermore, this takes into account no error whatsoever in the case of the L and M emission lines used in connection with the absorption limit for computing the M levels. Granting the probability of more exact measurement of emission lines than of absorption limits, yet the same relative error in the shorter wave-length emission lines as in our reference lines would introduce more error in the computed than in the directly measured results. The direct measurements are believed reliable to the accuracy stated. For these reasons, therefore, the experimental values of the M levels should be considered much more nearly correct than the computed ones.

The results seem quite definitely to offer at least partial evidence of a systematic error in the L_1 levels. However, there also seems to be shown an increasing accuracy in the L_1 levels with increasing atomic number. This cannot be accounted for as yet. Neither can all measurements and computations be completely reconciled. One possible explanation of a portion of the discrepancies may lie in the fact that compounds and not free metal atoms were used in the absorbing screens.

Two types of absorption discontinuities were found on the spectrograms—"white line" absorption and "limits" separating regions of unequal darkening.

M_1 and M_2, the former in particular, appeared as limits. The M_1 limit appeared less sharp than M_2 but much more pronounced probably because

the M_1 absorption continues with little diminution over the region where the M_2 absorption occurs.

On the other hand, M_3, M_4, and M_5 so far as here measured were distinctly of the "line" type for each of the elements. The short wave-length edge was very nearly if not exactly as sharp as the long wave-length edge. Five of the seven absorptions obtained among these levels gave conclusive evidence of this fact. The other two were too faint to warrant definite conclusion.

In order to investigate the reliability of the conclusion regarding the appearance of the M_3, M_4, and M_5 absorptions as "line" absorptions, photometric curves were made of some of the best plates of which a representative collection is shown in Fig. 2.

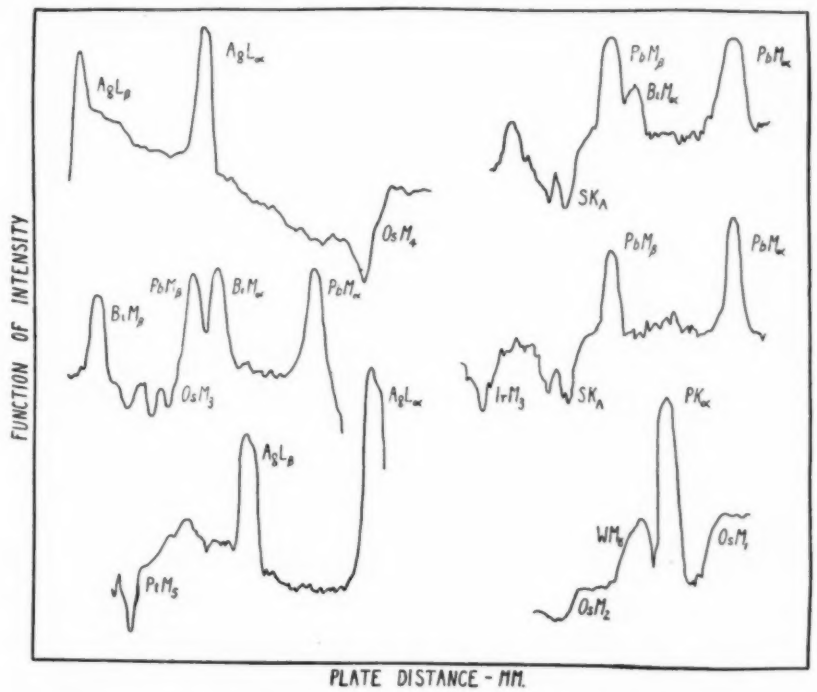

Fig. 2. Photometric curves showing the M_3, M_4, and M_5 absorptions.

Each of these curves represents the graphical average of three separate curves taken from different places on the plates. For purposes of comparison, one curve is given of the K-absorption due to sulphur in the crystal showing the "white line" absorption on the long wave-length side. For contrast, one curve is shown of osmium M_1 and M_2 which are distinctly of the "limit" type.

Because of the fact that the microphotometer available did not have particularly high resolving power, the edges of some of the absorptions and emission lines as well were not particularly sharp, so much so in fact that measurements on the wave-length from these photometric curves were not considered reliable. The conclusion regarding "line" absorptions, however, was fully substantiated.

The experimental verification of the existence of "white lines" is a matter of no little importance. Attention should be called to the fact that there must be a significant fundamental difference between "limits" and "white lines" in that the outer levels M_1 and M_2 are the former while the inner levels M_3, M_4, and M_5 are the latter. This fact must have some bearing on the theory of "white lines." Evidently the law of absorption for M_3, M_4, and M_5 is different from that for M_1 and M_2.

The failure of the earlier work on x-ray absorption spectra to show absorption lines (Fraunhofer lines) was explained upon the consideration that an electron cannot jump from an inner level to a level farther away from the nucleus since, in general, there is no vacant place to which it may go. Kossel, however, pointed out that this explanation should not apply to the peripheral levels. Subsequently, many cases have been mentioned in which continuous x-ray spectra have shown white lines.

In response to the report of Coster[6] on the complicated structure of the K-absorption edges of titanium, vanadium, chromium, and manganese and the L_{III} absorption edges of tin, antimony, tellurium, and iodine, Miss Chamberlain[7] offered the explanation, supported by experimental investigation, that the white line found on the long wave-length side of the absorption edge for the more highly oxidized compound was due to reduction of a portion of the compound to the free metal.

The presence in this investigation of absorption "lines" for some of the levels and of "limits" for other levels of the same series while, for each element, the same absorbing screen was used for all five levels has not found a satisfactory explanation.

The absence of IrM_5 and PtM_4 should not be interpreted as evidence of their non-existence; particularly so since IrM_4 and PtM_5 were obtained. It must be recalled that the only emission lines which are attributed to transitions involving the M_5 level are the l and η lines of the L-series, both of which are weak. The M_4 level is involved in transitions yielding L_{β_4} and one component of K_{β_1}. While it, too, is expected to be fairly weak yet it should be obtainable. For all the M_4 and M_5 discontinuities, experimental conditions, particularly in regard to the thickness of the absorbing screen, are very critical. It is therefore very difficult to obtain them.

No evidence was found of a component near any of the principal absorption discontinuities.

In conclusion, the writer wishes to express his appreciation to the members of the staff of the Department of Physics of the State University of Iowa for their interest and assistance, and especially to Professor G. W. Stewart who suggested the problem and under whose direction the work has been carried on.

PHYSICS LABORATORY,
UNIVERSITY OF IOWA,
JUNE 10, 1927.

[6] D. Coster, Zeits. f. Physik (July 2, 1924).
[7] K. Chamberlain, Phys. Rev. 26, p. 525 (1925).

FURTHER EXPERIMENTAL TESTS OF THEORIES OF THE ABSORPTION OF X-RAYS

By F. K. Richtmyer*

Abstract

When a beam of x-rays passes through a slab of absorbing material photo-electrons are in general expelled from all levels. If the beam is (1) monochromatic and (2) of wave-length shorter than the K absorption limit of the absorber, the ratio, R_L^K, of the number of photoelectrons coming from (K, L, $M \cdots$) levels to the number coming from (L, $M \cdots$) levels is given by the maximum value τ_{max} reached by the atomic absorption coefficient as the limit is approached from the short wave-length side to the minimum value τ_{min} reached as the limit is approached from the long wave-length side. Because of absence of data on scattering coefficients it is impossible to obtain accurate experimental values of R_L^K for purposes of comparing with experiment the theories of x-ray absorption proposed by Thomson, Compton, de Broglie and Kramers. A careful repetition of the measurements previously reported (Phys. Rev. **27**, 1 (1926) shows that, after making any reasonable assumption as to the magnitude of scattering coefficients, the experimental values of R_L^K are more nearly in agreement with Kramers' theory, excepting for a small observed variation of R_L^K with λ. However the absolute magnitude of the absorption discontinuity, i. e. $\tau_{max} - \tau_{min}$, is given very closely by de Broglie's theory.

Mass absorption coefficient of Sn in the wave-length range $\lambda_K/2 < \lambda < \lambda_K$. A brief report is also made of some preliminary measurements of a redetermination of the variation of absorption with wave-length in which it is hoped to attain considerably higher precision than previously reported. It is shown that in the wave-length range $\lambda_K/2 < \lambda < \lambda_K$ the observed values of mass absorption coefficient of Sn is a linear function of λ^3 and that the exponent of λ cannot differ from 3 by as much as 1 percent. There is no suggestion of a deviation from the λ^3 law as the absorption limit is approached from either side.

I. The Magnitude of the K Absorption Discontinuity

In a previous communication the writer[1] presented a critique, from the standpoint of experimental data, of the theories of the absorption of x-rays proposed, respectively, by J. J. Thomson,[2] A. H. Compton,[3] de Broglie,[4] and Kramers,[5] with particular reference to the magnitude of the K absorption discontinuity which these several theories predict. It was shown that the magnitude of this discontinuity, designated in the previous paper by

* The writer acknowledges with sincere appreciation his indebtedness to the Heckscher Research Council of Cornell University for the financial assistance which made these measurements possible. He also wishes to express his thanks to the Research Laboratory of the General Electric Company for the loan of certain important pieces of apparatus.

[1] Richtmyer, Phys. Rev. **27**, 1 (1926).

[2] Thomson, Conduction of Electricity through Gases, 2d ed., p. 321.

[3] A. H. Compton, Nat. Res. Council, Bul. **20**, 37 (1922).

[4] L. de Broglie, Journ. de Phys. et Rad. **3**, 33 (1922).

[5] Kramers, Phil. Mag. **46**, 836 (1923).

R_L^K,* as observed experimentally, is more nearly in agreement with Kramers' theory. Kramers' theory however predicts no variation of R_L^K with atomic number, whereas, experimentally, R_L^K *increases* with *decreasing* atomic number. The theories of Compton and de Broglie are in qualitative agreement with this latter experimental fact, but these theories predict a much larger variation of R_L^K with atomic number than is actually observed.

The advent of the Schrödinger wave theory has inspired new theories of the absorption of x-rays, by Wentzel[6] and Oppenheimer.[7] These later theories differ from the four earlier ones in that, while the latter agree with each other in giving the well known λ^3 law, the former yield more complicated relations for the variation of τ with λ ($\tau \equiv$ the atomic "fluorescent" absorption coefficient).

Any successful attempt to decide which, *if any*, of these six theories is correct must be based upon much more precise measurements of absorption coefficients, and *scattering coefficients*, than any yet reported by any investigator. I say *scattering coefficients*, since whereas theories give the true atomic absorption coefficient τ, experiment yields the *total* atomic absorption coefficient μ, which includes scattering; i.e., $\mu = \tau + \sigma$ where σ is the scattering coefficient. There are *theories* to predictt the value of σ as a function of λ, but there are no reliable *measurements*. To be sure, σ is, at least for the heavier elements and for not too short wave-lengths, small compared to τ. But σ, and its (probable) variation with λ cannot be neglected when, for example, one attempts to decide between the $\lambda^{2.92}$ law proposed (experimentally) by Allen[8] and the λ^3 law, proposed by the first four theories above mentioned, for the variation of absorption with wave-length.

Further, the values of R_L^K determined by the writer[1] and others are rendered ambiguous by the uncertainty of the value of σ at the wave-length λ_K. Various values of R_L^K can be obtained from the experimental data, depending on which particular theory of the variation of σ with λ is used. In the computation of R_L^K in the previous paper, it was assumed (1) that σ does not vary with λ and (2) that the value of σ is given, *to a first approximation*, by the intercept on the τ/ρ axis of the curve plotted between τ/ρ and λ^3. Assumption (1) is in agreement with the classical (Thomson's) theory of scattering, but assumption (2) differs from Thomson's theory in that the value of σ is determined from experiment.

On the hypothesis that the (true) absorption of x-rays is a quantum, photo-electric process, the ratio R_L^K gives the ratio of the number of $(K+L+M+\cdots)$ photo-electrons to the number of $(L+M+\cdots)$ photo-electrons emitted by an absorber when radiated by x-rays shorter than, but near to,

* R_L^K is defined as the ratio of the magnitude of the *true* atomic absorption coefficient τ_{max} on the short wave-length side of, but infinitely near to, the K absorption discontinuity, to the value of this coefficient τ_{min} on the long wave-length side of, but infinitely near to, that discontinuity.

[6] Wentzel, Zeits. f. Physik **38**, 518 (1926).

[7] Oppenheimer, Zeits. f. Physik **41**, 268 (1927).

[8] Allen, Phys. Rev. **24**, 1 (1924).

its K limit. The determination of this ratio is therefore a matter of considerable importance in connection with any theory of radiation and its interaction with matter.

As pointed out above, a precise determination of this ratio R_L^K is impossible until reliable data on scattering coefficients are available. Nevertheless, it seemed not undesirable to proceed as far as possible in obtaining precise data on the *absolute* magnitude of the K absorption discontinuity for several elements.

The method of measurement was similar to that previously described and involved nothing essentially novel, other than the precautions to reach maximum precision. Among these may be mentioned the following: (1) Measurements on a given element were made on one sample only in order to eliminate possible differences in samples. (2) The a.c. generator for supplying power was run from a *regulated* d.c. supply, but to secure still greater constancy manual regulation was used to supplement the automatic regulation. In this way the potential supplied to the x-ray tube, and also the current through the tube, were maintained constant to about 0.05 percent. (3) Read's "balance" method,[9] slightly modified, was used for measuring x-ray intensities. This method is particularly advantageous for making accurate measurements of ionization currents which cover a wide range of magnitudes since the electrometer is used as a zero instrument. Relative *rates of drift* of an electrometer, as frequently used, are not dependable unless the rates of drift which are compared are all of the same *order* of magnitude. Read's balance method, however, is quite independent of this source of error.

It has been shown by the writer[10] that, after correcting for the finite width of the spectrometer slits, (1) the width of the K absorption discontinuity of Mo, As and elements of the higher atomic number is zero within the limits of error of measurement; and (2) there is no deviation from the λ^3 law in the immediate neighborhood of the discontinuity. To measure the absolute magnitude of the discontinuity, it is only necessary therefore to obtain values of the absorption coefficient for a short range of wave-lengths on both sides of the K limit, plot the absorption coefficient as a function of λ^3, and project the curves from each side up to λ_K^3, as is shown in Fig. 1, which gives the absorption discontinuity for tin.* (The ordinates are mass absorption coefficients, μ/ρ, in c.g.s. units. The abscissas are the cubes of the wave-length in angstroms.) The two graphs, one on each side of the limit, are straight lines *with no suggestion of a deviation from linearity*

[9] H. S. Read, Phys. Rev. **28**, 898 (1926).

[10] Richtmyer, Phys. Rev. **26**, 724 (1925). See also Richtmyer and Bishop, Phys. Rev. **27**, 794 (1926).

* Parenthetically, this method yields a very precise determination for λ_K. Points a and b, which mark the *apparent* beginning of the discontinuity can be easily located with relatively high accuracy. The writer has shown (reference [10]) that the *observed* width of the discontinuity is exactly equal to the slit width. The wave-length of the discontinuity, therefore, is exactly half way between the wave-length corresponding to point a and that corresponding to point b.

as the limit is approached. Projecting these straight lines to the line λ_K^3 one finds that μ/ρ_{max} is 46.6; and μ/ρ_{min} is 7.98.

In this way the maximum and minimum values of μ/ρ at λ_K were determined for Mo, Ag, Sn and Au, as shown in the columns two and three of Table I.

To obtain the ratio R_L^K it is necessary first to subtract from the observed maximum and minimum values of μ/ρ the value of the mass scattering

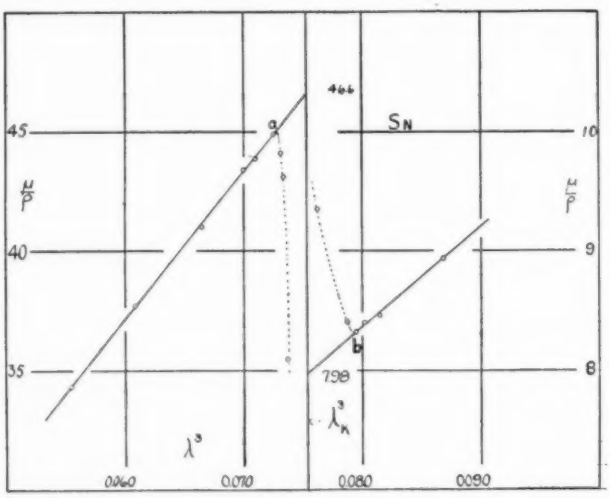

Fig. 1. The mass absorption coefficients of Sn in the neighborhood of the K absorption limit.

coefficient, σ/ρ, for the element concerned at its λ_K. These values of σ/ρ are unknown. They probably lie somewhere between 0.2 which is the value of σ/ρ given by Thomson's classical theory of scattering and, say, 1.0. Taking σ/ρ in turn as 0.0, 0.2 or 1.0, the values of R_L^K are given in columns four, five and six of the Table I. For comparison, the values of R_L^K as given

TABLE I

Observed and computed values of R_L^K.

Element	μ/ρ at K limit max.	min.	R_K^L observed $\sigma/\rho=0$	$=0.2$	$=1.0$	R_K^L calculated Kramers	de Broglie
Mo 42	81.2	12.4	6.55	6.63	7.02	5.5	14.4
Ag 47	54.7	9.08	6.05	6.12	6.65	5.5	13.3
Sn 50	46.6	7.98	5.86	5.98	6.56	5.5	12.4
Au 79	8.15	2.1	3.9	4.2	6.5	5.5	8.2

by the theories* of Kramers and of de Broglie are shown in the last two columns of the table. In any reasonable assumption for the value of σ/ρ, Kramers' theory is more nearly in *numerical* agreement with the observed values of R_L^K than is that of de Broglie.

* The theories of Thomson and of Compton give the same values of R_L^K as does de Broglie's theory. For further details see reference 1.

The situation is somewhat different, however, as regards the absolute magnitude of the discontinuity, i.e., the difference between columns two and three of the table. This difference (1) gives that part of the absorption due to the K electrons; and (2) is determined by experiment quite independently of scattering. An unambiguous comparison with theory is therefore possible. Fig. 2 shows such a comparison. The ordinates, τ_K, are the magnitudes of

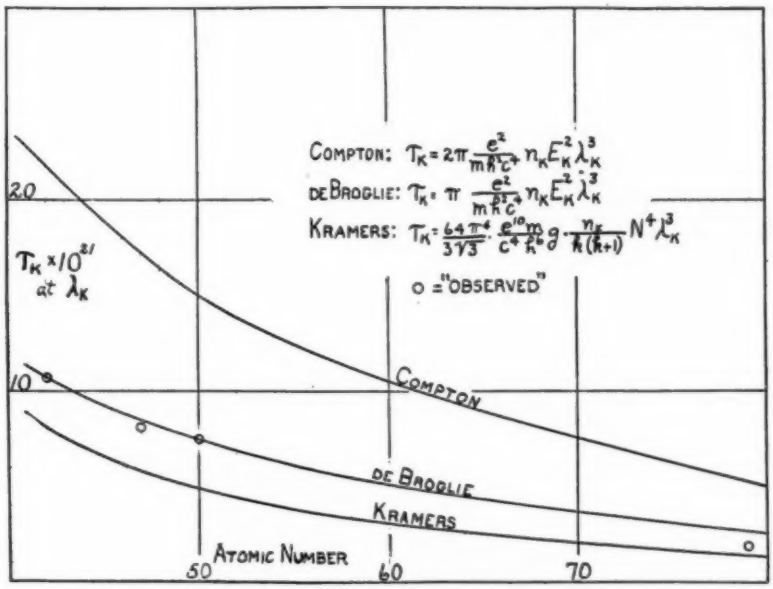

Fig. 2. The atomic absorption coefficients due to the K electrons, τ^K as a function of atomic number: Comparison of experiment with theory.

the discontinuities reduced to atomic (instead of mass) absorption coefficients. The full lines give the predictions of Compton, de Broglie and Kramers respectively. The circles give the observations, which are seen to be in excellent agreement with de Broglie's theory.

II. The λ^3 Law

It was pointed out by the writer[11] that the λ^3 law is only a close approximation to the truth; that if measurements of μ/ρ made for various wave-lengths far below the K limit be extrapolated to the K limit, the values of μ/ρ predicted by such extrapolation are somewhat larger than the observed values. Accordingly Allen[8] has proposed that n, the coefficient of λ, is 2.92, instead of 3.00 in the experimental formula

$$\mu/\rho = k\lambda^n + \sigma/\rho$$

In view of these experimental facts which show a slight departure from the λ^3 law, and of the theories of Wentzel[6] and of Oppenheimer[7] above mentioned, it seems desirable, with the improved technique now available, to make a

[11] Richtmyer, Phys. Rev. **18**, 13 (1921).

complete redetermination of absorption coefficients. The writer has started such a redetermination, with the hope of attaining a precision of 0.2 percent, or better if possible. It is not difficult to make measurements of absorption coefficients with a precision of the order of 1 or 2 percent; but to increase the precision several fold is quite another matter. A coming interruption of many months seems to make it desirable to report briefly some preliminary measurements on Sn covering the wave-length range $0.19 < \lambda < 0.42$A. These measurements are shown graphically in the curve *abc*, Fig. 3, in which μ/ρ is plotted as a function of λ^3. *Over the range bc the graph is seen to be a straight line within the limits of error of measurement.* Point *c* is very close to the *K* discontinuity. The writer is not prepared to state, without further investigation, that the part of the curve indicated by the dotted line *ab* makes a sharp break at *b* with the line *bc*. It is certain, however, that an extrapolation of the line *bc* toward shorter wave-lengths gives values of μ/ρ higher than

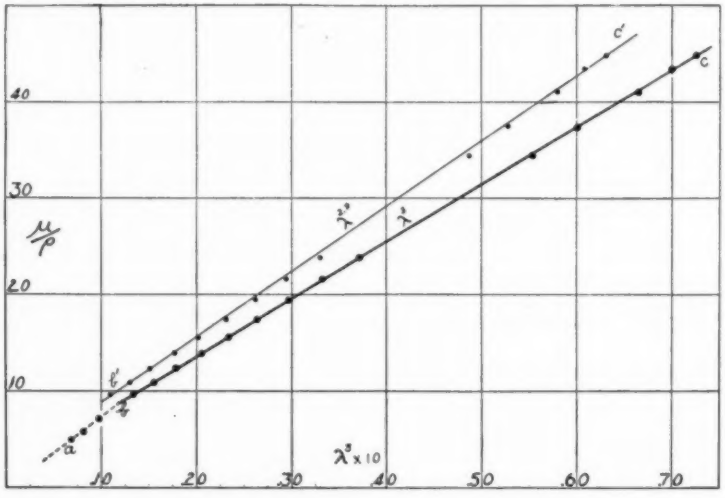

Fig. 3. The absorption coefficients of Sn in the range $\lambda_K/2 < \lambda < \lambda_K$.

observed by amounts much above the limits of precision. Incidentally, the *same* sample of tin was used for all these measurements; so that the apparent break at *b* in the graph *abc* is not due to the use of different samples of the absorber.

If, instead of λ^3, $\lambda^{2.9}$ is plotted as a function of μ/ρ (the $\lambda^{2.9}$ scale is not shown) the curve $b'c'$ results. This curve deviates from a straight line by amounts considerably in excess of experimental error. In other words *the experimentally observed (total) absorption coefficient of Sn in the wave-length range given approximately by* $\lambda_K/2 < \lambda < \lambda_K$ *is a linear function of* λ^3 *within experimental error.* The exponent of λ, if it does differ from 3, differs by less than one percent. *This law holds right up to the absorption limit*, as is seen by considering Figs. 1 and 3, in connection with the results reported in the paper[11] previously referred to, in which it was shown that even within the very narrow region at the absorption limit, a few thousandths of an angstrom

wide, where on account of the necessity of making observations with finite slit widths spectral regions from both sides of the limit overlap, observations taken in small steps through the limit were in complete agreement with the assumption that *there is no departure, within this narrow region, from the law of absorption which holds just outside the region*—which law is the λ^3 law.*

The writer hopes to resume these measurements in due course with improved apparatus. He wishes to take this opportunity to express his appreciation of the invaluable services of Mr. L. S. Taylor who assisted in making many of the measurements upon which this paper is based. (See abstracts of papers presented by Richtmyer and Taylor at meetings of the American Physical Society, Phys. Rev. **29**, 353, 606, 1927.)

CORNELL UNIVERSITY,
August, 1927.

* Of course, it is quite possible that if *accurate* ionization-chamber measurements could be made through an absorption limit, with sufficiently narrow slits one might find an indication of the *structure* of the limit such as has been observed in some instances by photographic means. Since, with a beam limited by two slits of equal width, the energy transmitted through the slits is proportional to the *square* of the slit width, such measurements present grave difficulties because of the low intensities involved. No such "structure" of an absorption limit has ever been observed by the writer.

ON THE SPECTRA OF GALLIUM, GERMANIUM AND INDIUM

By R. J. Lang

Abstract

The vacuum-spark spectra of gallium germanium and indium have been photographed in the ultra-violet by means of a two-meter vacuum spectrograph using a grating of 30,000 lines per inch. The known series lines of Ga III and Ge IV have been remeasured and certain new ones discovered. Term values have been recalculated. The series spectra of Ga II, Ge III, and In II have been worked out for the multiplets 4^3P-5^3S, 4^3P-4^3D, $4^3P-4^3P'$ and 4^1S-4^1P.

THE vacuum spark spectra of gallium, germanium and indium have been photographed in the ultra-violet using a two-meter vacuum spectrograph and a grating of 30,000 lines per inch ruled by Professor Wood of Johns Hopkins, which has been previously described.[1] In the case of gallium the metal of high purity was fused into a small hole in the end of an aluminum rod which was then used as the lower electrode in the spark. The upper was made of aluminum alone. Comparison plates were taken with pure Al electrodes also. The aluminum used was supplied by the Aluminum Company of America. It was found to be of exceptional purity and the author's appreciation of the kindness of the Aluminum Company is herein expressed. In the case of germanium and indium a small piece of the pure metal was used to tip each of the electrodes.

The notation adopted in this paper is the one now most generally employed, except that to save complexity in printing, the multiplicities are omitted unless needed to make the meaning clear. Thus in Ga III and Ge IV (Tables I and II) all of the terms are double and no difficulty arises. In Ga II, Ge III and In II (Tables VI, VII, X) there are triplets and single terms. Here the single terms have the multiplicity marked thus: $(4^1S–4^1P)$ while the triple terms are written without the multiplicity. To avoid any difficulty, however, both are included in Table VIII and IX.

Ga III

This spectrum was investigated by Carroll[2] who found most of the first members of the ordinary series. These have now been re-investigated and remeasured with greater accuracy, with the exception of the $4F–5G$ doublet, the values for which are quoted from Carroll's paper. The error of measurement is thought to be not greater than 0.03A in wave-length to about 1000A. Beyond this point the error is greater in some cases.

Table I gives the series lines and term values for Ga III. The second doublet of the principal series is new. Its identification rests upon the fact that an ordinary Rydberg formula applied to this pair and the pair at

[1] Lang and Smith, J.O.S.A. **12**, 523 (1926).

[2] Carroll, Phil. Trans. **A225**, 357 (1925).

1534A leads to a value for the $4S$ term which is approximately 246,000. The value of 247,790 recorded is chosen as probably more nearly correct as found by the values of $(\nu/R)^{1/2}$ for Cu I to Ge IV as shown in Table III. The doublet $4S-5P$ lies so far into the ultra-violet that the limit calculated by the Rydberg formula will be only approximate.

TABLE I

Series spectrum of Ga III.

Designation	λ(I. A. vac.)	Int.	γ	Δγ	Term values	
$4F_4-5G$	4383.09*		22815	6.2	$4S$	247790
$4F_3-5G$	4381.90*		22821		$5S$	107046
$4D_3-4F_4$	2424.47	6	41246	107	$4P_2$	180905
$4D_2-4F_3$	2418.21	5	41353		$4P_1$	182623
$4S-4P_1$	1534.51	10	65167	1718	$5P_2$	89792
$4S-4P_2$	1495.10	10	66885		$5P_1$	90315
$4P_2-5S$	1353.94	8	73858	1719	$4D_3$	103595
$4P_1-5S$	1323.15	6	75577		$4D_2$	103712
$4P_2-4D_2$	1295.45	2	77193	117		
$4P_2-4D_3$	1293.50	4	77310	1720	$4F_4$	62352
$4P_1-4D_2$	1267.21	3	78913		$4F_3$	62359
$4S-5P_1$	635.02	2	157475	523		
$4S-5P_2$	632.92	2	157998		$5G$	39538

* Wave-lengths as given by Carroll reduced to vacuum.

Taking then the values $4S$ to be 247,790 we arrive at the terms listed in Table I. Rao[3] has investigated part of the secondary spectrum of Ga III and gives the term values $5s=107{,}064$, $5p_1=87{,}046$, $5p_2=86{,}507$ and $6s=60{,}245$. These are based partly on Carroll's work, however, and cannot be considered as confirming the term values quoted in Table I. The $\Delta\nu$ value for the $5p$ terms does not check very well.

No trace of the satellite which should accompany one of the $4D$–$4F$ lines could be found. It will be very close to the main line, however, as shown by the group $4P$–$4D$.

NOTE ON INDIUM

Since the author's work on doubly-ionized indium was published[4] the $4F$–$5G$ line at 4071.4A has been resolved giving $\Delta\nu$ a value of 8.2. Since the value expected is 8.6 this may be taken as confirmation of Carroll's choice of these lines.

GE IV

This spectrum also was investigated by Carroll.[2] Table II contains the results of a remeasurement of the lines chosen by him.

[3] Rao, Phys. Soc. London Proc. **39**, 150 (1927).

[4] Lang, Proc. Nat. Acad. Sci. **13**, 341 (1927).

TABLE II

Series lines of Ge IV.

Designation	(I. A. vac.)	Int.	γ	$\Delta\gamma$	Term values	
$4D_3-4F$	1500.61	5	66640	255	$4S$	368684
$4D_2-4F$	1494.89	4	66895		$5S$	169439
$4S-4P_1$	1229.90	10	81307	2792	$4P$	284586
$4S-4P_2$	1189.07	10	84099		$4P$	287376
$4P_2-4D_2$	939.05	1	106491	253		
$4P_2-4D_3$	926.82	4	106744	2790	$4D$	177840
$4P_1-4D_2$	915.07	3	109281		$4D$	178095
$4P_2-5S$	868.44	2	115149	2786		
$4P_1-5S$	847.92	2	117935		$4F$	111200

COMPARISON OF TERM VALUES

The term values for similar configurations may be compared by plotting $(\nu/R)^{1/2}$ against atomic number for the same terms throughout the sequence Cu I, Zn II, Ga III, Ge IV. Table III gives the values of the $(\nu/R)^{1/2}$ and the differences. These differences are uniform and seem to confirm the values recorded in Tables I and II.

TABLE III

Values of $(\nu/R)^{1/2}$.

Term	Cu I	Diff.	Zn II	Diff.	Ga III	Diff.	Ge IV
$4S$	.7535	.3955	1.1490	.3531	1.5021	.3279	1.8300
$4P$	.5359	.3952	.9311	.3529	1.2840	.3263	1.6103
$4D$	.3357	.3252	.6609	.3107	.9716	.3014	1.2730
$4F$	.2504	.2513	.5017	.2521	.7538	.2512	1.0050
$5S$	.4180	.2992	.7172	.2705	.9877	.2523	1.2400
$5P$	.3432	.2848	.6280	.2749	.9029		

TABLE IV

Rydberg denominators and quantum defects.

	Ga III Term value	Ga III R. D.	Ga III q	Ge IV Term value	Ge IV R. D.	Ge IV q
$4S$	247790	1.9972	2.0228	368684	2.1858	1.8142
$5S$	107046	3.0374	1.9626	169439	3.2190	1.7810
$4P_1$	182623	2.3255	1.6745	287376	2.4718	1.5282
$4P_2$	180905	2.3365	1.6635	284586	2.4798	1.5202
$5P_1$	90319	3.3069	1.6931			
$5P_2$	89792	3.3226	1.6774			
$4D_2$	103712	3.0858	.9142	178095	3.1399	.8601
$4D_3$	103595	3.0877	.9123	177840	3.1422	.8578
$4F_3$	62359	3.9795	.0205	111200	3.9801	.0199
$4F_4$	62352	3.9800	.0200			
$5G$	39538	4.9979	.0021			

Table IV gives the term values, the Rydberg denominators (*R.D.*) and the quantum defects (q) for the various terms for Ga III and Ge IV. The term values seem to be very nearly correct on this scheme. The quantum defect becomes very small for the $4F$ terms and practically vanishes for $5G$.

Ga II and Ge III

The series spectra of Ga II and Ge III would be expected to follow those of Al II and Si III and the principal separations would have about the following values: in Ga II, $P_0P_1=950$, $P_1P_2=460$ and in Ge III, $P_0P_1=1675$, $P_1P_2=675$. Upon examining these spectra for triplets involving common separations of about these values it was found that the intervals 935 and 447 in Ga and 1640 and 763 in Ge were involved in several groups. Rao[3] also has chosen the triplet at 1800A as the first sharp triplet of Ga II in which these separations occur.

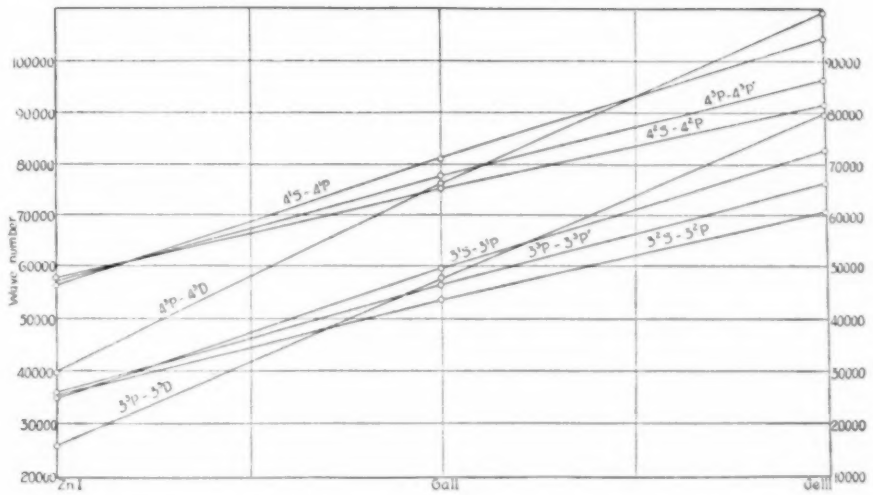

Fig. 1. Curves showing position of typical groups in Mg I – Si III and Zn I – Ge III.

Perhaps the most conspicuous, though usually not the most intense, group involving these main P intervals from a two-electron system is the PP' group. This group would be expected about 1500A in Ga II and near 1000A in Ge III. When found, these groups taken with the group found by Sawyer and Beese[5] for Zn I should obey the doublet laws. The multiplet in Ga at 1483A and that in Ge at 1160A involve the P separations chosen and obey the doublet law for position.

If one plots curves, as in Fig. 1, for these PP' groups of Mg I, Al II, Si III and also for the single lines 3^1S–3^1P as well as the doublets of the once more ionized atoms (stripped atoms) the curves so obtained are nearly straight and diverge slightly from each other fanlike as we proceed to higher atomic weight. The curve for the single lines crosses the other two between Mg I and Al II. Having plotted the PP' groups chosen for Zn I, Ga II and Ge III and also the stripped doublets, the location of the single lines

was fairly evident, since that for Zn I is already known. Very strong lines in Ga and Ge were located which satisfy the conditions for 4^1S–4^1P very well. The curves have almost exactly the same relative positions as in the Mg I–Si III sequence. In order to save space both sets of curves are placed in the same drawing. The lower curves and scale reading on left refer to the sequence Mg I–Si III, the upper curves and scale reading on right refer to sequence Zn I–Ge III.

The next group sought was $4P$–$4D$. The curve for this group in Mg I–Si III is nearly straight but has much steeper slope than those for PP' etc., and crosses these curves at Al II. The group for Zn I is known and the location of that for Ga II must be near the PP' group and the same P separations must be involved. Thus the group recorded was located in Ga II. The doublet law gives the corresponding group in Ge III. The curve so obtained crosses the other two at Ga II.

A difficulty arises, however, on account of the fact that three groups of Ga fall very close to 1500A. These are, one line of the doublets of the stripped atom (λ1494.86) the PP' group and the $4P$-$4D$ triplet. One would expect from the curves that the center of the PP' group should fall about $\nu = 67{,}000$ and that the diffuse group should be longer in wave-length, as they have been recorded, but this leaves one member of PP' unlocated unless it is blended with the doublet line above. The group is so complex and the interval $\Delta\nu = 935$ is repeated so frequently that it has been thought

TABLE V

λ (I. A. vac.)	Int.	ν	λ (I. A. vac.)	Int.	ν	λ (I. A. vac.)	Int.	ν
1537.61	1	65036	1527.41	1	65470	1483.95	5	67386
1536.91	1	65065	1515.19	3	65999	1483.52	3	67410
1536.39	3	65088	1514.57	5	66025	1483.15	0	67424
1536.09	1	65100	1514.35	0	66035	1477.83	0	67667
1535.40	7	65130	1505.01	4	66446	1473.73	2	67853
1535.53	15	65167	1504.41	4	66472	1463.65	5	68322
1533.00	1	65232	1504.12	0	66484	1454.90	1	68733
1531.46	1	65297	1494.86	15	66885			

well to record all of the lines present in the group in Table V. Undoubtedly there are other ways in which the groups may be arranged but on the whole the arrangement recorded seems the best one. Table VI shows the groups together with the separations and term values for Ga II and Table VII those for Ge III. The multiplets in Ge III are less in doubt than those of Ga II merely because they are not superimposed in any case.

The resonance line recorded at 2199A may be in doubt. It has about the correct position as shown by the value of the $4S$ term obtained and appears strongly in the spark in hydrogen becoming quite faint in the vacuum spark. The 4^1S and 4^1P terms, of course, depend on the identification of this line. The corresponding line in Ga has not been located for certain. The line at λ2500.94 (7) 39985 is approximately in the correct position but has already been classified otherwise.

TABLE VI

Series spectrum of Ga II.

Designation	λ (I. A. vac.)	Int.	γ	Δγ	Term values	
$4P_2-5S$	1845.30	9	54192	935	$5S$	57760
$4P_1-5S$	1813.98	8	55127			
$4P_0-5S$	1799.42	3	55574	447*	$4P_3$	111950
					$4P_1$	112885
$4P_2-4D_1$	1536.91	1	65065		$4P_0$	113332
$4P_2-4D_2$	1536.39	3	65088	934		
$4P_2-4D_3$	1535.40	7	65130		$4D_3$	46820
$4P_1-4D_1$	1515.19	3	65999	936	$4D_2$	46862
$4P_1-4D_2$	1514.57	5	66025	447	$4D_1$	46885
$4P_0-4D_1$	1505.01	4	66446			
$4P_2-4P_1'$	1504.41	4	66472			
$4P_1-4P_0'$	1494.86	?	66885	938		
$4P_2-4P_2'$	1483.95	5	67386			
$4P_1-4P_1'$	1483.52	3	67410	936		
$4P_0-4P_1'$	1473.73	2	67853	443		
$4P_1-4P_2'$	1463.65	5	68322			
4^1S-4^1P	1414.44	20	70700			

* Chosen by Rao.

TABLE VII

Series spectrum of Ge III.

Designation	λ (I. A. vac.)	Int.	ν	Δν	Term values	
4^1S-4^3P	2199.63	20	45462		4^1S	258962
$4P_2-4P_1'$	1183.34	10	84506		$4P_2$	211860
$4P_1-4P_0'$	1173.78	9	85195	1642	$4P_1$	213500
$4P_1-4P_1'$	1160.79	8	86148		$4P_0$	214263
$4P_2-4P_2'$	1159.62	8	86235	767		
$4P_0-4P_1'$	1150.55	9	86915	1644	4^1P	167086
$4P_1-4P_2'$	1137.92	10	87879			
					$4D_3$	112987
4^1S-4^1P	1088.42	20	91876		$4D_2$	113094
					$4D_1$	113166
$4P_2-5S$	1059.03	10	94426	1640		
$4P_1-5S$	1040.95	9	96066		$5S$	117434
$4P_0-5S$	1032.75	7	96829	763		
					$6S$	64930
$4P_2-4D_1$	1013.23	1	98694			
$4P_2-4D_2$	1012.50	4	98765	1643		
$4P_2-4D_3$	1011.49	6	98873			
$4P_1-4D_1$	996.64	4	100337	1644		
$4P_1-4D_2$	995.93	5	100409	766		
$4P_0-4D_1$	989.09	4	101103			
$4P_2-6S$	680.59	2	146931	1642		
$4P_1-6S$	673.07	1	148573			
$4P_0-6S$	669.58	0	149347	774		

TERM VALUES IN GA II AND GE III

In Ge III two members of a series are found at 1059A and 680A, and, while both lie well in the extreme ultra-violet, they have been used to deter-

mine the $4P$ terms. The other terms for Ge III then follow from the $4P$ term in the usual way. In Ga II no second members have yet been identified and it became necessary to estimate one of its terms. It was decided to get an approximate value for $4P$ by the use of the relation $(\nu/R)^{1/2}$ from the corresponding terms of the sequence Zn I to Ge III.

Table VIII gives the values of the $(\nu/R)^{1/2}$ for the various terms of the sequence Zn I to Ge III with differences, and in Table IX are recorded the term values with Rydberg denominators (*R.D.*) and quantum defects (q). The quantities enclosed in brackets are merely estimates.

TABLE VIII

Values of $(\nu/R)^{1/2}$

Term	Zn I	Diff.	Ga II	Diff.	Ge III
4^1S	.8309	.3493	(1.1802)	.3560	1.5361
4^3P	.6178	.3922	1.0100	.3795	1.3895
4^1P	.5142	———	(.8653)	———	.8183
4^3D	.3440	.3092	.6532	.3615	1.0147
5^3S	.4487	.2768	.7255	.3100	1.0355
6^3S	.2342	———	———	———	.7692

TABLE IX

Rydberg denominators and quantum defects.

Term Notation	Ga II			Ge III		
	Term value	*R. D.*	q	Term value	*R. D.*	q
4^1S	(152850)	———	———	258962	1.9529	2.0471
4^3P_2	111950	1.9802	2.0198	211860	2.1590	1.8410
4^1P	(82165)	———	———	167086	2.4312	1.5688
4^3D_3	46820	3.0620	.9380	112987	2.9565	1.0445
5^3S	57760	2.7566	2.2434	117434	2.8971	2.1028
6^3S	———	———	———	64930	3.9000	2.1000

SINGLY-IONIZED INDIUM

By the method described in the preceding pages the corresponding groups of single-ionized indium have been located also. The curves for the sequence Cd I, In II, etc., are not shown but are perfectly symmetrical with those for the Zn I–Ge III sequence. The wave-lengths and wave-numbers of the lines for In II are given in Table X.

Rao[5] has already chosen the $5P$–$6S$ triplet from wave-lengths given by Carroll. The intensity of the most refrangible member seems to be abnormally low but there is no other choice on these plates and the fact that the $5P$–$5D$ and $5P$–$5P'$ groups are found seems to confirm the choice made.

Sawyer and Beese[5] state that "in many two-valency-system spectra the frequency of the first PP' group is nearly a mean between the frequency

[5] Sawyer and Beese, Nature **116**, 936 (1925).

TABLE X

Series spectrum of In II.

Designation	λ (I. A. vac.)	Int.	γ	Δγ
$5P_2-6S$	2079.38	12	48091	2479
$5P_1-6S$	1977.43	10	50570	
$5P_0-6S$	1936.21	5	51647	1077*
$5P_2-5D_1$	1777.51	1	56258	
$5P_2-5D_2$	1774.79	10	56345	2479
$5P_2-5D_3$	1748.77	15	57183	
$5P_1-5D_1$	1702.51	6	58737	2478
$5P_1-5D_2$	1700.01	7	58823	1075
$5P_0-5D_1$	1671.89	5	59812	
$5P_2-5P_1'$	1741.59	5	57419	
$5P_1-5P_0'$	1716.55	6	58256	2479
$5P_2-5P_2'$	1674.04	10	59736	
$5P_1-5P_1'$	1669.51	5	59898	2477
$5P_0-5P_1'$	1640.10	5	60972	1074
$5P_1-5P_2'$	1607.38	5	62213	
5^1S-5^1P	1586.37	15	63037	

* Chosen by Rao.

of the first line of the principal series of singlets in the spectrum and the first line of the principal series of doublets of the once-more-ionized atom."

How well this rule is obeyed will be seen at once from Table XI provided we use the long wave-length member of the doublet as was done by Kichlu and Saha[6] and not the shorter line as Sawyer and Beese have done for Zn and Cd.

TABLE XI

Rule of Sawyer and Beese.

Element	$^1S-^1P$ 2 valency	$P-P'$ 2 valency	$^3S-^3P$ 1 valency
Ga	70700	67398	65167
Ge	91876	86196	81307
In	63037	59817	57185

In conclusion the author wishes to express to the Research Council of Canada his appreciation of a grant which has made this work possible.

UNIVERSITY OF ALBERTA,
EDMONTON, CANADA.
July, 1927.

Note added November 21: While this paper was at press Green and Loring published a report on Sn II and III (Phy. Rev. **30,** 574, 1927). The above results for In II seem to check very well with Sn III by Moseley curves and the prediction of these authors that the P separations of In II will be approximately 2420 and 1050 is very closely fulfilled and two members of the group PP' were located by them.

[6] Kichlu and Saha, Phil. Mag. **4,** 199 (1927).

INTENSITIES IN THE STARK EFFECT OF HELIUM: II

By Jane M. Dewey

Abstract

The intensities of the new spectral lines appearing in an electric field may be calculated from the quantum theory of perturbations. To apply the method to helium we consider the helium atom a perturbed hydrogen atom. Calculations are given here for a number of helium lines whose intensities have previously been measured. Measurements of the intensities of the groups $2S-nM$ and $2s-nm$ for $n=4$, 5, 6, and $M=S, P, D$, etc. are given and compared with the calculated intensities. The theory gives intensities of the correct order of magnitude and gives the variation with field approximately correctly but large deviations from the experimental values appear in all groups.

SINCE the previous communication[1] on this subject was written, Heisenberg and Foster have worked out a method of calculating the displacements and intensities of the lines in the spectrum emitted by helium in the presence of an electric field which should give valid results at all fields.[2] In a paper to appear shortly Foster gives calculations of the wave-lengths of these lines and compares them with the results of his measurements.[3] In this paper the results of calculations made by this method are given for the intensities of all lines on which measurements were reported in the previous paper. In addition new measurements of the intensities of lines lying in the violet portion of the helium spectrum are given.

Calculation of the intensities. In order to make the calculation we regard the helium atom as a perturbed hydrogenlike atom. The recent work of Heisenberg[4] on the helium spectrum shows that we may treat the orthohelium and parhelium spectra separately; each can be regarded as the spectrum emitted by a single electron, moving in a central field of force which differs slightly from a Coulomb field. To determine the effect of an external field on the helium atom we must determine the perturbation of a hydrogen atom by the two fields, an internal field, which we may attribute to the doubly charged nucleus and the interaction of the two electrons, and the external field which we apply.[4a] All we need know about the internal field (if we calculate the perturbation only to a first approximation) are the deviations of the empirically known helium terms from the corresponding hydrogen terms. We carry out the perturbation calculation by the method

[1] Dewey, Phys. Rev. **28**, 1108 (1926).

[2] Calculations for small fields are given by Unsold, Ann. d. Physik **82**, 355 (1927).

[3] Foster, Phys. Rev. **23**, 667 (1924); Proc. Roy. Soc. **A114**, 47 (1927).

[4] Heisenberg, Zeits. f. Physik **38**, 441 (1924), **39**, 499 (1926).

[4a] A corresponding calculation on the basis of the earliest methods of the quantum theory was given by Kramers, Zeits. f. Physik **3**, 199 (1920), and by Becker, *ibid*, **9**, 332 (1922).

given by Born, Heisenberg and Jordan[5] for the case in which the unperturbed system is degenerate. We try to find[6] the matrix $\mathbf{S}$ such that

$$\mathbf{W}=\mathbf{S}^{-1}\mathbf{H}(\mathbf{p}_0,\mathbf{q}_0)\mathbf{S} \tag{1}$$

is a diagonal matrix

$$\mathbf{q}=\mathbf{S}^{-1}\mathbf{q}_0\mathbf{S} \tag{2}$$

where $W(n,n)$ represents the change of the total energy by the perturbation, $W(n,m)$ is zero when n is not equal to m, $\mathbf{H}$ is the mean value of the perturbing energy, taken over the unperturbed system, $\mathbf{q}$ the coordinate of the electron in a given direction. The subscripts 0 refer to the unperturbed system. The necessary equation is

$$\det\left|W\delta(r,s)-H(r,s)\right|=0 \tag{3}$$

where r and s refer to the rows and columns of the determinant. In the case we are considering

$$\mathbf{H}=\mathbf{H}'+\mathbf{H}''$$

where $\mathbf{H}'$ refers to the inner and $\mathbf{H}''$ to the outer field.

The inner field can be regarded as a field of central symmetry, as it does not change the selection rule for the azimuthal quantum number. Its mean value, taken over the unperturbed motion, is directly given by the term values ν_r of the helium atom; if ν_0 is the term value of the corresponding hydrogen term, we get

$$\begin{aligned} H'(r,s)&=h(\nu_0-\nu_r) && \text{for } r=s\\ &=0 && \text{for } r\neq s\end{aligned}$$

The outer field F gives rise to a term eqF in the potential energy, its time-mean value is given by the coordinate of the "electric center" in the direction of the field. The matrix elements of eqF are calculated by Pauli[7]:

$$H''(r,r-1)=(3/2)a_0eF\left[(n^2-r^2)(r^2-m^2)/(4r^2-1)\right]^{1/2}$$

$$H''(r,r+1)=(3/2)a_0eF\left\{\left[n^2-(r+1)^2\right]\left[(r+1)^2-m^2\right]/\left[4(r+1)^2-1\right]\right\}^{1/2}$$

$$H''(r,s)=0 \text{ for } r\neq s\pm 1$$

where a_0 is the hydrogen radius, e the charge on the electron, n the principal quantum number, m the magnetic quantum number and F the electric field. To carry through the numerical calculation we consider the atom initially exposed to a very weak external magnetic field which removes the degeneracy with respect to the magnetic quantum number m. The system is then degenerate only with respect to the azimuthal quantum number and we may

[5] Born, Heisenberg and Jordan, Zeits. f. Physik **35**, 557 (1926). For a shorter account of the quantum theory of perturbations see Heisenberg, Math. Ann. **95**, 683 (1926).

[6] For details of the following calculations see J. S. Foster, Proc. Roy. Soc. (in press).

[7] W. Pauli, Zeits. f. Physik **36**, 336 (1927), Eqs. (60) and (66).

apply Eq. (3) to solve for W. If we insert the values of H in the determinant and insert for W its value $h(\nu_0-\nu)$, where ν is the frequency of the displaced helium term, and replace $\nu_0-\nu$ by x and $\nu_0-\nu_r$ by λ_r we obtain the determinant

$$\begin{vmatrix} h(x-\lambda_r) & \frac{3a_0eF}{2}\left(\frac{[n^2-(r+1)^2]\ [(r+1)^2-m]}{4(r+1)^2-1}\right)^{1/2} & 0 & \cdots \\ \frac{3a_0eF}{2}\left(\frac{[n^2-(r+1)^2]\ [(r+1)^2-m^2]}{4(r+1)^2-1}\right)^{1/2} & h(x-\lambda_{r+1}) & \frac{3a_0eF}{2}\left(\frac{[n^2-(r+2)^2]\ [(r+2)^2-m^2]}{4(r+2)^2-1}\right)^{1/} & \cdots \\ 0 & \frac{3a_0eF}{2}\left(\frac{[n^2-(r+2)^2]\ [(r+2)^2-m^2]}{4(r+2)^2-1}\right)^{1/2} & h(x-\lambda_{r+2}) & \cdots \\ \cdots & \cdots & \cdots & \cdots \\ \cdots & \cdots & \cdots & \cdots \end{vmatrix} = 0 \quad (5)$$

The subscripts refer to azimuthal quantum numbers. The λ's for the s, p and d terms are taken from Paschen's tables, for the higher terms they are calculated from the formulae of Waller.[8] The determinant has $n-m$ roots which give the displacements of the $n-m$ terms which have the quantum numbers n and m for which we have set up the determinant. Since the lower state will be practically undisturbed at any field obtainable in the laboratory the displacements of the terms of the upper state are the same as the displacements of the lines.

Having solved for the W's we can insert them in the determinant and regard it as a system of linear equations in the S's. We may write Eq. (2) in the form

$$q(r,u)=\sum_s \sum_t \tilde{S}^*(r,s)q_0(s,t)S(t,u) \qquad (6)$$

where $\tilde{S}^*$ indicates the transposed conjugate form of S. Since the final state is undisturbed

$$S(t,u)=\begin{cases} 1 \text{ for } t=u \\ 0 \text{ for } t\neq u. \end{cases}$$

Also

$$q_0(s,t)=0 \text{ for } s\neq t\pm 1$$

On solving (1) for the S's we obtain $n-m$ S's for each value of x which we insert in the equation, one corresponding to each index (azimuthal quantum number) appearing in the equation. Using the azimuthal quantum number as the second index of S and the number of the root x to which it corresponds as the first, Eq. (6) reduces to

$$q(k,l)=S(k,l-1)q_0(l,l-1)+S(k,l+1)q_0(l,l+1) \qquad (7)$$

where k is the azimuthal quantum number of the initial state and l of the final state. For instance

$$q(2P-4F)=S(4F,4S)q_0(2P-4S)+S(4F,4D)q_0(2P-4D)$$

[8] Waller, Zeits. f. Physik **38**, 635 (1926).

When two terms appear in this formula, one of them is in all the cases we shall consider very much larger than the other; for all the lines for which calculations are given in this paper the smaller will be disregarded. That is, for instance:

$$I(2P-4F)=\text{const.}\,[S(4F,4D)q_0(2P-4D)]^2$$

The S's are real and so normalized that

$$\sum_s S(r,s)^2=1$$

Then

$$\sum_r S(r,s)^2=1,$$

which gives a check on the correctness of the calculation. The S's must be calculated for each value of m. The relative intensities of the unperturbed lines which differ only in the magnetic quantum number are determined from the rules given by Kronig[9] and others. In most cases in these experiments the lines which have the same principal and azimuthal quantum numbers are superposed on the plates and their calculated intensities are added. The method of normalizing the S's and of summing superposed lines is equivalent to the assumption made in the calculations from the dispersion theory that the number of atoms in the states nS, nP, nD, etc., is the same. In making the calculations for orthohelium the fine structure was neglected and the calculations made as if the terms were single. This should not introduce appreciable error, since we can regard the fine structure as a perturbation of negligible magnitude.

Experimental Method

The experimental arrangement was as described in the previous paper except for certain minor changes. The operation of the Lo Surdo tube was improved by using a copper cathode with an aluminum end. The aluminum spattered less than molybdenum and the copper served to conduct away the heat. To keep the tube running smoothly it is necessary to keep the cathode below red heat. The tube was made of pyrex glass and a very massive anticathode also of aluminum was used. Instead of direct current generators rectified current from a high-tension transformer was used. A Coolidge tube was connected in series with the apparatus as a resistance. This was found very convenient as current through the filament of the Coolidge tube could be adjusted until the current put through the apparatus was just under the saturation current of the Coolidge tube. This reduced flashing somewhat, and protected the apparatus and transformer from damage in case for any reason the resistance of the Lo Surdo tube fell while it was in operation, so that it was not necessary to watch the apparatus so closely. A Hilger quartz spectrograph, type E, was used, with, as before, Ilford Rapid Chromatic plates, developed for four minutes in Rodinol 1/20 at 18°. The field was

[9] Kronig, Zeits. f. Physik **31**, 885 (1925).

determined from the separation of the lines of the group $2S$–$5M$ by comparison with the calculated separations. As it seemed probable that the displacement of the lines by variations in the field might make the more displaced lines appear weaker on the plates than the less displaced lines a very wide slit was used, 0.06 mm. This corresponds to a wave-length difference of about 0.5A on these plates and should reduce this error to a very small value. The effect of time on the blackening curves was investigated experimentally and found to be negligible. The blackening curves for the longer wave-lengths were taken with a tungsten filament lamp with a quartz plate cemented to one end. As it was found very difficult to obtain intensity enough from such a lamp at wave-lengths below about 3300A, a water cooled Finssen quartz mercury arc such as is used in hospitals was used for the shorter wave-lengths. The variation in intensity was obtained by varying the time of exposure. The lamp did not give a constant emission over short periods, showing irregular variations of periods shorter than a minute, but when all the exposures were long these variations were averaged out and reproducible results were obtained. The light emitted by this lamp was thus very similar to the light emitted by the Lo Surdo tube. At 3450A a blackening curve was taken with this lamp and also with the tungsten filament lamp and it was found that the two curves had the same form. The form of the blackening curves changes fairly rapidly with wave-length in the region in which these measurements were made and this may introduce considerable error into certain of the measurements, particularly into those on the lines of group $2s$–$4m$ (3185A), and to a less extent into the other measurements on the orthohelium lines; for the parhelium lines this error is small. A comparison of the intensities of the least disturbed lines gives the same values for the ratio of the intensities of these lines to within thirty percent for all lines on all exposures, even when the measured intensity of the lines is very different on the different exposures, and the agreement is usually better than this. For the lines in the visible region, whose intensity was given in the previous paper, the agreement was somewhat better, no disagreements larger than twenty percent being observed. As only two exposures were compared to obtain any of the ratios given in this paper the error should never be more than doubled in making this comparison.

Results

Parhelium lines. In Table I the calculated values of the intensities of the parhelium lines of the fourth group are given, together with the measured values, which are repeated from the previous paper for comparison with the calculation. The measured and calculated values of the intensities are so arranged as to add up to 100 for the entire group under consideration. The line $2S$–$4S$ was not observed. In Fig. 1 the calculated intensities of the lines of group $2S$–$5M$ are represented by solid lines and the points represent the measured intensities of these lines. The square of the field is used as abscissa and the relative intensity of the line as ordinate. The dotted lines are the straight lines which best represent the experimental data. The line

TABLE I

The calculated and measured intensities of the parhelium lines of the fourth group.

Field kv/cm	$2P-4P$ ∥	$2P-4P$ ⊥	$2P-4D$ ∥	$2P-4D$ ⊥	$2P-4F$ ∥	$2P-4F$ ⊥	$2S-4P$ ∥	$2S-4P$ ⊥	$2S-4D$ ∥	$2S-4D$ ⊥	$2S-4F$ ∥	$2S-4F$ ⊥
14.2 calc.	1.7	0.65	77	79	22	20	98	99	1.4	1.0	0.69	0.47
obs.	2.3	.86	77	77	23	22	96	96	2.5	2.0	1.0	1.7
16.2 calc.	2.1	0.79	74	77	23	22	97	98	1.7	1.3	0.89	0.77
obs.	2.3	.85	72	76	26	23	95	95	2.7	2.5	2.0	2.3
18.6 calc.	2.6	0.98	72	74	25	25	97	97	2.1	1.6	1.2	1.0
obs.	3.3	1.3	63	64	34	35	94	94	3.3	3.0	3.1	2.9
19.8 calc.	3.0	1.1	72	73	26	26	96	97	2.3	1.7	1.4	1.2
obs.	3.3	1.2	63	64	34	35	93	95	3.4	2.7	3.2	2.8
24.3 calc.	4.6	1.8	69	69	27	30	94	96	3.2	2.3	2.3	2.0
obs.	7.4	3.0	66	61	27	36	91	93	4.5	3.6	4.2	3.2

$2S$–$5S$ was always observed as a totally parallel polarized line. Its intensity is not given as the line is superposed on the group $2s$–$8m$. In Fig. 2 the lines represent the calculated values of the intensities of the lines of group $2P$–$5M$

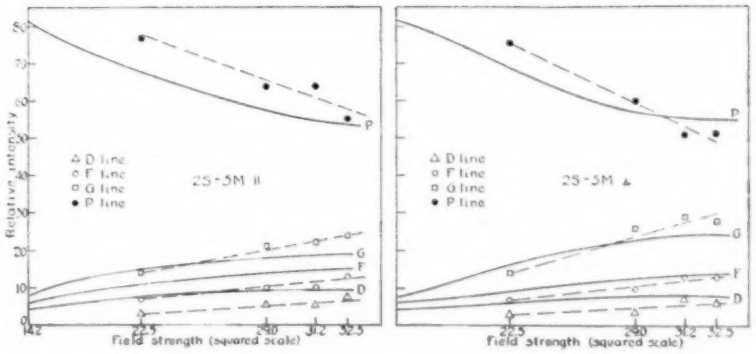

Fig. 1. Calculated and measured intensities of the lines of the group $2S-5M$.

and the points represent the measured values, which are taken from the data given in the previous paper. In Fig. 3 the intensities of the lines of the groups $2P$–$6M$ and $2S$–$6M$ are represented as in the previous paper, the intensities of the parallel components being given by lines above and the intensities of the perpendicular components by lines below the base line. The experimental values for the former group are taken from the first paper and for the latter are new.

It is obvious from the figures that the disagreement between theory and experiment is much larger than the experimental error. On the other hand the theory in every case gives the correct order of magnitude for the intensity and an approximately correct value for the polarization of the lines and predicts correctly which lines increase in relative intensity, which

decrease and which go through a maximum as we increase the field. We obtain a qualitative but not a quantitative agreement between theory and experiment. A comparison of Fig. 1 with Fig. 2 and of the two groups whose intensities are given in Fig. 4 with each other shows that the deviations are very similar for the groups of lines which have the same sets of initial states. This suggests that the assumption that the probability of exciting

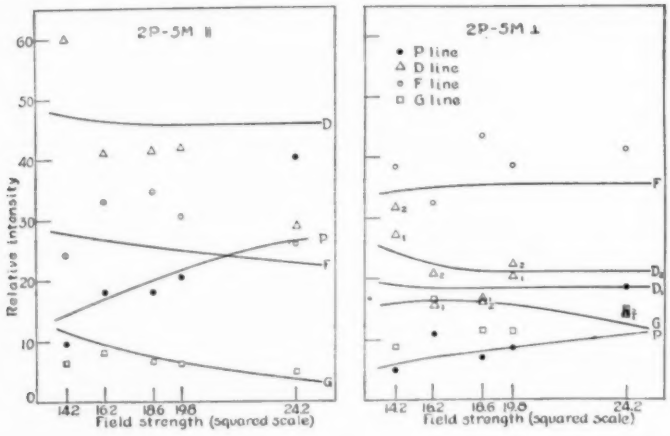

Fig. 2. Calculated and measured intensities of the lines of the group $2P-5M$.

the states nP, nD, nF, etc., is the same may not be warranted and that at least a part of the deviation may be due to differences in the number of atoms excited to the different states. In the fourth group, where the deviations are smaller compared to the experimental error, the deviations are not the same for the lines which have the same initial but different final states. In comparing the figures one should bear in mind that the intensity of the parallel components of the lines of group $2S-nM$ depends on the S's for the states where the magnetic quantum number m is 0, and the number of atoms excited to each of these states. The intensity of the perpendicular components of the lines of this group depends on the S's for m equal to one, and the intensities of the parallel components of the lines of group $2P-nM$ depend on both sets of S's. The intensity of the perpendicular components of the lines of the latter group depends largely on the S's for m equal to two. Because of the method of normalizing the S's and of expressing the measured values any deviation of a strong line causes an inverse deviation of all the other lines. The closeness with which the deviation of a line with a given initial and final state is repeated by the deviation of the line with the same initial but a different final state makes it unlikely that the deviation is due to experimental error.

Orthohelium lines. In Table II are given the calculated intensities of the groups of lines $2p$–$4m$ and $2s$–$4m$ and the measured values for the former group are repeated from the earlier paper and measured values given for the latter group. In Table III the same data is given for the fifth group. The measured and calculated values for the group $2p$–$6m$ are plotted for three

TABLE II

The calculated and measured intensities of orthohelium lines of the fourth group.

Field kv/cm	$2p-4p$ ∥	$2p-4p$ ⊥	$2p-4d$ ∥	$2p-4d$ ⊥	$2p-4f$ ∥	$2p-4f$ ⊥
14.2 calc.	0.072	0.028	85	86	15	14
obs.	.15	.07	86	89	14	11
16.2 calc.	0.099	0.037	81	84	19	16
obs.	.20		85	88	15	12
18.6 calc.	0.12	0.048	79	82	21	18
obs.	.23	.15	83	88	17	12
19.8 calc.	0.13	0.054	78	81	22	19
obs.	.25	.15	80	84	20	16
24.3 calc.	0.19		73		27	
obs.	.35		75		25	

	$2s-4s$ ∥	$2s-4d$ ∥	$2s-4d$ ⊥	$2s-4f$ ∥	$2s-4f$ ⊥
22.5 calc.	0.01		0.12		0.02
obs.			.003		
29.0 calc.	0.02	0.26	0.20	0.06	0.04
obs.	.001	.01	.005	.002	.001

TABLE III

Calculated and measured intensities of orthohelium lines of the fifth group.

Field kv/cm	$2p-5p$ ∥	$2p-5p$ ⊥	$2p-5d$ ∥	$2p-5d$ ⊥	$2p-5f$ ∥	$2p-5f$ ⊥	$2p-5g$ ∥	$2p-5g$ ⊥
14.2 calc.	0.6	0.25	39	42	35	41	25	17
obs.	1.2	.67	46	47	35	35	19	17
16.2 calc.	0.8	0.33	38	39	35	41	26	20
obs.			31	36	49	45	20	18
18.6 calc.	1.1	0.45	36	36	36	39	27	24
obs.	1.4	1.2	33	33	42	46	23	20
19.8 calc.	1.2	0.51	35	35	36	39	28	25
obs.	1.3	1.0	32	35	44	47	23	18
24.3 calc.	1.7	0.70	32	35	36	39	29	25
obs.	2.8	2.3	25	29	55	55	17	13

	$2s-5s$ ∥	$2s-5p$ ∥	$2s-5p$ ⊥	$2s-5d$ ∥	$2s-5d$ ⊥	$2s-5f$ ∥	$2s-5f$ ⊥	$2s-5g$ ∥	$2s-5g$ ⊥
22.5 calc.	0.07	98	98	0.8	0.7	0.7	0.6	0.4	0.3
obs.		99	100	.25	.15	.25	.17	<.1	<.1
29.0 calc.	0.11	96	97	1.3	1.2	1.2	0.9	1.0	0.6
obs.	.12	99	100	.27	.17	.29	.18	<.1	0.05

of the fields for which data were given in Fig. 4 and measurements of $2s$–$6m$ are given together with the calculated intensities in Table IV. Fig. 4 gives the measured intensity of the lines of group $2p$–$7m$ at three fields higher

TABLE IV

The calculated and measured intensities of the lines of the group 2s−6m.

Field kv/cm	2s−6s ‖	2s−6p ‖	2s−6p ⊥	2s−6d ‖	2s−6d ⊥	2s−6f ‖	2s−6f ⊥	2s−6g ‖	2s−6g ⊥	2s−6h ‖	2s−6h ⊥
22.5 calc.	0.7	87		5.2		3.2		3.0		1.1	
obs.		95		2.4		1.5		1.2		<.6	
29.0 calc.	1.2	78	83	8.6	7.0	5.9	4.8	4.3	3.2	2.5	1.8
obs.	.7	93	96	2.4	1.2	4.2	1.8	.75	.5	<.3	<.2

than those for which the intensities in this group were given in the previous paper and corrects an *erratum* in the intensities of this group at 19.8 kv/cm given in that paper. No calculations were made for this group as they would be extremely laborious and sufficient data has already been given to show

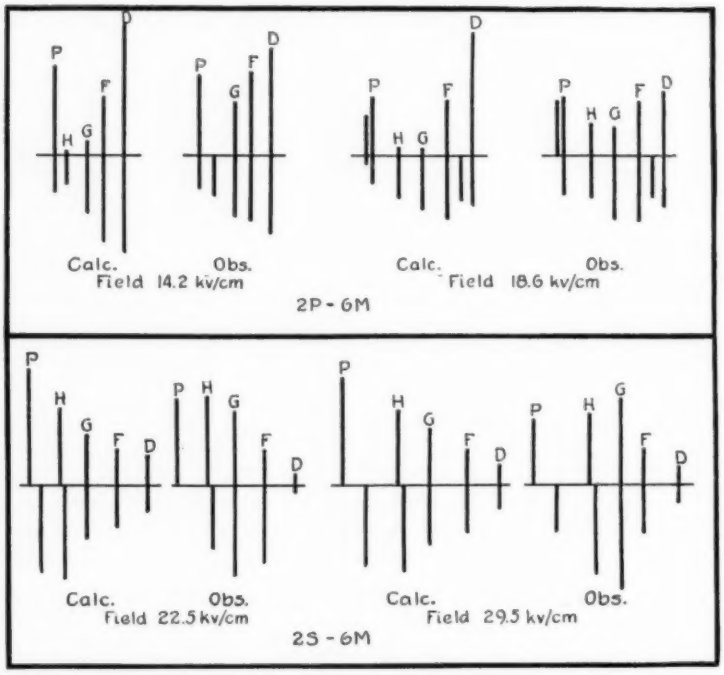

Fig. 3. Calculated and measured intensities of parhelium lines of the sixth group.

what agreement can be expected between the theory as applied here and experiment.

The deviation of the measured intensities of the orthohelium lines from the calculated intensities is considerably larger than for the parhelium lines. Particularly in the groups with the final state 2*s* the deviations are very large. The polarization of the weak lines does not agree with that given by the theory[10] and the deviations can not be regarded as depending only on the initial state. The deviations are in the same direction for lines with the same initial and different final state but are much larger for those with the final

[10] Cf. Table III of the previous communication.

state $2s$. The lines which represent large changes of azimuthal quantum number in the s groups appear with very slight intensity, the theoretical values being much larger. The experimental uncertainty is larger for these groups than for any others but should not be large as long as the weak lines are compared with each other. The deviations, however, are as large when this is done as when the intensity of the strong line is compared with that of a weak line. In the seventh group the total disappearance of the parallel component of the d line is interesting. This has been previously reported

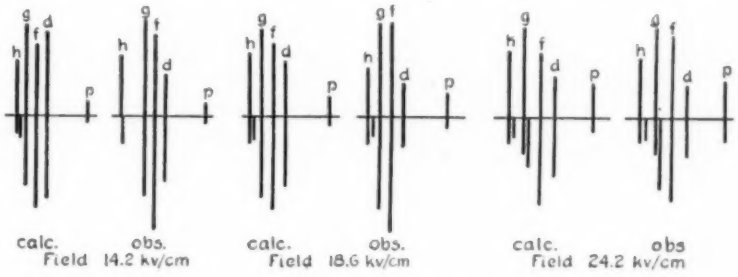

Fig. 4. Calculated and measured intensities of the lines of the group $2p-6m$.

by Foster. The theory predicts that the parallel component of a line with final state P will almost entirely disappear when the line is so displaced as have the same wave-length as the undisplaced P line. It will in general reappear when it is further displaced, as the line $2P$–$6H$ does. According to Foster's measurements the line $2p$–$7d$ crosses the position of the undisplaced p line at a field of about twenty kilovolts per centimeter, the field at which it is no longer observed. This line does not reappear at the fields which are used in our experiment; at a field of twenty-nine kilovolts per centimeter

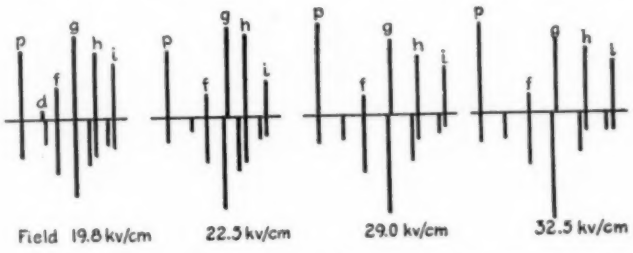

Fig. 5. Measured intensities of the lines of the group $2p-7m$.

it has an intensity of less than one one-thousandth the intensity of the whole group.

Conclusions

Calculations from the quantum theory of perturbations on the assumptions used here and to this approximation give only approximate values for the intensities of the new lines appearing in the Stark effect. The deviations are such as to suggest that they are partly due to differences in the number

of atoms excited to different states of almost the same energy. Apparently, factors come into play in the case of orthohelium other than those which influence the parhelium lines. No explanation of the deviations suggests itself. They may be due to the influence of the atoms on each other, which is here entirely neglected, and to the fact that we have neglected higher approximations of the theory in making the calculations.

The experiments and calculations described here were carried out at the University Institute for Theoretical Physics in Copenhagen. The author wishes to express her thanks to Prof. Niels Bohr for his interest and advice throughout the work and to Dr. Heisenberg for his assistance and suggestions on the theoretical part. Dr. Foster was kind enough to show her his results on the calculations of the wave-lengths in advance of publication. The research was assisted by a grant from the Rask-Örsted Foundation.

PRINCETON, NEW JERSEY,
JULY, 1927

THE ZEEMAN EFFECT OF THE SYMMETRICAL TOP ACCORDING TO WAVE MECHANICS

By Edward U. Condon†

Abstract

The alteration of the quantum-theoretical energy levels of a symmetrical top due to the action of a magnetic field on a charge which is fixed to the top, is investigated by means of the perturbation theory of the wave mechanics. The final formula for the change in the energy levels is given below in Eq. (10).

THE model of the rigid rotator with two different moments of inertia (symmetrical top) has proved useful in the theory of molecular spectra. Investigations of the unperturbed energy levels and radiation amplitudes (matrix components of the electric moment) according to wave mechanics have been given by Reiche, Reiche and Rademacher, Kronig and Rabi, and by Manneback.[1] Dennison[2] has also treated the problem by the matrix methods. Reiche has investigated the first-order Stark effect while Manneback has investigated the second-order Stark effect as well.

The Zeeman effect, i.e., the perturbation of the energy levels of the top by a magnetic field, has not been hitherto investigated. The results of the calculation of this perturbation are here communicated.

The notation here used is that of Kronig and Rabi. The top has two of its moments of inertia equal to A and the third, about the axis of symmetry, equal to C. The electrical properties of the top are summarized in the assumption that a charge, e, is fixed to the top at a point whose distance off the axis of symmetry is a, while the distance along the axis of symmetry from the center of gravity of the top to the foot of the perpendicular from this charge on to the axis is c.

The wave equation can be conveniently derived with the aid of a variation principle due to Fock.[3] The Lagrangian function for the particle in a magnetic field is

$$L=T-(e/c)\boldsymbol{A}\cdot\boldsymbol{v} \tag{1}$$

where T is the kinetic energy, $\boldsymbol{A}$ the vector potential, and $\boldsymbol{v}$ the velocity of the charged particle. Using the Eulerian angles θ, ϕ, ψ, one can write the magnetic term as

$$(e/c)\boldsymbol{A}\cdot\boldsymbol{v}=H(\alpha\dot{\theta}+\beta\dot{\phi}+\gamma\dot{\psi}) \tag{2}$$

† National Research Fellow.

[1] Reiche, Zeits. f. Physik **39**, 444, (1926); Reiche and Rademacher, Zeits. f. Physik **42**, 453 (1927); Kronig and Rabi, Phys. Rev. **29**, 262 (1927); Manneback, Phys. Zeits. **28**, 72 (1927).

[2] Dennison, Phys. Rev. **28**, 318 (1926).

[3] Fock, Zeits. f. Physik **38**, 242 (1926).

in which H is the field strength and

$$\begin{aligned}\alpha &= -2\pi\mu\nu \cdot a\cos\phi(c\cos\theta + a\sin\theta\sin\phi)\\ \beta &= 2\pi\mu\nu \cdot a(a\cos\theta - c\sin\phi\sin\theta)\\ \gamma &= 2\pi\mu\nu[a^2\cos^2\phi + (c\sin\theta - a\cos\theta\sin\phi)^2]\end{aligned} \tag{3}$$

where μ is the electronic mass and ν the electronic Larmor precession frequency for unit field strength.

The Hamiltonian function is obtained in the usual way by expressing $p_\theta\dot{\theta} + p_\phi\dot{\phi} + p_\psi\dot{\psi} - L$ as a function of the momenta, p_θ, p_ϕ, and p_ψ. The result is

$$\begin{aligned}H = &\frac{1}{2A}(p_\theta + H_\alpha)^2 + \frac{1}{2}\left(\frac{\cos^2\theta}{A\sin^2\theta} + \frac{1}{C}\right)(p_\phi + H_\beta)^2 + \frac{1}{2A\sin^2\theta}(p_\psi + H_\gamma)^2\\ &- \frac{\cos\theta}{A\sin^2\theta}(p_\phi + H_\beta)(p_\psi + H_\gamma)\end{aligned} \tag{4}$$

Applying Fock's variation process to this Hamiltonian function, one finds the following form for the wave-equation on neglecting terms in H^2:

$$DU + \frac{8\pi^2 E}{h^2}U = \frac{2\pi i H}{h}\Delta U \tag{5}$$

Here D is the differential operator occurring in the wave-equation for the unperturbed top while Δ is a linear differential operator of the first order representing the action of the magnetic field:

$$\begin{aligned}DU \equiv &\frac{1}{A\sin\theta}\frac{\partial}{\partial\theta}\left(\sin\theta\frac{\partial U}{\partial\theta}\right) + \left(\frac{\cos^2\theta}{A\sin^2\theta} + \frac{1}{C}\right)\frac{\partial^2 U}{\partial\phi^2} + \frac{1}{A\sin^2\theta}\frac{\delta^2 U}{\partial\psi^2}\\ &- \frac{2\cos\theta}{A\sin^2\theta}\frac{\partial^2 U}{\partial\phi\,\partial\psi}\end{aligned} \tag{6}$$

$$\begin{aligned}\Delta U \equiv &\frac{1}{A\sin\theta}\frac{\partial}{\partial\theta}(\alpha U\sin\theta) + \frac{\alpha}{A}\frac{\partial U}{\partial\theta} + \left(\frac{\cos^2\theta}{A\sin^2\theta} + \frac{1}{C}\right)\left(\frac{\partial}{\partial\phi}(\beta U) + \beta\frac{\partial U}{\partial\phi}\right)\\ &+ \frac{1}{A\sin^2\theta}\left(\frac{\partial}{\partial\psi}(\gamma U) + \gamma\frac{\partial U}{\partial\psi}\right) - \frac{\cos\theta}{A\sin^2\theta}\left(\frac{\partial}{\partial\phi}(\gamma U) + \frac{\partial}{\partial\psi}(\beta U)\right.\\ &\left. + \beta\frac{\partial U}{\partial\psi} + \gamma\frac{\partial U}{\partial\phi}\right).\end{aligned} \tag{7}$$

The unperturbed equation ($H = 0$) is degenerate in that the energy levels depend only on the quantum numbers, j and n, while the unperturbed characteristic functions are:

$$U_{jmn} = \Theta_{jmn}(\theta) \cdot e^{in\phi} \cdot e^{im\psi} \tag{8}$$

Since ψ does not occur explicitly in the perturbation term, ΔU, this coordinate remains separable and it is thus unnecessary to apply the special apparatus

of the perturbation theory for degenerate systems. According to the simple perturbation theory,[4] the amount of the perturbation becomes:

$$\Delta E_{jmn}=\frac{ihH}{4\pi}\int \bar{U}_{jmn}\Delta U_{jmn}\sin\theta\, d\theta\, d\phi\, d\psi \tag{9}$$

in which it is supposed that the characteristic functions have been normalized and where $\bar{U}_{jmn}$ means the conjugate complex function to U_{jmn}.

The computation of the perturbation energy is readily effected since besides integrals over exponential functions the only integral needed is

$$\int_0^\pi \Theta_{jmn}^2(\theta)\cdot\cos\theta\cdot\sin\theta\, d\theta=-nm/j(j+1)$$

The integral is a simple consequence of well-known properties of the hypergeometric function, to which $\Theta_{jmn}(\theta)$ is related.[5] The result, therefore, for ΔE_{jmn} is

$$\Delta E_{jmn}=-mh\nu_L\left[\frac{\mu(c^2+\frac{1}{2}a^2)}{A}+\frac{n^2}{j(j+1)}\left(\frac{\mu(c^2+\frac{1}{2}a^2)}{A}-\frac{\mu a^2}{C}\right)\right] \tag{10}$$

in which ν_L is the Larmor precession frequency for a particle of mass μ and charge e in a field of strength H, i.e.,

$$\nu_L=eH/2\mu c$$

The ratio $n^2/j(j+1)$ is to be given the value 1 when $j=n=0$.

One sees that the alteration of the energy levels for a molecule represented by this model will therefore be small compared with the Zeeman effect for atoms in the ratio of electron mass to nuclear mass.[6] (The distances a and c are of the same order of magnitude as the distances of the nuclei from the center of gravity of the top-molecule.) The formula deviates from that of the old quantum theory in the appearance of $j(j+1)$ in place of j^2, the same change as occurs in the formula for the unperturbed energy levels.

The model of a symmetrical top is often used for discussions of band spectra for diatomic molecules having states with a resultant electronic angular momentum about the line joining the two nuclei. In this case the moment of inertia, C, arises solely from the electronic structure of the molecule, hence the $\mu a^2/C$ is of the order of magnitude 1. The other terms may be neglected in comparison with it.

The minus sign which affects this term can then give rise to an inverted Zeeman effect, as already noted by Lenz as a consequence of the old theory. If $n=0$ in both initial and final states, there is no Zeeman effect of atomic order of magnitude. If $\Delta n=0$ there is a splitting into the normal Lorentz

[4] Schrödinger, Ann. d. Physik **80**, 437 (1926).

[5] See e.g. Reiche, Zeits. f. Physik **39**, 453, Eq. (44) (1926).

[6] For a review of the present status of theory and experiment concerning Zeeman effect of band spectra, see section on Zeeman effect by Kemble in the Report of the National Research Council on Molecular Spectar in Gases.

triplet (when one applies the selection rules for m as given quantum mechanically by Dennison, Kronig and Rabi, and Reiche) except that the spacing decreases with increasing j, i.e., as one moves away from the origin of a band. The spacing varies as $1/j(j+1)$ or almost inversely as the square of j. But if $n=0$ in one state and $n=1$ in the other then an inversion of one set of levels occurs. This has the consequence that a pattern of $2j+1$ equidistant lines appears, due to the non-splitting for $n=0$ and the splitting for $n=1$. The extreme width of the pattern is $2/(j+1)$. In other words for such bands the broadening due to the Zeeman effect will vary with the inverse first power of j instead of the inverse second.

This calculation was carried out while the writer was a visitor at the summer semester of the Institute for Theoretical Physics at Munich. I take this opportunity to express to Professor Sommerfeld and his co-workers in Munich my appreciation of friendly advice and discussions during the semester and of the hearty *Münchner Gemütlichkeit*, which pervades the life of the institute.

ZÜRICH, SWITZERLAND,
August 8, 1927.

ELECTRONIC STATES AND BAND SPECTRUM STRUCTURE IN DIATOMIC MOLECULES
VI. THEORY OF INTENSITY RELATIONS FOR CASE *b* DOUBLET STATES. INTERPRETATION OF CH BANDS λλ3900, 4300*

By Robert S. Mulliken

Abstract

Theoretical *intensity equations* (Eqs. 8–22 of text) are obtained by means of the summation rule for all possible branches (including "main" and "satellite" branches) in transitions between *doublet* electronic states falling under Hund's *case b*. A revised *notation* is proposed, *applicable to all known bands* and capable of simply describing any band line, for any type of multiplicity. The energy differences between F_1 and F_2 terms (s parallel or antiparallel to j_k in case b) are considered qualitatively for a series of cases between case a and case b, for normal and inverted doublets (cf. Fig. 1); with normal doublets, as is shown elsewhere in detail by Kemble, a special case is possible in which s is oriented nearly as $\pm\epsilon$, while $\sigma \backsim \sigma_k$, for all but the lowest values of j, so that the Kramers and Pauli formula should hold rather accurately; it is concluded that the ^2P common final state of CHλλ3900 and 4300 is an example of this case.

It is shown on the basis of the work of Hulthén and Kratzer that in CHλ4300 the structure (missing lines, number of branches, combination rules, satellite series, term-form) and qualitative intensity relations are in excellent agreement with the theory for a case b $^2D \rightarrow {}^2P$ transition; in the case of λ3900 the agreement is equally good with the theory for a case b $^2S \rightarrow {}^2P$ transition. Initial term values are given (cf. Tables III and VII) for both bands, making use of Kratzer's accurate formulas for the final term values. The ^2D initial state of λ4300 shows a very small inverted doublet separation, diminishing with increasing j_k. The F_1 and F_2 levels of the ^2S initial state of λ3900 are very close together, but there is evidence that the F_2 levels are slightly the higher.

The three observed levels of the CH molecule are probably low-lying levels. Their relation to the electron levels of the carbon atom is discussed. It is likely that the ^2P, ^2D, and ^2S levels of CH are respectively derived from the three lowest states, ^3P, ^1D, and ^1S, of carbon.

Theory of Intensity Relations

In a previous paper (V of the present series[1]) intensity equations corresponding to Hund's case b (cf. IV of this series[2]) have been obtained, with the help of the summation rule, for $^2S \rightarrow {}^2S$ bands ($\sigma_k' = 0 = \Delta\sigma_k = \sigma_k''$). In the present paper similar equations are obtained for $\Delta\sigma_k = 0$ and ± 1 and any values of σ_k, for doublet electronic states. The equations for $\Delta\sigma_k = \pm 1$ are then applied to the interpretation of the CH bands λ3900 and λ4300.

* Part of paper presented at Washington meeting of American Physical Society, Phys. Rev. **29**, 921A (1927).

[1] R. S. Mulliken, Phys. Rev. **30**, 138 (1927): V.

[2] R. S. Mulliken, Phys. Rev. **29**, 637 (1927): IV.

For the general procedure used in obtaining the intensity equations, reference should be made to V. We first write the equations which are applicable (neglecting the separation into doublets arising from interaction of j_k and s, and also neglecting σ-type doubling) for each of the three transitions $\Delta j_k = 0, \pm 1$, for each of the cases $\Delta\sigma_k = 0, \pm 1$. For the present purpose, these are best written in the compact form given by Hönl and London,[3] rather than in the more extended and obvious form given in III[4] of this series. As in V, *the j and j_k values of the new mechanics will be used*; and *in the equations below, j, j_k, and σ_k will always represent the larger of the two quantities j' and j'', j_k' and j_k'', or σ_k' and σ_k''.* After substituting j_k and σ_k for j and σ (their j numbering already corresponds to that of the new mechanics), the Hönl and London equations are as follows[5]:

For $\Delta\sigma_k = 0$ with $\Delta j_k = 0$,

$$i_0 = 2(2j_k+1)\sigma_k^2/j_k(j_k+1) \tag{1}$$

For $\Delta\sigma_k = 0$ with $\Delta j_k = \pm 1$,

$$i^{\pm} = 2(j_k^2-\sigma_k^2)/j_k \tag{2}$$

For $\Delta\sigma_k = \pm 1$ with $\Delta j_k = 0$

$$i_0 = (2j_k+1)(j_k+\sigma_k)(j_k-\sigma_k+1)/j_k(j_k+1) \tag{3}$$

For $j_k \to j_k-1$, if $\sigma_k \to \sigma_k-1$, or for $j_k-1 \to j_k$, if $\sigma_k-1 \to \sigma_k$,

$$i^{\pm} = (j_k+\sigma_k)(j_k+\sigma_k-1)/j_k \tag{4}$$

For $j_k-1 \to j_k$, if $\sigma_k \to \sigma_k-1$, or for $j_k \to j_k-1$, if $\sigma_k-1 \to \sigma_k$,

$$i^{\pm} = (j_k-\sigma_k)(j_k-\sigma_k+1)/j_k \tag{5}$$

We have now to consider the subdivision of the intensity corresponding to a given value of each of the quantities Δj_k and $\Delta\sigma_k$ into intensities of individual lines corresponding to particular values of j and Δj. The problem is in general more complicated than for the ${}^2S \to {}^2S$ transitions treated in V in that we have to consider transitions $\Delta j_k = 0$ as well as $\Delta j_k = \pm 1$. The equations for the cases $\Delta j_k = \pm 1$, borrowed from Sommerfeld and Hönl's paper on line spectrum multiplets, have been given in V (Eqs. 2–4, q.v.). For $\Delta j_k = 0$ the appropriate Sommerfeld and Hönl equations (Eqs. (5), (15), (20) of their paper[6] with notation, etc., suitably modified—cf. V—to fit the present case) are as follows:

$\Delta j = 0$,

$$i^0 = (2j_k+1)(2j+1)[j(j+1)+j_k(j_k+1)-s(s+1)]^2/jj_k(j+1)(j_k+1). \tag{6}$$

$\Delta j = \pm 1$,

$$i^{\pm} = (2j_k+1)[(j+j_k)(j+j_k+1)-s(s+1)][s(s+1)-(j-j_k-1)(j-j_k)] \\ /jj_k(j_k+1). \tag{7}$$

[3] H. Hönl and F. London, Zeits. f. Physik **33**, 803 (1925).

[4] R. S. Mulliken, Phys. Rev. **29**, 391 (1927): III.

[5] The proportionality constants are here so chosen that the sum of the intensities of all transitions to or from any state is equal to *twice* the a priori probability of that state; this factor two disappears in the final equations, since each j_k state gives rise to two j states.

[6] A. Sommerfeld and H. Hönl, Sitzungsber. der Preuss. Akad. der Wiss., phys.-math. Klasse, p. 141 (1925).

The procedure is now exactly analogous to that used in V. For *any* transition $\Delta j_k = +1$ or -1 between *doublet* electronic states, Eqs. (2a), (2b), and (3a) of V hold for the relative intensities of the components corresponding to the three possible combinations of j values. For a transition $\Delta j_k = 0$, there are for doublet electronic states ($s = \frac{1}{2}$) *four* possible j transitions, viz., $Q_1(j = j_k + \frac{1}{2})$, $Q_2(j = j_k - \frac{1}{2})$, ${}^QP_{21}(j' = j_k' - \frac{1}{2},\ j'' = j_k'' + \frac{1}{2})$, ${}^QR_{12}(j' = j_k' + \frac{1}{2},\ j'' = j_k'' - \frac{1}{2})$, where the symbols Q, P, R as usual denote $(j' - j'') = 0, -1, +1$, or, when used as superscripts, indicate similarly the value of Δj_k; in regard to the subscripts (cf. the following section. By appropriately substituting $j_k - \frac{1}{2}$ or $j_k + \frac{1}{2}$ for j in Eqs. (6) and (7), putting $s = \frac{1}{2}$, reducing, and omitting a common factor 8, the following equations for the relative intensities of these branches are obtained (the corresponding equations for line spectra are given by Sommerfeld and Hönl in the table at the top of p. 151 of their paper[6]):

$$Q_1(j = j_k + \tfrac{1}{2}), \qquad i_4 = j_k(2j_k + 3) \tag{6a}$$

$$Q_2(j = j_k - \tfrac{1}{2}), \qquad i_5 = (j_k + 1)(2j_k - 1) \tag{6b}$$

$${}^QP_{21} \text{ or } {}^QR_{12}(j = j_k + \tfrac{1}{2}), \quad i_6 = 1 \tag{7a}$$

For the case $\Delta j_k = 0$, the sum Σ^0 of the expressions i_4, i_5, and $2i_6$ (i_6 is taken twice because it corresponds to two components which are always simultaneously present) is $(2j_k + 1)^2$. For the case $\Delta j_k = \pm 1$, the corresponding sum $\Sigma^{\pm}(i_1 + i_2 + i_3$ of Eqs. (2a), (2b), (3a) of V) is $4j_k^2 - 1$ (cf. V). The intensity expression for any value of $\Delta\sigma_k$, Δj_k, and Δj can now be obtained by multiplying any desired one of the Eqs. (6a), (6b), (7a) of the present paper and (2a), (2b), (3a) of V, by a quantity i_x/Σ, where $\Sigma^{\pm}$ is used if $\Delta j_k = +1$ or -1, but Σ^0 if $\Delta j_k = 0$, while i_x is chosen—from Eqs. (1)–(5) above—to correspond to whatever values of $\Delta\sigma_k$ and Δj_k are desired.

For the case $\Delta\sigma_k = 0$, the final equations for the ten possible branches are as follows (in the special case $\sigma_k = 0$, the intensities vanish for four branches, and the remaining intensities agree with those given by Eqs. (5)–(7) of V):

$$P_1 \text{ or } R_1, \quad i = 2(j_k + 1)(j_k^2 - \sigma_k^2)/j_k(2j_k + 1) \tag{8}$$

$$P_2 \text{ or } R_2, \quad i = 2(j_k - 1)(j_k^2 - \sigma_k^2)/j_k(2j_k - 1) \tag{9}$$

$${}^PQ_{12} \text{ or } {}^RQ_{21}, \quad i = 2(j_k^2 - \sigma_k^2)/j_k(4j_k^2 - 1) \tag{10}$$

$$Q_1, \quad i = 2\sigma_k^2(2j_k + 3)/(j_k + 1)(2j_k + 1) \tag{11}$$

$$Q_2, \quad i = 2\sigma_k^2(2j_k - 1)/j_k(2j_k + 1) \tag{12}$$

$${}^QP_{21} \text{ or } {}^QR_{12}, \quad i = 2\sigma_k^2/j_k(j_k + 1)(2j_k + 1) \tag{13}$$

For the case $\sigma_k \to \sigma_k - 1$, (or, $\sigma_k - 1 \to \sigma_k$) the final equations are:

$$P_1(\text{ or, } R_1), \quad i = (j_k - \sigma_k)(j_k - \sigma_k + 1)(j_k + 1)/j_k(2j_k + 1) \tag{14}$$

$$P_2(\text{ or, } R_2), \quad i = (j_k - \sigma_k)(j_k - \sigma_k + 1)(j_k - 1)/j_k(2j_k - 1) \tag{15}$$

$${}^PQ_{12}(\text{ or, } {}^RQ_{21}), \quad i = (j_k - \sigma_k)(j_k - \sigma_k + 1)/j_k(4j_k^2 - 1) \tag{16}$$

$$R_1(\text{ or, } P_1), \quad i = (j_k + \sigma_k)(j_k + \sigma_k - 1)(j_k + 1)/j_k(2j_k + 1) \tag{17}$$

$$R_2(\text{ or, } P_2), \quad i = (j_k + \sigma_k)(j_k + \sigma_k - 1)(j_k - 1)/j_k(2j_k - 1) \tag{18}$$

$$^{R}Q_{21}(\text{ or, } {}^{P}Q_{12}),\quad i=(j_k+\sigma_k)(j_k+\sigma_k-1)/j_k(4j_k^2-1) \tag{19}$$

$$Q_1,\quad i=(j_k+\sigma_k)(j_k-\sigma_k+1)(2j_k+3)/(j_k+1)(2j_k+1) \tag{20}$$

$$Q_2,\quad i=(j_k+\sigma_k)(j_k-\sigma_k+1)(2j_k-1)/j_k(2j_k+1) \tag{21}$$

$$^{Q}P_{21}\text{ and }{}^{Q}R_{12},\quad i=(j_k+\sigma_k)(j_k-\sigma_k+1)/j_k(j_k+1)(2j_k+1) \tag{22}$$

Eqs. (20), (21), (22) are applicable for both cases $\Delta\sigma_k=\pm 1$, but, as indicated, the application of the other equations to the P, R, ^{P}Q, and ^{R}Q branches is reversed when the sign of $\Delta\sigma_k$ is reversed.

A Proposed Notation

The existence of satellite series for which $\Delta j\neq\Delta j_k$ has forced the adoption of a notation for such series. The notation used in Eqs. (8)-(22) for doublet bands is based on the following principles: (1) the large letter P, Q, or R denotes the value of Δj in accordance with the usual conventions; (2) a superscript letter is added to denote in a similar manner the value of Δj_k, which is really more important than Δj (even when case *a* is approached; where j_k loses its significance as a quantum number) in determining the *form* of the branches (cf. I of this series,[38] p. 492); in case the superscript letter is identical with the larger letter (e.g., ^{R}R), it may ordinarily be omitted without danger of confusion; (3) the subscripts denote, in the order given, the initial and final types of rotational states, e.g., $^{P}Q_{12}$ indicates a transition from an F_1 (*i.e.*, a j_k+s) to an F_2 (*i.e.*, a j_k-s) state; the notation $^{P}Q_{12}$ might be read "P-form Q_{12}"; when the initial and final subscripts are identical, only a single subscript need be written (e.g., $^{R}R_{11}$ can be written R_1); the notation F_1, F_2 as used for the general case is a natural extension of that previously adopted for ^{2}S states (cf. V) following Kratzer's method of designation; (4) each *individual* line in a series is to be denoted (in harmony with the prevailing convention) by a number in *parentheses* giving the value of j'' for the line (e.g., $^{R}Q_{21}(1\frac{1}{2})$). This notation has been chosen with the ideals of maximum simplicity and expressiveness tempered by the idea of changing as little as is consistently possible the customary designations of series in well known band spectra.

The notation here proposed (including the A, B subscripts discussed below) can be extended to case *b* electronic states of any degree of multiplicity; the various states which correspond to various orientations of s with respect to j_k can be denoted as F_1, F_2, F_3, $\cdots$, starting with F_1 for the parallel orientation; subscripts can then readily be assigned to the band-lines. The same system can also be used for case *a* electronic states (cf. definition on p. 794 below) and is very satisfactory for transition cases between *a* and *b*; a number of such transition cases will be discussed in VII of the present series. Thus *the notation proposed is uniformly applicable to all known bands of diatomic molecules.*

The use of superscripts is not really essential, and may be entirely omitted if desired, but it is very helpful in making obvious the classification of a line in terms of Δj_k. A possible alternative procedure, but only in the case of *doublet* electronic states, would be to dispense with the numerical subscripts in favor of the superscripts.

It will probably be best always to use the j values of the new mechanics, although the conventional j values, which are always $\frac{1}{2}$ unit higher, might be used; for simplicity in printing, but for no other reason, half-integral j values, which occur for odd molecules, might possibly be replaced by the next higher integers, as is commonly done in the case of line spectra.

In the National Research Council Report on Molecular Spectra, Birge has used a notation in which symbols such as P_4^+ and R_6^- have the same meaning as $P_1(3\frac{1}{2})$ and $R_2(5\frac{1}{2})$ here. Birge uses a number in parentheses in the form $P^+(4)$ to denote the empirical ordinal number M of a line in its series, counting the first line as 1. The use of such symbols as P^+ and P^-, while better than the present subscript notation in that it brings directly to mind the quantities $+\epsilon$ and $-\epsilon$, is unfortunately hardly capable of extension to triplet and higher multiplicities. The ordinal number M might be retained by writing e.g. $P_2[6]$ when $M=6$ but $P_2(6)$ if $j''=6$. In view of recent progress, however, M will probably be needed less often than formerly.

Extension of Theory and Notation to Include σ-Type Doubling

Eqs. (8)–(22) and the notation proposed above are incomplete in one respect: they neglect σ-type doubling. Empirically (cf. II[7] and VII of this series, and treatment of CH bands below) and theoretically[8] every rotational state $F_i(j)$, $i=1, 2$, etc., is single if $\sigma_k=0$ (S states), double if $\sigma_k>0$ (P, D, $\cdots$ states). Since this σ-type doubling is of an entirely different nature from the multiplicity due to the spin and indicated by the numerical subscripts, it seems desirable to use literal subscripts such as A and B to distinguish the two rotational sub-levels—following the method first used for singlet electronic states, in II.

Selection rules. Certain selection rules are operative which reduce the number of observed branches below the conceivable number. The following formulation of these rules for *singlet* electronic states is in agreement with the experimental facts (cf. II). The observed P and R branches ($\Delta j=\pm 1$) differ from the observed Q branches ($\Delta j=0$) in the following way: (1) in $^1P\rightarrow{}^1S$ (or $^1S\rightarrow{}^1P$) transitions the P and the R branch go only from (or to) one set—which we shall (*ordinarily*) *define* as the "B" set—of the ^1P rotational levels, while the Q branch goes only from (or to) the *other* set of levels which we shall (*ordinarily*) *define* as the "A" set; (2) in $^1D\rightarrow{}^1P$ (and presumably in $^1P\rightarrow{}^1P$, etc.) transitions, two branches of each kind occur, in such a way that if the two sets of initial levels were suitably labelled a, b and the two sets of final levels c, d, then the P and R branches could be said to correspond to combinations $a\rightarrow c$ and $b\rightarrow d$; and if so, the Q branches would correspond to $a\rightarrow d$ and $b\rightarrow c$.

For singlet states, $j=j_k$ and $\sigma=\sigma_k$. Since in general (doublets, triplets, etc.) the existence of σ-type doubling is associated with $\sigma_k>0$, rather than with $\sigma>0$, according to Hund's theoretical work[8,9] (cf. IV, Swan bands, in

[7] R. S. Mulliken, Phys. Rev. **28**, 1202 (1926): II.
[8] F. Hund, Zeits. f. Physik **36**, 657 (1926).
[9] F. Hund, Zeits. f. Physik **40**, 742 and **42**, 93 (1927).

regard to experimental evidence), we may expect that the above selection rules which hold when $s=0$, also hold *in general*, but in such a way that the permitted transitions depend in Hund's case b on the value of Δj_k rather than on that of Δj. These expectations are supported by the data on the OH, ZnH, and other bands, as will be shown in VII. For case a, where j_k is no longer a quantum number, the proper selection rules are readily obtained by an imagined adiabatic passage from case b to case a.[10]

Notation: assignment and meaning of subscripts A and B. In the preceding paragraph A and B rotational sub-states *for P electronic states* are arbitrarily defined in a way which will probably ordinarily prove unambiguous. Suitable definitions of A and B rotational states for S, D and other electronic states are somewhat difficult to give. One would naturally wish to give the designation A (or B) always to states which have something in common physically, and which differ in respect to this common property, or perhaps quantum number, from all states designated B (or A).

In II, after A and B states had been defined as above for ^1P electronic states, the question was raised as to whether the rotationally single ^1S states should be classed as A or B states, and whether—in (^1P, ^1S) *and other* combinations—the Q, or the P and R, branches show "crossing-over" ($A\rightarrow B$, $B\rightarrow A$). Since (cf. II, p. 1205, ref. 4) "the terms are presumably of the same rotational type for all ^1S states," it seemed evident that crossing-over is impossible in $^1S\rightarrow{}^1S$ transitions. Since the latter have only P and R branches, it was concluded that crossing-over is absent here (*i.e.*, in this case, that only $B\rightarrow B$ combinations occur), and by analogy probably in general in such branches, but that it is characteristic of Q branches; also, that ^1S states are B states. (We should now specify $\Delta j_k=\pm 1$ rather than P and R branches, and $\Delta j_k=0$ rather than Q branches.) These conclusions furnished automatically a means of classifying states as A or B,[11] and it also appeared that the designations A and B had the desired sort of physical significance.

But recent theoretical work of Hund[9] indicates that S states may be physically of either of two types which differ in a way at least partly like that in which A and B sub-states of P or other electronic states differ.[12]

[10] In case a, the *scale* of the doubling depends markedly, to be sure, on the orientation of s,—cf. ref. 15a and text (N_2 bands) of ref. 2.

[11] But in the case of a band not involving an S state, the choice of A or B for a particular set of rotational states would be indeterminate unless a P, S band having a common initial or final state were known.

[12] Extending work of Heisenberg, Hund has shown[9] that the observed peculiarities of the He_2, N_2, N_2^+, and Swan bands can be accounted for very beautifully by the new quantum mechanics. This not only yields the characteristic alternate missing or weakened lines but also gives correct selection rules for the σ-type doubling. For molecules *with equal nuclei*, and $\sigma_k>0$, it appears that A and B sub-states differ in that the one set has a Schrödinger ψ function (whose electronic factor is) symmetrical in the nuclei, the other, one which is antisymmetrical (of course this is not necessarily the *only* difference). If $\sigma_k=0$, the (electronic part of) ψ may be *either* symmetrical or antisymmetrical. These symmetry properties give rise to characteristic selection rules. In the case of He_2 this theory is in exact agreement with the scheme of energy levels given[7] in II. In the case of the N_2, N_2^+, and Swan bands, the Heisenberg-Hund explanation is simpler and more satisfying than that suggested by the writer in IV. The new interpretations also yield interesting conclusions in regard to nuclear spin.

Hund's work also indicates[12] that *physically like* states combine in transitions $\Delta j_k = 0$ and physically *unlike* states in transitions $\Delta j_k = \pm 1$. These results rob the designations A and B and the "Q crossing-over rule," as given above, of any sure claim to physical meaning in the sense desired, and in fact make it likely that "A" states of some electronic states or molecules may be physically *similar* to "B" states of others, and vice versa.

The theory is unfortunately not sufficiently developed or verified as yet to make it feasible to assign systematically the desired physically significant subscripts. Hence it seems best for the present to use the designations A and B merely as a necessary means of indexing observed terms. Later when the nature of σ-type doubling is better understood, these can be readily replaced by other physically appropriate literal subscripts.

The following arbitrary procedure for assigning the designations A and B is suggested: (1) in the case of a P state for which a (P,S) combination is known, the designations A and B are ordinarily[15] to be assigned according to the definition already given (item (1) above under "Selection rules"), or if necessary[15] in the reverse manner; (2) starting from the designations for a P state, the designations A, B for S and D levels are ordinarily[15] to be assigned on the basis of the convention that branches having $\Delta j_k = \pm 1$ correspond to $A \rightarrow B$ or $B \rightarrow A$ transitions while branches having $\Delta j_k = 0$ correspond to $A \rightarrow A$ or $B \rightarrow B$ transitions; *this convention is precisely opposite to that which was used in II*[13,14] and which was there thought to have a

---

The same selection rules which exist in σ-type doubling for molecules with equal nuclei, and which are there explained by the symmetry character of the ψ functions, are found in molecules with unequal nuclei (cf. II, also VII and present discussion of CH bands). Hund concludes (*l. c.*, foot p. 111) that the same cause must be effective here, in other words that even with very unequal nuclei, the ψ functions are nearly symmetric or antisymmetric.

[13] This change is desirable because, since it is based on the same considerations which meet with such success in explaining alternating intensities, Hund's selection principle (*real* "crossing-over" in a physical sense in the branches $\Delta j_k = \pm 1$) is probably[14] correct. If this is true, the new convention will then, *for a given band-system or group of connected band-systems*, give the same designation A (or B) only to physically similar states, and thus will minimize confusion when the ultimate physically significant subscripts are assigned.

[14] The absence of $^1S \rightarrow {}^1S$ and $^1P \rightarrow {}^1P$ transitions in He_2 seemed to constitute strong evidence for the writer's conclusions in II, but is now explained by another selection principle given by Hund according to which $\Delta\sigma_k = 0$ is not possible if the two states concerned happen to be alike in symmetry character. That this last condition is fulfilled for the known He_2 bands is shown for the ^1P states, if we grant the correctness of Hund's *other* selection principles,[12] by the identical missing-line type of all the known $m^1P \rightarrow 2^1S$ bands, and for the ^1S states by the identical type of the $m^1S \rightarrow 2^1P$ bands. The absence of $^1S \rightarrow {}^1S$ transitions between the known ^1S states of He_2 is *also* required in Hund's theory by the impossibility of crossing-over for the P and R branches here, since the known ^1S states are all of one symmetry type.

[15] If for a P, D or other state, observed combinations linking it (directly or indirectly) with an S state are not known, the designations A and B must be assigned arbitrarily; if a P, S combination is later discovered, it may then turn out that the A, B designations assigned for the P state conflict with rule (1) above; in this case the designations need not be changed, but in accordance with rule (2) the S state levels must now be designated as B levels. In case a P state should be found to combine in opposite ways with two different S states, as seems possible according to Hund's theory, rule (1) must again be suspended for one of the bands and the S levels for this band must also be designated B levels.

physical meaning; it leads to an opposite labelling of D states (e.g., in He_2, Fig. 2 of II), leaves previous designations unchanged for P states, and, contrary to II, causes S rotational levels to be designated ordinarily as A levels. In some cases exceptions must be made to the above procedure[15]; no objection can be made to this on theoretical grounds, since the use of the above arbitrary labelling scheme is purely a matter of convenience. Such a scheme, even with exceptions, seems preferable, however, to a purely random procedure, and probably cannot easily be bettered until a sure basis is established for a physically descriptive nomenclature.

Complete notation. The notation discussed in the section entitled "A Proposed Notation," and used in Eqs. (8)–(22), can now be extended by the addition of subscripts A and B. The latter will be used with substantially the same conventions (cf. item 3 of the first paragraph of the above section) as for the numerical subscripts; these conventions have in fact already been used for σ-type doubling in II (cf. Eqs. 1 and 2).[7] The probable A, B selection rules, analogous, in the way required by the assumptions stated above, to those involved in Eqs. (1) and (2) of II, as here revised according to item 2 of the preceding paragraph, can now be embodied in the notation. The notation for the entire set of expected branches in the general case for doublet bands is as given in Table I, where the notation given in parentheses is *complete*, while that outside the parentheses is to be used under ordinary circumstances if there is no danger of misunderstanding. The meaning of the notation will be made clearer by a study of Fig. 2 as an example of the general case.—The method of designating A and B states given in the preceding paragraph has been so chosen that Table I always corresponds to the expected selection rules, even under the exceptional circumstances mentioned in ref. 15.

TABLE I

Notation for expected branches in general case of transition between doublet electronic states of Hund's case b type.

Main branches		Satellites	Main branches	Satellites
$P_{1A1B}({}^{P}P_{1A1B})$	$P_{2A2B}({}^{P}P_{2A2B})$	${}^{P}Q_{1A2B}$	$Q_{1B}({}^{Q}Q_{1B1B})$	${}^{Q}P_{2B1B}$
$R_{1A1B}({}^{R}R_{1A1B})$	$R_{2A2B}({}^{R}R_{2A2B})$	${}^{R}Q_{2A1B}$	$Q_{1A}({}^{Q}Q_{1A1A})$	${}^{Q}P_{2A1A}$
$P_{1B1A}({}^{P}P_{1B1A})$	$P_{2B2A}({}^{P}P_{2B2A})$	${}^{P}Q_{1B2A}$	$Q_{2B}({}^{Q}Q_{2B2B})$	${}^{Q}R_{1B2B}$
$R_{1B1A}({}^{R}R_{1B1A})$	$R_{2B2A}({}^{R}R_{2B2A})$	${}^{R}Q_{2B1A}$	$Q_{2A}({}^{Q}Q_{2A2A})$	${}^{Q}R_{1A2A}$

Special cases. In the general case, all the indicated twenty branches are to be expected, but only half of them in ${}^2S\rightarrow{}^2P$ and ${}^2P\rightarrow{}^2S$ transitions. In these two cases, the Q, ${}^{Q}P$, and ${}^{Q}R$ branches with subscript B ordinarily[15] drop out, because of the absence of B sub-states for ${}^2S$ terms; half of the P, R, ${}^{P}Q$, and ${}^{R}Q$ branches also drop out (ordinarily[15] those with the BA subscript if the *initial* state is ${}^2S$, those with the AB subscript if the *final* state is ${}^2S$). In such transitions, the subscripts can therefore usually be considered as understood and can therefore be omitted when the electronic transition is specified. In ${}^2S\rightarrow{}^2S$ transitions, only six branches are possible, all of which are alike in respect to literal subscripts, so that the latter can usually be omitted.

If bands are discovered in which there are branches where the usual σ-type selection rules do not hold (this seems to be the case in some of the OH satellite series), the new branches can easily be designated by the method proposed above.

Intensity relations. According to Hund's theory, A and B rotational sub-states should have the same a priori probability, except in the case of molecules with equal nuclei. In III, it was assumed[4] (cf. pp. 399–400) that, aside from the alternate missing lines in He_2, A and B sub-states are practically identical in respect to probabilities of transition as a function of σ, j, $\Delta\sigma_k$, Δj, etc., and in respect to a priori probabilities, and it was found that the experimental data on singlet systems support this assumption. A similar assumption may therefore reasonably be made in general. In accordance with this, we shall expect Eqs. (8)–(13) and (14)–(22) to hold, in the case of doublet bands—multiplied by suitable weight factors for alternate lines in case the nuclei are equal—for any line without regard to its literal subscripts. Thus, with unequal nuclei, two lines differing only in their literal subscripts (such as occur in the general case of twenty-branch bands) should have the same intensity. Similar considerations may be expected to hold in the case of triplet and higher multiplicities.

General Considerations in Regard to the Order of F_1 and F_2 Levels

In order correctly to interpret observed band structures in transitions between doublet electronic states, it is necessary to consider how the sign and magnitude of the separation of corresponding F_1 and F_2 levels (*i.e.*, of levels $F_1(j+1)$ and $F_2(j)$, which in case b have the same j_k) should vary in passing from ideal case a to ideal case b, and how it should differ for normal and inverted doublets. The present discussion is qualitative only; the problem is treated elsewhere by Kemble[16,16a] from a quantitative standpoint.

For simplicity, let us consider only doublet states ($s=\frac{1}{2}$). Theory[16] and experiment (cf. VII) agree in requiring that in an imagined transition from a very strong negative magnetic interaction (case a, inverted doublets) through zero interaction (case b) to a very strong positive interaction (case a, normal doublets), the σ_k+s (e.g., $^2P_{1\ 1/2}$, if $\sigma_k=1$) states of inverted case a pass into the $j_k+s(F_1)$ states of case b and thence into the $\sigma_k-s(^2P_{1/2})$ states of normal case a, while the $\sigma_k-s(^2P_{1/2})$ states of inverted case a pass into the j_k-s states of case b and thence into the $\sigma_k+s(^2P_{1\ 1/2})$ states of normal case a. These relations are illustrated in Fig. 1. Case b and the two cases a are of course only ideal limiting cases. Strictly speaking, ideal case b does not always exist, since when the magnetic interaction is zero, s ceases to be definitely oriented with respect to j_k, j loses its significance as a quantum number, the designations F_1 and F_2 are no longer appropriate, and the structure becomes indistinguishable from that for the case $s=0$ of a molecule

[16] E. C. Kemble, Phys. Rev. **30**, 387 (1927). Cf. E. C. Kemble and F. A. Jenkins, Phys. Rev. **29**, 607A (1927).

[16a] E. C. Kemble, forthcoming paper in Phys. Rev.

with $2s$ less electrons[17]; the rotational energy is now given by the nuclear kinetic energy $E^m = B[j_k(j_k+1)-\sigma_k^2]+\cdots$ alone. But even when the primary magnetic interaction is zero, as always in ^2S states, the magnetic field developed by molecular rotation will usually (at least for the larger values of j_k) permit quantization of j.

It will be convenient to use the designations F_1 and F_2, first applied to case b, throughout the entire range of magnetic interactions. Thus in the region of case a those states which on gradually decreasing the magnetic interaction would pass into F_1 (or F_2) states of case b will be *defined* as F_1 (or F_2) states; in exceptional cases, however (cf. second paragraph following), another method of definition will be used.

In fully developed case a, F_1 and F_2 states of equal j are widely separated and it is natural to divide the sets of lines constituting e.g. a $^2P\rightarrow{}^2S$ band into a $^2P_{1/2}\rightarrow{}^2S$ and a $^2P_{1\ 1/2}\rightarrow{}^2S$ sub-band, the subscript of ^2P referring to the value of σ (equal to $\sigma_k \pm \frac{1}{2}$), which is constant in case a for each sub-band. When the magnetic interaction is small, however, σ is no longer constant, the states $F_1(j+1)$ and $F_2(j)$ form more or less close doublets, and the division into sub-bands and the designations $^2P_{1/2}$ and $^2P_{1\ 1/2}$ become artificial.

Considering a ^2P state by way of example, the lowest F_2 state of case b, $F_2(\frac{1}{2})$, shows a peculiar behavior. For inverted doublets, nothing unusual happens: the widely separated lowest states $F_1(1\frac{1}{2})$ and $F_2(\frac{1}{2})$ of case a pass smoothly into a close doublet in case b, the separation falling to zero with the magnetic interaction. For normal doublets, however, we have on the one hand in case a the $^2P_{1\ 1/2}$ states with $j=1\frac{1}{2}, 2\frac{1}{2}, \cdots$ and the $^2P_{1/2}$ states with $j=\frac{1}{2}, 1\frac{1}{2}, \cdots$, and on the other hand in case b the F_2 states with $j=\frac{1}{2}, 1\frac{1}{2}, \cdots$ and the F_1 states with $j=1\frac{1}{2}, 2\frac{1}{2}, \cdots$. All the $^2P_{1\ 1/2}$ states go over into corresponding F_2 states, and all the $^2P_{1/2}$ states except $j=\frac{1}{2}$ into F_1 states. There remain to be correlated the $^2P_{1/2}$ state with $j=\frac{1}{2}$ and the case b state $F_2(\frac{1}{2})$, and it appears that the one must go over into the other[18] in spite of the fact that all the other $^2P_{1/2}$ states are correlated with F_1 states of case b. On account of the latter it seems best to define the lowest $^2P_{1/2}$ state likewise as $F_1(\frac{1}{2})$ regardless of the fact that this conflicts with the method of definition given above, and to say that $F_1(\frac{1}{2})$ of case a goes over into $F_2(\frac{1}{2})$ of case b; in intermediate cases one might speak merely of $F(\frac{1}{2})$.—A similar procedure can be used for ^2D and other states.

In general, the part of the total molecular energy which varies with j includes both nuclear kinetic energy and magnetic energy. Considering always a pair of corresponding levels $F_1(j+1)$ and $F_2(j)$, it will be seen that the kinetic energy part of the difference F_1-F_2 (measured by Bm^2, m being the vertical vector in Fig. 1) is always positive, with a minimum value zero in case b at the point where the magnetic interaction is zero. The magnetic energy part of the difference F_1-F_2, on the other hand, is always negative

[17] Some of the apparently singlet system ($s=0$) bands of helium[7] and hydrogen (O. W. Richardson, Proc. Roy. Soc., 1926) may perhaps really have $s=1$ but with a magnetic interaction too small to produce an observable fine structure. In such a case the observable intensity and other relations should be exactly the same as for true singlets.

[18] Cf. ref. 16, also F. Hund, Zeits. f. Physik 42, 113 (1927), Fig. 8.

except in a region extending from the place where the magnetic interaction and energy are zero to a place, lying on the normal-doublet side of zero, where the intensity of the interaction is such that s stands perpendicular to σ_k ($\pm\epsilon$ positions) so that the *energy* is again zero. In this region (cf. Fig. 1) the magnetic part of $F_1 - F_2$ is positive. The *net* difference $F_1 - F_2$ is evidently negative in case a, either normal or inverted, but positive in the region just described as well as for some distance outside in the direction of normal case a (possibly also in some part of the inverted-doublet region).—For a given interaction, the sign of $F_1 - F_2$ may in some cases change as j is increased.[16,16a]

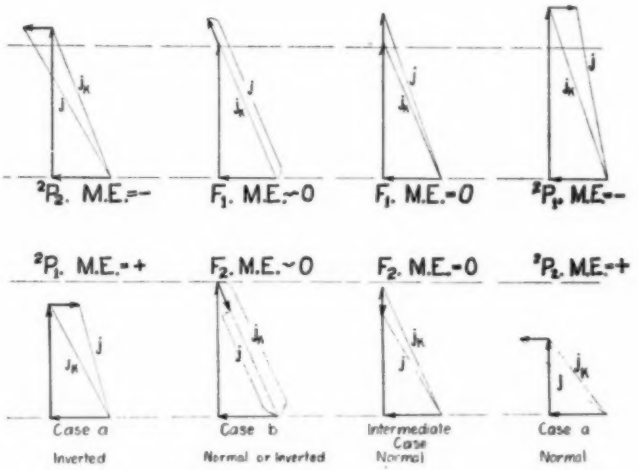

Fig. 1. Vector diagrams showing composition of σ_k (horizontal, medium length heavy line), m (long vertical line), and s (short vector) to give j_k and j, for various orientations of s. The proportions used correspond to $\sigma_k = 1$, $s = \frac{1}{2}$, with $j = 2$ (for F_2 and related states, lower line) or $j = 3$ (for F_1 and related states, upper line); this gives $j_k = 2\frac{1}{2}$ in case b. The j and j_k values are in terms of the old numbering, but, even aside from this, the geometrical relations shown should not be taken too literally, in view of the new mechanics. The figure gives an idea how the kinetic energy (proportional to m^2) and magnetic energy (M. E.) vary in passing from case b through intermediate cases to either normal or inverted case a. The kinetic energy is a minimum at case b, for F_1 terms, a maximum for F_2 terms. The designation "M. E.~0" instead of "M. E. = 0" for case b is intended to suggest that the ideal case b is not possible (j would not be quantized if there were no magnetic interaction); cf. discussion in text.

The special case in which s lies near the $\pm\epsilon$ positions for very low (and therefore also for higher) values of j is of interest; here the magnetic energy should be practically zero, and the existing, kinetic energy, difference should be given (aside from changes required by the new mechanics) by the Kramers and Pauli formula[19]

$$E^m = Bm^2 + \cdots = B\left[(j^2 - \sigma^2)^{1/2} \mp \epsilon\right]^2 + \cdots$$

[19] The Kramers and Pauli formula is always formally a correct expression (in the old quantum theory) for the nuclear kinetic energy (cf. E. C. Kemble, Bulletin on Molecular Spectra, pp. 310–12), although the quantities σ and ϵ in general vary with j and have no particular physical significance.

with $\epsilon \sim s \sim \frac{1}{2}$ and $\sigma = \text{const.} = \sigma_k$. This gives $F_1(j+1) > F_2(j)$ for all values of j, but with $F_1 - F_2$ approaching zero as j increases. As Kratzer has shown,[20] the experimental ΔF values for the common final electronic state of the CH bands λλ3900 and 4300 can be accurately reproduced by such a formula, with integral j values, $\sigma = 1$, and $\epsilon = \frac{1}{2}$, and it seems very probable that this ^2P state is one in which the above situation is actually realized.

The above conclusion is strongly supported, as Kemble shows elsewhere[16] by the fact that Kratzer's value of B and the probable value of the magnetic interaction (cf. last section of present paper) have the right magnitude to cause s to lie close to the $\pm\epsilon$ positions. For $F_1(1\frac{1}{2})$ and $F_2(1\frac{1}{2})$ there are to be sure considerable deviations, and for $F_2(\frac{1}{2})$ a large deviation, from the ϵ positions, but it so happens that the total, magnetic plus kinetic, energy is almost the same as if the ϵ positions had been maintained.[16a]

Application of the Theory to Interpretation of the CH Bands λ3900 and λ4300

General. The following interpretation of the CH bands λ3900 and λ4300 is based on the data and analysis of Heurlinger and Hulthén[21] and on the very thorough analysis of Kratzer.[20] Kratzer's conclusions are here critically reviewed and in some cases modified, in the light of the present theory, and additional conclusions in regard to missing lines and intensity relations are given, based on the data of Hulthén.

The bands λ3900 and λ4300 have two sets of $\Delta_2 F''$ values in common (cf. Kratzer's Table 20), showing that both bands have the same final electronic state.[22b] According to Hulthén's analysis, there are twelve branches in the λ4300 band but only six, with typical Q combination defects, in λ3900. From Hulthén's data and reproductions, the order of intensity of the branches for low values of j is $R > Q > P$ in λ4300, but $Q > P > R$ in λ3900. Assuming that additional weak branches for which $\Delta j \neq \Delta j_k$ have passed unnoticed, all of these relations are in agreement with theory if the λ4300 and λ3900 bands are $^2D \rightarrow {}^2P$ and $^2S \rightarrow {}^2P$ transitions respectively. We shall now attempt to show in detail that this interpretation is in agreement with the observed facts.

Notation. The notation proposed in the first part of the present paper will be used in designating lines, branches F and ΔF values, etc. Tables II

[20] A. Kratzer, Zeits. f. Physik **23**, 298 (1924).

[21] T. Heurlinger, Diss. Lund, 1918. T. Heurlinger and E. Hulthén, Zeits. f. Wiss. Phot. **18**, 241 (1919). E. Hulthén, Zeits. f. Physik **11**, 284 (1922); Dissertation Lund (1923).

[22] In Kratzer's Tables 1–4 for λ4300 there are small systematic deviations from the expected equalities in the sense that the $(R-Q)$ $\Delta_1 F$'s are pretty consistently slightly larger than the $(Q-P)$ $\Delta_1 F$'s. The uniform direction of these deviations is not explainable by such relations as $F'_{1A} \neq F'_{1B}$ and $F'_{2A} \neq F'_{2B}$ nor by any reasonable modification of the adopted term-scheme. The writer is convinced that the discrepancies in question are a result of slight errors in the experimental data. (*b*) If all the recorded frequencies are relatively slightly too high in the P branches, the above discrepancies would be accounted for, *as well as* the discrepancies between the $\Delta_2 F_{1B}''$ values (cf. Kratzer's Table 20) for the λ3900 and λ4300 bands. In the latter case it is very improbable that the existence of the observed near-agreement between data on two different bands could be due to chance, and there is no theoretical reason here for expecting *slight* discrepancies.

TABLE II

Revised notation for CH λ4300.

Present	P_{1B1A} (3½)	P_{1A1B} (3½)	Q_{1A} (2½)	Q_{1B} (2½)
Kratzer	P_1 (4)	P_3 (4)	Q_1 (3)	Q_3 (3)
Hulthén	$P_{11}(4)$	$P_{12}(4)$	$Q_{11}(3)$	$Q_{12}(3)$
Present	R_{1B1A} (1½)	R_{1A1B} (1½)	P_{2B2A} (2½)	P_{2A2B} (2½)
Kratzer	R_1 (2)	R_3 (2)	P_2 (4)	P_4 (4)
Hulthén	$R_{11}(2)$	$R_{12}(2)$	$P_{21}(4)$	$P_{22}(4)$
Present	Q_{2A} (1½)	Q_{2B} (1½)	R_{2B2A} (½)	R_{2A2B} (½)
Kratzer	Q_2 (3)	Q_4 (3)	R_2 (2)	R_4 (2)
Hulthén	$Q_{21}(3)$	$Q_{22}(3)$	$R_{21}(2)$	$R_{22}(2)$
Present	F_{1A}' (2½) =	F_{1B}' (2½)	F_{2A}' (1½) =	F_{2B}' (1½)
Kratzer	F_1 (3) =	F_3 (3)	F_2 (3) =	F_4 (3)
Present	F_{1A}'' (1½)	F_{1B}'' (1½)	F_{2A}'' (½)	F_{2B}'' (½)
Kratzer	f_1 (2)	f_3 (2)	f_2 (2)	f_4 (2)

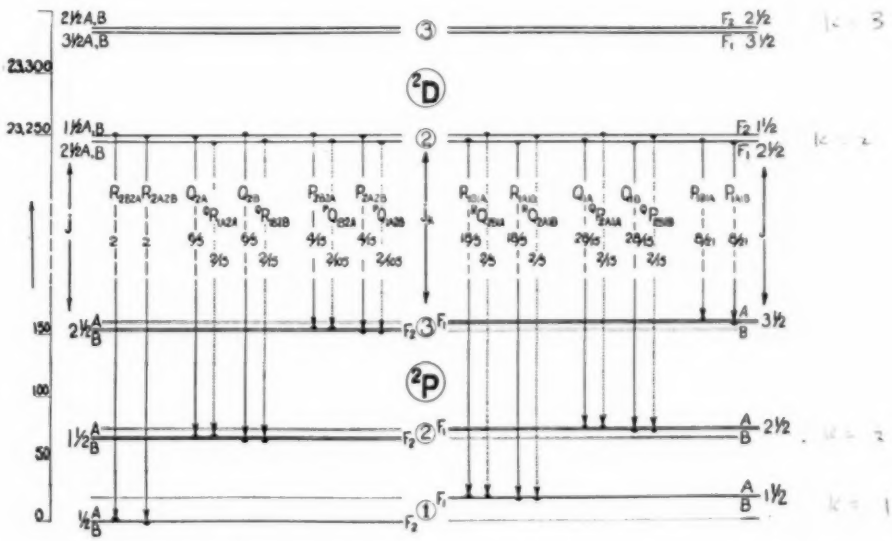

Fig. 2. *Lowest rotational levels, and first line of each branch, with theoretical intensity, for CH* λ4300. The rotational levels shown are all drawn to scale, in accordance with Kratzer's analysis (see *text, "analysis of* λ4300*" and following section*), except that the A-B doublet separations in the ^2P states, and the F_2-F_1 separations in the ^2D states, are *exaggerated three-fold*. The existence of a *latent* $A-B$ doubling is to be assumed in each F_1 and F_2 level of the ^2D states (giving altogether four ^2D levels for each value of j_k). The correctness of the assignment of j and j_k values and of subscripts in Fig. 2 is made probable by theoretical considerations given in the text.

The twelve "main" branches (full lines in Fig. 2) are identified in the text with the twelve observed branches; out of the eight predicted weak satellite branches, only the few strongest lines have been found (cf. Table V). In regard to intensity relations in the higher members of the main branches cf. Table IV. That the summation rule ($\Sigma i = p = 2j+1$) is fulfilled for each individual rotational level can readily be verified for the levels with $j_k' = 2$ and for those with $j_k'' = 1$ (to make the test for other levels, additional lines would need to be drawn in the figure).

and VII show in what way the notations of Hulthén and Kratzer correspond to that adopted here; they also give the *first line* to be expected in each (strong) branch. The correctness of the designations and of the assignment of j values will be made probable in the subsequent discussion. The assignment of the literal subscripts in Table I is based on a study of λ3900, taken in connection with the A,B selection rules assumed to hold in λ4300 (cf. Table I).

Analysis of λ4300. The λ4300 band will be discussed first. The structure can best be understood by a study of Fig. 2. This shows how the energy levels are numbered and arranged and how transitions between them can give rise to the predicted twenty branches. The "main" branches, represented by full lines in Fig. 2, correspond to the twelve known branches; the predicted intensities of the remaining ("satellite") branches are so low that one can hardly hope to do more than find a few of their strongest lines. The figure is so drawn that each "satellite" line is placed adjacent to a "main" line which should actually lie close to it in the spectrum. Only the first line of each branch is shown, together with its theoretical intensity as calculated from Eqs. (14)–(22). The general course of the theoretical intensities for higher values of j_k can be seen from an inspection of the equations (also cf. Table V): in the main branches, the intensity should rise steadily (neglecting the Boltzmann factor), in the satellite branches it should fall steadily, with increasing j_k.

Kratzer's analysis shows,[23] by verifying certain combination relations (cf. Tables 1–4 of his paper) that the twelve known branches actually are related as in Fig. 2. It also shows[23,24] that $F_{1A}' = F_{1B}'$ and $F_{2A}' = F_{2B}'$ within experimental error (in regard to assignment of A or B subscripts, (cf. text preceding Table II); in other words, the σ-type doubling is vanishingly small

[23] Kratzer's relations in his Table 1–2 are of the type $R_{1B1A}(j) - Q_{1A}(j) = Q_{1A}(j+1) - P_{1B1A}(j+1)$. According to the present interpretation (this can be understood from a diagram such as Fig. 2, after drawing in additional lines of each strong branch), which follows Mecke's term-scheme,[24] the experimental verification of this equation shows that $F_{1B}'(j+1) - F_{1A}'(j) = F_{1A}'(j+1) - F_{1B}'(j)$, which is the same thing as $F_{1B}'(j+1) + F_{1B}'(j) = F_{1A}'(j+1) + F_{1A}'(j)$. From this we conclude that $F_{1A}'(j) = F_{1B}'(j)$; the equalities $\Delta_1 F_{1A}'(j) = \Delta_1 F_{1B}'(j)$ and $\Delta_1 F_{2A}'(j) = \Delta_1 F_{2B}'(j)$ have also been established by Kratzer[25] in another way (cf. his Table 5).

Kratzer assumed that the P, Q, and R branches all involve (what are here defined as) $B \to A$ and $A \to B$ transitions only, in which case the quantities on both sides of the first equation of the preceding paragraph should represent exactly $\Delta_1 F_{1A}'(j)$, i.e. $F_{1A}'(j+1) - F_{1A}'(j)$. Experimentally there is no means of deciding, from the present data, between Kratzer's and Mecke's term-schemes, but the latter is to be preferred for reasons stated in the text.

Kratzer's relations in his Tables 3–4 are of the type $R_{1B1A}(j) - Q_{1A}(j+1) = Q_{1A}(j) - P_{1B1A}(j+1)$. According to Mecke's term-scheme, the quantities on the left and right sides of the equation should represent respectively $\Delta_1 F_{1A}''(j) + F_{1B}'(j+1) - F_{1A}'(j+1)$ and $\Delta_1 F_{1A}''(j) + F_{1A}(j) - F_{1B}'(j)$, and their equality again shows $F_{1A}'(j) = F_{1B}'(j)$, in addition to verifying the assignment of j'' values and other features of the term-scheme.

[24] Kratzer thinks that the equality $\Delta_1 F_{1A}'(j) = \Delta_1 F_{1B}'(j)$ may possibly not hold for $j < 3\frac{1}{2}$, and similarly with $\Delta_1 F_{2A}'(j) = \Delta_1 F_{2B}'(j)$ for $j < 2\frac{1}{2}$. (Kratzer's statement is that the equalities are definitely established by the data only for $m \geqq 4$). But this now seems highly improbable, since the separations $F_A - F_B$ should theoretically diminish steadily with j, and since the *lowest possible* values of j, according to Fig. 2, are $2\frac{1}{2}$ for F_1' and $1\frac{1}{2}$ for F_2'.

in the initial, ^2D, states of λ4300. Thus there is no direct experimental evidence that this doubling is present, but the assumption of its latent existence gives an explanation of the presence of twelve strong branches in this band as compared with six in the otherwise very similar λ3900 band, and also explains the apparent absence of crossing over. The assumption that crossing over really is present was first suggested by Mecke,[25] from analogy with the He_2 λ5733 band; the aptness of this analogy is evident, since the latter is now classified[7] as $^1D \rightarrow {}^1P$.

FORM AND INTERPRETATION OF FINAL TERMS (COMMON TO ΛΛ3900, 4300)

Having established the combination relations, Kratzer showed that the observed $\Delta_1 F''$ values in λ4300 can be accurately reproduced (cf. his Tables 7 and 8)[26] by assuming the following (Kramers and Pauli) term-forms[27]:

$$F_{iA}''(j) = 14.207\left\{\left[(j+\tfrac{1}{2})^2-\sigma^2\right]^{1/2}-\rho\right\}^2-1.447\times10^{-3}\left\{\left[(j+\tfrac{1}{2})^2-\sigma^2\right]^{1/2}-\rho\right\}^4+\cdots \tag{24}$$

In Eq. (24), $\sigma=1$, and $\rho=+\frac{1}{2}$ for $i=1$, $-\frac{1}{2}$ for $i=2$; the appearance of $j+\frac{1}{2}$ in place of j is equivalent to the use of the integral j values of the old quantum theory.[28] For the F_{iB}'' terms the same equations hold except for a slight change in the coefficients (to 14.170 and 1.436×10^{-3}).

In his Table 22, Kratzer shows that when differences $F_{1A}''(j)-F_{2A}''(j-1)$ and $F_{1B}''(j)-F_{2B}''(j-1)$ are formed from F'' values calculated from the above equations, these agree excellently, even for the lowest values of j, where these differences are large, with corresponding differences[29] obtained from the experimental data *for λ3900*. We can therefore adopt Kratzer's expressions for F'' as correct empirical expressions, aside from a possible additive constant, for the *entire* energy of the molecule (including nuclear rotational and vibrational energy, magnetic energy, etc.) in the common final electronic state of CH ΛΛ3900 and 4300. Kratzer's Tables 7–8 and 22 indicate that the errors in the F'' values calculated from these expressions

[25] R. Mecke, Phys. Zeits. **26,** 219 (1925); Zeits. f. Physik **28,** 261 (1924).

[26] In Kratzer's Tables 7 and 8, the first line of each table ($m=1$) should be omitted since "$m=1$" is physically non-existent according to the present interpretation. In the line "$m=2$," under $\Delta f_1(m)$ in Table 7, the datum 55.4 should be added in the "observed" column (cf. Kratzer's Table 3), while in the line "$m=3$" under $\Delta f_2(m)$ in the "observed" column in Table 7 the datum 86.6 should be replaced by 86.9 (cf. Table 3).

[27] Kratzer shows beyond reasonable doubt (pp. 308–9, 310–11) that the coefficient B of the quadratic term in the F'' expressions should really be *slightly* different for F_{1A}'' than for F_{2A}'' and for F_{1B}'' than for F_{2B}''; also that the B values for F_1' and F_2' must differ slightly.

[28] Kratzer's m and $m-1$ of his Eqs. (10a) and (10b), respectively, *both* correspond to $j+\frac{1}{2}$ in the present numbering.

[29] The experimental differences here are somewhat affected by slight contributions from the *initial* states, but these can be discounted (cf. discussion below under λ3900). In Kratzer's Table 22, the datum 18.05 can be added in the column $R_4(m)-R_2(m)$ opposite $m=2$ (this addition is based upon two new R lines identified by the writer,—cf. below under λ3900). Approximate $\Delta_1 F''$ values can also be calculated from λ3900, which after allowance for combination defects due to the presence of only six branches (cf. Fig. 3), agree with those of Kratzer's Tables 7–8. They supply a new "observed" $\Delta_1 F$ for "$m=2$", under "$\Delta f_2(m)$" and under "$\Delta f_4(m)$", which agrees with the calculated values (these particular ΔF's cannot be obtained for λ4300).

should not exceed one or two tenths of a wave number unit, at least for small and moderate j values. In Figs. 2 and 3, the spacing of the F'' levels is in accordance with Kratzer's F'' equations. The lowest levels are taken as $F_{2\alpha}''(\frac{1}{2})$ and $F_{1\alpha}''(1\frac{1}{2})$, where $\alpha=A$ or B; the levels $F_{1\alpha}''(\frac{1}{2})$ calculated by Kratzer in his Tables 7–8 are here supposed non-existent.[28]

The altogether probable interpretation of Kratzer's F'' equations, which give an asymptotic equality[30] of $F_{1\alpha}''(j)$ and $F_{2\alpha}''(j-1)$ for large j values,

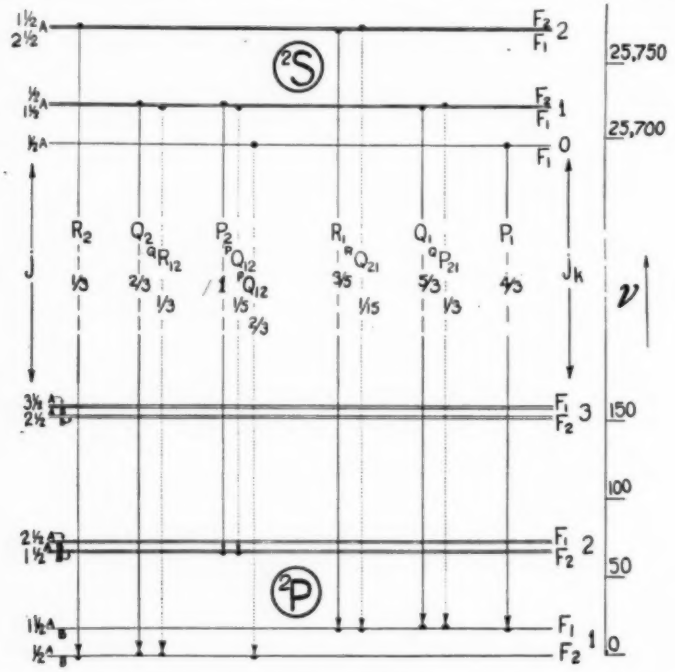

Fig. 3. *Lowest rotational levels, and first line of each branch, with its theoretical intensity, for CH* λ3900. The rotational levels shown are all drawn to scale, as in Fig. 2, except that the A-B doublet separations in the ^2P states, and the F_2-F_1 separations in the ^2S states, are exaggerated. The actual $F_2'-F_1'$ separations are so small that it is not certain even that $F_2'>F_1'$. The assignment of j and j_k values and of numerical subscripts is discussed in the text. The literal subscripts, here omitted, can be read from the diagram (assuming that all ^2S states are A states); they have been assigned in analogy to $^1S\rightarrow{}^1P$ transitions (cf. text, table I and paragraph following).

The theoretical intensity given for the first line of each branch has been calculated from Eqs. (14)–(22), from which also the trend for higher j values can be determined. On account of the smallness of the $F_2'-F_1'$ separations, all satellites except $^PQ_{12}(\frac{1}{2})$ should be superposed on, and add to the intensity of, the corresponding main lines. The fulfillment of the summation rule can readily be verified for the levels $F_1'(\frac{1}{2})$, $F_2'(\frac{1}{2})$, $F_1''(1\frac{1}{2})$, $F_2''(\frac{1}{2})$.

is that they correspond to a *normal* ^2P electronic state, approximating Hund's case b, in which the coefficient B and the magnetic interaction happen to be of such magnitudes that s is oriented approximately as $\pm\epsilon$ even for low values of j, so that the magnetic energy approximately vanishes and the Kramers

[30] It is possible[29] that at some high value of j the separation $F_{1\alpha}''(j)-F_{2\alpha}''(j-1)$ passes through zero to negative values, or that it reaches a minimum and again increases.

and Pauli formula with $\sigma = \sigma_k = 1$ is applicable (cf. preceding section, p. 795–6). Granting this, the proper assignment of F_1'' and F_2'' designations, and the correct j values, are immediately obvious from Kratzer's F'' expressions, while the j_k values are given by $j - \frac{1}{2}$ for the F_2'' and by $j + \frac{1}{2}$ for the F_1'' levels. The missing lines in λ3900 and λ4300 are incapable (cf. Fig. 2) of giving decisive evidence in support of this assignment of j values and of F_1'' and F_2'' designations, but the intensity relations for low values of j, both in λ3900 and in λ4300, are in agreement with it, and it has accordingly been adopted in Tables II–III and Figs. 2–3.

Missing lines in λ4300. In Hulthén's table of frequencies for λ4300 (Dissertation,[21] pp. 52–53), many lines are given which do not belong to the twelve main series. Hulthén has arranged part of these in series to form a second band[31] (probably this is a 1,1 vibrational transition, while the main band is 0,0, —as suggested by Kratzer[32]); but many, in part intense, lines, remain. The first lines of the P_1, Q_1 and R_1 branches as given by Hulthén are exactly the same as in Fig. 2, but his P_2, Q_2 and R_2 branches all begin with j values one unit higher than those of Fig. 2. Hulthén notes (Dissertation, p. 45) that the first line of each series is already rather strong, and concludes that earlier lines are missing for theoretical reasons. This is exactly the present point of view,[33] except that one more line should be present in each of the P_2, Q_2 and R_2 branches. As a matter of fact, lines of fairly appropriate intensity are present in Hulthén's tables in the proper positions (cf. following paragraph) as follows[33]: $\nu = 23{,}248.0$ (int. 4) fits as $R_{2B2A}(\frac{1}{2})$ plus $R_{2A2B}(\frac{1}{2})$; $\nu = 23{,}181.0$ (int. 3) as $Q_{2B}(1\frac{1}{2})$ plus $Q_{2A}(1\frac{1}{2})$, while $\nu = 23{,}181.7$ (int. 3) is now regarded[34] as $Q_{2B}(2\frac{1}{2})$ plus $Q_{2A}(2\frac{1}{2})$; $\nu = 23{,}094.6$

[31] Hulthén states in his dissertation that the two bands have a common set of final terms, but, as Dr. Hulthén has stated in a letter to the writer, this is erroneous.

[32] Kratzer also suggested that the two bands might constitute two components of an electronic doublet.

[33] Kratzer has attempted to extend all the branches down to low values of j and has tentatively picked out lines which fit fairly well in the following positions (cf. his Tables 14–15).

(*a*) $P_1(3)$, $Q_1(2)$, $P_2(3)$, $P_2(4)$, $Q_2(3)$, $P_3(3)$, $Q_3(2)$;
(*b*) $P_-(2)$, $Q_2(2)$, $R_2(2)$, $P_4(2)$, $Q_4(2)$, $R_4(2)$, $R_3(1)$;
(*c*) $P_4(3)$, $P_4(4)$, $Q_4(3)$.

The lines are given in Kratzer's notation. In this assignment, many observed frequencies have been used more than once. A critical examination shows that there are discrepancies of one wave number unit or more (well beyond the probable experimental error) for all members of the first group (*a*), in respect to combination relations which they should satisfy (cf. Kratzer's Tables 16–19, etc.) in view of the demonstrated relation[23] $F_{iA}' = F_{iB}'$; these deviations can be explained only if the equalities $F_{iA}' = F_{iB}'$ suddenly fail for the lowest values of j, which is very improbable;[25] accordingly these lines may probably be rejected. The lines in group (*b*) cannot be tested by combination relations, but $R_2(2)$ at least can be rejected as not falling properly on the extrapolation of the R_2 branch. The lines in group (*c*) definitely satisfy the proper combination relations. Having shown that many of Kratzer's lines are probably not genuine, we shall rather arbitrarily throw out all the remaining lines of group (*b*), except $R_4(2)$, as unproven, and also shall reject $P_4(3)$ of group (*c*) as fortuitous (this is justifiable, since an extrapolation of the recognized lines of the P_4 branch would lead to an intensity below 1 for $P_4(3)$, whereas the observed line is of intensity 3). This leaves $R_4(2)$, $Q_4(3)$, and $P_4(4)$,—or $R_{2A2B}(\frac{1}{2})$, $Q_{2B}(1\frac{1}{2})$, and $P_{2A2B}(2\frac{1}{2})$ in the present notation; these correspond to the frequencies which are discussed in the text (q. v.).

[34] Hulthén assigned 23,181.0 as $Q_{2A}(2\frac{1}{2})$ and 23,181.7 as $Q_{2B}(2\frac{1}{2})$.

(int. 1) as $P_{2B2A}(2\frac{1}{2})$ plus $P_{2A2B}(2\frac{1}{2})$, or possibly as $P_{2A2B}(2\frac{1}{2})$ only. The double use of the frequencies 23,248.0, 23,181.7, and 23,094.6 is entirely reasonable, since the previously assigned lines show that the doublet separations $R_{2B2A}-R_{2A2B}$, $Q_{2A}-Q_{2B}$, and $P_{2B2A}-P_{2A2B}$ each converge toward zero with j; even for $j''=1\frac{1}{2}$, R_{2B2A} and R_{2A2B} are not resolved, while according to the present interpretation,[34] the same is true of $Q_{2A}(2\frac{1}{2})$ and $Q_{2B}(2\frac{1}{2})$. The intensity relations $R>Q>P$ for the newly assigned lines are also correct (cf. Fig. 2).

Form and interpretation of initial terms of λ4300. We can test the assignments just made, and at the same time calculate the values of F' (denoting by F' the *entire* energy of excitation), by means of certain theoretical relations which will be evident from Fig. 2. They are as follows:

$$F_{iA}'(j)=F_{iB}'(j)=R_{iBiA}(j-1)+F_{iA}''(j-1)=R_{iAiB}(j-1)+F_{iB}''(j-1)=Q_{iA}(j)+F_{iA}''(j)=Q_{iB}(j)+F_{iB}''(j)=P_{iBiA}(j+1)+F_{iA}''(j+1)=P_{iAiB}(j+1)+F_{iB}''(j+1),\text{ with } i=1 \text{ or } 2. \quad (25)$$

The values of F' as calculated for a few of the lowest j values are given in Table III. It will be seen that the lines assigned above, all of which involve the level $F_2'(1\frac{1}{2})$, give values for this level which not only are concordant among themselves, but whose mean fits satisfactorily into the series of F' levels.

It is important to note that the j' values are definitely fixed (granting the correctness of the designations of the various branches as P, Q, and R) by the j'' values, and are subject to uncertainty only in so far as the latter are uncertain. The assignment of the designations F_1' and F_2' to particular initial levels in Fig. 2 and Table III and Eq. (25) is however based solely on the theory, according to which the twelve main branches should correspond to $F_1'\rightarrow F_1''$ and $F_2'\rightarrow F_2''$ transitions; the correctness of the F_1'', F_2'' designations was made probable (cf. above) by theoretical considerations, and the F_1' and F_2' designations then follow. The subscripts A and B for the initial states are also fixed by those of the final states in accordance with the assumed selection rules implied in Table I; those for the final states are determined from λ3900 (see below).

From Table III it can be seen that $D=F_2'(j)-F_1'(j+1)$ has at first a small positive value which decreases, but less and less rapidly, with increasing[35] j. It is of interest to follow D to high values of j. Starting from $D(4\frac{1}{2})=F_2'(4\frac{1}{2})-F_1'(5\frac{1}{2})=+0.49$, we can obtain successive values of D for increasing j by adding successive values of $\Delta_1D(j)=\Delta_1F_2'(j)-\Delta_1F_1'(j+1)$, starting with $\Delta_1D(4\frac{1}{2})=[F_2'(5\frac{1}{2})-F_2'(4\frac{1}{2})]-[F_1'(6\frac{1}{2})-F_1'(5\frac{1}{2})]$.[36] For $\Delta_1D(4\frac{1}{2})$ we find $173.44-173.65=-0.21$, giving $D(5\frac{1}{2})=+0.28$. The series

[35] Kratzer's Table 6 shows in another way that $\Delta_1F_{1A}'=\Delta_1F_{1B}'>\Delta_1F_{2A}'=\Delta_1F_{2B}'$; also that (*granting* $F_2'>F_1'$) $F_2'-F_1'$ decreases, but with diminishing rapidity, as j increases.

[36] The Δ_1F_1' values can be obtained from Kratzer's Table 1 and the Δ_2F_2' values from his Table 2; in each case the *mean* of his two mean values should be used, since on account of $F_{1A}'=F_{1B}'$ and $F_{2A}'=F_{2B}'$, his two means in each table should differ only because of experimental error.

of $\Delta_1 D$ values continues as follows: -0.12, -0.11, -0.14, -0.14, -0.06, -0.04, -0.21, -0.05. $+0.03$, -0.02, $+0.06$, $+0.15$, $+0.16$, -0.10, $+0.02$, $+0.19$, $+0.04$, while the D values, beginning with $D(6\frac{1}{2})$, are $+0.16$, $+0.05$, -0.09, -0.23, -0.29, -0.33, -0.54, -0.59, -0.56, -0.58, -0.52, -0.37, -0.21, -0.31, -0.29, -0.10, -0.06. These D values are probably correct within a few tenths or perhaps half a wave number unit, since the cumulative errors in the mean ΔF values used in the calculation, plus slight errors in the F'' values used in obtaining D in Table III, probably do not exceed this amount.

TABLE III

Initial term values for λ4300, referred to $F_{2B}''(\frac{1}{2})$ as zero level.

Source	$F_1'(2\frac{1}{2})$	$F_2'(1\frac{1}{2})$	$F_1'(3\frac{1}{2})$	$F_2'(2\frac{1}{2})$	$F_1'(4\frac{1}{2})$	$F_2'(3\frac{1}{2})$	$F_1'(5\frac{1}{2})$	$F_2'(4\frac{1}{2})$
$R_{iBiA}(j-1)$	23,246.4 *	248.0 *	333.94*	335.1 *	450.31	450.98	595.38	595.79
$R_{iAiB}(j-1)$	246.4 *	248.0 *	333.74*	334.9 *	450.23	451.02	595.32	595.85
$Q_{iA}(j)$	246.47*	248.24*	333.95	335.42*	450.27	450.91	595.18	595.76
$Q_{iB}(j)$	246.27*	248.06*	333.85	335.00*	450.19	451.00	595.36	595.87
$P_{iBiA}(j+1)$	246.62*	248.3 *	333.99	334.75	450.35	450.93	595.47	595.78
$P_{iAiB}(j+1)$	246.20*	247.9 *	333.81	335.06	450.18	451.08	595.33	595.90
Average	23,246.40	248.08	333.90	335.04	450.26	450.99	595.34	595.83
$F_2'-F_1'=D$	1.68		1.14		0.73		0.49	

Notes. (*a*) A* indicates that the same line has been used twice in the calculation on account of an unresolved A–B doublet (e. g. $R_{iBiA}(1\frac{1}{2})$ and $R_{iAiB}(2\frac{1}{2})$, (*b*) The F'' values used in accordance with Eq. (25) to obtain the above results are those given in Kratzer's Tables 7 and 8 (and calculated from Eq. 24), except that a correction of -3.54 wave numbers has been made to all, in order that the lowest level $F_{2B}''(\frac{1}{2})$ shall serve as an arbitrary zero of energy. (*c*) The slight systematic discrepancies between the F' values calculated using F_{iA}'' and F_{iB}'' values may be attributed to slight inaccuracies in Kratzer's F'' formulas.

The diminishingly rapid contraction of an initially small separation $F_2'-F_1'$ is exactly the situation expected for a very nearly ideal case *b* electronic state.[37] The term-separation should here correspond chiefly to *magnetic* energy, the nuclear kinetic energy being given very nearly for both F_2 and F_1 by $B[j_k(j_k+1)-\sigma_k^2]+\cdots$. Neglecting the magnetic energy, this gives $\Delta_1 F(j_k)=F(j_k+1)-F(j_k)=2B(j_k+1)$; σ_k does not appear in $\Delta_1 F$ (cf. discussion in I, pp. 490–92).[38] If we compute $\Delta_1 F$ values from Table III, using the means of the pairs $F_1'(2\frac{1}{2})$ and $F_2'(1\frac{1}{2})$, $F_1'(3\frac{1}{2})$ and $F_2'(2\frac{1}{2})$, etc., the successive $\Delta_1 F$ values are roughly 87, 116, 145, or 29×3, 29×4, 29×5. These are of the expected form if $2B\sim29$ and if $j_k=2$ for $F_1'(2\frac{1}{2})$ and $F_2'(1\frac{1}{2})$, 3 for $F_1'(3\frac{1}{2})$ and $F_2'(2\frac{1}{2})$, etc. These j_k values are exactly those demanded by the theory, for case *b* with $s=\frac{1}{2}$, to match the

[37] Kratzer (Eqs. 12 and Table 9) represents F_1' and F_2' by Kramers and Pauli formulas with $\sigma=0.5$, and $\rho=-\frac{1}{2}$ for F_1' and $\rho=+\frac{1}{2}$ for F_2'. This reversal of the ρ values in the Kramers and Pauli formula is a necessary consequence of the observed inversion of the order of the F_1' and F_2' levels as compared with the F_1'' and F_2'' levels. The corresponding reversal of the j values involves the interpretation of certain branches as having $\Delta j=+2$ or -2 (this can be seen by reversing the order of the two j' values corresponding to a given j_k, in Fig. 2, but leaving the j'' values, which are the same as Kratzer's except for the downward shift of $\frac{1}{2}$ unit to the new mechanics, untouched). Kratzer does not mention this point, but it is a convincing argument against his use of the Kramers and Pauli formula here.

[38] R. S. Mulliken, Phys. Rev. **28**, 481 (1926): I.

j' values which were already fixed by other considerations (cf. above). If the above interpretation is correct, the relation $F_2'' > F_1'$ shows that the ^2D state is inverted (cf. discussion in preceding section, p. 794-5), unlike the ^2P final state. An explanation of this and of the small magnitude of the magnetic energy will be given in the last section of the paper.

Intensity relations in λ4300. The experimental data on intensity relations for the twelve recognized branches, obtained from Hulthén's table of data (Dissertation, pp. 52–53), are given in Table IV for the early lines of each branch (data on higher-numbered lines can be found in Hulthén's table). The course of the observed intensities agrees qualitatively with the theoretical predictions. For the lowest values of $\bar{\jmath}$ (mean of j' and j'') the predicted order of intensity $R > Q > P$ is obviously fulfilled. The data also support the predicted intensity relation $R_1(j+1) > R_2(j)$ for low values of j, with asymptotic equality for high values of j, as well as the corresponding relations for the P and Q branches. The expected equality of intensity of branches differing only in respect to literal subscripts is very definite.

TABLE IV

Observed intensities in λ4300 (eye estimates).

j''	R_{1B1A}	R_{1A1B}	R_{2B2A}	R_{2A2B}	Q_{1A}	Q_{1B}	Q_{2A}	Q_{2B}	P_{1B1A}	P_{1A1B}	P_{2B2A}	P_{2A2B}
½	———	———	4(4)		———	———	———		———	———	———	———
1½	10*(7.2)		4(5.3)		———	———	3(2.4)		———	———	———	———
2½	6(7.6)		5(3.2)	5(3.2)	4(3.7)		3(4.8)		———	———	1(0.5)	
3½	5(4.2)	5(4.2)	6	6	3(3.2)	3(3.2)	6*(3.5)	4(3.5)	4(0.8)		3(0.6)	3(0.6)
4½	6	6	7	7	4(4.4)	4(4.4)	5	6	4(0.8)	4(0.8)	4(1.1)	4(1.1)
5½	7	7	8	8	6*	4	5	5	4(1.3)	4(1.3)	5	5
6½	8	8	7	12*	6	6*	9*	7	5	5	9*	6
7½	7	12*	7	7	6	9*	7	7	6	9*	7	7
8½	7	7	6	6	7	7	8	6	7	7	6	6
9½	6	6	5	5	6	6	6	7	6	6	5	5
10½	5	5	6*	4	6	6	5	5	5	5	4	4
11½	4	4	7*	3	5	5	5	4	4	4	4	4
12½	7*	3	5*	3	10*	4	7*	4	4	4	7*	4

Notes. For the first one or two lines of each branch, the intensity given represents the sum of the intensities for an unresolved doublet. The figures *in parentheses* are i values, calculated for a few of the lines from Eqs. (14)–(22); in the cases where an unresolved doublet was observed, the sum of the (equal) i values of the components is given. A* denotes superposition of a line of another branch.

Quantitatively, the agreement is not good. The P branches are much too strong, being as intense as the Q branches and more intense than the R branches for high values of j. The Q branches are relatively weaker than predicted; their maximum intensity is equal to that of the P branches and less than that of the R branches. These deviations are very similar to those[4] in the He_2 λ5733 band ($^1D \rightarrow {}^1P$), and suggest that the Hönl and London equations are inaccurate when σ_k is large—possibly because of a lack of the rigid coupling of σ_k assumed by the theory. In the present case as in λ5733, however, the intensity type is very different[4] from that for other values of σ_k' and σ_k'', and strongly supports the classification $D \rightarrow P$.

The relative intensities of lines such as $R_1(j+1)$ and $R_2(j)$ appear to approach equality too rapidly with increasing j. Possibly this is because we are not dealing with an *ideal* case b transition.

Satellite lines in λ4300. As already noted above (first paragraph under "analysis of λ4300"), the predicted intensities of the "satellite" lines are for the most part so low that one cannot hope to detect these lines by ordinary methods. The most intense satellite lines, according to the theory, should be as follows (cf. Eqs. (14)–(22) and Fig. 2), in order of diminishing intensity: ${}^{R}Q_{21}(1\frac{1}{2})$, int. 0.40, calculated wave number equal to $R_1(1\frac{1}{2})+1.7$; ${}^{R}Q_{21}(2\frac{1}{2})$, int. 0.19, position $R_1(2\frac{1}{2})+1.1$; ${}^{Q}R_{12}(1\frac{1}{2})$ and ${}^{Q}P_{21}(2\frac{1}{2})$, each int. 0.13, respective positions $Q_2(1\frac{1}{2})-1.7$ and $Q_1(2\frac{1}{2})+1.7$; ${}^{R}Q_{21}(3\frac{1}{2})$, int. 0.12, position $R_1(3\frac{1}{2})+0.7$, etc.; in each case the *intensity* given applies to *each* of the two possible combinations of literal subscripts; the calculated *positions*, which are the same for both combinations of literal subscripts because the $A-B$ doublets in the corresponding "main" lines are not resolved, were readily obtained from the data of Table III taken in connection with the diagram of Fig. 2.

Lines are present in Hulthén's table (Dissertation, pp. 52–3) which may be identified with the four theoretically most intense satellite lines; these are given in Table V. Three fall in positions not hitherto assigned to other lines, and have reasonable intensities. In view of the large number of u-n assigned lines in λ4300, too much weight should not be attached to these agreements. Nevertheless, the presence of lines in the predicted positions, in all cases where a detectable intensity is expected, gives marked support to the theory. Further work on the intensity relations and satellite lines in λ4300 would be desirable.

TABLE V

Satellite lines in λ4300

Identification	Wave No.	Int.	Position	
			Obsd.	Calcd.
${}^{R}Q_{21}(1\frac{1}{2})$	23,230.1	2(0.80)	$R_1(1\frac{1}{2})+1.7$	$R_1(1\frac{1}{2})+1.7$
${}^{R}Q_{21}(2\frac{1}{2})$	23,261.7	1(0.38)	$R_1(2\frac{1}{2})+1.2$	$R_1(2\frac{1}{2})+1.1$
$[{}^{Q}R_{12}(1\frac{1}{2})$	23,179.4*	4*(0.27)	$Q_2(1\frac{1}{2})-1.6$	$Q_2(1\frac{1}{2})-1.7]$
${}^{Q}P_{21}(2\frac{1}{2})$	23,174.6	1(0.27)	$Q_1(2\frac{1}{2})+1.6$	$Q_1(2\frac{1}{2})+1.7$

Notes. In each case the satellite line, like the main line, is here regarded as an unresolved doublet corresponding to both possible combinations of the literal subscripts. The position $\nu=23,179.4$ is already occupied by the strong line $Q_{1A}(4\frac{1}{2})$, so that the independent presence of ${}^{Q}R_{12}(1\frac{1}{2})$ cannot be proved.

Analysis of λ3900. As already noted, the observed relations in λ3900—six strong branches, with Q combination defects and intensities in the order $Q>P>R$, indicate a ${}^2S\rightarrow{}^2P$ transition.

Kratzer has shown by a comparison of Δ_2F'' values (cf. his Table 20) that the two P and R branches of λ3900 have final states identical with those of two of the P, Q, and R branches (P_3, P_4, Q_3, Q_4, R_3, and R_4 in Kratzer's notation) of λ4300, and in another way (cf. his Table 21) that the two Q branches of λ3900 have their final states in common with the *other* two P, Q, and R branches (P_1, P_2, Q_1, Q_2, R_1, R_2 in Kratzer's notation) of λ4300.

In accordance with the considerations advanced in the section above on "Extension of theory to σ-type doubling," we may reasonably expect to find selection rules, in particular, the existence of "crossing-over" in the P

and R but not in the Q branches, analogous to those for $^1S \rightarrow {}^1P$ bands. This expectation is fulfilled; the designations of the branches used here (Table VI and Fig. 3) and the choice of subscripts A and B have been made accordingly; literal subscripts for λ4300 (cf. Table II), which could not be assigned on the basis of the structure of that band alone, were thereby also determined. The assignments of j' values and of the designations F'_1 and F_2' here are based, in accordance with the theory—in particular with the selection rule $\Delta j = 0, \pm 1$—on the j'', F_1'', F_2'' assignments already made. Fig. 3 and Table VI have been constructed on this basis. The final levels in Fig. 3 are drawn identical with those in Fig. 2.

TABLE VI

Revised notation for CH λ3900.

Present[a,e]	$P_1(1\frac{1}{2})$	$Q_1(1\frac{1}{2})$	$R_1(1\frac{1}{2})$	$P_2(1\frac{1}{2})$	$^PQ_{12}(\frac{1}{2})$	$Q_2(\frac{1}{2})$	$R_2(\frac{1}{2})$
Hulthén[b,e]	$P_1(2)$	$Q_1(2)$	$R_1(2)$	$P_2(3)$	$P_2(2)$	$Q_2(2)$	$R_2(2)$
Kratzer[b,e]	$P_3(2)$	$Q_1(2)$	$R_3(2)$	$P_4(3)$	$P_4(2)$	$Q_2(2)$	$R_4(2)$
New	$F_1'(\frac{1}{2})$			$F_2'(\frac{1}{2})$		F'' (cf. Table II)	
Kratzer[d]	$G_1(1), G_3(1)$			$G_2(1), G_4(1)$			

Notes. (*a*) Literal subscripts have been omitted (cf. "Special cases" under "Extension of Theory and Notation to σ-type Doubling," above). (*b*) The lines $R_1(1\frac{1}{2})$ and $R_2(\frac{1}{2})$ were not identified by Hulthén or Kratzer (cf. text). (*c*) Hulthén's and Kratzer's m numbering is the same as the present j_k numbering. (*d*) Kratzer assumed the existence of a special set of initial states G_1 and G_2 for the Q branches, distinct from G_3 and G_4 of the P and R branches, and did not assume "crossing over" in P and R branches. Mecke's suggestion[16] that there are only two sets of initial states, and that crossing over occurs, has been adopted here. (*e*) Hulthén's $P_2(2)$ is now classified as the first member of the satellite series $^PQ_{12}$, while higher members of the P_2 branch are believed to consist of a P_2 and $^PQ_{12}$ line superposed, but with the latter becoming weaker and weaker as j increases; similarly the Q_2, R_1 and Q_1 lines are presumably unresolved doublets consisting of a main line and a satellite (cf. Fig. 3).

Missing lines and satellite series in λ3900. Fig. 3 shows the first possible line in each branch as predicted by the theory. As will be seen from the figure, there is no likelihood of detecting any satellite line in this band except $^PQ_{12}(\frac{1}{2})$. This is actually present according to Hulthén's data (cf. Table VI). All other satellite lines, for low values of j, should be so close to their companions as to be unresolvable, on account of the smallness of the separations $F_2' - F_1'$ (cf. below); for high values of j their predicted intensities are too low for observation. In several cases the intensities of main lines should, however, be appreciably increased for low j by unresolved satellites (cf. Fig. 3).

The first line of each branch as recorded by Hulthén is exactly that predicted for a $^2S \rightarrow {}^2P$ transition,[39] except for the absence of the first R_1 and of the first R_2 line. On examination of Hulthén's reproduction, however (Dissertation, p. 56, Fig. 12, 2), a weak line is found in the calculated position in each case: $R_1(1\frac{1}{2})$, calculated,[40] $\nu = 25{,}756.7$, measured from Hulthén's

[39] Hulthén gives an additional line $P_1(1)$, equivalent in the present notation to an impossible line $P_1(\frac{1}{2})$.

[40] The calculation is made by using Kratzer's calculated F'' values in conjunction with the mean F' values obtained from the P and Q lines (cf. "initial terms of λ3900," and Table VIII).

reproduction,[41] $\nu = 25{,}756.5$; $R_2(\frac{1}{2})$, calculated, $\nu = 25{,}774.6$, measured 25,774.6.

Hulthén has shown that the P_2, Q_2, and R_2 lines, also the line ${}^PQ_{12}(\frac{1}{2})$, show identical Zeeman effects, while the P_1, Q_1, and R_1 lines have a different Zeeman effect. These two kinds of Zeeman effect are evidently due to the F_2'' and F_1'' states respectively (no appreciable Zeeman splitting is to be expected[42] for the initial, ${}^2S$, states with their very narrow doublets $(F_2 - F_1)$).

The fact that the "satellite" line ${}^PQ_{12}(\frac{1}{2})$ fits perfectly as the first member of the P_2 branch, both in position and Zeeman effect, is as expected (taking into account the lack of appreciable separation of F_2' and F_1' for low j), and so is not an argument against the assignment given. If the line in question really were $P_2(\frac{1}{2})$, it would follow that there are two states $F_1'(\frac{1}{2})$ and $F_2'(-\frac{1}{2})$ both with $m = j_k' = 0$ (cf. Fig. 3). This lacks sense, but with the j numbering used by the writer in I–IV of this series, these two states would have appeared as $F_1'(1)$ and $F_2'(0)$, derived from $m = \frac{1}{2}$. The existence of this line (and of an analogous line in the OH bands) thus led the writer to conclude[37] that a level $F_2(0)$ exists in ${}^2S$ states. But the revised j numbering of the new mechanics shows the invalidity of the conclusion, while the theory for Hund's case b now satisfactorily explains the existence of the line.

Intensity relations in λ3900. From Hulthén's reproduction (Dissertation, p. 56, Fig. 12, part 2) it is clear that the Q lines are much stronger than the P and R lines, as predicted. So far as can be seen, the P lines are stronger than the R lines for low j values, as expected; evidence for this is perhaps also Hulthén's failure to notice the first lines of each R branch (cf. above).

Even for fairly large values of j, there is a perceptible difference in intensity between the components of each of the doublets which are formed by lines corresponding to the same values of j_k but opposite orientations of s (i.e., $P_1(j+1)$ and $P_2(j)$, $Q_2(j+1)$ and $Q_1(j)$, $R_1(j+1)$ and $R_2(j)$). These differences, which are such that $P_1 > P_2$, $Q_1 > Q_2$, $R_1 > R_2$, for the components of a doublet, become very marked for the smallest values of j, as can be seen from Hulthén's reproduction (cf. also Hulthén's statement on p. 43). The observed differences are of exactly the kind predicted (cf. theoretical intensities given in Fig. 3, and Eqs. (14)-(22)). They give valuable confirmation of the assignment of the subscripts 1 and 2, hence of the j values, for given j_k values, in both the bands λλ3900 and 4300.

Initial state terms of λ3900. The discussion preceding Table III, for λ4300 (q.v.), is again applicable here with minor changes (Fig. 3 should be substituted for Fig. 2, and Table VII for Table III, while in Eq. (25) the terms $F_{iB}(j)$ and all sums including lines with subscript B or BA should be omitted; other changes are obvious). F' values for λ3900, calculated as in λ4300 with the help of Kratzer's F'' values assumed as correct, are given in Table VII.

[41] In a letter to the writer, Dr. Hulthén agrees that these lines are probably genuine.

[42] Cf. E. C. Kemble, National Research Council Report on Molecular Spectra in Gases, p. 349.

TABLE VII

Initial term values for λ3900, referred to $F_{2B}''(\frac{1}{2})$ as zero level.

Source	$F_1'(\frac{1}{2})$	$F_1'(1\frac{1}{2})$	$F_2'(\frac{1}{2})$	$F_1'(2\frac{1}{2})$	$F_2'(1\frac{1}{2})$	$F_1'(3\frac{1}{2})$	$F_2'(2\frac{1}{2})$	$F_1'(4\frac{1}{2})$	$F_2'(3\frac{1}{2})$
$^PQ_{12}(j)$	25,698.72								
$P_i(j+1)$	698.93	724.09	724.11	774.56	774.52	850.14	850.19	950.68	950.81
$Q_i(j)$		724.13	724.03	774.64	774.53	850.22	850.19	.80	.71
$R_i(j-1)$				774.49	774.57	850.22	850.29	.78	.87
Average	25,698.83	724.11	724.07	774.56	774.54	850.20	850.22	950.75	950.80
$F_2'-F_1'$		−0.04		−0.02		0.02		0.05	

The agreement of the F' values calculated from P, Q, and R branches gives strong support to the correctness of Kratzer's F'' values, and to the term scheme given in Fig. 3. For the lowest values of j, it is evident that $F_1'(j+1)=F_2'(j)$ within experimental error. For higher values of j there is evidence,[43] but not entirely satisfactory, that $F_2'(j)>F_1'(j+1)$. Only one case (the initial state of the CaH B bands) is definitely known in which $F_2>F_1$ for a ^2S state; usually $F_1>F_2$.[1] Both F_1' and F_2' can be expressed for low values of j by $F'(j_k)=25{,}698.8+12.62j_k(j_k+1)$, with $j_k=0, 1, 2, \cdots$; if we assume $j_k=j-\frac{1}{2}$ for the F_1', $j+\frac{1}{2}$ for the F_2' terms, everything is exactly as expected for a ^2S electronic state.[44]

RELATION OF ELECTRON LEVELS OF CH MOLECULE AND CARBON ATOM

Evidence for low-lying states of CH as initial states of λλ3900 and 4300 bands. The bands λλ3900 and 4300 discussed above are especially conspicuous in the flames of burning hydrocarbons.[45] Kayser designates them

[43] The extension of Table VII to higher values of j gives differences F_2-F_1 which are comparable with the errors probably involved (errors of measurement and of Kratzer's calculated F'' values). An indirect method has been used by Kratzer (Table 22), as follows; according to Fig. 3, we expect

(*a*) $\quad Q_2(j_k)-Q_1(j_k)=F_{1A}''(j_k)-F_{2A}''(j_k)+F_2'(j_k)-F_1'(j_k)$

(*b*) $\quad P_2(j_k)-P_1(j_k)=F_{1B}''(j_k)-F_{2B}''(j_k)+F_2'(j_k-1)-F_1'(j_k-1)$

(*c*) $\quad R_2(j_k)-R_1(j_k)=F_{1B}''(j_k)-F_{2B}''(j_k)+F_2'(j_k+1)-F_1'(j_k+1)$

After subtracting $F_{1\alpha}''-F_{2\alpha}''$ (calculated; $\alpha=A$ or B) from (*a*), (*b*), or (*c*), the remainder should give $F_2'-F_1'$. Also, (*c*) − (*b*) should give $\Delta_2F_2'(j_k)-\Delta_2F_1'(j_k)$. The results obtained from the data (cf. Kratzer's Table 22) are, from (*a*), $F_2'-F_1'=-0.015j_k$; from (*b*), $F_2'-F_1'=+0.01j_k$; from (*c*), $F_2'-F_1'\sim 0.18$ (nearly constant); also, from (*b*) and (*c*), $\Delta_2F_2'>\Delta_2F_1'$. These results are puzzling and partially inconsistent from the point of view of the present theory; except for the evidence from the Q branches (relations *a*), they however indicate $F_2(j_k)>F_1(j_k)$. The opposite conclusion $F_1>F_2$ indicated by the Q branches supports Kratzer's assumption that these have different initial states than the P and R branches (cf. Table VI, note *d*); this, however, is in disagreement with the theory for ^2S states. It seems possible that the discrepancies are due to small systematic errors in the measurements (cf. ref. 22) or in the calculated F'' values (which are based on the data of λ4300, where systematic errors are probably present[22]).

[44] Kratzer suggests the use of the general Kramers and Pauli term with $\rho=\frac{1}{2}$, and leaves σ undetermined. Kratzer gives $B\cong 12.52$ (Eq. 14a of his paper), but this is apparently due to a misprint or oversight.

[45] Additional probable CH or CH^+ bands have been described by Fortrat (Compt. Rendus, **178**, 1272, 1924) and by McDonald (Phys. Rev. **27**, 246, 1926 and **29**, 212, 1927). McDonald's bands λλ2264, 2367 (which have a common final state) are either of the $^1S\rightarrow{}^1S$ type, or else of the $^2S\rightarrow{}^2S$ type with the doublets unresolved. If the former, they are probably due to CH^+, if the latter, to CH. According to McDonald, neither of these bands nor Fortrat's λ3143 band have any energy levels in common with the λ3900 and λ4300 bands.

the C+H bands. Aside from the chemical evidence, their small moment of inertia speaks for a hydride emitter.[20] Kratzer suggested CH and CH_2 as possible emitters.[20] There is, however, no evidence in the band structure of anything more complicated than a diatomic emitter. The fact that the observed electronic states are of a *doublet* type shows that the emitter contains an odd number of electrons. This is true of CH, but not of such molecules as CH^+, CH_2, etc. The evidence is then strongly in favor of CH as the emitter.

The fact that the CH bands are strongly excited in flames is evidence (assuming that the excitation is primarily thermal) that the initial energy of the CH molecules before emission of the bands is not very great, hence that their final ^2P state is near the normal state of the CH molecule. The magnitude of the magnetic interaction (see last section) also indicates this. The fact that the λ3900 band is emitted less intensely than the λ4300 band (cf. Hulthén, Dissertation, p. 42) may be partly due to the higher energy required for the initial state of the former.

Correlation of energy levels of carbon atom and CH molecule. According theory of line spectra and atomic structure,[46] the carbon atom should have a ^3P normal state. Somewhat above this there should be a metastable ^1D state, followed by a metastable ^1S state. These states ^3P, ^1D, and ^1S represent all the possible arrangements of the two equivalent $2p$ electrons of the outer shell of the carbon atom. Of the low levels mentioned, only the normal, ^3P, state is yet known.[47]

The process of formation of a CH molecule from one of these carbon atoms and a normal hydrogen atom is conveniently treated from the point of view used by Hund in his recent fundamental papers.[9] As the hydrogen atom approaches the carbon atom, it will first produce something like a Stark effect in the latter. When this is sufficiently strong (cf. ref. 46, p. 78), the resultant orbital angular momentum k of the carbon atom should be oriented with respect to the line joining the two nuclei giving a quantized component σ_k which may have any integral value from 0 to k. The resultant spin s_C of the carbon atom should then be oriented with respect to σ_k, giving a quantized component σ_s between s_C and $-s_C$; as the nuclei come closer, the spin $s=\frac{1}{2}$ of the hydrogen atom should also orient itself with respect to σ_k, giving for the resultant spin two possibilities $s=s_C\pm\frac{1}{2}$, or merely $s=\frac{1}{2}$ if $s_C=0$. (This description of the behavior of the spin applies to case a, but must be altered if the effect of nuclear rotation is large.) Thus one may expect the ^3P carbon atom to give rise to the following molecular states: $\sigma_k=1$, $s=\frac{1}{2}$ or $1\frac{1}{2}$ (^2P and ^4P), and $\sigma_k=0$, $s=\frac{1}{2}$ or $1\frac{1}{2}$ (^2S and ^4S); the ^1D carbon atom to $\sigma_k=2$, 1, and 0, $s=\frac{1}{2}$ (^2D, ^2P, ^2S); the ^1S atom to $\sigma_k=0$, $s=\frac{1}{2}$ (^2S).

If the approach of the hydrogen nucleus to the carbon nucleus were sufficiently close, the CH molecule should resemble a nitrogen atom in order

[46] F. Hund, "Linienspektren und Periodisches System," especially pp. 139–142. J. Springer, Berlin, 1927.

[47] J. C. McLennan and A. B. McLay, Trans. Roy. Soc. Canada **20**, III, p. 363 (1926); I. S. Bowen, Phys. Rev. **29**, 231 (1927).

and spacing of electronic levels, just as the molecules BO, CO, NO respectively resemble atoms Na, Mg, and Al. In this case, the lowest states of CH should be those derived from the low-lying states ^4S, ^2D and ^2P of the nitrogen atom,[46] namely, ^4S; ^2D, ^2P, ^2S; ^2P, ^2S. It seems probable, however, on account of the relatively small nuclear charge of the hydrogen atom, that the approach of the CH molecule to the term-arrangement of a united atom is much less close than in the case of such molecules as BO, CO, etc., although (cf. following paragraph) the distance between the nuclei is about the same for all. The observed ^2P, ^2D, and ^2S states of CH are more readily explained as being respectively not very far removed from the ^3P, ^1D, and ^1S states of the carbon atom, the chief effects of the hydrogen atom being then to alter the multiplicity and to remove the metastability of the ^1D and ^1S atomic states. If the relation suggested is correct, the observed states all have $\sigma_k = k$; five other states derived from the same atomic states (all with $\sigma_k \neq k$; cf. preceding paragraph) might also be expected.

It is of interest that the equilibrium separation of the nuclei r_0, as calculated by Kratzer from the coefficients B ($B = 12.62$, $r_0 = 1.20 \times 10^{-8}$ cm for the ^2S state, $B = 14.19$, $r_0 = 1.13 \times 10^{-8}$ cm for the ^2P state, and $B = 14.57$, $r_0 = 1.11 \times 10^{-8}$ for the ^2D state), decreases in the order S, P, D. This might be ascribed to decreasing symmetry, and consequent increasing polarization by the hydrogen atom, of the outer electron shell of the carbon atom, in this order.

Mecke's systematic comparison[48] of the r_0 values for hydride molecules indicates that the H nucleus in general remains near but probably essentially outside the outer electron shell of the other atom, so that r_0 diminishes with the size of the latter. Thus the series of r_0 values for the lowest known states (^2P, ^3S, ^2P, ^1S respectively) of CH, NH, OH, FH, is 1.13, 1.10, 0.96, and 0.92×10^{-8} cm.[49]

Doublet widths in CH. The magnitude and sign of the magnetic interaction in the ^2P and ^2D states of CH call for some comment. As Mecke has shown[48b,50] there is empirically a semi-quantitative relation between the multiplet separations for various hydride spectra and the multiplet separations for the lowest P terms[51] of various corresponding atoms. Mecke has calculated the doublet separation for CH on this basis from $\Delta\nu = 15.5$ for the boron atom, obtaining[52] $\Delta\nu = 24$. This quantity should represent approximately the doublet separation, between $F_1(\frac{1}{2})$ and $F_2(1\frac{1}{2})$, which would exist

[48] R. Mecke, Zeits. f. Physik **42**, 390 1927.

[49] The data for CH, OH, FH are as given by Birge in the Bulletin on Molecular Spectra, p. 230–2, while the value for NH is from Hulthén and Nakamura (Nature, Feb. 12, 1927).

[50] R. Mecke, Zeits. f. Physik **36**, 795 (1926).

[51] In every case Mecke compares, without specific explanation, the *lowest* P term of an atom with the lowest double term of a molecule. The justification for this procedure is very likely that, in the case of most of the hydrides at least, the molecular states in question are actually the result of the union of a normal hydrogen atom with a metal or other atom in its lowest P state.

[52] Mecke calculates "$\Delta\nu_{red.}$", which here has the value 25. In general he finds that the *observed* $\Delta\nu$'s differ from this quantity in approximately the ratio 1/1.05. Assuming this factor here, we expect $\Delta\nu = 24$ for CH.

if case *a* were realized. We cannot expect the latter to be true with so small a magnetic interaction; but this estimated $\Delta\nu$ can be used as a measure of the magnetic interaction in calculating the actual position of the F_1 and F_2 states. This Kemble has done,[16a] with results that agree well with the empirical course of the ΔF values, accounting, as already remarked, for the observed near approach of s to the $\pm\epsilon$ orientations even for low j values.

The very small inverted $\Delta\nu$ for the ^2D state of CH can be explained in the following way in agreement with the supposition that this state is derived from ^1D of the carbon atom. In the latter, the two outer electrons ($2p$ electrons) each have $k=1$, $s=\frac{1}{2}$, the k's being parallel, the s's antiparallel. Now the energy of interaction between the k and the s of a single electron should be of larger magnitude[53] and of *opposite sign* as compared with that between the k of one electron and the s of another; in the former case, the sign corresponds to that in a normal doublet, in the latter—where it is the same as for two ordinary magnets—to that in an inverted doublet. For the two $2p$ electrons of the ^1D carbon atom, there are four (s,k) energies to be considered, but as is readily seen, their sum is zero. If now a hydrogen atom with $k=0$, $s=\frac{1}{2}$ is brought near, the resulting ^2D doublet separation comes only from the two orientations of the spin of the *hydrogen* atom in the magnetic field of the k's of the carbon electrons. Hence the doublet should be narrow[54] and inverted, as observed. This agreement gives support to the suggested relation of the ^2D of CH to the ^1D of carbon, but other possibilities involving similar relations of the k and s vectors are of course not excluded.

WASHINGTON SQUARE COLLEGE,
NEW YORK UNIVERSITY,
August, 1927.

[53] Cf. J. C. Slater, Phys. Rev. **28,** 291 (1926) for quantitative formulas and discussion.

[54] That the separation should not be negligible is indicated by data on atomic spectra. Cf. e. g. the term values in Table XI of Bowen's paper,[47] in particular the small inverted a^3D term ($\Delta\nu=-16$), which is evidently a term for which $\Delta\nu$ would be zero,—cf. Slater's Eq. (26),—if only the energy of interaction of each electron with its own spin were taken into account, since various other combinations of the same $2p$ electrons, such as $b^4P(\Delta\nu=-246)$, $b^2P(\Delta\nu=-168)$, $5k^4P(\Delta\nu=+270)$, give much larger values of $\Delta\nu$.

THE INFRA-RED RADIATION OF NITROGEN

By A. H. Poetker

Abstract

Extension of the first positive group of nitrogen bands. An investigation of the infra-red portion of the first positive group of nitrogen bands by thermocouple and prism has extended that group to the region of 1.5μ. The broad radiation maxima corresponding to the 0, +1, and +2 sequences have been broken up into individual bands. Their observed maxima occur at the positions calculated from the known vibration levels of this group. For higher accuracy the region from 7500 to 10500A was photographed under a dispersion of 9A per mm with neocyanin plates. The bands were recorded as far as 10500, the beginning of the 0 sequence. The measurements of the heads and principal lines within this range are given in tables. From these results values for the bands of the 0 sequence are found, and those of the −1 and −2 sequences are improved.

Reassignment of vibration numbers. The new data point very definitely to a modification of the assignment of vibration quantum numbers as previously made by Birge, in that the lowest final level should be dropped, and the other vibration quantum numbers should be diminished by one. The evidence pointing to this as the more probable assignment is discussed.

Oxygen triplet λ9265. Incidentally, the hitherto unresolved O triplet at 9265A appeared clearly resolved on these plates. The wave-lengths were measured as: 9265.67, 9262.61, and 9260.31.

Introduction

THE considerable progress made in recent years towards unravelling the very complex spectrum of nitrogen has made the further extension of that spectrum beyond the region of the visible very desirable. Such an extension on the side of the infra-red is particularly inviting because the beautiful regularity of the bands at the red limit of the visible might be expected to continue into the adjacent region. These bands, from the green through the yellow and red, belong to the first positive group of nitrogen, now universally ascribed to the neutral N_2 molecule. The visible spectrum of this group has been adequately investigated, particularly by Deslandres,[1] Von der Helm,[2] and under high dispersion by Birge.[3] The last named also gives the measurements of the most conspicuous lines or groups of lines between λ6800 and λ7650 as obtained by a Hilger constant deviation spectroscope. Croze,[4] using a prism spectrograph of small dispersion detected ten other bands and measured their heads.

Turning now to radiometric methods, Pfund[5] got the energy curve of the first positive group from .59 to 1.2μ. It showed the most marked maxi-

[1] Deslandres, Comptes rendus, **134**, 747 (1902).
[2] Von der Helm, Zeits. f. Wiss. Phot. **8**, 405 (1910).
[3] Birge, Astrophys. Jour. **39**, 50 (1914).
[4] Croze, Ann. d. Physique **1**, 97 (1914).
[5] Pfund, Jour. Opt. Soc. Amer. **9**, 193 (1924).

mum of the entire system at .90μ and two decided maxima beyond at 1.06 and 1.20μ respectively. The various sequences of the group could not be analyzed into individual bands with his apparatus. Yet from a theoretical standpoint the individual bands are of primary interest. Hence it was thought worth while to refine methods of investigation for the purpose of getting as much as possible of the detailed structure of these higher sequences of the group.

I. Thermocouple Method

Apparatus. A powerful source was a primary requisite. Hence the discharge tube was made of generous proportions. It was of the usual type for this kind of work, shaped like the Greek letter Π, from the central section of which (50 cm in length) the light was taken end-on. It was made of Pyrex, was 1.5 m in over-all length, of 18 mm bore, and supplied with cylindrical iron electrodes 15 cm long and of 2 cm diameter.

Nitrogen, obtained by bubbling air through a solution of pyrogallic acid to remove the oxygen, was fed into the tube continuously through a fine capillary, its supply being so adjusted with the exhaustion as to give the greatest brilliancy of discharge. A 5 KVA transformer applied about 2000 volts to the tube, and the current through the tube when making a run was about 0.7 ampere.

An auto-collimating prism spectrometer was built up. The arrangement will be clear from Fig. 1. The light entering the slit S_1 placed at the focus of

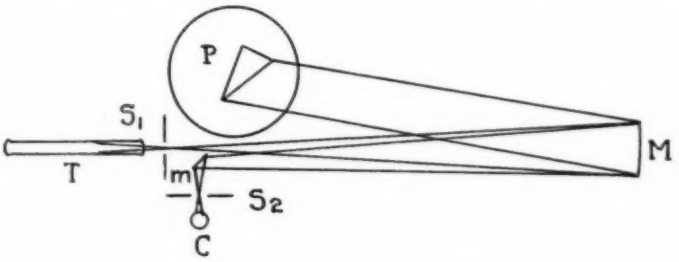

Fig. 1. Diagram of apparatus.

the concave mirror M was reflected as a parallel beam to the 30° reflecting glass prism P. Here, after refraction and reflection, it returned to the mirror M, thence, after a further reflection at m, was focused on the second slit S_2 and fell upon the thermocouple C placed immediately behind it. The dispersion of this system varied from about 140A per mm in the region of 7000A, to 450A per mm at 15,000A. The mirror was of 10 cm aperture and 90 cm focal length. The prism had a 10 by 10 cm reflecting surface, and was mounted on a spectrometer table of very delicate adjustment, the turning of the table being read on a graduated scale by an optical system 250 cm long. The entire spectrometer system,—slits, prism table, mirrors and thermocouple,—was mounted on a single I-beam.

The detector was a three-junction conpensating vacuum thermopile kindly made for me by Professor Pfund.[6] Preliminary trials indicated the

[6] Pfund, Phys. Zeits. 13, 870 (1912).

absolute necessity of shielding it from all stray radiation, air currents, minute changes of temperature, etc. Hence great pains were taken to house it properly. A double housing of good insulating material was provided, and every possibility of stray radiation on the second slit was guarded against. Still further asbestos shields protected the whole system from the heat of the discharge tube.

The galvanometer was a high sensitivity Leeds and Northrup instrument giving a 19 mm deflection per microvolt at 1 m distance, and with a period of about 12 seconds. It was operated at a scale distance of about 3.5 m. The leads connecting it with the thermopile were shielded from magnetic disturbances by being run through metal conduits, and the galvanometer was

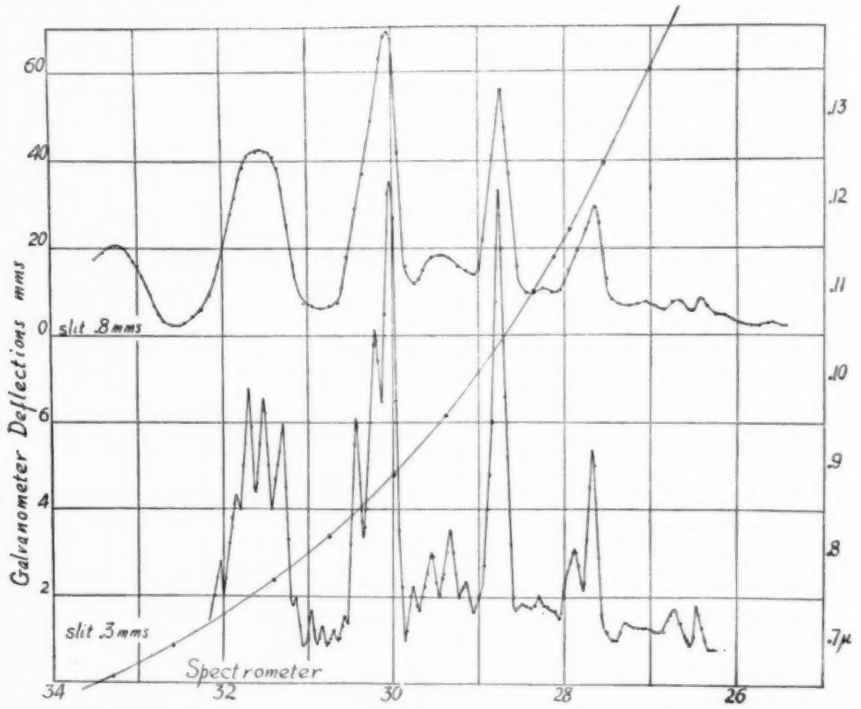

Fig. 2. Radiation curves of the first positive group of nitrogen.

protected as much as possible by thorough insulation from even gradual changes in temperature. The entire arrangement gave a combination of sensitivity and stability that was almost ideal.

In making a set of readings the discharge was run intermittently, each discharge lasting 15 secs. which was ample time to bring the galvanometer to its full deflection. This enabled the tube to be run at current densities which if steady would have caused the glass to soften. After each run the spectrometer table scale was calibrated anew from the strong lines of Na and K in this region. Light from an arc containing these substances was focused on the slit directly through the discharge tube.

Results. A general survey of the field with wide slits (0.8 mm) gave the upper curve of Fig. 2, which, except for the small maxima on the right and

the one at .95μ, is very like the curve obtained by Pfund. Narrowing the slits to 0.3 mm brought out the band structure of these general maxima as shown in the lower curve of Fig. 2. Of the larger maxima of the preliminary curve only that at 1.04μ remains unresolved. This could not be made to show structure with the use of the prism. The maximum at 1.20μ could be broken up only into two minor ones at 1.183 and 1.222μ respectively. The last group of bands recorded by Croze is seen to consist of three intensely strong bands beginning at 0.89μ followed by several very weak ones. The next group or sequence comprises one band at 1.042μ of as great intensity as any of the spectrum, and somewhat separated from four weak bands that follow. Of the two following sequences only two or three bands could be located with certainty.

To determine if possible the more detailed structure of these higher maxima a plane grating of 15,000 lines per inch was substituted for the prism.

TABLE I

Radiation maxima for higher sequences of first positive group.

Seq. Δn	$n' \rightarrow n''$	Calculated Maxima (μ)	Prism Princ. Max.	Prism Int.	Prism Minor Max.	Prism Int.	Structure by Grating	Int.	Remarks
−2	5→3		0.736	7					
	4→2		.747	10					
	3→1		.761	10					
	2→0		.775	9					Partly due to O
−1	7→6				0.787	2			
	6→5				.802	3			
	(5→4)				.811	3			Argon
					.822	4			N series lines
	4→3				.833	3			
	3→2		0.845	9					Partly due to O
	2→1		.867	12					
	1→0		.886	16					
0	5→5	.9146			0.917	3			
	4→4	.9375			.939	5			
	3→3	.9617			.963	5			
	2→2	.9873			.988	2			
	1→1	1.0143							
							1.035	3	
	0→0	1.0429	1.042	16			1.041	5	
							1.043	5	
							1.046	3	
+1	3→4	1.1043			1.108?	2			
							1.128	2	Oxygen
	2→3	1.1418							
							1.174	1	
	1→2	1.1820	1.183	4			1.178	1	
							1.182	1	
							1.187	1	
							1.210	1	
	0→1	1.2253	1.222	7			1.218	1	
							1.222	2	
							1.229	2	
+2	1→3	1.4107			1.41	2			
	0→2	1.4789			1.47	2			

Since this gave a dispersion of less than 20A per mm the slit could now be widened to 1 mm. This broke each of the unresolved maxima of the lower curve of Fig. 2, at 1.042, 1.183 and 1.222μ, into four peaks as shown in the column "Structure" in Table I. Since the spectrum was normal the second order Balmer lines could be conveniently used for calibration.

Since under this high dispersion the galvanometer readings were hardly sufficient by be accurately read except in the regions of maxima, a light-sensitive thalofide cell was tried in the hope of its being a more sensitive detector. It was operated on a battery circuit of 80 volts, the dark deflection being balanced out in the galvanometer by a potentiometer method. Since the cell shows fatigue and gradual recovery, readings were taken at regular intervals of 45 secs. A high resistence short period galvanometer was substituted for this part of the work. The region of greatest sensitivity for the thalofide cell is from 0.9 to 1.2μ. While the deflections in this region were greater than with the thermocouple, the stability was less; drift due to slow changes in the resistence of the cell was almost unavoidable. The results, however, checked the previous work unmistakably.

The energy maxima for the various bands as averaged from the results of the several runs are given in Table I. The possible error is 0.002μ, and for the last two sequences even greater. The values under "Calculated Maxima" are those deduced by Birge[7] from his analysis of the vibration levels for this group, except that ¼ the wave-number interval between successive first heads was added to obtain the approximate position of the maximum intensity of the band. The initial and final vibration quantum numbers, n' and n'', used for band designation differ slightly throughout from those given by Birge, and will be justified in Part III. The oxygen lines are quite pronounced in the spectrum. They were detected as sharp narrow peaks with the grating and account for the shift of the centre of gravity of the .850 and .772 bands.

II. Photographic Method

The accuracy of the photographic method is so far superior to that of the thermopile, that it is desirable for purposes of analysis to have photographic results as far out as possible. The intensity of some of the bands of these higher sequences assured good photographic results even under fairly high dispersion. The region, therefore, from 7500 to 10,500A was investigated by this method.

An auto-collimating plane grating spectrograph previously described[8] was used. It gave a dispersion of 9A per mm in the first order. Tube and excitation were as described in Part I, except that for continuous running the current through the tube was reduced to about 0.5 amperes. Also greater purity of the nitrogen was obtained by bubbling the air through a mixture of KOH and pyrogallol and then removing the water vapor by tubes of P_2O_5. Though this did not prevent the strongest O lines from registering, it did eliminate their over-exposure and halation otherwise present.

[7] Birge, private communication. Equations of n'' and n' functions were later published in Birge and Sponer, Phys. Rev. **28**, 259 (1926), Eqs. (8) and (9).

[8] Poetker, Phys. Rev. **30**, 418 (1927).

Neocyanin plates were used hypersensitized by an ammonia bath.[8] Exposures averaged 15 hours for the range from 7500 to 9000A, and a full day for the range beyond. The slit widths used were about 0.02 mm and 0.1 mm respectively.

Results. Fig. 3 shows one of the plates for the lower range. Comparison with the radiation curve of Fig. 1 brings out the beautiful correspondence with the results obtained by thermocouple. The sensitivity of the neocyanin plates is falling off rapidly at 8800A which accounts for the apparently diminished intensity of the band beginning at 8912A. Though many of the lines are still incompletely resolved, a single band in this region shows on these plates about 125 lines. If more closely examined by superposition, the first three bands of this complex, at 8912, 8722, and 8542A, will be found to be very similar in detailed structure, and with well-defined heads, as in the sequences of lower wave-length. Distinctive heads or close similarity of structure can hardly be recognized in the next two bands, though this improves again in the ones that follow. The stronger lines that interrupt the regularity of the bands at various places include the strong oxygen doublet and triplet at 8446 and 7775A, the nitrogen series lines (especially those of the $^4P^4P'$ group in the vicinity of 8200A), and finally about eight fairly intense argon lines.

The heads of the bands and the more intense lines were accordingly measured on my plates. In general, this could be done for the lower range to within 0.04 or 0.05A, except perhaps where several lines were fused into one. The method followed was that adopted in previous work on the hydrogen infra-red.[8]

The wave-lengths and wave-numbers of about 125 of these lines are given in Table II. In many cases the line given is the first member of a close doublet or triplet. The lines known as not belonging to the molecular spectrum have been omitted for the sake of brevity. The intensities are only visual estimates, and allowance must be made in the last two bands for the diminished sensitivity of the plates.

I have arranged in Table III what seems to be the series of first heads, and possibly of the second and fourth, for this sequence. Similar first differences are found to exist between several other prominent lines in the first three bands and again in the last two (at 8047 and 7896A), but they cannot be traced across the intervening two with equal certainty. This might be interpreted as indicating that all these bands do not belong to the same sequence, but are partly fragmentary traces perhaps of an entirely different system; still on the other hand, the general regularity of all the other bands in the whole region makes this alternative unlikely.

For the following sequence, from 9000 to 10,500A, it is much harder to get satisfactory results. Beyond 8940A, as was evident from the thermocouple investigation, the spectrum is quite weak. This coupled with the greatly reduced sensitivity of the neocyanin makes the plates under high dispersion too weak for reproduction. The bands appear to be equally com-

Fig. 3. Infra-red portion of first positive group of nitrogen.

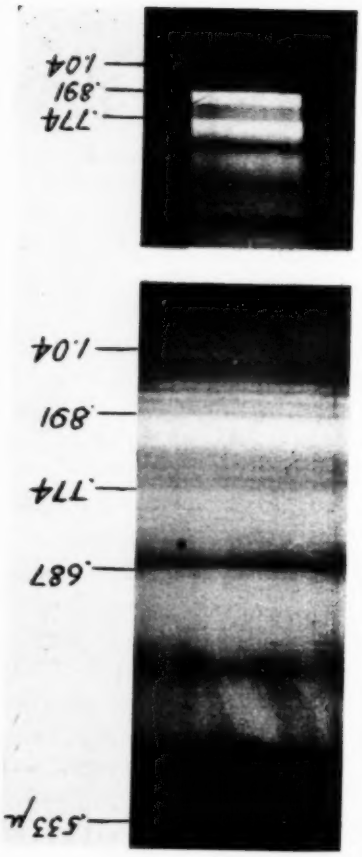

Fig. 4. First positive group of *N* showing new sequence extending from 10500A to 9000A. (Mag. 4x).

Fig. 5. Same under lower dispersion. (Mag. 6x).

TABLE II

Wave-lengths and wave-numbers of principal infra-red lines of nitrogen spectrum. In the second column the numbers are visual estimates of the intensities, while the letters denote the character of the lines; b, broad, perhaps multiple; h, hazy, diffuse; v, shades towards violet; r, shades towards red.

λ(I. A. air)	Int.	ν(vac.)	λ(I. A. air)	Int.	ν(vac.)	λ(I. A. air)	Int.	ν(vac.)	λ(I. A. air)	Int.	ν(vac.)
8936.60	2	11186.87	8504.82	2	11754.81	8137.10	2	12286.02	7828.07	3	12771.03
11.57	3r	11218.29	00.59	2	60.66				24.27	3	77.24
10.68	3	19.41	8496.88	2	65.79	30.85	2b	95.46	20.50	2	83.39
8892.08	3	42.88				13.13	2h	12322.31	02.39	2	12813.07
91.04	3	44.19	88.11	3	77.95	8097.07	2	46.76	7792.04	2	30.08
			68.15	3v	11805.72	78.84	2	74.62			
79.27	3h, r	59.10	62.12	2	14.13	64.47	2	96.67	7769.44	2	12867.40
72.31	2	67.93	11.18	2	85.68				53.05	3	94.61
71.17	3	69.38	10.29	3	86.93	47.26	2b	12423.18	39.56	3	12917.08
67.82	3	73.64				32.55	2	45.93	30.22	4	32.72
62.53	3	80.37	03.96	2b	95.88	30.23	2	49.52	18.55	3	52.24
			8397.10	2	11905.61	29.07	2	51.32			
58.75	2	85.18	86.31	2	20.92	19.38	2	66.37	17.59	3	53.85
52.74	4	11292.84	79.94	2	29.99				15.48	3	57.40
31.38	4	11320.15	74.70	2	37.45	8007.63	2	12484.66	02.44	3	79.33
8792.30	2	70.47				7999.92	2	96.70	7677.72	3	13021.12
75.35	4v	92.43	69.02	1b	45.55	89.58	2v	12512.86	76.85	3	22.59
			63.14	3b	53.95	82.13	2	24.54			
44.95	4b	11432.04	51.45	2	70.68	76.51	2	33.37	69.68	3	34.77
22.28	3	61.75	41.48	1	84.99				64.05	3	44.35
03.31	3	86.73	32.87	2	97.37	72.17	2	40.19	60.80	3b	49.88
8691.33	4	11502.56				68.31	2	46.13	54.52	3	60.59
75.46	3	23.60	8326.16	1	12007.04	59.37	3b	60.36	44.19	3	78.24
			8299.06	2h	46.25	39.20	2	92.27			
66.40	3	35.65	84.51	1	67.41	12.17	1	12635.29	7638.57	2	13087.86
60.81	3h	43.10	74.80	1	81.57				26.13	3h, r	13109.21
54.55	3b	51.45	05.59	1	12183.47	11.27	2	36.72	13.00	3	31.82
45.48	3v	63.56				7896.28	2	60.71	03.96	3	47.43
39.45	3v	71.64	04.62	1	84.91	81.93	2	83.76	7592.97	3	66.46
			8187.38	2	12210.57	79.72	2	87.32			
8607.84	4v	11614.13	82.14	1	18.39	65.36	2	12710.48	89.91	2	71.77
8595.58	3	30.70	76.36	2	27.02				72.27	3	13202.45
78.47	3	53.89	72.78	2	32.38	58.07	3b	22.28	53.31	3	35.59
63.48	3	74.29				55.76	1	26.02	36.90	3	64.41
41.73	2	11704.02	63.65	1	46.06	50.76	2	34.12	35.90	3	66.17
			58.43	2	53.90	40.85	2	50.21			
23.15	2	29.53	57.63	2	55.10	33.66	3	61.92	31.06	3	74.69
11.64	3	45.39	48.21	2b	69.26						

plex, so that with the widening of the slit the individual lines are somewhat run together. In the band at 1.04μ about 30 lines or groups of lines could be distinguished and measured. The most noticeable feature about this part of the spectrum is that the characteristic heads of great intensity seem to have given way to a more uniform and gradual distribution. As a result the banded structure is almost lost under high dispersion, and under low, the accuracy of measurement is considerably reduced.

Some small spectrograms were taken with a small constant deviation Hilger spectroscope from the other end of the central portion of the discharge tube. Fig. 4 is an enlargement of a typical plate. It reveals the 1.04μ band quite clearly and brings out very well the even banded structure of the region just beyond the 8900A maximum. Filters cut out the spectrum below 8500A in this plate except for a one minute exposure.

Fig. 5 is an enlargement of the spectrum obtained with a still more powerful prism spectrograph. The exposure is only 8 minutes, but this was repeatedly sufficient to register these bands between 9000 and 10,500A, though the plates are of very low sensitivity in this region.

I have used the small Hilger spectrograms to get the approximate positions of the heads and the maxima of the bands for this sequence (Table IV). From the results obtained with the same instrument in hydrogen an

TABLE III

Series of first, second and fourth heads of −1 sequence.

$n'\rightarrow n''$	λ(air) I. A.	Int.	ν (vacuo)	First Difference	Second Difference
7→6	7896.28	2	12660.71		
				237.53	
6→5	8047.26	2	12423.18		.74
				238.27	
5→4	8204.62	1	12184.91		1.09
				239.36	
4→3	8369.02	1	11945.55		2.17
				241.53	
3→2	8541.73	2	11704.02		1..74
				242.27	
2→1	8722.28	3	11461.75		1.19
				243.46	
1→0	8911.57	3	11218.29		
7→6	7879.72	2	12687.32		
				237.80	
6→5	8030.23	2	12449.52		1.15
				238.95	
5→4	8187.38	2	12210.57		.94
				239.89	
4→3	8351.45	2	11970.68		1.26
				241.15	
3→2	8523.15	2	11629.53		1.65
				242.80	
2→1	8703.31*	3	11486.73		1.05
				243.85	
1→0	8892.08	3	11242.88		
7→6	7858.07	3	12722.28		
				237.62	
6→5	8007.63	2	12484.66		.98
				238.60	
5→4	8163.65	1	12246.06		.42
				239.02	
4→3	8326.16	1	12007.04		2.23
				241.25	
3→2	8496.88	2	11765.79		.94
				242.19	
2→1	8675.46	3	11523.60		1.04
				243.23	
1→0	8862.53	3	11280.37		

* Coincident with a *N* series line but more intense than such series line should be.

TABLE IV

Approximate positions of maxima and heads of 0 sequence.

$n'\rightarrow n''$	λ(air) I. A.	Maxima ν(vac.)	First Diff.	λ(air) I. A.	Heads ν(vac.)	First Diff.
5→5	9133	10946		9180	10890	
			267			265
4→4	9362	10679		9409	10625	
			264			273
3→3	9599	10415		9657	10352	
			276			281
2→2	9860	10139		9927	10071	
			545			542
1→1	———			———		
0→0	10420	9594		10491	9529	

accurate dispersion curve was available, but the extremely low dispersion (700A per mm in this region) and the hazy outlines of the banded structure make the most careful measurements rather rough. To compensate if possible for this, the results of Table IV were averaged from a half-dozen plates. The second band of the sequence was too faint to be measured on any of these plates.

In this upper range under high dispersion about 200 lines or groups of lines could be clearly measured. I give the more prominent of these in Table V. Because of their faintness, the width of the slit used, and the use of a low

TABLE V

Wave-lengths and wave-numbers of principal infra-red lines of nitrogen spectrum.
Notation same as in Table II.

λ(I. A. air)	Int.	ν(vac.)	λ(I. A. air)	Int.	ν(vac.)	λ(I. A. air)	Int.	ν(vac.)	λ(I. A. air)	Int.	ν(vac.)
10498.4		9522.6	1058.3	2	9745.5	9593.7		10420.6	9157.3	2b	10917.3
90.8		29.5	48.7	2	54.7	77.6		38.2	52.3	2	23.2
86.1		33.8	41.8	2	61.2	59.3		58.2	48.7	2	27.5
75.7		43.3	28.3		74.1	55.3		62.5	44.9	1	32.1
71.5		47.1	07.5		94.0	53.2		64.8	41.1	1	36.6
65.4		52.6	10191.5		9809.4	9550.5	b	10467.8	24.1	2	57.0
61.1		56.6	44.5		54.8	45.1	b, h	73.7	17.3	2	65.2
57.4		60.0	40.3		58.9	37.4		82.2	12.0	1	71.5
53.3		63.7	33.4		65.6	06.6		10516.1	04.5	1	80.6
48.4		68.2	16.7		81.9	9491.9	1	32.4	9099.3	2	86.8
42.1		74.0	07.9		90.5	82.7	2b	42.6	96.2	2	90.6
37.5		78.2	10097.3		9900.9	34.8	1	96.2	92.6	2	94.9
24.4		90.2	14.5		82.8	17.6	1	10615.5	88.7	1	99.7
20.9	2	93.4	9940.2		10057.4	13.2	2	20.5	80.2	1	11010.0
16.3	2	97.7	34.5		63.2	09.8	3b, h	24.3	58.3	2	36.6
12.9	2	9600.8	9920.6		10077.3	05.8	2	28.8	9049.5	3b	11047.3
04.2		08.8	14.5		83.5	9397.6	1	38.1	45.7	2b	51.9
10397.1		15.5	9868.4		10130.6	92.2	4	44.2	37.4	2	62.1
95.3		17.1	64.4		34.7	86.2	3	51.0	33.3	2b, h	67.1
90.4		21.7	20.0		80.5	76.3	2	62.3	19.6	1	83.9
87.8		24.1	17.5		83.1	56.0	2	85.4	10.1	2	95.6
83.3		28.3	15.2		85.5	42.5	2	10700.8	06.2	2	11100.4
73.2	2	37.6	9704.8		10301.4	26.2	3	19.5	03.9	1	03.3
65.9	2	44.4	9697.7		09.0	22.7	2	23.6	00.4	1	07.6
59.6	2	50.3	88.4		18.8	19.1	2	27.7	8975.8	2b	38.0
10356.0	2	9653.6	86.3		21.0	9296.4	2	53.9	59.7	1	58.0
49.1	2	60.1	69.1		39.4	86.6	2	65.3	53.8	2	65.4
47.0		62.0	67.4		41.2	57.5	2	99.1	52.1	2	67.5
39.9		68.7	65.1		43.7	9196.9	2b	10870.2	48.2	2b, h	72.4
37.0		71.4	45.0	b	65.2	94.4	2b	73.2	41.7	2	80.5
16.4	2	90.7	41.6	b	68.6	9182.0	2	10887.9			
05.3		9701.1	35.7	b	75.2	78.5	3	92.0			
10271.0	2	33.5	33.6		77.5	74.9	2	96.3			
66.1	2	38.1	25.4	b	86.3	70.9	2	10901.1			
62.3	2	41.7	23.2	b	88.7	66.6	3	06.2			

power eye-piece in the comparator telescope in their measurement, the accuracy is considerably reduced, and since the error in some cases may amount to several tenths of an angstrom, only one decimal place is carried. The intensities, where added, are merely to indicate some relative distinction.

III. DISCUSSION

Birge[9] has made an assignment of the vibrational quantum numbers for the bands of the first positive group of nitrogen, as well as for the second and

[9] Birge, Phys. Rev. **23**, 294 (1924).

fourth. He has incorporated his results in the recent Bulletin of the National Research Council on Molecular Spectra in Gases, where he gives in Fig. 10 (p. 126) a comprehensive diagram of the vibrational energy levels and the bands involved in these groups. It was with the idea of checking this assignment by finding and measuring the bands it predicted in the extension of the first positive group in the infra-red that the present work was undertaken.

It has already been remarked that the assignment of vibration quantum numbers here proposed differs slightly from that previously suggested by Birge. The change was adopted as the only satisfactory way of reconciling several flaws in what was otherwise a perfect agreement between theory and experiment, prediction and observation. The reconciliation is effected by dropping the 0 level of the Birge assignment for the final (so-called A) levels. This involves that the Δn characterizing the sequences be diminished by one in each case, the green bands thus being the -5 sequence, the yellow bands the -4, and the newly resolved batch at 1.04μ the 0 sequence. Had better data been available Birge would undoubtedly have made the same assignment.

The reasons for considering this the more probable assignment may be briefly summarized as follows:

1. The band whose head was measured by Croze as λ9108 and which was designated as the 0→0 transition by Birge is conspicuous for its absence. And yet this 0→0 transition should theoretically be the strongest band of the entire group. The head of the weak band present lies considerably farther out. The only strong line I can find on my plates in this neighborhood is one which invariably measures up as λ9122.6 and which, I am confident, is the argon line measured (radiometrically) by Meissner[10] as λ9123.00. Hence even this could not have been on Croze's plates since he used chemically prepared nitrogen.

2. On the other hand, the band with its maximum at 1.042μ is as strong as any in the whole group—being equalled in intensity only by the band at 8912A. This fits in very well with its new assignment as the 0→0 transition.

3. The intensity distribution according to the new assignment of the whole group of bands is more symmetric, more in accord with the distribution found in other systems, and especially with that of the similar second positive group of this same neutral N_2 molecule. This intensity distribution for the higher sequences is given in Fig. 6. Comparison with Birge's Fig. 13[11] will indicate several points of close similarity between this and the distribution for the second positive group, especially the sudden drop after the initial member in the intensity curve of the 0 sequence.

4. Again, the absence in Birge's diagram[11] (Fig. 10, p. 126) of the bands due to transitions to the 0 final level in the very complete green and yellow sequences is rather suggestive of its non-existence. On the other hand, the established presence of such bands (Croze's 7887 and Birge's 6968) in the red and deep red sequences would be conclusive evidence for its existence.

[10] Meissner, Phys. Zeits. **17**, 549 (1916).

[11] Birge, Molecular Spectra in Gases, p. 135.

But the assignment of these bands to their former places made them at best sad misfits in the sequences concerned, as is evidenced by their respective abnormally high and low first differences.[12] Only the first two bands of the -2 sequence were included in my recent plates, but fortunately I had an old plate from some preliminary work under lower dispersion (18A per mm) extending well down into this sequence. It was not particularly good, but

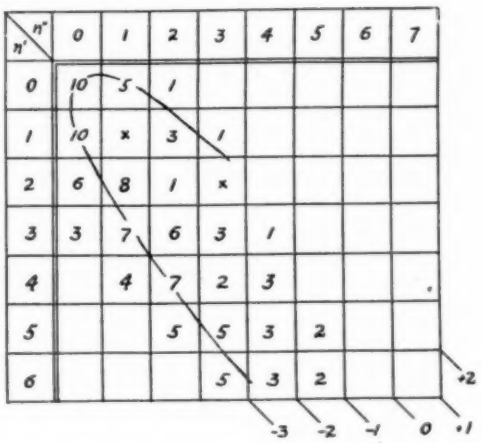

Fig. 6. Intensity distribution of first positive group of nitrogen.

using known N series lines, O and A lines present, the bands in question could be measured with sufficient accuracy for a decisive test of their assignment. For in this part of the spectrum the bands are sharply defined and unmistakable. I give in Table VI the series for the first and second heads as roughly measured from this plate. The error may easily amount to several tenths of an angstrom, but the values are better than data so far available,

TABLE VI

Series of first and second heads of the -2 sequence.

$n' \to n''$	λ(air) I. A.	ν(vac.)	First Diff.	λ(air) I. A.	ν(vac.)	First Diff.
7→5	7164.6	13953.7		7152.2	13977.9	
			208.0			209.4
6→4	7273.0	13745.7		7260.9	13768.5	
			211.2			211.1
5→3	7386.5	13534.5		7374.0	13557.4	
			211.9			211.7
4→2	7504.0	13322.6		7491.0	13345.7	
			213.4			213.9
3→1	7626.13	13109.21		7613.00	13131.82	
			214.60			213.74
2→0	7753.05	12894.61		7739.56	12917.08	

and the table is given to show how forced is the inclusion of the λ7896 band in the -2 sequence; the first difference would jump from 215 to 234, an

[12] Birge, Astrophys. Jour. **39**, 50 (1914), see Table IV.

excess of about 18 cm^{-1}. As for the λ6968 band, Birge's[12] table indicates sufficiently its misplacement. But it is doubtful whether this is a real band. Again using an old plate (panchromatic), I found that only one of the three heads given by Birge for this band had anything corresponding to it on the plate, a line at 6966A, which was evidently to be attributed to argon. Not even under low dispersion could anything like a clear-cut band be detected here.

These reasons seem to me conclusive evidence in favor of the modified assignment.[13] For the rest, my findings, as is evident from the tables, confirm the general analysis of the genesis of this first positive group of nitrogen, and add new data for the more accurate determination of the relative vibration term values. The initial bands of either the -1 or -2 sequence suggest themselves by their regularity for a study of the quantum analysis of the individual bands, but no attempt has been made to attack this problem which has so far resisted all efforts at its solution.

It has been mentioned that the stronger oxygen lines were present on these plates. An additional remark on the λ9265 triplet might be made. As is well known, it is the first member of the first subordinate series, 2^3P-3^3D. I am not aware of its having been clearly resolved before. Paschen gives it as λ9264.28 and lists it as shading towards violet. The three components were clearly distinguishable on a number of my plates. The measurements averaged from several plates are given in Table VII. These give the aver-

TABLE VII

Oxygen triplet λ *7265*

λ(air) I. A.	Int.	ν(vacuo)	Designation
9265.67	3	10789.57	$2^3P_2-3^3D_{1,2,3}$
9262.61	2	10793.13	$2^3P_1-3^3D_{1,2,3}$
9260.31	1.5	10795.81	$2^3P_0-3^3D_{1,2,3}$

age term value for 3^3D as 12,415.17. The intensities are only relative visual estimates.

The experimental work of this investigation was done at Johns Hopkins University, and, in conclusion, I should like to express my thanks for the courtesy there shown me, and in particular to Dr. Pfund for making me the thermocouple and suggesting the investigation.

MARQUETTE UNIVERSITY,
MILWAUKEE, WIS.
September 1, 1927.

[13] These results were communicated to Prof. Birge, who concurs in the new assignment.

THE STRUCTURE OF THE SWAN BANDS

By John D. Shea

Abstract

Frequency of the lines of the Swan spectrum.—Data obtained by Leinen, Komp, Hindrichs and Johnson have been used in a detailed quantum analysis of the Swan bands. The very recent data by Johnson have been employed only in the study of the multiplicity of the lines. Tables of the frequencies of the lines and their combination differences are given for the (0, 0), (0, 1), (1, 0), (1, 1) and (1, 2) bands.

Quantum analysis of the Swan spectrum.—Quantum numbers have been assigned to all lines of the R and P branches of the above bands. The Q branch is not observed in these bands. The combination principle is verified in the case of all the above bands. A new method for obtaining accurate numerical values of the constants of the rotational energy function, $E=B_0m^2+D_0m^4+F_0m^6+H_0m^8+\cdots$, has been developed, assuming the theoretical relations between rotational and vibrational constants recently derived by Kratzer, Kemble, and Birge. The so-called method of zero sums has been re-formulated for rapid use in band spectra computations.

Molecular constants of the carrier.—The moment of inertia of the Swan band carrier for infinitely small vibration is found to be 15.84×10^{-40} gm cm^2 for the initial state in the emission process, and 17.03×10^{-40} gm cm^2 for the final state, with a probable error of less than 0.1 percent. The constants of an assumed law of force of the form $F=k_1(r-r_0)+k_2(r-r_0)^2+k_3(r-r_0)^3+\cdots$ are evaluated.

Multiplicity of the lines.—For small values of j the R branches consist of triplets, the P branches of doublets, the separation decreasing as j increases. Empirical formulas for this separation as a function of j are given. The separation for corresponding j values in the various bands shows interesting numerical relations. The well-known "staggering" of alternate lines has been investigated quantitatively for the (0, 0) band, and can be explained by the assumption of a double moment of inertia, either in the initial or final state, in agreement with Mulliken's prediction of σ-type doubling for these bands. The necessary difference of the two values of the moment of inertia is 0.012 percent. The molecule C^-C^- is suggested as the probable carrier of the Swan bands, provided such a doubly charged molecule can exist.

Introduction

THIS paper[1] deals with the analysis, on the basis of quantum theory, of the Swan bands resulting from the vibrational quantum transitions (0,0) (λ5165), (0,1) (λ5635), (1,0) (λ4737), (1,1) (λ5129) and (1,2) (λ5585). Certain theoretical relations have been tested, and the more important constants for the carrier have been evaluated with a high degree of accuracy.

The so-called Swan bands were first observed by Wollaston[2] in 1802, but the bands were not described until Swan[3] investigated them in 1857. The bands, which are quite complex, occur in the visible portion of the spectrum.

[1] Preliminary results of this investigation have been reported to the American Physical Society in the following abstracts: Phys. Rev. **25**, 716 (1925) Abstract 9; Phys. Rev. **27**, 245 (1926) Abstract 14.

[2] Wollaston, Trans. Roy. Soc. London, **11**, 365 (1802).

[3] Swan, Trans. Roy. Soc. Edinburgh, **21**, III, 411 (1857).

Although the existence of these bands has been known for more than a century, the molecule to which they are due is still in doubt.[4,5,6] The molecule undoubtedly contains at least two carbon atoms. Whether or not one or more hydrogen atoms are also present has not been decided. These bands are observed in the Bunsen flame, in stars of spectral types *R* and *N*, in comets,[7] in the carbon arc, in vacuum tubes with carbon electrodes containing an inert gas at low pressures,[6] and in the furnace spectra of King.

Excellent photographs of these bands have been published by Johnson.[6] Cut (b) in the frontispiece of the Bulletin of the National Research Council, Vol. XI, Part 3, December 1926, entitled "Molecular Spectra in Gases," was prepared by the writer from an enlargement made from a plate taken by Birge with the large concave grating at the University of Wisconsin. This cut is of the (0,0) and (1,1) bands, the lines of the (0,0) band being labeled with their correct quantum numbers.

The Swan system consists of five sequences[8,9] of bands with the head of the first band of each sequence in the vicinity of the following wave-lengths: λλ6191 (0,2), 5635 (0,1), 5165 (0,0), 4737 (1,0) and 4381 (2,0). These correspond to the sequences $n''-n'=+2, +1, 0, -1$ and -2. Thus in the $+1$ sequence the λ5635 band is produced by a transition in emission from the vibrational state $n'=0$ to the vibrational state $n''=1$.

TABLE I

Schematic representation of the Swan bands.

n'	$n''=0$	1	2	3	4	5	6
0	5165	5635	6188				
1	4737	5129	5585	6120			
2	4381	4716	5096	5541	6060		
3		4371	4698		5502	6005	
4			4364	4683		5473	5958
5					4673		

Table I contains the vibration quantum number assignments of the Swan bands. It is the same as that given by Mecke[10] and Birge.[11] Each band corresponds in emission to a transition from the vibration state n', given at the left of the row in which a particular band occurs, to the vibration state n'', given at the top of the column.

[4] Watts, Phil. Mag. (6) **28**, 117 (1924).

[5] Kayser, Handbuch der Spectroscopie, Vol. V, 226 (1910) and Vol. VII, 139 (1924).

[6] Johnson, Trans. Roy. Soc. London **A227**, 157 (1927).

[7] Wright, Lick. Obs. Bull. **7**, 8 (1912) See also Fig. 171 p. 435 Vol. I, Russell, Dugan and Stewart, Astronomy, (1926).

[8] For an introduction to the quantum theory of band spectra see Sommerfeld, Atombau, 4th edition, Chapter 9.

[9] For a more detailed account see the Report of the National Research Council on Molecular Spectra in Gases, 1926. The nomenclature of this paper is the same as that in the report of the National Research Council, and reference will be made to it as "Report."

[10] Mecke, Phys. Zeits. **26**, 217 (1925).

[11] Birge, Phys. Rev. **23**, 294 (1924).

The structure of the Swan bands has been investigated by Thiele,[12] Leinen,[13] Heurlinger,[14] and others.[5,6] The individual lines of the various bands can be arranged in ten series, such that the second frequency difference of the lines in each series is approximately a constant. These series can be conveniently considered as two sets of doublets and two sets of triplets. The two sets of doublets (and similarly for the triplets) are found by taking alternate lines of what seems at first to be a single doublet series. The basis of this division lies in the fact that if it is not made, the second differences show a systematic irregularity due apparently to a slight mutual displacement of alternate lines. Leinen, Thiele and other early investigators made the division into ten series. Heurlinger assumed only five series, which he interpreted on the quantum theory as a doublet P branch and a triplet R branch. It has recently become evident that the band series of homopolar molecules as a rule consist of lines which alternate in intensity,[15] and the application of this rule suggests that the true interpretation of the Swan bands is to assume two P branches (each composed of doublets), and two R branches (each composed of triplets). Each P or R branch consists of alternate strong and extremely weak lines, and the two P branches (similarly the two R branches) interlace in such a fashion that the faint lines of one almost coincide with the strong lines of the other. In the tables, the lines of each band are listed in order, as if there were only one doublet P and one triplet R branch, merely for convenience.

Several investigators have measured the wave-lengths of the lines in different portions of the Swan spectrum. Only the measurements giving the wave-lengths to 0.001A were used in this work. Hindrichs,[16] about 1904, measured the lines of the bands in the $n''-n'=-1$ sequence. These measurements, although made under fairly high dispersion, do not seem to be as accurate as those of later investigators. Leinen[13] measured the lines of the $n''-n'=0$ sequence, the measurements being published in 1905. He used an electric arc as source, and lists but two heads, the (0,0) and (1,1). Komp,[17] about 1911, measured the lines of the $n''-n'=+1$ sequence. Since the work reported in this paper was completed, a paper by Johnson[6] has appeared which gives accurate measurements of the lines of many of the Swan bands, including several which are not considered in the present paper. His data were obtained, for the most part, under low temperature conditions, and give only lines which are relatively near the head. Combining these measurements with the older ones would produce little if any change in the results already obtained before Johnson's paper appeared, and accordingly this has not been done.

[12] Thiele, Astrophys. J. **8**, 1 (1898).

[13] Leinen, Zeits. f. wiss. Phot. **3**, 137 (1905).

[14] Heurlinger, Untersuchungen über die Struktur der Bandenspektra, Dissertation, Lund (1918).

[15] Report, Chapter IV, Section 5e, p. 200 et seq.

[16] Hindrichs, Ueber Messungen und Gesetzmassigkeiten in der Vierten Kohlebande. Bonn Diss. (1904).

[17] Komp, Zeits. f. wiss. Phot. **10**, 117 (1911–12).

The Combination Principle and Its Verification

The lines of the three possible branches, P, Q, and R of the usual quantum theory, are defined as follows:

$$P_j = \nu_0 + F_{j-1}' - F_j'' \tag{1a}$$

$$Q_j = \nu_0 + F_j' - F_j'' \tag{1b}$$

$$R_j = \nu_0 + F_{j+1}' - F_j'' \tag{1c}$$

In these equations F_j is the "term" value (i.e., the energy divided by hc) expressed as a function of j, the resultant angular momentum of the molecule in $h/2\pi$ units, ν_0 is the frequency of the origin. The Q branch is not observed in the Swan bands. From experimental data it is possible to evaluate only m, the angular momentum due to the rotation of the nuclei. Assuming for the present that m and j are parallel, one may write $m = j - \epsilon$, where j is assumed to be an integer. However, it is possible that j may be a half-integer, and in order to distinguish this case, we write $m = k - \alpha$, where k is an exact half-integer.[18] For the sake of convenience, a line will always be referred to in terms of its j for the final state, as shown by Eqs. (1a)–(1c).

In the particular case of the Swan bands m is known to be approximately a half-integer, and hence if the resultant angular momentum is integral, ϵ is approximately one half. If the resultant angular momentum is half-integral, then α is nearly zero.

From Eqs. (1a) and (1c) it follows that

$$R_j - P_j = F_{j+1}' - F_{j-1}' = 2\Delta F_j' \tag{2a}$$

$$R_{j-1} - P_{j+1} = F_{j+1}'' - F_{j-1}'' = 2\Delta F_j'' \tag{2b}$$

In these equations $F_{j+1} - F_{j-1}$ is defined as being equal to $2\Delta F_j$.[19] Eqs. (2a) and (2b) are the essential equations in a test of the combination principle. Thus Eq. (2a) indicates that although both R_j and P_j are functions of the initial and final states, their difference is a function of the initial state only. If now the values of $2\Delta F_j'$ are evaluated from the observed lines in two different bands of an n'' progression (i.e., having the same initial vibration state) these values should be identical within the limits of experimental error. This relation should hold whether the lines are perturbed or not. The same argument applies to the values of $2\Delta F_j''$ for the various bands of an n' progression. This identity of the values of $2\Delta F_j$ for different bands is known as the combination principle. In the case of bands in which a Q branch is observed, additional combinations are possible. In all bands thus far analyzed, perturbations have been found to occur in pairs, and each pair of perturbed lines may be explained as due to an irregularity in one energy level, usually in the initial state. Thus if F_j' is greater than expected by any

[18] ϵ (or α) is thus interpreted as a measure of the angular momentum due to electronic motion. The more recent interpretation of the new wave mechanics is not pertinent in the present investigation.

[19] By this definition of $2\Delta F_j$, it follows that $2dF/dj = 2\Delta F_j$ to a high degree of approximation. (Report, Chap. IV, Eq. (78).).

given amount, the R_{j-1} and P_{j+1} lines will both be displaced to the violet by this same amount. This fact is very useful, as it definitely fixes the relative values of j for the R and P lines, provided perturbations exist. Perturbations do exist in the Swan bands, and with these as a basis, the writer has assigned relative values of j to all the series lines of the (0,0), (0,1), (1,0), (1,1) and (1,2) bands. Then by the use of Eqs. (2a) and (2b) the values of $2\Delta F_j'$ and $2\Delta F_j''$ have been evaluated. The equalities predicted by the combination principle were then found to exist, thus proving that the previous assignment of vibration quantum numbers is correct. The series and the corresponding values of the combination differences are given in Tables II to VI. In these tables the measurements for each band are listed

TABLE II

Frequencies of the lines of the (0,0) band, and their combination differences.

j	R^r	R^c	R^v	P^r	P^v	$2\Delta F''^r$	$2\Delta F''^v$	$2\Delta F'''$	$2\Delta F'^v$
1									
2									
3		19389.05							
4		393.16							
5		397.83							
6	19400.88	402.53							
7	406.31	407.55							
8	411.42	412.80	19414.52						
9	417.22	418.30	419.80						
10	422.83	424.01	425.33						
11	429.03	429.95	431.13						
12	435.13	436.15	437.13						
13	441.77	442.57	443.50						
14	448.29	449.19	449.93					87.16	87.30
15	455.38	456.13	456.89	19354.61	19355.27	100.77	100.86	93.68	93.92
16	462.41	463.22	463.88	354.61	355.27	107.80	107.95	100.11	100.28
17	469.93	470.64	471.28	355.27	355.85	114.66	114.79	106.56	106.82
18	477.41	478.18	478.70	355.85	356.40	121.56	121.78	113.53	113.27
19	485.25	486.07	486.64	356.40	357.37	128.85	128.70	119.55	119.73
20	493.40	494.08	494.64	357.86	358.45	135.63	135.63		126.13
21	501.85	502.43	502.95		359.94		142.49	132.47	132.62
22	510.28	510.92	511.26	360.93	361.46	149.35	149.46	139.01	139.00
23	519.22	519.81	520.22	362.84	363.43	156.38	156.38	145.44	145.48
24	528.05	528.73	528.90	364.84	365.44	163.21	163.29	151.81	151.86
25	537.52	538.07	538.42	367.41	367.95	170.11	170.12	158.17	158.34
26	546.82	547.49	547.49	369.88	370.39	176.94	177.10	164.63	164.67
27	556.77	557.32	557.62	372.89	373.40	183.88	183.92	171.20	171.16
28	566.51	567.22	567.22	375.62	376.33	190.99	190.89	177.41	177.46
29	577.05	577.41	577.72	379.36	379.86	197.69	197.55	183.72	183.94
30	587.18	587.84	587.84	382.79	383.28	204.39	204.56	190.25	190.14
31	598.11	598.72	598.87	386.80	387.27	211.31	211.45	196.48	196.70
32	608.76	609.38	609.38	390.70	391.14	218.06	218.24	202.89	203.05
33	620.23	620.79	620.79	395.22	395.67	225.01	225.12	209.20	209.35
34	631.27		631.85	399.56	400.03	231.71	231.82	215.59	215.76
35	634.24		643.80	404.64	405.03	238.60	238.77	221.84	221.99
36	654.71		655.26	409.43	409.86	245.28	245.40	228.28	228.40
37	667.13		667.72	414.96	415.40	252.17	252.32	234.51	234.62
38	679.09		679.62	420.20	420.64	258.89	258.98	240.85	241.01
39	691.98		692.56	426.28	426.71	265.70	265.85	247.09	247.20
40	704.39		704.88	432.00	432.42	272.39	272.46	253.39	253.57
41	717.69		718.27	438.59	438.99	279.10	279.28	259.61	259.70
42	730.54		731.03	444.78	445.18	285.76	285.85	265.88	266.00
43	744.43		744.90	451.81	452.27	292.62	292.63	272.06	272.14
44	757.65		758.12	458.48	458.89	299.17	299.23	278.37	278.43
45	772.06		772.31	466.06	466.47	306.00	305.84	284.46	284.58
46	785.64		786.12	473.19	473.54	312.45	312.58	290.84	290.68
47				481.22	481.63			296.84	296.92
48	814.80		814.96	488.80	489.20	326.00	325.76		
49	830.19		830.19					309.12	309.28
50	844.39		844.74	505.68	505.68	338.71	339.06	315.30	315.30
51	860.26		860.75	514.89	514.89	345.27	345.86	321.40	321.49
52	875.09		875.44	522.99	523.25	352.10	352.19	327.58	327.77
53	891.42		891.81	532.68	532.98	358.74	358.83	333.62	333.68
54	906.64		907.01	541.47	541.76	365.17	365.25	339.82	339.78
55	923.44		923.86	551.60	552.03	371.84	371.83	345.63	345.82
56	939.04		939.43	561.01	561.19	378.03	378.24	351.87	351.91
57	956.32		956.71	571.57	571.95	384.75	384.76	357.63	357.78
58	972.43		972.76	581.41	581.65	391.02	391.11	363.78	363.83
59	990.15		990.52	592.54	592.88	397.61	397.64	369.71	370.04
60	20006.94		20006.94	602.72	602.72	404.22	404.22	375.75	375.80

TABLE II (cont.)

Frequencies of the lines of the (0,0) band, and their combination differences.

j	R^r	R^s	R^q	P^r	P^q	$2\Delta F^{rr}$	$2\Delta F^{rq}$	$2\Delta F^{rr}$	$2\Delta F^{rq}$
61	20024.83		20025.21	19614.40	19614.72	410.43	410.49	381.95	381.70
62	041.24		041.97	624.99	625.24	416.25	416.73	387.64	387.70
63	060.45		060.66	637.19	637.51	423.26	423.15	393.02	393.53
64	077.87		077.87	648.22	648.44	429.65	429.43	399.64	399.41
65	096.70		097.07	660.81	661.25	435.89	435.82	405.49	405.29
66	114.33		114.56	672.38	672.58	441.95	441.98	411.12	411.20
67	133.91		134.20	685.58	685.87	448.33	448.33	416.95	416.86
68	152.13		152.13	697.38	697.70	454.75	454.43	422.81	422.78
69	171.95		171.95	711.10	711.42	460.85	460.53	428.51	428.51
70	190.52		190.52	723.62	723.62	466.68	466.90	434.31	434.31
71	210.85		211.11	737.64	737.64	473.21	473.47	439.94	439.92
72	229.55		229.55	750.36	750.60	479.19	478.95	445.50	445.76
73	250.50		250.73	765.35	765.35	485.15	485.38	451.27	451.27
74	269.71			778.28	778.28	491.43		456.92	457.15
75	291.09			793.58	793.58	497.51		462.38	
76	310.50			807.33		503.17		468.36	
77	332.49			822.73		509.76		473.99	
78	352.17			836.51		515.66		479.70	
79	374.44			852.79		521.65		485.23	
80	394.76			866.94		527.82		490.69	
81	417.36			883.75		533.61		496.46	
82	437.76			898.30		539.46		501.88	
83	460.79			915.48		545.31		507.21	
84	481.62			930.51		551.11		512.59	
85	505.29			948.20		557.09		518.29	
86	526.27			963.33		562.94		523.55	
87	550.37			981.74		568.63		528.74	
88	571.48			997.53		573.95		534.24	
89	596.15			20016.13		580.02		539.20	
90	617.85			032.28		585.57		544.85	
91	642.61			051.30		591.31		550.06	
92	664.65			067.79		596.86		555.35	
93	689.79			087.26		602.53		560.38	
94	712.21			104.27		607.94		565.64	
95	737.74			124.15		613.59		570.83	
96	760.43			141.38		619.05		576.08	
97	786.39			161.66		624.73		581.13	
98	809.27			179.30		629.97		586.25	
99	835.54			200.14		635.40		591.25	
100	858.73			218.02		640.71		597.03	
101	885.25			238.51		646.74		601.21	
102	908.85			257.52		651.33		607.54	
103	935.93			277.71		658.22		611.24	
104	959.61			297.61		662.00		616.14	
105	986.85			319.79		667.06		620.87	
106	21010.84			338.74		672.10		625.95	
107	038.40			360.90		677.50		630.69	
108	062.63			380.15		682.48		635.89	
109	090.50			402.51		687.99		639.90	
110				422.73				644.82	
111				445.68					
112				465.56					
113				488.71					
114				509.21					
115				532.37					
116				553.31					
117				576 71					
118				598.06					
119				622.57					
120				645.17					
121				667.69					

TABLE III

Frequencies of the lines of the (0,1) band, and their combination differences.

j	R^r	R^s	R^q	P^r	P^q	$2\Delta F^{rr}$	$2\Delta F^{rq}$	$2\Delta F^{rr}$	$2\Delta F^{rq}$
1									
2									
3									
4									
5									
6			17787.48						
7			792.30						
8			797.57						
9		17801.65	803.14						
10		807.59	808.93						
11		813.89	815.09						
12		820.45	821.44						

TABLE III (cont.)

Frequencies of the lines of the (0,1) band, and their combination differences.

j	R^r	R^c	R^o	P^r	P^o	$2\Delta F''_r$	$2\Delta F''_o$	$2\Delta F''_r$	$2\Delta F''_o$
13		17827.30	17828.18						
14		834.31	835.16						
15		841.68	842.47						
16	17848.39	849.33	849.98	17740.70		107.69			99.28
17	856.57	857.27	857.87	741.74	17742.40	114.83	114.87	105.47	105.61
18	864.42	865.34	865.91	742.92	743.72	121.50	121.62	112.02	112.08
19	873.19	873.83	874.41	744.55	745.19	128.64	128.64	118.13	118.44
20	881.49	882.52	882.97	746.29	746.90	135.20	135.62	124.74	142.76
21	890.90	891.56	892.02	748.45	749.07	142.45	142.49	130.82	131.24
22	900.03	900.56	901.06	750.67	751.28	149.36	149.28	137.49	137.59
23	909.60	910.30	910.73	753.41	753.97	156.19	156.33	143.86	143.78
24	919.32	920.28	920.28	756.17	756.78	163.15	163.50	150.15	150.25
25	929.58	930.12	930.52	759.45	760.05	170.13	170.47	156.54	156.91
26	939.30	940.61	940.61	762.78	763.37	176.52	177.24	163.02	162.97
27	950.49	951.05	951.43	766.56	767.15	183.93	183.90	168.84	169.54
28	961.16		961.94	770.46	771.07	190.70	190.87	175.60	175.58
29	972.54		973.23	774.89	775.47	197.65	197.76	181.83	182.06
30	983.53		984.35	779.33	779.88	204.20	204.47	188.22	188.39
31	995.39		996.31	784.32	784.84	211.07	211.47	194.23	194.58
32	18007.30		18008.00	789.30	789.77	218.00	218.23	200.61	200.97
33	019.81		020.44	794.78	795.34	225.03	225.10	206.95	207.16
34	031.95		032.64	800.35	800.84	231.60	231.80	213.44	213.46
35	044.97		045.63	806.37	806.98	238.60	238.65	219.47	219.67
36	057.66		058.35	812.48	812.97	245.38	245.38	225.78	226.01
37	071.17		071.91	819.19	819.62	251.98	252.29	231.95	232.13
38	084.54		085.15	825.71	826.22	258.83	258.93	238.22	238.46
39	098.33		099.20	832.95	833.45	265.38	265.75	244.45	244.63
40	112.44		112.92	840.09	840.52	272.35	272.40	250.43	250.81
41	127.05		127.58	847.90	848.39	279.15	279.19	256.97	256.95
42	141.22		141.75	855.47	855.97	285.75	285.78	263.12	263.16
43	156.42		156.94	863.93	864.42	292.49	292.52	269.18	269.24
44	171.16		171.61	872.04	872.51	299.12	299.10	275.40	275.45
45	186.94		187.46	881.02	881.49	305.92	305.97	281.49	281.47
46	202.16		202.63	889.67	890.14	312.49	312.49	287.75	287.87
47				899.19	899.59			293.71	293.79
48	233.89		234.52	908.45	908.84	325.46	325.68		
49			251.23					306.09	305.98
50			267.56	927.80	928.54		339.02		311.93
51	284.64		285.18		939.30		345.88		318.02
52	301.14		301.64		949.54		352.10	324.15	324.02
53	318.93		319.64	960.49	961.16	358.44	358.48	330.02	330.07
54			336.69	971.12	971.57		365.12	335.89	336.11
55	354.74		355.29	983.04	983.53	371.70	371.76		341.92
56	372.36		372.78	994.33	994.77	378.03	378.01	348.00	347.99
57	391.41		391.85	18006.74	18007.30	384.67	384.55	353.92	353.93
58	409.45		409.90	018.44	018.85	391.01	391.05	359.97	359.90
59	429.03		429.48	031.44	031.95	397.59	397.53		365.81
60	447.68		448.07		044.09		403.98	371.83	371.82
61	467.64		468.03	057.20	057.66	410.44	410.37		377.63
62	486.67		487.02		070.44		416.58		383.49
63	507.14		507.62		084.54		423.08		389.36
64	526.68		527.04		097.66		429.38		395.18
65	547.90		548.27		112.44		435.83		400.83
66			568.10		126.21		441.89		406.52
67			590.14		141.75		448.39		412.29
68			610.20		155.81		454.39		418.53
69			632.11		171.61		460.50		424.00
70			653.09		186.20		466.89		429.48
71			675.93		202.63		473.30		435.15
72			697.03		217.94		479.09		441.41
73			720.34		234.52		485.82		446.44
74			742.02		250.59		491.43		452.18
75			765.86		268.16		497.70		457.38
76			787.41		284.64		502.77		463.52
77			812.13		302.34		509.79		468.48
78			834.40		318.93		515.47		474.92
79			859.34		337.21		522.13		479.66
80			882.25		354.74		527.51		485.42
81			907.48		373.92		533.56		490.84
82			930.72		391.41		539.31		496.29
83			956.50		411.19		545.31		501.69
84			980.14		429.03		551.11		507.15
85			19006.87		449.35		557.52		512.18
86			030.43		467.96		562.47		518.08
87			057.35		488.79		568.56		522.81
88			081.77		507.62		574.15		526.36
89					528.99				533.87
90					547.90				

successively. For the (1,0) band, Johnson's data have been substituted for the much poorer data of Hindrich's which were originally used. In this band, as well as in the (1,2) band, the series assignments have been carried to

TABLE IV

Frequencies of the lines of the (1,0) band, and their combination differences.

j	R^r	R^c	R^v	P^r	P^v	$2\Delta F''$	$2\Delta F'''$	$2\Delta F^{IV}$	$2\Delta F^{V}$
1									
2	21135.36	21138.65	21142.55						
3	139.86	142.55	145.99						
4	144.86	146.50	149.64						
5	149.13	150.90	153.63						
6	153.63	155.38	157.74						
7	158.82	160.16	162.18						
8	163.71	165.07	166.83						
9	169.10	170.22	171.75						
10	174.34	175.51	176.85						
11	180.09	181.05	182.25						
12	185.69	186.72	187.76						
13	191.86	192.64	193.62						
14	197.77	198.71	199.54						
15	204.24	205.04	205.89						
16	210.54	211.41	212.26						100.32
17	217.47	218.13	218.81		21104.72		113.41		106.69
18	224.20	224.99	225.53		104.72		120.27	113.32	112.98
19	231.49	232.11	232.73	21104.15	105.15	126.77	126.96	119.48	119.84
20	238.61	239.36	239.80	104.72	105.15	133.89	134.21	126.34	126.24
21	246.24	246.92	247.34	105.15	105.87	141.09	141.05	132.47	132.75
22	253.71	254.42	254.82	106.14	106.61	147.57	147.81	139.24	138.96
23	261.78	262.40	262.82	107.00	107.96	154.78	154.44	145.36	145.23
24	269.62	270.30	270.62	108.35	109.19	161.27	161.11	152.09	151.77
25	278.11	278.75	279.04	109.69	110.63	168.42	168.12	158.17	158.09
26	286.49	286.95	287.23	111.45	112.21	175.04	174.74	164.82	164.70
27	295.08	295.68	297.06	113.29	114.05	181.79	181.63	171.07	170.93
28	303.86	304.35	304.77	115.42	116.02	188.44	188.33	177.28	177.57
29	312.44		313.50	117.80	118.11	195.64	195.39	183.90	183.86
30	321.93		322.86	119.96	120.49	201.97	202.37	189.68	190.29
31	330.22		330.89	122.76	123.21	207.46	207.68	196.45	196.84
32	341.35		341.83	125.48	126.02	215.87	215.81	202.94	203.24
33	351.67		352.32	127.28	127.65	224.39	224.67	209.56	209.54
34	360.82		361.31	131.79	132.29	229.03	229.02	215.96	215.95
35	371.25		371.83	135.71	136.37	235.54	235.46	221.76	222.25
36	381.40		381.77	139.06	139.33	242.34	242.44	228.02	228.12
37	393.12		393.91	143.23	143.71	249.89	250.20	234.49	234.50
38	402.52		403.10	146.91	147.27	255.61	255.83	240.97	
39	413.85		414.10	152.15		261.70		247.02	247.14
40	424.80		425.22	155.50	155.96	269.47	269.26	253.16	253.02
41	436.44		437.26	160.69	161.08	275.75	276.18	259.93	259.84

TABLE V

Frequencies of the lines of the (1,1) band, and their combination differences.

j	R^r	R^c	R^v	P^r	P^v	$2\Delta F''$	$2\Delta F'''$	$2\Delta F^{IV}$	$2\Delta F^{V}$
1									
2									
3									
4									
5									
6									
7									
8									
9									
10									
11									
12									
13									
14	19582.91	19583.58	19584.57						
15	589.26	590.41	591.26					92.87	92.57
16	596.50	597.38	598.11	19490.04	19491.01	106.46	106.37	98.66	99.40
17	603.86	604.60	605.36	490.60	491.01	113.26	113.59	105.49	105.78
18	611.07	612.02	612.41	491.01	491.60	120.06	120.42	111.90	111.72
19	619.09	619.74	620.23	491.96	492.88	127.13	126.86	118.19	118.62
20	626.57	627.55	627.98	492.88	493.40	133.69	134.15	125.01	125.10
21	635.13	635.75	636.35	494.08	494.64	141.05	141.11	131.03	131.38
22	643.24	643.80	643.80	495.54	496.17	147.70	147.63	137.53	137.57
23	652.08	652.69	653.09	497.60	498.18	154.48	154.51	143.59	143.63
24	660.81	661.25	661.25	499.65	500.17	161.16	161.08	150.23	150.26
25	669.97	670.61	670.93	501.85	502.43	168.12	168.18	156.63	156.46
26	679.09	679.62	679.62	504.18	504.79	174.91	174.83	163.05	163.12
27	688.75	689.38	689.59	506.92	507.49	181.83	181.89	169.38	169.34
28	698.34	698.92	699.20	509.71	510.28	188.63	188.64	175.63	175.77
29	708.42	708.96	709.19	513.12	513.61	195.30	195.35	182.01	182.00
30	718.27	719.12	719.12	516.33	516.92	201.94	202.20	188.61	188.56
31	727.59	728.12	728.12	519.81	520.40	207.78	207.72	194.37	194.69
32	739.47	740.06	740.06	523.90	524.43	215.57	215.63	199.54	199.39
33	751.43	751.75	751.75	528.05	528.73	223.38	223.02	206.79	207.08

TABLE V (cont.)

Frequencies of the lines of the (1,1) band, and their combination differences.

j	R^r	R^c	R^v	P^r	P^v	$2\Delta F^{rr}$	$2\Delta F^{rv}$	$2\Delta F^{vr}$	$2\Delta F^{vv}$
34	19761.51	19761.95	19761.95	19532.98	19533.48	228.83	228.53	213.91	213.68
35	773.12	773.59	773.95	537.52	538.07	235.60	235.52	219.75	219.79
36	784.33		784.90	541.47	541.76	242.57	242.57	225.63	225.87
37	797.15		797.68	547.49	547.72	249.66	249.96	232.30	232.30
38	807.93		808.48	551.60	552.03	255.90	256.45	238.47	238.49
39	820.63		821.13	558.68	559.19	261.95	261.94	244.77	244.71
40	832.50		832.96	563.16	563.77	269.34	269.19	250.19	250.93
41	845.61		846.21	569.76	570.20	275.85	276.01	256.92	256.94
42	857.96		858.55	575.58	576.02	282.38	282.53	263.16	263.30
43	871.65		872.14	582.45	582.91	289.20	289.23	269.20	269.29
44	883.75		884.74	588.76	589.26	294.99	295.48	275.54	275.64
45	898.30		898.83	596.11	596.50	302.19	302.33	281.36	282.02
46	911.43		911.91	602.39	602.72	308.71	309.17	287.90	287.76
47	926.00		926.50	610.40	611.07	315.60	315.43	293.72	293.83
48	939.43		939.77	617.71	618.08	321.72	321.69	299.96	299.93
49	954.48		954.99	626.04	626.57	328.44	328.42	305.89	305.89
50	968.44		968.79	633.54	633.88	334.90	334.91	312.07	312.16
51	983.73		984.20	642.41	642.83	341.32	341.37	318.12	318.06
52	998.50		998.58	650.32	650.73	348.18	347.85	324.12	324.12
53	20014.11		20015.24	659.61	660.08	354.50	355.16	330.78	330.15
54	028.71		029.06	667.72	668.43	360.99	360.63	336.28	337.02
55	044.98		045.41	677.83	678.22	367.15	367.19	342.13	342.11
56	060.45		060.66	686.58	686.95	373.87	373.71	347.60	347.71
57	077.87		077.87	697.38	697.70	380.49	380.17	354.27	354.13
58	092.14		092.54	706.18	706.53	385.96	386.01	360.86	360.65
59	109.02		109.33	717.01	717.22	392.01	392.11	365.34	365.74
60	125.35		125.63	726.80	726.80	398.55	398.83	371.54	371.69
61	143.28		143.78	737.48	737.64	405.80	406.14	377.64	377.70
62	159.79		159.79	747.71	747.93	412.08	411.86	383.60	384.10
63	176.40		176.78	759.68	759.68	416.72	417.10	389.69	389.69
64	193.78		193.78	770.10	770.10	423.68	423.68	393.74	394.12
65	212.27		212.71	782.66	782.66	429.61	430.05	400.94	400.56
66	229.55		229.55	792.84	793.22	436.71	436.33	406.24	406.68
67	248.38		248.38	806.03	806.03	442.35	442.35	413.09	412.73
68	265.27		265.52	816.46	816.82	448.81	448.70	418.19	418.19
69	285.04			830.19	830.19	454.85	454.85	423.92	423.94
70	302.47			841.35	841.58	461.12	460.89	430.00	429.69
71	322.37			855.04	855.35	467.33	467.02	435.53	
72	339.97			866.94		473.03		441.02	
73	360.90			881.35		479.55		446.58	
74	378.64			893.39		485.25		452.75	
75	394.92			908.15		486.77		457.81	
76	417.36			920.83		496.53		459.30	
77	437.76			935.62		502.14		469.16	
78	457.25			948.20		509.05		474.43	
79	479.05			963.33		515.72		479.84	
80	497.77			977.41		520.36		485.45	
81	518.98			993.60		525.38		490.83	
82	538.94			20006.94		532.00			
83	561.25								
84	580.85								
85	603.39								
86	623.21								
87	646.36								
88	666.32								
89	689.79								
90	710.11								
91	734.21								
92	754.35								
93	778.38								
94	799.03								
95	823.49								
96	844.53								
97	868.96								
98	890.51								
99	915.03								
100	935.93								
101	959.61								

somewhat larger values of j than given in Tables II to VI but seem too uncertain to warrant publication.

In all cases the values of $2\Delta F^r$ have been obtained by the use of red component of the P and R branches. The values of $2\Delta F^v$, however, have been obtained from the violet component of the P branch and the central component of the R branch, where it exists, otherwise from the violet component. This has been done because, as is shown later in the paper, the violet component of the P branch corresponds to the central component of the R

TABLE VI

Frequencies of the lines of the (1,2) band, and their combination differences.

j	R^r	R^c	R^v	P^r	P^v	$2\Delta F''^v$	$2\Delta F''^v$	$2\Delta F''^r$	$2\Delta F''^r$
1									
2									
3									
4									
5									
5									
6									
7									
8									
9									
10			17967.21						
11			973.23						
12	17977.30	17978.39	979.47						
13	984.35	985.18	986.09					78.73	78.80
14	991.10	992.02	992.92	17898.57	17899.59	92.43	92.43	85.16	85.15
15	998.46	999.29	18000.12	899.19	900.03	99.27	99.26	91.51	91.46
16	18005.88	18006.74	007.30	899.59	900.56	106.29	106.18	97.90	98.21
17	013.79	014.52	015.24	900.56	901.08	113.23	113.44	104.80	104.69
18	021.68	022.49	023.09	901.08	902.05	120.60	120.44	110.68	110.76
19	030.10	030.82	031.44	903.11	903.76	126.99	127.06	118.08	117.27
20	038.56	039.29	039.83	904.60	905.32	133.96	133.97	123.49	123.50
21	047.56	048.19	048.66	906.61	907.32	140.95	140.87	129.72	129.69
22	056.39	057.20	057.66	908.84	909.60	147.53	147.60	136.18	136.17
23	065.95	066.49	066.94	911.38	912.02	154.57	154.47	142.32	142.28
24	075.31	076.02	076.40	914.07	914.92	161.24	161.10	148.74	148.71
25	085.15	085.91	086.28	917.21	917.78	167.94	168.13	155.03	155.07
26	095.31	095.96	096.27	920.28	920.95	175.03	175.01	161.09	161.25
27	105.77	106.32	106.70	924.06	924.66	181.71	181.66	167.51	167.42
28	116.29	117.05	117.05	927.80	928.54	188.49	188.51	173.80	173.77
29	127.05		127.58	931.97	932.55	195.08	195.03	180.00	180.15
30	138.32		139.03	936.29	936.90	202.03	202.13	186.44	186.14
31	150.03		150.94	940.61	941.44	209.42	209.50	192.43	192.59
32	161.37		162.05	945.89	946.44	215.48	215.61	199.98	199.51
33	173.59		174.29	951.05	951.43	222.52	222.86	204.87	205.00
34	185.56		186.20	956.50	957.05	229.06	229.15	211.07	211.02
35	198.37		199.06	962.52	963.27	235.83	235.79	217.27	217.53
36	210.75		211.33	968.29	968.67	242.46	242.66	223.57	223.72
37	224.02		224.70	974.80	975.34	249.22	249.36	229.71	229.86
38	236.78		237.36	981.04	981.47	255.74	255.89	225.29	235.97
39	250.59		251.23	988.73	988.73	261.86	262.50	242.01	241.97
40	263.86		264.36	994.77	995.39	269.09	268.97	248.10	248.25
41	278.33		278.94	18002.49	18002.98	275.84	275.96	254.18	254.23
42	292.04		292.71	009.68	010.13	282.36	282.58	260.46	260.50
43	306.91		307.54	017.87	018.44	289.04	289.10	266.37	266.43
44	321.20		321.77	025.67	026.28	295.53	295.49	272.43	272.57
45	336.69		337.21	034.48	034.97	302.21	302.24	278.55	278.54
46	351.34		351.88	042.65	043.23	308.69	308.65	284.10	283.86

branch. The combination principle is tested by comparing the values of $2\Delta F_j'$ for all bands having the same initial vibration state, and the values of $2\Delta F_j''$ for all bands having the same final vibration state. In general the discrepancies are less than about 0.15 cm^{-1} and fall within the limits of experimental error.

THE DETERMINATION OF THE CONSTANTS OF THE MOLECULAR CARRIER

Birge[20] and others have recently developed the quantum theory, with certain assumptions, to such a point that it is now possible to determine certain constants for the molecule giving rise to a band spectrum with a comparatively high degree of accuracy. The first assumption is that the law of force between the two nuclei of the molecule can be represented by:

$$F(\text{dynes}) = k_1(r-r_0) + k_2(r-r_0)^2 + k_3(r-r_0)^3 + \cdots \qquad (3)$$

The second important assumption is that the values of the energy levels can be represented by an expression of the form[21]:

[20] Birge, Nature **116**, 783 (1925); Phys. Rev. **27**, 245 (1926); Report, Chap. IV.

[21] Birge, Report, pp. 173–175, 234–237.

$$E/hc=(E^n+E_m)/hc=E^nhc+B_nm^2+D_nm^4+F_nm^6+H_nm^8+\cdots. \quad (4)$$

where $m=j-\epsilon=k-\alpha$ and E^n is the energy due to vibration. Kemble,[22] considering only the first three terms on the right of Eq. (4), has obtained expressions for B_0, B_1, D_0 and D_1. The relations are simplified if the case of the non-vibrating molecule is considered, i.e., if $n=0$. Neglecting the electronic energy, as is done in Eq. (4), one can write:

$$E_m/hc=F_m=B_0m^2+D_0m^4+F_0m^6+H_0m^8+\cdots. \quad (5)$$

The constants of the molecule referred to above are the values of k_1, k_2, and k_3 of Eq. (3) and the value of B_0 of Eq. (5). The moment of inertia I_0 of the molecule is determined from B_0, since $B_0=h/8\pi^2I_0$.

Expressions for the values of the k_1, k_2, k_3, etc., which will be called here the k_i (i taking on the values 1, 2, 3, $\cdots$), can be developed for the cases of a molecule rotating, but having only infinitesimal vibration, and of a molecule vibrating, but having only infinitesimal rotation. The expressions for the k_i for the first case involve only quantities which can be derived from rotational data alone. The expressions for the k_i for the second case involve the values of B_0 and B_1, which must be determined from rotational data, in addition to quantities which can be determined from vibrational data.[23]

In the actual determination of the constants it is better in view of the relative accuracy of the two types of data to eliminate the k_i from the expressions for the k_i derived for the two cases considered. The following relations are then obtained:

$$D_0=-4B_0^3/(\omega^{0^2}) \quad (6)$$

$$F_0=(2-\alpha\omega^0/6B_0^2)D_0^2/B_0 \quad (7)$$

$$H_0=3F_0D_0/B_0-5D_0^3/B_0^2+F_0^2/D_0-8D_0^2x/3\omega^0 \quad (8)$$

where ω^0 is the limiting frequency of vibration for infinitesimal amplitude, $\alpha=B_0-B_1$, and $x=(\omega^0-\omega^1)/2\omega^0$, ω^1 being the frequency of vibration for the state $n=1$. Eq. (6) is due to Kratzer,[24] Kemble,[22] and others, while Eqs. (7) and (8) are due to Birge.[25] Kemble, using only terms inclusive of D_n in Eq. (4) has derived a theoretical expression for β'' in

$$D_n=D_0+\beta''n \quad (9)$$

This is as far as usable theoretical relations had been developed at the time the present investigation was carried on.

Since the expression for the frequency of the lines of a band involve the values of the rotational energy for both the initial and final states, Eqs. (1a) and (1c), it is inconvenient to make use of these expressions. The combination differences, however, Eqs. (2a) and (2b), involve only the energy values

[22] Kemble, J. Optical Soc. Am. **12**, 1 (1926).
[23] Birge, Report, p. 235 et. seq.
[24] Kratzer, Zeits. f. Physik **3**, 289 (1920).
[25] Birge, Report, p. 237; Nature, **116**, 783 (1925).

for a single state. Substituting Eq. (5) in either Eq. (2a) or (2b) there results:

$$2\Delta F_j = 4B_0 m + 8D_0 m^3 + 12F_0 m^5 + 16H_0 m^7 + \cdots \tag{10}$$

Eqs. (6) to (8) are expressions for D_0, F_0 and H_0 in terms of quantities derivable from vibrational data, but each of these are functions of B_0. As B_0 is not accurately known at first, Eq. (10) can most conveniently be solved by the method of successive approximations.

In the case of the Swan bands m is not an exact half-integer, and it is therefore necessary to determine α (or ϵ) at the same time that B_0 is determined. In the course of the investigation it was found that α itself is a function of k of the form

$$\alpha = \alpha_0 + \zeta_0 k^2 + \theta_0 k^4 + \cdots \tag{11}$$

with an analogous expression for ϵ. This is not without precedent, as Birge[26] found it necessary to use a variable α in the case of the CuH bands. In the case of the Swan bands it was found necessary to include only the first two terms of Eq. (11).

The method of calculation actually used will now be briefly outlined. The quantities which are derivable from vibrational data are assumed to be accurately known, due to the fact that the percent error in their determination is very small It is then necessary to express Eq. (10) as a function of the unknowns, which are B_0, B_1 and α (or ϵ). The resultant expression is unwieldy and the method of successive approximations is used.

Let B_s be an assumed value of B_0, i.e., an approximate value of B_0 determined in any suitable manner. With this value of B_0 approximate values of D_0, F_0, and H_0 are calculated, these being denoted by D_s, F_s, and H_s. Approximate values of $2\Delta F_j$ may then be calculated by means of Eq. (10) using the values of B_s, D_s, F_s and H_s. Residuals are then formed, in the sense of observed value of $2\Delta F_j$ minus the calculated value. Corrections to the value of B_s are then determined from these residuals in the following manner. The variation of Eq. (10) with respect to the quantities which are variable is

$$\delta 2\Delta F_j = 4m\delta B_0 + 8m^3 \frac{\partial D_0}{\partial B_0}\delta B_0 + 12m^5 \frac{\partial F_0}{\partial B_0}\delta B_0 + 12m^5 \frac{\partial F_0}{\partial B_1}\delta B_1 + 16m^7 \frac{\partial H_0}{\partial B_0}\delta B_0 + 16m^7 \frac{\partial H_0}{\partial B_1}\delta B_1 + \cdots \tag{12}$$

B_1 differs but little from B_0 and hence B_s may be used as an approximate value of B_1. The variation of $2\Delta F_j$ is, except for terms of higher order than the first, the residual found by means of the approximate values of the constants. If α (or ϵ) is to be determined it may be included in Eq. (12) and evaluated along with the δB_0 and δB_1. In the actual case of the Swan bands it was also necessary to include a term due to ζ_0 of Eq. (11). Sub-

[26] Birge, Report, pp. 174–175, 236. See also Kemble, Report, p. 346.

stituting $k-\alpha$ for m in Eq. (12) and for α its expanded form in Eq. (11), one has

$$\delta 2\Delta F_j = a+\delta B_0\left(4k+8k^3\frac{\partial D_0}{\partial B_0}+12k^5\frac{\partial F_0}{\partial B_0}+16k^7\frac{\partial H_0}{\partial B_0}\right)+ck^2$$

$$+\delta B_1\left(12k^5\frac{\partial F_0}{\partial B_1}+16k^7\frac{\partial H_0}{\partial B_1}\right)+\cdots \qquad (13)$$

where $a=-4B_0\alpha_0+\cdots$ and $c=-12B_0\zeta_0-24D_0\alpha_0+\cdots$.

The most probable values of the unknowns in Eq. (13) are given by the method of least squares. However, as no rapid method of least squares has been formulated to cover such a case as this the labor involved is excessive. After much consideration it was decided to solve Eq. (13) by the method introduced into modern literature by Norman Campbell under the name of "Zero Sums."[27] The method of zero sums consists of dividing the observational equations up into as many groups as there are unknowns, and then adding the observational equations of each group. One then has as many simultaneous equations ("normal" equations) as there are unknowns, and the solution is made in any convenient way. This method, when applied to Eq. (13) reduces enormously the amount of work necessary. Let one consider a rational integral function where values of the dependent variable are given for equidistant values of the independent variable, and make a change of variable, if need be, so that the independent variable has successive values which differ by unity, but which are not necessarily integral. The observational equations of any one of the "Zero Sums" groups may then be represented by

$$y_x=a_0+a_1(x_c+r)+a_2(x_c+r)^2+a_3(x_c+r)^3+\cdots \qquad (14)$$

in which r is either an integer or a half-integer, depending upon whether there is an odd or even number of observations in the group, and varies from $-u$ to $+u$, where $u=(n-1)/2$, n being the number of observations in the group. x_c is the central or average value of the independent variable for the group. If now the average of n consecutive observational equations be taken, there results, by application of the binomial expansion,

$$(1/n)\sum_{r=-u}^{r=+u} y_x=a_0+a_1Z_1+a_2Z_2+a_3Z_3+\cdots \qquad (15)$$

where, if $A=\dfrac{n^2-1}{12}$; $B=\dfrac{3n^2-7}{20}A$; $C=\dfrac{3n^4-18n^2+31}{112}A$

$$\begin{array}{lll} Z_0=1 & Z_3=x_c^3+3Ax_c & Z_6=x_c^6+15Ax_c^4+15Bx_c^2+C \\ Z_1=x_c & Z_4=x_c^4+6Ax_c^2+B & Z_7=x_c^7+21Ax_c^5+35Bx_c^3+7Cx_c \\ Z_2=x_c^2+A & Z_5=x_c^5+10Ax_c^3+5Bx_c & \end{array} \qquad (16)$$

[27] Campbell, Phil. Mag. (6) **39**, 177 (1920). The writer believes this method to be essentially the same as that given by Tobias Mayer in 1748. See Whittaker and Robinson, Calculus of Observations, p. 258.

Eq. (15) is rigorous, but the left hand side in practice contains the algebraic sum of the errors, divided by n, and will therefore be referred to as a normal place.

Now Eq. (15) may be applied to both Eq. (10) and Eq. (13) Thus it is not necessary to calculate the individual residuals, but the algebraic sum of the residuals may be computed at once by the application of Eq. (15). The original values of $2\Delta F_j$ are divided into as many groups as there are unknowns, and the sums of the $2\Delta F_j$ are found for each group. From this point until the approximations are finished it is not necessary to deal with the individual values. In the actual work on the Swan bands an equation, analogous to Eq. (13), was set up for the vibrational state $n=1$. The inclusion of the data for the vibration state $n=1$ practically doubled the number of observational equations, but only increased the number of unknowns from four to six, the two additional unknowns being the values of a and c of Eq. (13) for the state $n=1$. In the present investigation about one hundred and seventy values of $2\Delta F_j$ were available.

The various constants discussed above were evaluated, with the results which follow. The constants for the vibration state $n=1$ are not listed, as the theoretical basis upon which they were computed is not sufficiently well founded to warrant their publication.

Initial State	*Final State*
$\alpha' = 0.0487 - 7.36\times10^{-6}k^2$	$\alpha'' = 0.0324 - 2.55\times10^{-6}k^2$
$B_0' = 1.7495$ cm^{-1}	$B_0'' = 1.6260$ cm^{-1}
$D_0' = 6.8673\times10^{-6}$ cm^{-1}	$D_0'' = -6.5040\times10^{-6}$ cm^{-1}
$F_0' = 0.9068\times10^{-11}$ cm^{-1}	$F_0'' = 1.2365\times10^{-11}$ cm^{-1}
$H_0' = -3.14\times10^{-16}$ cm^{-1}	$H_0'' = -1.64\times10^{-16}$ cm^{-1}
$B_0' - B_1' = 0.01730$ cm^{-1}	$B_0'' - B_1'' = 0.01487$ cm^{-1}
$I_0' = 15.84\times10^{-40}$ gm cm^2	$I_0'' = 17.03\times10^{-40}$ gm cm^2
$r_0' = 1.265\times10^{-8}$ cm	$r_0'' = 1.311\times10^{-8}$ cm
$k_1' = 10.92\times10^5$ dyne cm^{-1}	$k_1'' = 9.28\times10^5$ dyne cm^{-1}
$k_2' = -3.44\times10^{14}$ dyne cm^{-2}	$k_2'' = -2.68\times10^{14}$ dyne cm^{-2}
$k_3' = 2.75\times10^{22}$ dyne cm^{-3}	$k_3'' = 2.25\times10^{22}$ dyne cm^{-3}

The above values are obtained from the central component of the R branch and the violet component of the P branch. The value of B_0 is believed to be within 0.10 percent of the true value. α_0 is difficult to determine, and the error in its determination may be as high as ten percent. ζ_0 is believed to be accurate to at least five percent. The value of I_0 has essentially the same accuracy as B_0. Fig. 1 gives the residuals of $2\Delta F_j$. In this figure, in order to eliminate somewhat the rather large individual errors of the observations, the residuals are grouped in sets of five, and the average of each set plotted, except for the first and last points on the curve, where the mean of a smaller number of residuals is used. If there is a trend present, it is believed to be so small as not appreciably to affect the constants.

Johnson's published values of I_0' and I_0'' are 16.236×10^{-40} and 17.410×10^{-40}, and while he does not claim for these values an accuracy greater than 0.5 percent, they differ from the present values by over two percent. His values of the moment of inertia, as well as the numbering of the lines, were determined by a graphical method proposed some years ago by Birge. His procedure, while very rapid, is rather indeterminate for complex bands

such as those studied here, and has since been superseded by more definite and precise methods,[28] the most accurate of which is that used in the present investigation. Any one of the new methods indicates that Johnson's numbering of j' and j'' is too large by one unit. This incorrect numbering accounts

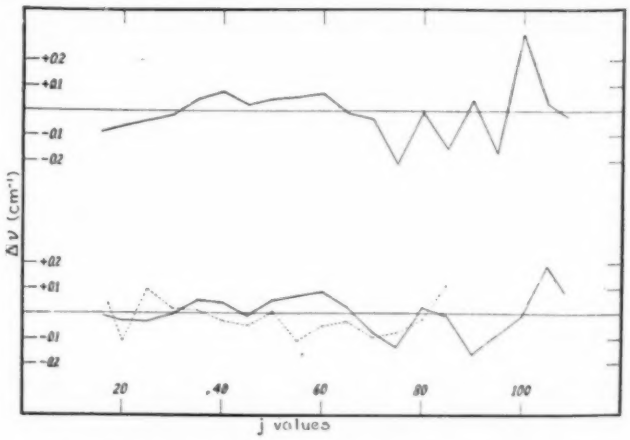

Fig. 1. Mean Residuals of $2\Delta F$. Upper: $2\Delta F''$ (0, 0) band. Lower: $2\Delta F'$, solid line (0,0) band, dotted line (0, 1) band.

entirely for the above discrepancy. Fig. 2 is a plot of the first differences of $2\Delta F_j''$ for the (0,0) band. The circles are the values determined from Leinen's data, and the filled in circles are the values given by Johnson. A curve passed through these points and extrapolated back to $m=0$ (or $j=0.5$ approxi-

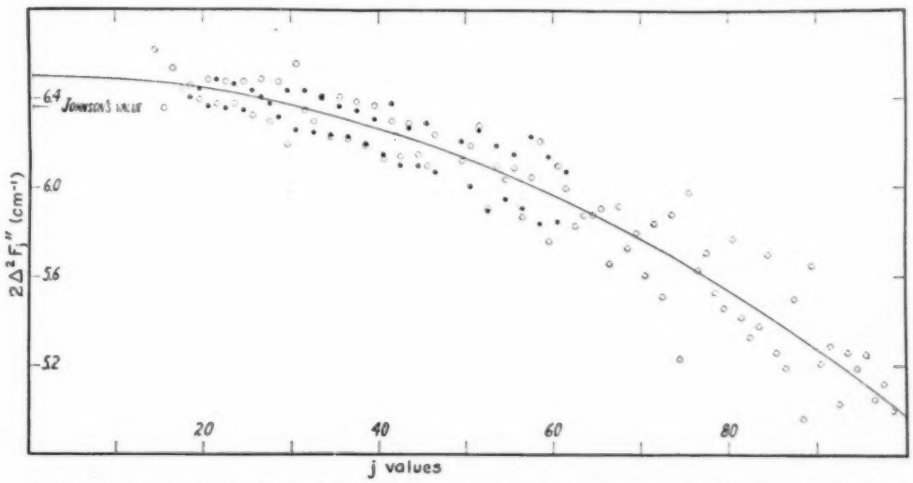

Fig. 2. Values of $2\Delta^2 F_j''$ for the (0, 0) band. Open circles from Leinen's data, solid circles from Johnson's data. Abscissae are j values, ordinates cm^{-1}.

mately) gives the value of $4B_0$, since from Eq. (10) we obtain, to a high degree of approximation,

$$2\Delta^2 F_j = 4B_0 + 24D_0 m^2 + \cdots \tag{17}$$

[28] See Report, pp. 169–175.

The theoretical curve resulting from the constants determined by the writer has been drawn on the figure, as well as the value of $4B_0$ given by Johnson. It is quite apparent that his value is too small. Precisely similar relations hold for the initial state.

In order to determine the frequencies of the origin of the various bands, the contribution due to rotation was calculated and then subtracted from the frequencies of the R and P lines, as indicated in the following equations.

$$\nu_0 = R_j - (F_{j+1}' - F_j'') \tag{18a}$$

$$\nu_0 = P_j - (F_{j-1}' - F_j'') \tag{18b}$$

The following values have been calculated for the frequency of the origin:

(0,0) band, 19379.20 ± 0.2 cm^{-1}
(0,1) band, 17761.10 ± 0.2 cm^{-1}
(1,1) band, 19513.50 ± 0.4 cm^{-1}
(1,0) band, 21131.60 ± 0.5 cm^{-1}

These values are for the mean of the red and violet components. They differ slightly from the values of the origin determined by Johnson, whose values are for the central component. Until a satisfactory explanation of the triplet separation has been developed any value for the origin is somewhat meaningless.

Multiplicity of the Lines

The interpretation of the separation of the components of the doublets and triplets is, to say the least, difficult. Mulliken's interpretation[29] is probably correct, but expressions based upon this interpretation for the separation have not yet been published in sufficient detail to use.[30] None of the other theoretical expressions thus far derived seem to apply in the case of the Swan bands. The R branch consists of triplets for small values of j, and the triplet separations decrease as j increases. In the vicinity of $j=30$ the central component approaches so close to the violet component that it is no longer possible to resolve these two components. In the vicinity of $j=70$ the separation between the resulting two components has become so small that it is no longer possible to resolve them. In the case of the P branch the lines can be carried back only to $j=16$ approximately, but even at this point, with an arc as source, there is no evidence of a triplet structure. Johnson, using a tube fitted with carbon electrodes and filled with argon at 30 mm pressure, has obtained a triplet P branch. Fig. 3 is a plot of the separations of the various components of the (0,0) band, Johnson's data being used. In this figure the lines of the R branch are indicated by the large circles, and the lines of the P branch by the smaller filled-in circles. The vertical axis represents the mean position of the red and violet components of the R branch. The red components of the P branch have been made to coincide,

[29] Mulliken, Phys. Rev. **29**, 637 (1927).

[30] Kemble and Jenkins, Phys. Rev. **29**, 607 (1927), Abstract 8; See also Phys. Rev. **30**, 171 (1927).

arbitrarily, with the red components of the R branch. It is apparent from the plot that the violet component of the P branch coincides with the central component of the R branch, while the central component of the P branch falls between the red and central components of the R branch. Now the central component is observed by Johnson only when using the vacuum tube as a source. There is no evidence whatsoever of a central component

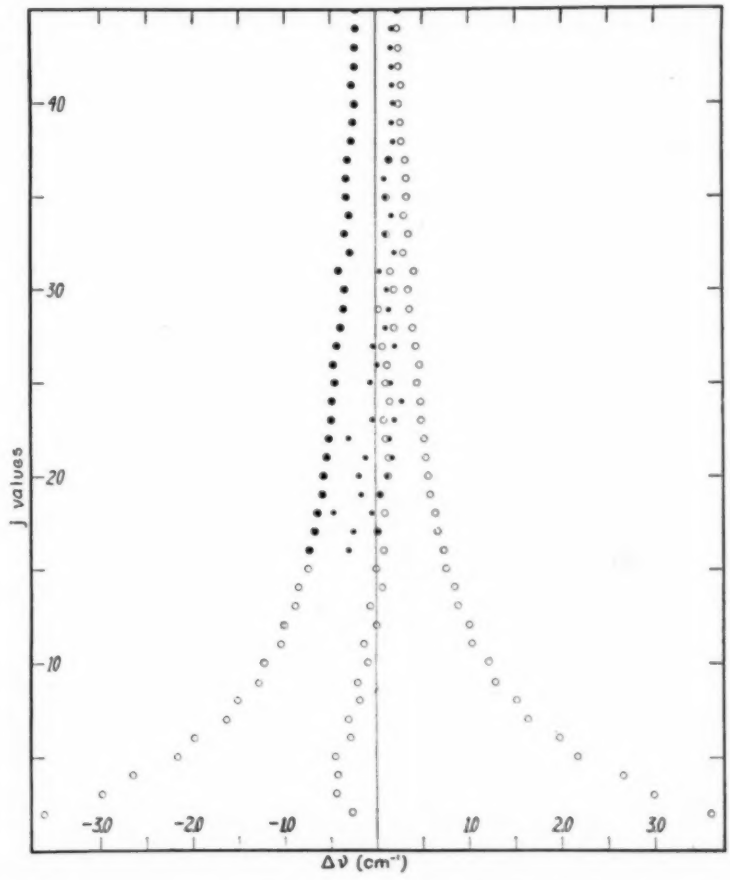

Fig. 3. Component separations of the R and P branches of the (0, 0) band. Large circles represent lines of the R branch with the mean position of the red and violet components taken as the vertical axis. For the P branch the red component is plotted arbitrarily in coincidence with the red component of the R branch, such points being indicated by filling in the large circles. The smaller filled-in circles then represent the position of the violet and (in a few cases) central component of the P branch.

when the arc is used as a source. It is therefore evident that these P lines do not correspond to the central component of the R branch, and their true explanation should be a matter of some interest.

Heurlinger[14] concluded that the separations were a function of m^{-1}. That this is the case is clearly brought out by the fact that the separation of the red and violet components of the R branch can be represented within the

limits of experimental error from about $j=10$ to $j=70$ by the very simple expression $R^v-R^r=c/k$, where c is a constant and $k=j-0.5$. In the region $j=2$ to $j=10$ the separation may be represented by the addition of a term of the form Ae^{-dk}, where A and d are constants. These expressions are, of course, empirical, and are not suggested as a basis for an interpretation of the separation. Any expression which can be made use of theoretically must involve the j for both the initial and final states of the molecule. The basis of this statement lies in the following observed relations, which seem to be true, on the average, except for the R lines for which $j=2$:

$$(R^v-R^r)_{(1,0)}-(R^v-R^r)_{(0,0)}=(R^v-R^r)_{(1,1)}-(R^v-R^r)_{(0,1)}=(R^v-R^r)_{(1,2)}-(R^v-R^r)_{(0,2)} \tag{19a}$$

$$(R^v-R^r)_{(0,1)}-(R^v-R^r)_{(0,0)}=(R^v-R^r)_{(1,1)}-(R^v-R^r)_{(1,0)} \tag{19b}$$

$$(R^v-R^r)_{(1,1)}>(R^v-R^r)_{(1,0)}>(R^v-R^r)_{(0,1)}>(R^v-R^r)_{(0,0)} \tag{19c}$$

Eq. (19a) is a function of the initial state, and Eq. (19b) is a function of the final state. The differences involved in Eqs. (19a) and (19b) are all quite small, of the order of the experimental error, and at the same time are one-half, or less, the resolving power of the grating used. The necessity of exempting the lines R_2, in the above relations, suggests that Johnson may be in error in his assignment of these particular lines.

In the early portion of this paper a slight mutual displacement of alternate observed lines was discussed. This will now be taken up quantitatively, and, for convenience, the amount of the displacement will be denoted by the term "stagger" and the phenomenon itself as "staggering." Fig. 4 shows the amount of staggering, for the (0,0) band, of the violet component of the P branch and of the central component of the R branch to $j=36$, and of the violet component of the R branch from $j=37$ to $j=100$. Johnson's data were used from $j=0$ to $j=47$, and Leinen's from $j=48$ to $j=100$. The amount of staggering was determined by forming a table of differences, using alternate lines, and then interpolating to halves by means of the formula[31]:

$$f_{0.5}=f_0+\tfrac{1}{2}f_{0.5}'-(f_0''+f_1'')/16+\cdots \tag{20}$$

Curves plotted for the staggering of the various branches indicate that in the vicinity of the origin the stagger is zero for all branches except for the red component of the R branch, the stagger near the origin for this component being about 0.2 cm^{-1}. This seems to be real. In Fig. 4 the stagger of the P branch is indicated by the small filled-in circles, while that of the R branch is indicated by the larger open circles. The dotted curve was plotted from values of $S=1.967\times10^{-4}j^2$. If this is interpreted as due to a change in the moment of inertia of the molecule, a corrective term should be added, due to the effect of this change in B_0 on the value of D_0. The solid curve of Fig. 4 was plotted from values of $S=1.967\times10^{-4}j^2-2.36\times10^{-9}j^4$, where the coefficient of j^4 is the change in D_0 produced by a change in B_0 of 1.967×10^{-4}. It is made on the assumption that the final state alone is double, although the assumption that the initial state is double is equally tenable. If the

[31] See, for example, S. Newcomb's Logarithmic Tables, p. 64, Section 29.

initial state alone is double then the coefficient of j^4 would be a trifle less. Mulliken[29] has predicted that the staggering in the Swan bands is due to a so-called rotational doubling (σ-type doubling). Such rotational doubling can be considered as the effect of a double moment of inertia. Thus Mulliken's prediction is verified in the case of the Swan bands, the two moments of inertia, if the final state alone is concerned, differing by 0.012 percent.

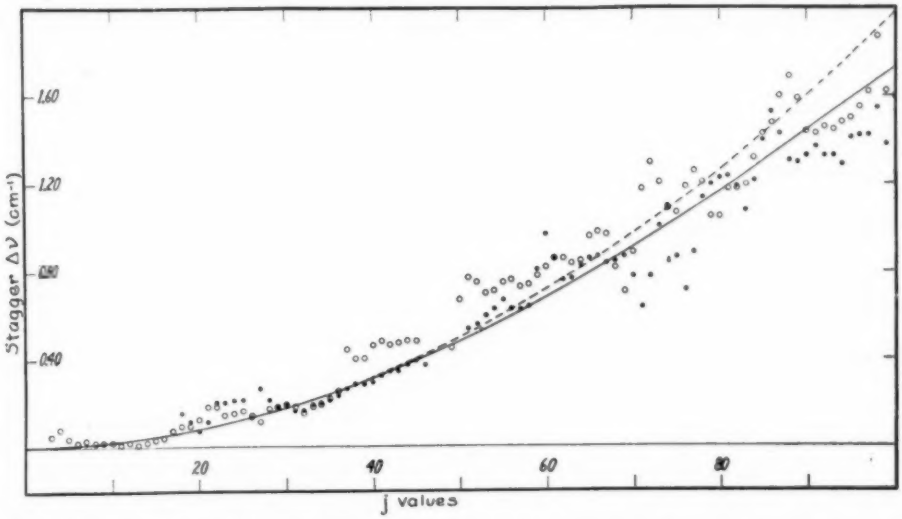

Fig. 4. "Staggering" for the (0, 0) band. Open circles refer to the R branch, filled-in circles to the P branch. Dotted curve, $S=\Delta Bj^2$; Solid curve, $S=\Delta Bj^2+\Delta Dj^4$.

In regard to Johnson's suggestion that the Swan bands may be due to CH-HC (acetylene), the writer wishes to point out that the Swan bands have never been produced in absorption in acetylene, nor in any cold gas. Combination bands, having the same vibrational energy changes as the Swan bands, have not been observed. The writer, from a consideration of these facts, and from the sources of the Swan bands, believes that the carrier is either C-C or, if such a compound is possible, $C^- - C^-$ [4,32]. Except for the fact that it is without precedent, the doubly negatively charged molecule would be preferable in that it has the same number of electrons as N_2, and the second positive group of nitrogen is known to be quite similar to the Swan spectrum. On the tetrahedron model of the chemist, with electrons occurring in pairs in the vicinity of the vertices of the tetrahedron, this assumption gives a structure which would seem to be stable.

In conclusion I wish to extend thanks to Professor R. T. Birge, under whose guidance the present work was done, for his many helpful suggestions, and to Dr. A. S. King of Mt. Wilson Observatory for his kindness in providing me with enlargements of furnace spectrograms.

PHYSICAL LABORATORY,
UNIVERSITY OF CALIFORNIA,
August 29, 1927.

[32] J. J. Thomson, Nature 86, 466 (1911).

ABSORPTION OF POTASSIUM IONS IN VARIOUS GASES

By F. M. Durbin

Abstract

Loss by scattering, retardation or neutralization suffered by a beam of positive potassium ions in traversing helium, argon, hydrogen, nitrogen, air and oxygen. —The absorption of potassium ions accelerated by 8.5 to 350 volts has been measured in helium, argon, hydrogen, nitrogen, air and oxygen. A magnetic deflection apparatus was used in which the metal parts were entirely enclosed in glass. The rays were observed that traversed a fixed distance at various pressures without being deflected from a semicircular path by scattering, retardation, or neutralization. A free path for absorption may be deduced which varies with the gas and velocity of the ions; it is larger than the value given by the kinetic theory for an argon atom in the gases used, varying from 10 times in the case of fast rays in helium to 1.4 times for slow rays in oxygen. At low velocity the free path decreases rapidly and approaches the kinetic theory value.

IT IS well known that positive rays with high velocity are able to capture electrons from the gas molecules through which they pass and become neutralized. Very slow positive ions were investigated by Dempster[1] and were found to show great differences in the rate at which they became neutralized in passing through helium. The present paper describes experi-

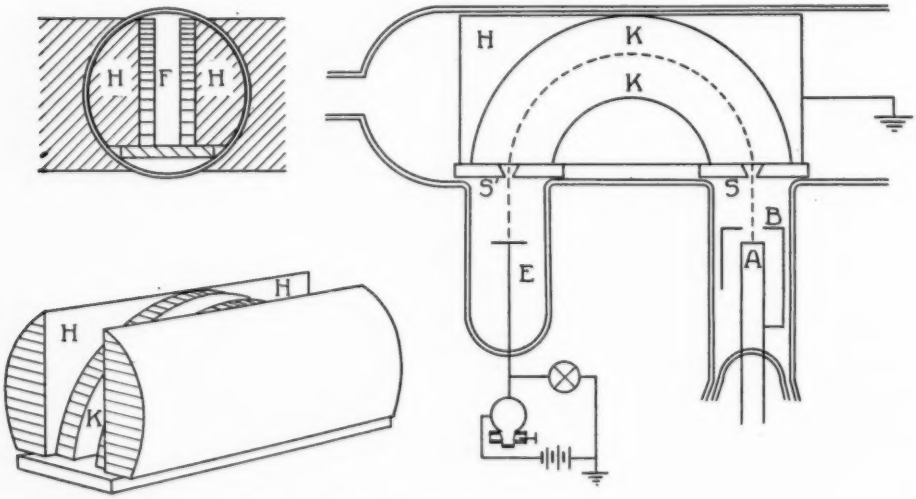

Fig. 1. Diagram of apparatus.

ments in which ions of one kind, positively charged potassium, were allowed to pass through air, hydrogen, nitrogen, helium, oxygen, and argon and the decrease in the intensity of the rays observed in each case.

[1] A. J. Dempster, Phil. Mag., 3, p. 115 (1927).

The apparatus used is illustrated in Fig. 1. It is similar to that described in the paper just referred to but modified so that the metal parts may be completely enclosed in glass tubes. The rays were obtained by heating a potassium catalyst on the platinum strip A. The material was kindly supplied by Mr. Kunsman and was found to give a very steady emission of potassium ions.[2] After passing the opening in the brass cylinder B, the ions were accelerated to the first slit S by potential differences varying from 9 to 350 volts. The ions were then deflected magnetically in a circular path of 7 cm diameter so as to pass the second slit S'. Those completing the path as charged particles were measured by the charge given to the electrode E. The initial emission was kept constant by means of a galvanometer connected in the circuit between A and S. The electromagnet had pole pieces closely fitting the outside of the glass tube as shown in the cross section, and inside the tube were placed two iron pole pieces H separated by a narrow slot about 3 mm wide shown at F. By cutting back the pole faces as indicated at H the field was concentrated to a narrow area K on either side of the path of the ions. Fields as high as 4750 gauss were used.

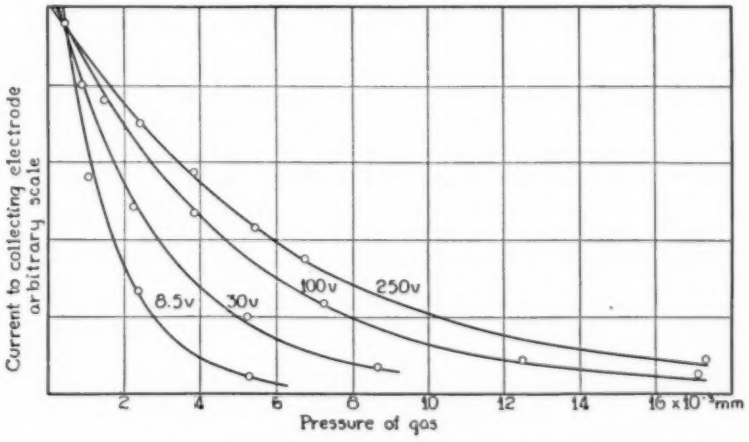

Fig. 2. Variation with the pressure of helium of the number of positive ions reaching the collecting electrode.

Gas was kept flowing into the apparatus through a small capillary from a reservoir whose pressure was varied. The pressures in the apparatus were measured by means of a MacLeod gauge. The number of ions reaching the electrode with various pressures of gas was observed, the initial intensity and the magnetic field being kept constant.

The decrease in the rays with increasing pressure is shown in Fig. 2 for helium gas. The ordinates are the currents observed and the abscissas the pressures of the helium. The curves as drawn are exponential curves passing through the first point, and the observations as indicated lie very close to the exponential curves. The slow rays are much more weakened than the faster rays. From the curves the constant of the exponential factor may be

[2] C. H. Kunsman, Journal of Industrial and Engineering Chemistry, **17**, 971 (1925).

found and interpreted as a mean free path for the removal of the ion from its original path by scattering, retardation or neutralization. If L is this free path reduced to atmospheric pressure, $N=N_0e^{-xp/760L}$, where p is the pressure in millimeters and x is the distance covered by the rays. This free path may be compared with that given by the kinetic theory if we suppose the potassium ion to have the same diameter as the argon atom. In all cases the ions have velocities greater than the gas molecules through which they are moving so that the simple kinetic theory formula for a rapidly moving particle gives a value that is within 5 percent of the correct value. In helium the curves shown give a free path 9.8; 7.5; 4.5 and 2.3 times the kinetic theory free path at 0°C, for the 250, 100, 30 and 8.5 volt rays respectively. Thus disturbances sufficient to remove an ion from the original bundle occur less frequently than the collisions with the helium atoms. The velocity

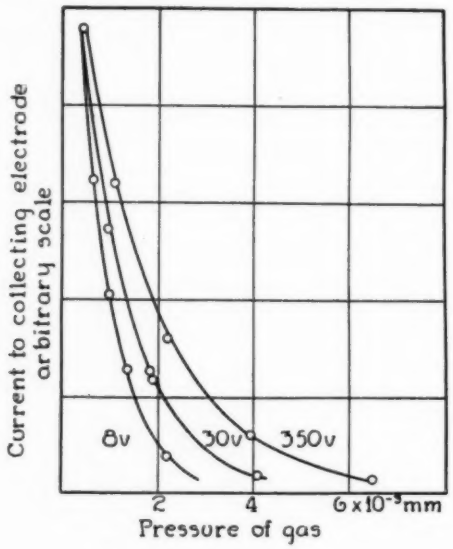

Fig. 3. Variation with the pressure of nitrogen of the number of positive ions reaching the collecting electrode.

of the 8.5 volt ions is 3.24×10^5 cm per sec. while the average velocity of the helium atoms is 1.2×10^5 cm per sec. Thus with velocities only slightly greater than those of the kinetic theory, many of the potassium ions pass through the helium atoms at a collision, without neutralization and without appreciable changes in direction or velocity.

With other gases similar results were obtained. Fig. 3 shows the decrease of the positive ion current with pressure in nitrogen. A collision with a nitrogen molecule is much more effective in throwing the potassium ion out of the original beam than a collision with a helium atom. However the mean free paths deduced from the three curves in Fig. 3 are 4.13, 2.81 and 2.07 times the kinetic theory free path for an argon atom in nitrogen, showing that even here not every collision is effective in removing the ion from the original group.

In hydrogen, oxygen, air and argon similar observations were made and the decrease with pressure was found to agree well with exponential curves from which a mean free path for absorption could be deduced. These mean free paths are plotted in Fig. 4 for rays of different speed in the various gases used. The ordinate is the ratio of this mean free path to the kinetic theory mean free path for an argon atom in the gas used. There is a decided decrease in the free path at low velocities and the curves suggest an extrapolation to the ratio unity at very low speeds. Oxygen is most and helium least

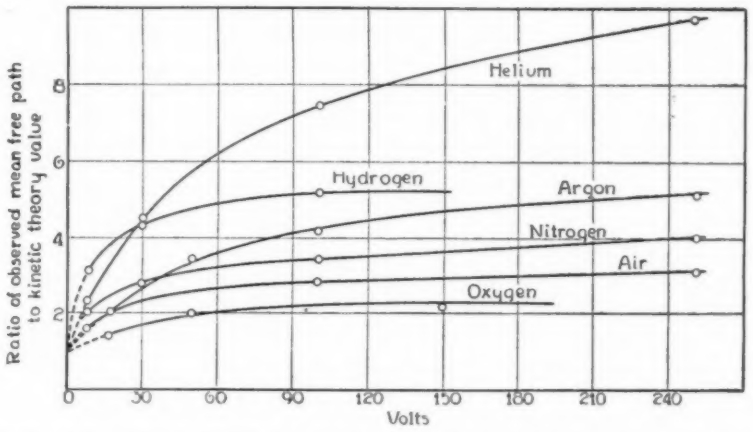

Fig. 4. Ratio of the mean free path for absorption to the kinetic theory value of the mean free path as a function of the velocity of the potassium ions in various gases.

effective in weakening the rays. In the case of oxygen the effect is probably due to neutralization of the potassium ion, and accompanying this process there is in all probability ionization of the oxygen molecule. Thus if it should prove possible to separate the effects due to scattering and retardation of the rays and examine the weakening due to neutralization by itself, we may hope to investigate the question of ionization of gases by ions of different kinds and its dependence on the velocity of the moving particles.

The author is indebted to Professor Dempster for assistance in designing the apparatus used and in preparing this paper.

UNIVERSITY OF CHICAGO,
September 1, 1927.

POST-ARC CONDUCTIVITY AND METASTABLE STATES IN MERCURY

By M. L. Pool

Abstract

A mercury arc, excited between an anode and a Wehnelt cathode, was interrupted by a relay run by a rotating commutator. By means of a second relay run by the same commutator galvanometric current measurements could be made at any instant before or after the arc was interrupted.

Post-arc conductivity ascribed to residual positive ions and electrons.—Residual positive ions and electrons formed during the arc have been found to remain in measureable quantities under certain conditions for 1/10 sec. after the arc has been turned off. These ions and electrons cannot be rapidly removed from the arc space by the application of potentials to collecting electrodes because there are formed about the electrodes space charge sheaths which effectively restrict the potentials applied to a small region. The *thickness of these space charge sheaths* about both the anode and cathode gradually increase with time and finally fill the entire arc space, whereupon the post-arc current ceases. For ion concentrations from 10^{12} to about 10^{7} the decay of the post-arc current is closely exponential for all voltages and for various forms of collecting electrodes. For concentrations below 10^{7} the decay becomes much more rapid. *The critical restriking potential*, previously attributed to the existence of long-lived metastable atoms, is accounted for by the distorted electrical fields which are set up in the neighborhood of the filament as a result of electron diffusion from a region of high electron and positive ion concentration. The location of this region in the arc space is markedly dependent upon the filament temperature. The critical restriking potential is most sharply defined for low filament temperatures and for heavy arc currents. Cathode ray oscillograph curves show that impurities do not effect the critical potential.

Introduction

ATTEMPTS to measure the life of metastable atoms have been made by various investigators within the past five years. Among the apparently more direct methods of attack there are the post-arc absorption method and the post-arc conductivity method. The former was perfected by Dorgelo,[1] and his value for the longest life of a metastable mercury atom is 1/200 sec. The latter was devised by Kannenstine[2] in his work on metastable helium. Using his method on mercury Marshall[3] has reported the value 1/22 sec. If these values are true the life of a metastable mercury atom is of the order of a hundred thousand times that of an ordinary, excited mercury atom.

But Eckart[4] has pointed out that post-arc conductivity may equally well be accounted for on the hypothesis that 1/22 sec. measures the time that

[1] Dorgelo, Physica, 429 (1925).
[2] Kannenstine, Astrophys. Journal **55**, 343 (1922); **59**, 133 (1924).
[3] Marshall, Astrophys. Journal **60**, 244 (1924).
[4] Eckart, Phys. Rev. **26**, 454 (1925).

positive ions remain in the arc space after the arc has been turned off. Among the things to be desired from a positive ion hypothesis is an explanation as to how the critical restriking potential can be accounted for and an estimate of the time required to sweep the arc space free of the residual ions.

This paper is a report of a series of experiments which have been made in order to obtain more definite knowledge regarding the characteristics of low-voltage post-arc conditions, and in particular regarding the factors upon which the critical restriking potential depends.

Apparatus and Method

A drawing of the discharge tubes used is shown in Fig. 1. A typical electric circuit is shown in Fig. 2. R_1 and R_2 are two relays run by a commutator

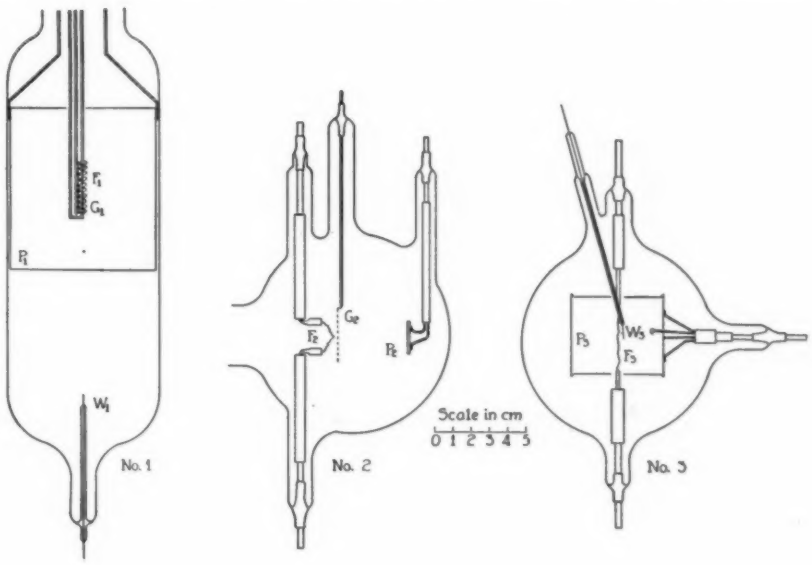

Fig. 1. Diagrams of the various tubes used. W_1 and W_3 are 4 mil tungsten wires, 1 cm long. G_1 is a nickel grid spiral supported on nickel leads. G_2 is a nickel grid 2.8×3.2 cm. P_1 is a nickel cylinder with open ends, area 214 cm². P_2 is a nickel plate, area 5.3 cm². P_3 is a nickel cylindrical can with closed ends, area 94 cm². F_1 is a tungsten filament, while F_2 and F_3 are oxide-coated platinum filaments.

of three segments. R_1 turns the arc on and off. By means of R_2 the galvanometer can be thrown into the circuit for any predetermined length of time (say 1/400 sec.) at any time before or after the stopping of the arc. By means of two movable sliding contacts this sampling of the current in the grid circuit at various instants could be done not only quite rapidly, but also without in any way affecting the rotation rate of the commutator. By merely a throw of a switch the galvanometer when either in the grid circuit or in the plate circuit could be replaced by a Western Electric cathode ray oscillograph. In some cases excitation of the mercury vapor was obtained by placing R_1 in the primary of an electrodeless discharge circuit.

Observations and Interpretation

A. *Post-arc currents and photoelectron emission.* Since there is ample evidence that two metastable states exist in the mercury atom and since the results of several experiments have been easily interpreted by supposing that an electron remains in either one of these states at least somewhat longer than in an ordinary excited state, one might well venture to say that in a mercury arc a large concentration of these longer lived excited atoms would be rapidly built up. If the arc is now stopped and if the electron in the metastable orbit eventually reverts to the normal level by the emission of radiation or if the metastable atom on collision with the electrode liberates electrons, one would expect it possible to detect electronic currents for an appreciable time after the stopping of the arc—especially so if the radiation is handed on from atom to atom until the energy finally escapes from the arc space.

Tube No. 1, Fig. 1, was therefore built for the purpose of measuring this anticipated current and of determining whether it were not possible to account for all post-arc conductivity by supposing that electrons are ejected from the electrodes.

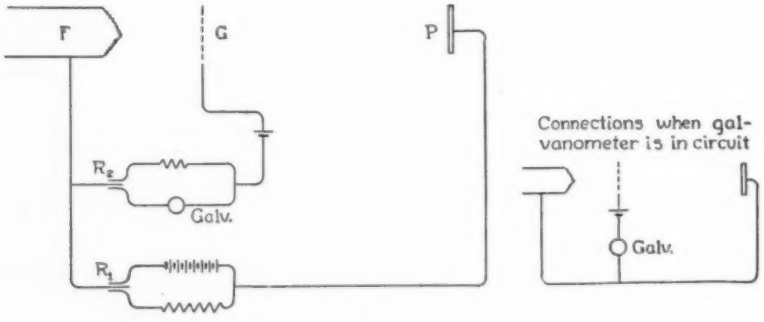

Fig. 2. Diagram of electrical circuits.

Thus in Fig. 3, the currents between the plates P_1 and filament F_1, 1/40 sec. after the arc has been turned off, are plotted as ordinates against the plate voltages as abscissas. The plate was maintained at any particular potential shown in Fig. 3 during the entire post-arc time, and 1/40 sec. after the arc had been stopped the galvanometer was put into the circuit for 1/150 sec. The potential drop across the filament was 5.6 volts and the plate voltage was measured from the positive side of the filament. It is seen that the plate current has its maximum negative value when the plate is -7.2 volts with respect to the center of the filament. As the plate voltage is made more negative the current markedly decreases and becomes virtually zero when the plate is -60 volts. If the post-arc plate current is due to photoelectron emission from the plate or to the Osterhuis effect, one would expect the current to reach a saturation value. However, if the current is due to the removing of residual ions and electrons, we can easily explain the curve observed by supposing that 60 volts applied to the plate for 1/40 sec. has practically swept the arc space free of these ions and electrons.

B. *Post-arc currents with various voltages on collecting electrode.* We shall now consider in detail the behavior of post-arc conductivity with various voltages applied to different collecting electrodes for the purpose of deciding whether or not that behavior is in accord with the assumption that only residual ions and electrons contribute to the post-arc currents observed.

Tube No. 2 as shown in Fig. 1 was used in obtaining the curves of Fig. 4. The currents between the grid G_2 and the filament F_2 are plotted against the time as measured from the instant at which the arc is stopped. The ordinates are in micro-amperes. The electrical circuit is shown diagrammatically and

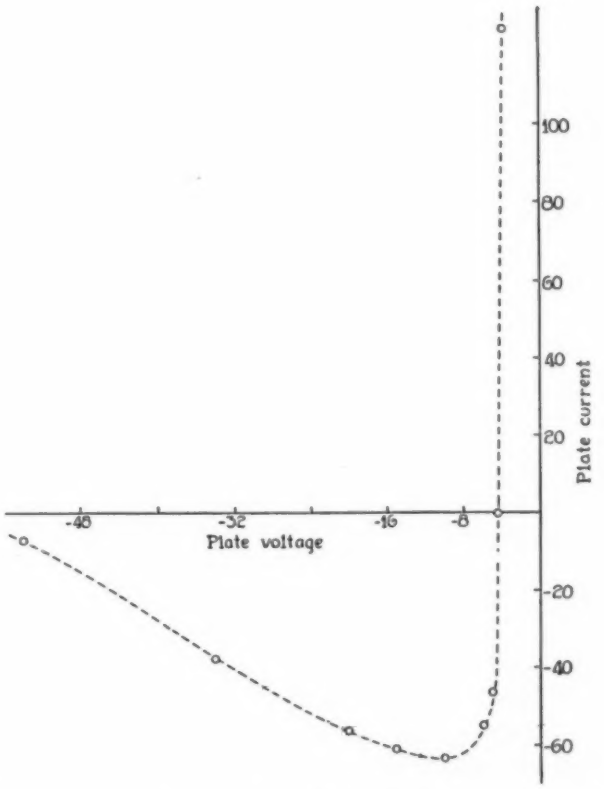

Fig. 3. Post-arc currents between P_1 and F_1 for various plate voltages 1/40 sec. after stopping the arc.

signifies that the arc was formed between the filament and the plate, and that during the time the arc was on, the grid G_2 was out of the circuit. The potential drop across the filament was 1.8 volts. When the potential applied to the plate is removed and the arc thus stopped, the grid is immediately made a few volts positive with respect to the filament; the current flowing between these two electrodes was measured by a sensitive galvanometer. The galvanometer, however, was not in the grid circuit during the entire post-arc time, as might be concluded from the abbreviated drawing. The details of the grid circuit are shown in Fig. 2. It is seen that the galvanometer

can be thrown into the grid circuit (for 1/400 sec.) at various times after the arc had been stopped. The circles on the curves represent the instantaneous values of the current flowing in the grid circuit. Therefore, the smooth curve through these observed values shows how the current changes with time; the area under a curve is proportional to the quantity of electricity removed. The potential of the grid with respect to the filament is indicated at the left of each curve.

When the grid is made 3.0 volts positive with respect to the filament, it is seen from the curve +3.0 that at first the current is flowing in a direction opposite to that of the electrical field impressed. If $t=0$ designates the time when the arc is turned off, then at $t=0.005$ sec. the value of this negative

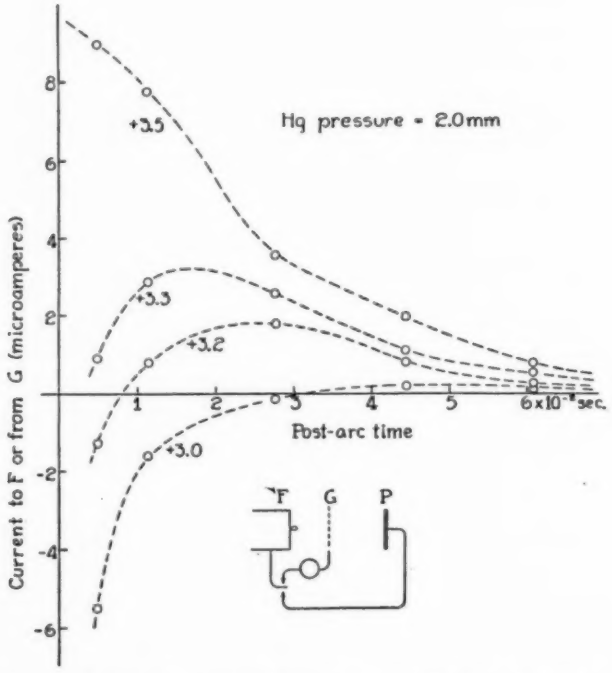

Fig. 4. Decay of post-arc currents between G_2 and F_2 when the grid potential is in the neighborhood of +3.2 volts.

current is 5.5 microamperes. This negative current persists until $t=0.03$ sec. Thereafter, a small positive current is detected which becomes virtually zero when $t=0.08$ sec.

Curve +3.3 shows that the current for all post-arc times is positive, but that the maximum current is reached only after 0.018 sec. after the arc had been turned off. Curve +3.5 shows that the current is a maximum at the beginning of the post-arc time and decreases rapidly at first and then more slowly later.

In order to interpret the above post-arc current curves it is undoubtedly necessary to bring into consideration the variation of the concentration of positive ions and electrons in different parts of the arc space. For an arc

running under constant conditions concentration measurements have been made by several investigators using an exploring electrode according to the method of Langmuir.[5] The results obtained indicate that in the neighborhood of the filament there exists a region of negative space charge; between this negative space charge and the anode there is a region of high positive ion and electron concentration[6] (this region will be designated by $H\pm$); and in the neighborhood of the plate there is a region of low positive ion and electron concentration. At any instant in any small element of volume chosen outside the negative space charge about the filament, the concentrations of ions and electrons are nearly the same. In a low-voltage arc the ratio of the concentration of positive ions in the region $H\pm$ to the concentration near the anode is often as great as 100 to 1.

When the exciting potential applied to the anode is removed, it is to be expected that the ions and electrons in $H\pm$ rapidly decrease in number by recombining and by diffusing to regions of lower ion and electron concentration. It would also be expected that during this period of readjustment the current flow between the filament and an electrode, maintained at a small difference of potential, may be largely dependent upon the size of $H\pm$ and its location with respect to the electrode, and in addition upon the size of the negative space charge about the filament.

In the light of the above concepts let us, as an example, consider curve +3.2, Fig. 4. For $t=0.005$ sec. the current is flowing in a direction opposite to that of the applied field; i.e., the electrons, instead of going into the grid, are first diffusing into the filament from the region of negative space charge immediately surrounding it. The value of this electron diffusion current at this particular instant is 1.3 microamperes. At $t=0.01$ sec. the current is in the direction of the applied field and is 0.5 microamperes. This means that the electrons are diffusing about as rapidly into the filament as into the grid. At $t=0.03$ sec. the current is 1.8 microamperes. This means that the distorted fields existing immediately after the stopping of the arc have now nearly disappeared, and that the positive ions together with remaining electrons are moving under the influence of the applied potential.

C. *Influence of filament temperature on post-arc currents.* In Fig. 5 the post-arc currents in microamperes between the filament and plate of tube No. 2 are plotted as ordinates against the post-arc time as abscissas for the case in which the temperature of the filament is quite low. The arc was formed between the filament and the grid. If the filament is made very hot, the curves of Fig. 5 change over to those of Fig. 6. In Fig. 5 curve +3.3 (plate 3.3 volts positive with respect to the filament) begins with a positive value and decreases to zero for $t=0.021$ sec., has a maximum negative value for $t=0.035$ sec. and then approaches zero with increase in post-arc time. But in Fig. 6 curve +3.3 begins with a negative value, has a maximum

[5] Langmuir, Gen. Elec. Rev. **26**, 731 (1923).

[6] McCurdy, Phil. Mag. **48**, 898 (1924). Compton, Turner, McCurdy, Phys. Rev. **24**, 597 (1924). Compton and Eckart, Phys. Rev. **25**, 139 (1925). McCurdy and Dalton, Phys. Rev. **27**, 163 (1926).

positive value for $t=0.045$ sec., and then approaches zero with increase in post-arc time. The zero was the galvanometric deflection taken 1/4 sec. after the arc had stopped. The deflection then observed, due to thermionic emission from the filament, was, however, very small, especially when the plate was less than 3.5 volts with respect to the filament.

Since the curves of Figs. 5 and 6 are distinctly different in type and since they were obtained under identical conditions—barring the temperature change of the filament—we shall attempt to account for them by bringing into consideration the thickness of the electron space charge about heated filaments. If a hot filament emitting electrons is placed in a vacuum, there exists, as is well known, a negative space charge extending from the filament to the plate. If gas is admitted into the vacuum so that an arc may be formed this negative space charge existing throughout the tube contracts

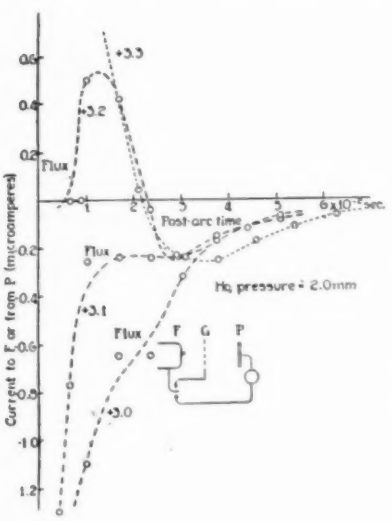

Fig. 5.

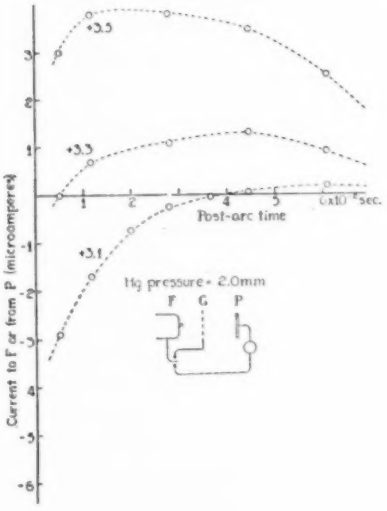

Fig. 6.

Fig. 5. Post-arc currents between G_2 and F_2 for low filament temperature, showing critical potential at +3.2 volts.

Fig. 6. Post-arc currents between P_2 and F_2 for high filament temperature.

inward toward the filament. If the filament is quite hot, the thickness of the negative or electron space charge, even for heavy arc currents, may be several millimeters. However, if the temperature of the filament is decreased, the thickness of the space charge decreases also. If the temperature is sufficiently decreased so that every electron emitted by the filament is immediately removed, the electron space charge becomes virtually zero.[7] Under these conditions where ionization is present there exists a thin positive ion space charge closely surrounding the filament. Surrounding this positive space charge is the region $H\pm$.

The curves in Figs. 5 and 6 may be interpreted then in the following way: For example, in curve +3.3, Fig. 5, when $t=0.01$ sec. we see that positive

[7] Compton, Turner and McCurdy, Phys. Rev. **24**, 597 (1924).

ions are moving into the filament and continue to do so until $t=0.03$ sec. In curve $+3.3$ of Fig. 6 the electron diffusion into the filament from the negative space charge about the filament reduces the positive current to a low value. This electron diffusion current in curve $+3.1$ predominates until $t=0.04$ sec. In curve $+3.1$ of Fig. 5 the diffusion of electrons from $H\pm$ through the positive ion space charge about the filament is so great that the observed current is negative during the entire post-arc time.

The points of significance brought out in the above three sets of curves are that the post-arc currents vary with time in a rather complicated manner, that there exists a critical potential about which the current curves change very rapidly in form, and that the behavior of these currents with respect to change in filament temperature and for various voltages upon collecting electrodes can be accounted for by residual ions and electrons.

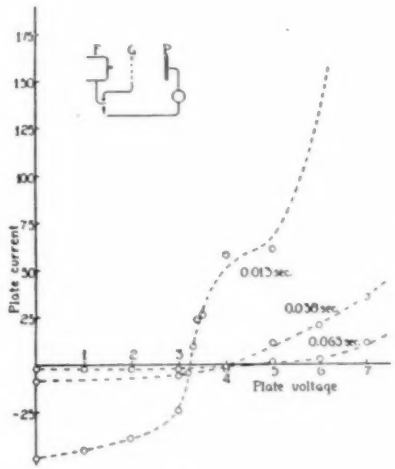

Fig. 7.

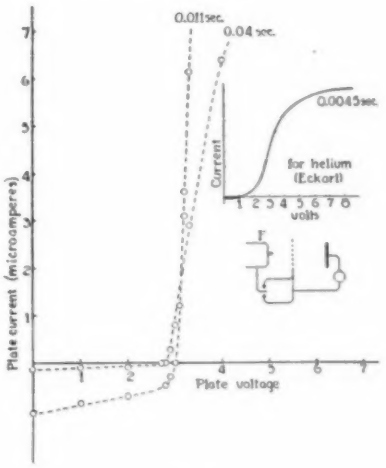

Fig. 8.

Fig. 7. Post-arc currents between P_2 and F_2 for constant time-waits after stopping the arc, low filament temperature.

Fig. 8. Post-arc currents between P_2 and F_2 for constant time-waits, medium filament temperature. Insert is Eckart's curve for helium where the time-wait was 0.0045 sec.

The curves to be considered immediately following verify and bring out under different conditions the phenomena already considered and indicate that the critical restriking potential observed in low-voltage arcs does not necessitate the existence of long-lived metastable atoms, but that the critical potential may be due to the peculiar potential gradients existing in the arc space.

D. *Post-arc currents for constant time-waits.* Experiments were made with tube No. 2 in which the post-arc current in the plate circuit was measured as a function of the plate voltage for constant time-waits after the stopping of the arc. In Fig. 7 the current in the plate circuit at $t=0.013$ sec. is negative until the plate is raised to $+3.2$ volts with respect to the filament; thereafter, the current is positive for greater plate voltage. If,

however, $t=0.038$ sec., the plate current is negative until the plate is raised to +4.2 volts. These curves were obtained when the filament temperature was quite low and are in good agreement, as may be seen, with the curves in Fig. 5.

With an increase in filament temperature the curves of Fig. 8 were obtained. As before the plate current at a given time-wait is plotted against the plate voltage. It is seen that these curves are in accord with those of Fig. 6.

Eckart has made similar measurements in helium. He found that the currents increased rather slowly with increase in plate voltage and concluded that the post-arc conductivity was due not to the ionization of metastable atoms, but to residual positive ions remaining in the arc space. However,

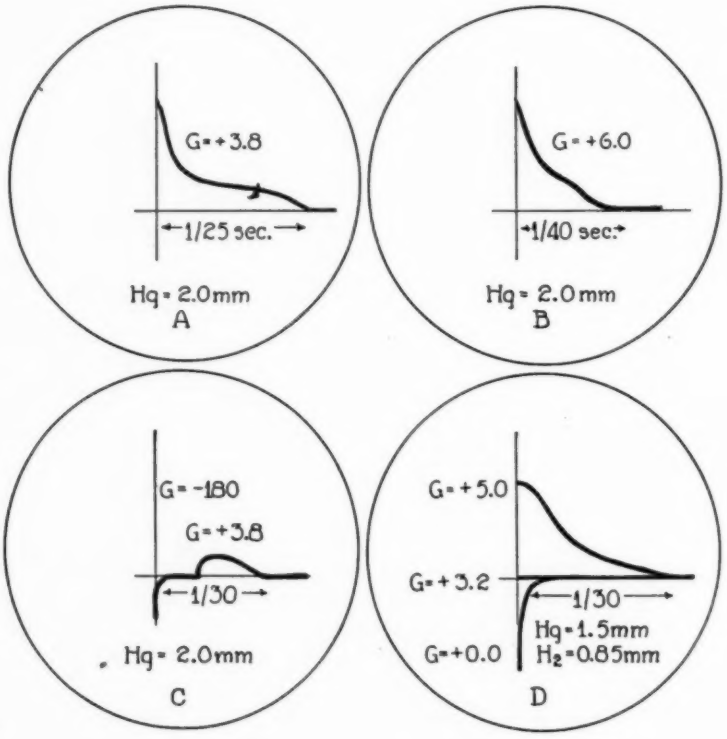

Fig. 9. Cathode ray oscillograph curves showing post-arc current decay between grid and filament as a function of grid voltage.

it is possible, as is seen in Fig. 8, to obtain curves that rise very rapidly when the plate is made about +3 volts with respect to the filament. One might naturally then conclude that this sudden increase in post-arc current is best explained as due to the ionizing of long-lived metastable atoms. But it will be noticed that the points at which the curves of Figs. 7 and 8 cross the axis are dependent upon the time-waits. This phenomena would be hard to account for solely by metastable atoms, but is obviously in agreement with the concept of changing potential gradients in the post-arc space due to diffusion and recombination of residual positive ions and electrons.

E. *Cathode ray oscillograph curves.* Fig. 9 shows some post-arc current curves obtained by placing a Western Electric cathode ray oscillograph between the grid and filament. The arc was formed between the filament and plate. The large circle represents the size of the screen; it is evident that detailed examination of these curves was possible. For curve *A* the grid was +3.8 volts with respect to the filament; whereas for curve *B* the grid was +6.0 volts. In the former the conductivity persisted for about 1/25 sec., in the latter the persistence was about 1/40 sec. The difference in the two curves may be accounted for by saying that in curve *A* the positive ions in the neighborhood of the filament move into the filament quite slowly and consequently liberate electrons from the filament for a longer time than do the more rapidly moving positive ions in curve *B*.

Curve *D* shows the type of conductivity obtained in mercury at 1.5 mm pressure when the grid is 0, +3.2, and +5 volts with respect to the filament and when hydrogen was admitted to a pressure of 0.85 mm. The introduction of air, nitrogen, carbon dioxide, helium, and argon has little or no effect upon the curves obtained. For pressures less than 0.5 mm a shorter persistence is noticed which might be expected when molecular diffusion begins to be effective. For example, if the pressure of Hg is 0.002 mm and that of H_2 is 0.01 mm, the current persists only 1/400 sec. Curves obtained with extremely pure mercury[8] were very much the same as those obtained with impure mercury.

F. *Experiments with electrodeless discharge.* In some of the experiments the mercury vapor was excited by an electrodeless discharge. While the discharge was on, the filament was hot but was disconnected from both the grid and plate. When the discharge was stopped, the grid was immediately made a few volts positive with respect to the filament. Observations made by means of the cathode ray oscillograph showed no post-arc currents at all, nor any indications of restriking until the grid was made about +4.6 volts. It is believed that these observations are additional evidence to support the concept of rapidly diffusing electrons with energies corresponding to the lowest radiating potential. Of course in an electrodeless discharge there does not exist any region $H\pm$, because throughout the discharge the distribution of ions and electrons is about the same. Consequently, when the discharge is stopped, approximately as many electrons would tend to diffuse in one direction as in another, and therefore large electron emission from the filament is not possible until it is made sufficiently negative to repel these diffusing electrons.

G. *Critical restriking potentials.* The experiments described above suggest that post-age conductivity is due (1) to the diffusion of positive ions and electrons from regions of high electron and positive ion concentrations to regions of lower electron and positive ion concentrations and (2) to the motion of these electrons and ions under the influence of the distorted fields existing when the arc is interrupted. Upon removing the exciting potential

[8] This mercury was upon two occasions kindly furnished by Professor W. D. Harkins; it had been distilled a great many times in his experiments on isotopes.

on the anode, the filament receives a shower of rapidly diffusing electrons; in order to repel them the filament must be made about five volts negative with respect to the region from which they come. If the filament is made still more negative, electrons in the neighborhood of the filament are driven to the plate and the arc current appears to persist for a few hundredths of a second. If the filament is able to emit electrons copiously the arc may restrike through the ionization of excited atoms that might be present in the arc space.

The question now arises whether or not there is any fresh ionization produced by the voltages applied in the curves of Figs. 4, 5, 6, 7, 8, 9; i.e., whether there is any restriking of the arc at all with the small applied potentials, or whether the currents observed are entirely due to the ions and electrons present in the arc space when the arc is interrupted.

The total quantity of electricity carried to the electrodes in curve *A*, Fig. 9, is approximately 10^{-4} coulombs which would require an average concentration over 500 cc. of at least 13×10^{11} ions per cc at the instant the arc was interrupted. From 0.01 to 0.04 sec. after the stopping of the arc the quantity of electricity removed by the electrodes was 5.5×10^{-5} coulombs which requires an average concentration of 6.9×10^{11} ions per cc at the beginning of the interval. The arc during this experiment was quite intense and the arc current was 0.3 amperes.

By means of a Langmuir exploring electrode (to be considered in detail later) the concentrations of ions and electrons about midway between the cathode and anode at various times after a 0.04 ampere arc was interrupted have been calculated; the results are given in Table I. If the concentration

TABLE I

Concentration of ions and electrons midway between cathode and anode at various times after the interruption of a 0.04 ampere arc.

Post-arc time	Current	No. of ions per cc.
0.0055 sec.	280×10^{-6} amps.	3.34 $\times10^{11}$
.0074 "	176 "	1.67 "
.0092 "	108 "	.78 "
.0112 "	66 "	.28 "
.0152 "	33 "	.12 "
.019 "	20 "	.051 "
.029 "	5 "	.0052 "
.040 "	1 "	.00033 "

after 0.01 sec. obtained from Table I is multiplied by 0.3/0.04, the ratio of the arc currents, we have a concentration of 4.4×10^{11}. This value is in fair agreement with 6.9×10^{11} mentioned above. Working with steady uninterrupted arcs Compton and Eckart[6] have measured concentrations near the cathode as high as 48×10^{11}.

Consequently, we may say that the post-arc currents observed in the above experiments are due probably entirely to residual ions and electrons and that metastable or excited atoms undoubtedly play only a minor role in the post-arc phenomena here considered. However, Dorgelo[1] has shown by absorption methods that metastable atoms actually do exist in the arc

space 1/200 sec. after the arc had been turned off. These apparent long-lived atoms (1/200 or 1/22 sec.) can be accounted for by metastable atoms of short life (say 10^{-6} sec.) which are continuously being formed by the comparatively slow process of recombination of positive ions and electrons. Dorgelo has also observed that impurities markedly decrease the "life" of the metastable atom. As may be expected impurities, although having little or no effect on the rate of recombination of ions and electrons, would however decrease the concentration of metastable atoms by increasing their rate of disappearance after they have been formed.

H. *Time required to remove ions and electrons from arc space.* If large quantities of ions and electrons really exist in the arc space for 1/50 to 1/10 sec. after the arc has been turned off, one would expect it to be possible to rapidly sweep them from the arc space by the application of a high negative potential to the plate. However, Eckart observed that no effect on the post-arc current was noticed even when a negative voltage of -135 was applied and remarked that the result was somewhat disconcerting. A similar and

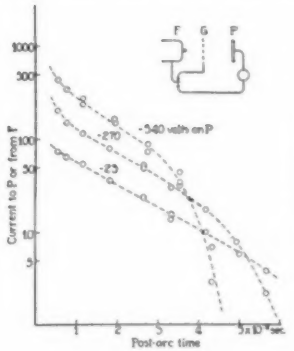

Fig. 10.

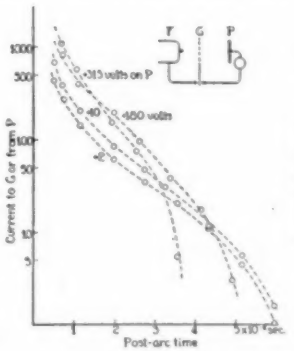

Fig 11.

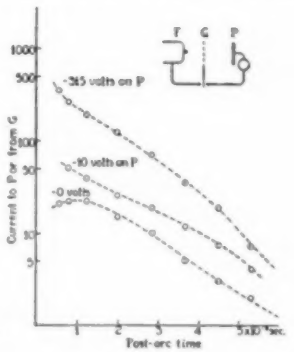

Fig. 12.

Fig. 10. Log plot of post-arc currents between P_2 and G_2 of tube No. 2 when P is highly negative.
Fig. 11. Log plot of post-arc currents between P_2 and G_2 when P_2 is highly positive.
Fig. 12. Log plot of post-arc currents between P_2 and G_2 when P_2 is highly negative.

related phenomena has been observed by Langmuir with regard to currents collected by negative electrodes placed in an arc running under constant conditions.[9] But before attempting to account for the slowness with which the ions are actually removed, we shall first consider a few experiments which were made with various high potentials on different collecting electrodes in order to observe the factors governing the removal of ions and electrons from the arc space after the arc has been interrupted.

Fig. 10 shows how the logarithm of the post-arc currents decreases with time when the plate is placed 540, 270, and 23 volts negative with respect to the filament. These potentials were upon the plate during the entire post-arc time. The arc was formed between the filament and grid. If curve -540 is compared with curve -23, it is seen that the rate of decay is approximately the same up to $t=0.03$ sec. Then for curve -540 the rate

[9] Langmuir, Science **58**, 290 (1923).

rapidly increases and when $t=0.045$ sec. the post-arc current has ceased. Curves in Fig. 11 show how the post-arc current decreases when the plate is made positive with respect to the grid; the filament is not in the post-arc circuit. Curves in Fig. 12 show the rate of decrease when the plate is made negative with respect to the grid; again the filament is not in the post-arc circuit.

Since the current curves in Fig. 10 are exponential for the greater portion of the post-arc time, we may write $i=i_0e^{-Kt}$ where K is 54.5, 55, and 70 respectively for curves -23, -270, and -540. Similar curves were obtained over an appreciable range in mercury vapor pressure; the value of K for different pressures is given in Table II. The increase in K for vapor pressures

TABLE II

Values of K for different pressures of mercury vapor.

Pressure	Temp.	K for plate -4.5 volts	K for plate -180 volts
.08 mm	78°C	180	285
.37	105	68	69
1.25	130	49	54
5.2	162	53	53
18.3	200	55	58

less than 0.5 mm is accounted for, as before, by molecular diffusion. The constancy of K for higher vapor pressures may well be expected in view of Eq. (2), below, since the mean free path L in the equation is raised to the 1/5 power. Eckart has reported that "some hasty experiments using mercury instead of helium showed that all phenomena were essentially the same and yielded values for b $[b=1/K]$ of 0.01 to 0.02 sec."

Fig. 9*C* shows the type of post-arc currents between the grid and filament as observed by the cathode ray oscillograph when the grid for 1/60 sec. is made 180 volts negative with respect to the filament; thereafter the grid is put at 3.8 volts. The latter portion of the curve is very much like the curve in Fig. 9A, where the grid at all times is $+3.8$ volts with respect to the filament. According to these observations the persistence of post-arc currents is not in any marked way dependent upon the potentials applied to the collecting electrodes.

I. *Experiments with anode completely enclosing cathode.* In order to test the dependence of the persistence of post-arc currents upon the size of collecting electrodes tube No. 3[10] was used. Here the anode was a cylinder 5 cm in diameter with closed ends. The filament leads passed through small holes in the center of the end plates. The arc was formed between the filament F_3 and the cylindrical anode P_3.

In Fig. 13 the ordinates represent the logarithm of the currents between the anode P_3 and a 4 mil wire 1 cm long placed near the filament (see Fig. 1). Post-arc measurements were made with the filament completely out of the circuit. Since Figs. 13 and 10 are plotted on the same scale, it is easily

[10] Tube No. 3 was made and used by Dr. F. M. Kannenstine in some of his work on metastable helium.

noticed how much more rapid is the rate of decay of the post-arc current in the former than in the latter. For tube No. 3 the post-arc current ceases after 0.018 sec. when −93 volts is put on the plate; for tube No. 2 the current persists for 0.045 sec. even when −270 volts is applied. Curve 0 in Fig. 13 shows how the current flows between the wire and plate when no voltage is applied.

Related observations are plotted in Fig. 14. Here the currents between P_3 and the wire W_3 at a definite time after the stopping of the arc are plotted as ordinates against the potential of the wire as abscissas. The voltages are applied to the wire for 0.0125 sec., then the galvanometer is put into the

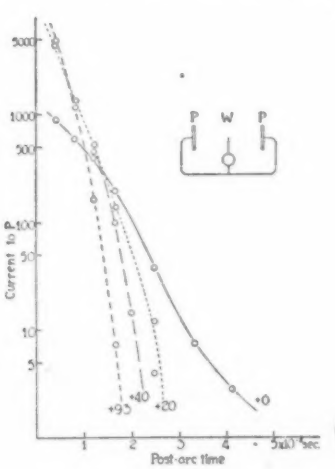

Fig. 13

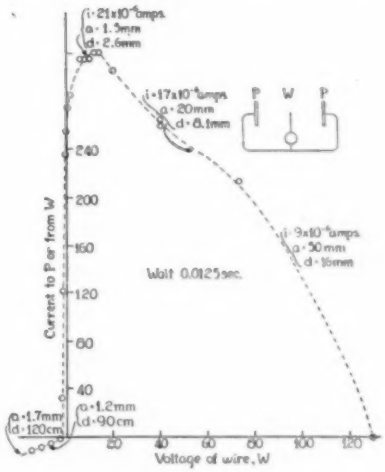

Fig. 14.

Fig. 13. Log plot of post-arc currents between P_3 and W_3 for tube No. 3 when W_3 is positive.
Fig. 14. Post-arc currents between P_3 and W_3 0.0125 sec. after stopping the arc as a function of the potential difference.

circuit for 1/400 sec. It is seen that the post-arc current has decreased to zero in less than 0.0125 sec. when 130 volts is applied and that the curve is quite unsymmetrical about the axes. Zero current is also obtained when the wire is put 1.7 volts negative with respect to the plate.

J. *Space charge sheaths about collecting electrodes.* The behavior of the post-arc currents shown in Figs. 10 to 14 may be accounted for by bringing into consideration the concept of space charge sheaths. Langmuir[11] has shown that for low gas pressures (say 0.002 mm) the current carried by ions between any pair of electrodes cannot exceed a definite value; this value depends on the form of the electrodes, on the potential difference between them, and on the charge and mass of the ions, but not in any way upon the concentration of ions.

McCurdy[12] has derived an equation which gives at high gas pressures (say 2 mm) the limiting currents that may be obtained between coaxial

[11] Langmuir and Mott-Smith, Gen. Elec. Rev. **27**, 449, 538, 616, 762, 810 (1924).
[12] McCurdy, Phys. Rev. **27**, 157 (1926).

cylindrical electrodes. McCurdy's equation when evaluated for electrons in mercury vapor is:

$$i=1.74\times10^{-6}\frac{L^{1/2}V_0^{3/2}}{(aB)^{3/2}} \tag{1}$$

For positive ions in mercury vapor the numerical coefficient is 1.94×10^{-8}. L is the mean free path of the mercury atoms, V_0 is the potential of the collecting electrode with respect to the outer electrode, a is the radius of the outer electrode, and B is a function of the ratio of the two radii.

In the experiments here described the ions and electrons were in many cases drawn to plane electrodes; the corresponding current limiting equation may be obtained as follows: Poisson's space charge equation for plane electrodes is $d^2V/dx^2=4\pi\rho=4\pi i/u$, where u is the velocity of advance of an ion.

But

$$u=3Eel/4mv_t$$

where v_t is the random velocity of agitation.

Since

$$\tfrac{1}{2}mv_i^2=V_ie=\tfrac{1}{2}eEL(M/1.134m)^{1/2}$$

$$\frac{d^2V}{dx^2}=\frac{16}{3}\pi i\left(\frac{m}{Eel}\right)^{1/2}\left(\frac{M}{1.134m}\right)^{1/4}$$

Putting $dV/dx=E$ and integrating, we have

$$E^{3/2}=8\pi i\left(\frac{m}{el}\right)^{1/2}\left(\frac{M}{1.134m}\right)^{1/4}(x-d)$$

$E=0$ when $x=d$, where d is the distance to the plane electrode which is the source of ions or electrons. Integrating again and solving for d,

$$d=\left[\frac{(2.27)^{1/2}}{16\pi^2}\,\frac{e}{m}\left(\frac{5}{3}\right)^3\frac{1}{M^{1/2}}\,\frac{V_0^3L}{i^2}\right]^{1/5}$$

Evaluating for mercury, the thickness of the positive sheath is given by

$$d=4.5\times10^{-4}(V_0^3A^2L/i^2)^{1/5} \tag{2}$$

For the negative sheath the numerical coefficient is 1.74×10^{-3}. In addition to the symbols used before, A is the area of the electrode.

Eqs. (1) and (2) have been applied to the observations made with tubes Nos. 2 and No. 3. In Table III there is given a set of data and calculations for curves +93 and +20 of Fig. 13. In this table t is the time after the arc had been stopped, d is the thickness of the positive space charge upon the cylindrical plate P, a is the radius of the negative space charge around the wire W, n is the number of ions per cc, i is the current in amperes.

Calculations for the curve marked +20 in Fig. 3 show that the thickness of the positive space charge sheath on the cylindrical electrode P is 1.5 mm

at time $t=0.0045$ sec. The radius of the negative space charge sheath about the wire W is 0.77 mm and the number of electrons and ions per cc is 2.2×10^9. For $t=0.025$ sec. the thickness of the positive sheath is 19 mm, the radius of the negative sheath is 17 mm and the number of ions and electrons per cc is 1.6×10^5. It is admitted that in the determination of the radius of space charge sheaths and of the number of ions per cc there is a large error present even when the arc is working under steady conditions. In this set of experiments an attempt has been made to determine the size of these sheaths

TABLE III

Applications of Eqs. (1) and (2) to the observations.

t	i	d	a	n
		For curve +93, Fig. 13		
0.0045 sec.	316×10^{-6} amp.	3.2 mm	1.3 mm	1.3×10^9
.0085	77	5.6	4.1	1.0×10^8
.0125	12.5	12.0	7.2	1.0×10^7
.0170	0.4	41.0	12.0	1.9×10^5
		For curve +20, Fig. 13		
0.0045 sec.	300×10^{-6} amp.	1.5 mm	0.8 mm	2.2×10^9
.0085	106	2.3	1.1	5.2×10^8
.0125	35	3.5	1.9	10.0×10^7
.0170	10	8.8	6.8	2.9×10^6
.0250	0.5	19.0	17.0	1.6×10^5

at various instants during the changing conditions that exist immediately after the stopping of the arc. Consequently, no estimate is made as to the accuracy of the results. However, it will be recalled that the radius of the cylindrical electrode P is 25 mm and that the radius of the sheath about the wire W for $t=0.025$ sec. is 17 mm. This value is not unreasonable because for $t=0.028$ sec. no current was obtained—an indication that all ions and electrons have been removed, or what is equivalent, that the sheaths have swept throughout the arc space and may be considered as ceasing to exist.

When the post-arc potentials on P and W are reversed, very much smaller currents are obtained. Calculations give unreasonably large values for the thickness of the negative space charge sheath upon P, even when $t=0.005$ sec. The interpretation is that the large surface of P makes the removal of the electrons quite rapid, and before any galvanometric measurements can be made a large percent of these electrons have been removed. Thus for $t=0.005$ sec. there exists no negative space charge on P; throughout the arc space there is, however, a predominance of positive ions and consequently there exists everywhere a positive ion space charge.

The writer is particularly grateful to Professor A. J. Dempster for helpful suggestions and criticism during the course of this investigation.

RYERSON PHYSICAL LABORATORY,
UNIVERSITY OF CHICAGO,
August 22, 1927.

THE RELATIVE INTENSITIES OF POSITIVE RAYS FROM THE ISOTOPES OF LITHIUM

By John Leslie Hundley

Abstract

The relative intensities of positive rays from the isotopes of lithium were investigated for various lithium compounds at different temperatures, using Dempster's method of positive ray analysis. It was found that there is in general a change in the ratio Li_7/Li_6 with temperature, the ratio decreasing at higher temperatures and increasing at lower. An application of Richardson's law shows that the two isotopes have different work functions, Li_6 having a greater work function than Li_7. The ratio b_6/b_7 is constant over wide ranges of temperature for a given lithium compound, but is different for different compounds.

IN INVESTIGATIONS of the relative intensity of positive rays from the isotopes of lithium, A. J. Dempster[1] and G. P. Thomson[2] have observed variable results; these might be attributed to different rates of evaporation for the two isotopes. However, F. W. Aston[3] found no difference in the ratios for ions from lithium iodide under different discharge conditions; M. Morand[4] has observed a difference in the ratios with different currents from a mixture of salts, but concluded that the effect was due to an overlapping of the Li_6 and Li_7 beams.

The object of the experiments described here was to study the emission of positive ions from different lithium compounds at different temperatures. Emission of positive ions from heated salts has been found by a number of investigators[5] to follow an equation of the form known as Richardson's law. A variation in the ratio with temperature might be interpreted as a difference in the work functions of the isotopes. Neglecting $T^{1/2}$, Richardson's law may be stated:

$$I = Ae^{-b/T} \tag{1}$$

The ratio of intensities Li_7/Li_6 at a temperature T is then

$$I_7/I_6 = Ae^{-(b_7-b_6)/T} \tag{2}$$

If the work functions are the same, the ratio should be independent of the temperature. A change in the ratio with temperature may be considered as due to different values of b for Li_6 and Li_7. By writing an equation of the form (1) for each isotope, with different constants b_6 and b_7, the temperature T can be eliminated, giving

$$\log I_6 = (b_6/b_7)\log I_7 + \text{const.} \tag{3}$$

[1] A. J. Dempster, Phys. Rev. **18**, 420 (1921).
[2] G. P. Thomson, Phil. Mag. **42**, 857 (1921).
[3] F. W. Aston, Phil. Mag. **47**, 385 (1924).
[4] M. Morand, Comptes rendus, p. 460, Feb. 15, 1926.
[5] O. W. Richardson, Emission of Electricity from Hot Bodies, p. 250

The method of investigation was similar to that used by Dempster.[6] The positive rays were produced from substances which were heated on a platinum strip; they passed through the slit into a magnetic field which bent them in a half-circle of about 7.5 cm diameter. It was found convenient to use a grid potential of 50 to 100 volts between the source and slit. The grid potential and the magnetic field were kept constant, and two accelerating potentials, V_6 and V_7, were used to bring the Li_6 and Li_7 ions respectively on to a second slit. When $V_6 : V_7 = 7:6$ the paths are identical, even in the stray magnetic field before the first slit. The rays were finally caught in a Faraday cylinder. In Dempster's experiments, the intensity of a beam passing through the second slit was measured by neutralizing the positive ion current by a negative current from an ionization chamber. Beta-rays from a radioactive source were shot into the ionization chamber through a slit, the width of which could be varied by means of a micrometer screw. In the present experiments two radioactive sources and two adjustable slits were used on the ionization chamber; one slit was adjusted to balance the Li_6 intensity and the other the Li_7, the radioactive source being about ten times as strong for the Li_7 as for Li_6. A sector that could be revolved inside the ionization chamber opened the chamber to ionizing radiations from one or the other source and at the same time changed the accelerating potential to bring the Li_6 or Li_7 rays on to the second slit. The object of this arrangement was to measure the two intensities at one temperature in a very short time, thus decreasing the possibility of errors due to changing temperature or surface conditions of the emitting source. A Lindemann quadrant electrometer was used to indicate exact neutralization of the positive ray current. The radioactive sources were kept in fixed positions, and the slits were calibrated on an arbitrary scale by the rate of charge of the electrometer system, to which suitable capacities were added.

The platinum strips bearing the lithium compounds were baked out in vacuum, and in the experiments all pressures were below MacLeod gauge measurements. With magnetic field and grid potential constant, the ratio of intensities Li_7/Li_6 is found from the slit widths of the compensating ionization chamber using the calibration curves for the slits. By the rotating sector and switch, very rapid adjustments could be made; the final comparison of the intensity of the Li_6 and Li_7 at a given temperature could be made in a small fraction of a minute. The time between comparisons at different temperatures was also short, being only a few minutes. Usually the emission was steady enough for careful adjustments.

The first experiments were made with a mixture of lithium phosphate and iron oxide, prepared by melting the compound with iron filings in an oxygen flame. This type of source is described by C. H. Kunsman[7] as one which gives a very steady emission of positive ions. Lithium chloride was tried in the same way, but the intensity of emission falls off so rapidly that measurements could not be made. The phosphate alone was also tried, and

[6] A. J. Dempster, Phys. Rev. **11**, 316 (1918); A. J. Dempster, Phys. Rev. **18**, 415 (1921).
[7] C. H. Kunsman, Phys. Rev. **25**, 892 (1925).

was found to give an emission that was too unsteady for satisfactory results. Other successful experiments were carried out with lithium silicate, lithium aluminate and spodumeme ($Li_2O \cdot Al_2O_3 \cdot 4SiO_2$). These compounds were obtained in as pure a state as possible and put on platinum strips in the form of thin layers of fine powder. All have high melting points, the lowest being that of the silicate, which is in the neighborhood of 1200°C. The highest temperatures used in the experiments were below 1200°C. The aluminate and spodumene give very steady emissions over a wide temperature range.

An attempt was made to observe the rates of emission from lithium metal, using a small iron furnace to heat the metal, and bombarding the

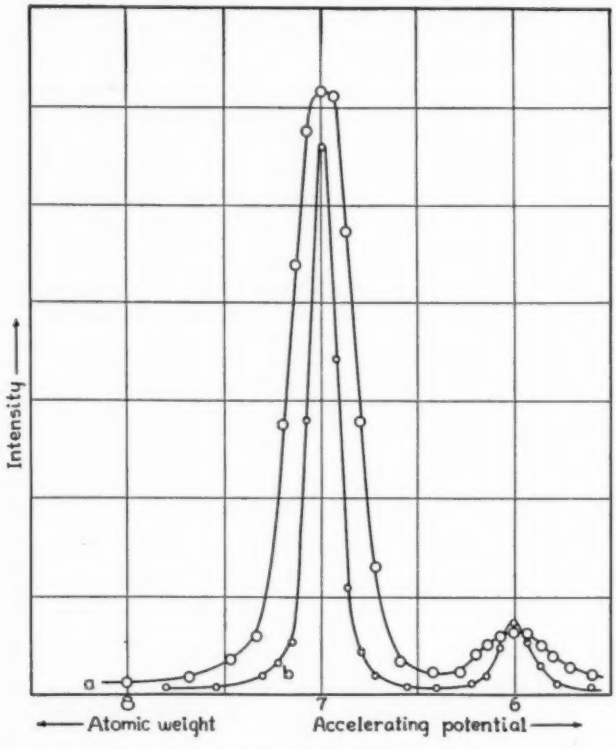

Fig. 1. (*a*)l ithium silicate; slits 0.75 mm and 2.0 mm; (*b*) lithium phosphate and iron oxide, slits 0.75 mm and 1.0 mm.

metal with electrons from a hot tungsten wire. With the current between the furnace and hot filament constant, intensity changes were produced by changes in the furnace temperature.

Fig. 1 shows intensity plotted against accelerating voltage, or atomic weight. Curve (a) is for lithium silicate, with the first slit 0.75 mm and the second slit 2.0 mm. Curve (b) is for the lithium phosphate-iron oxide mixture, with the first slit 0.75 mm and the second slit 1.0 mm. For the sake of comparison, divisions on the intensity scale are different in the two curves. It is seen that the two isotopes are sharply separated in each case. The first slit was kept narrow, 0.25 to 0.75 mm, and the second slit was set

at 2.0 mm in the experiments. The object of this was to make sure that the maximum of each bundle was received by the measuring apparatus in spite of possible small variations in accelerating potential or magnetic field. On curve (a) a variation of the accelerating voltage of 2 volts on either side of the exact maximum causes a very small variation in the intensity through the slit, while such a change in the accelerating voltage would cause a large current variation with the slit arrangement used for curve (b).

The curve (a), which was taken with the source at a high temperature, shows a broadening of the Li_7 beam to a considerable distance on either side; the intensity at atomic weight 6 is increased by scattered rays from Li_7. This curve, although an extreme example, illustrates the necessity for background corrections. It was found that the intensity at an accelerating voltage corresponding to atomic weight 8 was slightly less than the lowest intensity between atomic weights 6 and 7, and greater than the intensity at a corresponding point between 6 and 5. The pressure conditions used were always such that the two peaks Li_7 and Li_6 were sharply defined, and the lowest intensity between peaks was never very much greater than the intensity at atomic weight 8. From a consideration of the intensity curves it was concluded that the intensity at atomic weight 8 was very close to the background intensity that should be deducted from the intensity at atomic weight 6. Further discussion of this point will be taken up later.

It was found that the ratio of intensities Li_7/Li_6 varies with the temperature. In general, for higher temperatures the Li_6 intensity becomes relatively stronger. On decreasing the temperature to a former value, the former ratio is reestablished. This variation is shown by the data of Table I, from a lithium phosphate-iron oxide source; I_6' I_7 and I_8 indicate the intensity at atomic weights 6, 7 and 8 respectively.

TABLE I

Variation with temperature of source (lithium phosphate-iron oxide) of the ratio Li_7/Li_6.

Heating current	I_7	I_6'	I_8	$R=\frac{I_7}{I_6'-I_8}$
3.00 amp.	357	22.9	3.6	18.5
2.86	147	4.8	1.3	42.0
2.68	24	.4	—	60. (uncorrected)
3.00	347	24.0	3.5	17.0
2.87	165	6.2	1.5	35.1

These observations are directly at variance with those of Aston, who found a constant ratio under different conditions. It is possible that in his experiments the particular variable responsible for a change in ratio was not altered. The behavior shown is to be expected if Li_6 has a larger work function than Li_7. In subsequent experiments, the intensities Li_7 and Li_6 were measured and the ratio b_6/b_7 which would be necessary to account for the different ratios Li_7/Li_6 was determined by plotting log I_6 against log I_7, making use of Eq. (3). In determinations of b_6/b_7 from a set of data, it is essential that no change occur except in the temperature of the emitting

surface. Then a point on the graph is obtained for each temperature at which the intensities are measured.

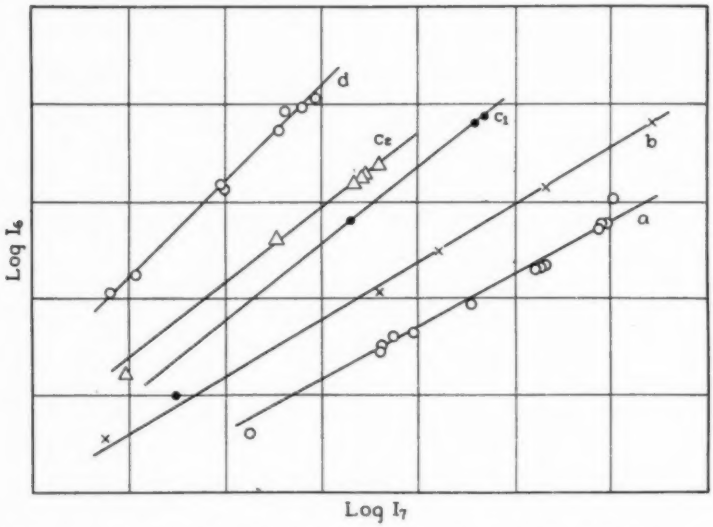

Fig. 2. (*a*) Lithium silicate; (*b*) lithium aluminate; (c_1) and (c_2) lithium phosphate—iron oxide mixtures; (*d*) spodumeme ($li_2O \cdot Al_2O_3 \cdot 4SiO_2$).

Fig. 2 shows curves obtained by plotting log I_6 against log I_7. The value of a scale division on the log I_6 scale is twice that of the log I_7 scale. The scale is the same for each curve, but the origins have been shifted to prevent overlapping.

The data from which curve (a), for lithium silicate, and curve (d) for spodumeme ($Li_2O \cdot Al_2O_3 \cdot 4SiO_2$) were plotted are shown in Table II. The

TABLE II

Data for curves (a) and (d) of Fig. 2. R is the ratio $I_7/(I_6' - I_8)$.

Data for curve (a)								Data for curve (d)			
I_7	I_6'	I_8	R	I_7	I_6'	I_8	R	I_7	I_6'	I_8	R
190.	19.25	3.2	11.9	21.2	2.4	1.2	17.6	207.	7.0	1.85	40.2
63.	6.3	1.5	13.1	209.5	21.9	3.5	11.3	40.	.6	.3	130.
135.	12.5	2.0	12.9	26.	2.7	1.2	17.3	201.	5.4	1.2	47.9
200.	21.2	3.8	11.5	138.	13.8	2.4	13.1	230.	6.7	1.3	42.6
55.6	6.15	1.6	12.2	53.4	4.95	1.2	14.2	85.5	1.1	.35	114.
190.	19.9	2.5	10.9	89.	7.95	1.3	13.4	73.5	.9	.3	122.
52.	5.7	1.6	12.7	131.5	12.0	1.6	12.6	145.	2.5	.45	70.7
								248.	7.4	1.4	35.4

observations in most cases fit well on straight lines. This would be expected on the theory that the differences were due to a difference in the work function. The greatest divergence occurs at low temperatures where the ratios are largest and the difficulty in measuring I_6' and I_8 are greatest. The values of b_6/b_7 deduced from the curves are:

(a)	lithium silicate	1.08
(b)	lithium aluminate	1.20
(c_1)	lithium phosphate-iron oxide	1.56
(c_2)	lithium phosphate-iron oxide	1.56
(d)	Spodumeme	1.95

The two sets of data tabulated above represent the range of temperature changes possible with constant slit width and constant potentials. By decreasing the slit width at high temperatures and decreasing the grid and accelerating potentials, it was possible to obtain smaller ratios Li_7/Li_6; at low temperatures it was necessary to use a larger emitting surface, wider slit and higher potentials. Four such changes were made with spodumeme,

TABLE III

	I_7	I_6'	I_8	R	b_6/b_7
A	281.	12.9	2.8	27.8	2.02
	320.	16.	3.0	24.5	2.26
	141.	2.9	.8	67.	
B	307.	18.4	3.1	20.	
	93.	2.3	1.0	72.	2.06
C	104.5	4.1	1.4	38.	
	296.	20.9	4.0	16.9	1.79
D	178.5	19.1	2.4	10.7	
	90.	6.1	1.3	18.7	1.81

giving the data of Table III. The values of b_6/b_7 for spodumeme were computed by Eq. (3) using intensities at two different temperatures to eliminate the constant. The mean value of b_6/b_7 is 1.99, which is in agreement with the value 1.95 found graphically for spodumeme for a very low range of temperatures.

Other measurements were also made with the other three substances, in addition to those used in the graphs in Fig. 2. Two sets of data, each at three temperatures, with the lithium phosphate-iron oxide mixture gave ratios R from 7.5 to 40, and values of b_6/b_7 computed from the intensities were 1.58 and 1.50 in one case, and 1.50 and 1.51 in the other. The value deduced from the graphs shown in Fig. 2 is 1.56. Two observations, each at two temperatures, with lithium silicate gave ratios R from 9.8 to 17.5, and b_6/b_7 was computed to be 1.10 and 1.18. Two observations, each at two temperatures, with lithium aluminate gave b_6/b_7 as 1.22 and 1.14, while R varied from 14.0 to 26.5.

The experiments with lithium metal were not satisfactory because of a large background. Over a small temperature range there appeared to be a decrease in the ratio Li_7/Li_6 with increasing temperature; numerical values were uncertain because the background intensity, measured in the usual way, amounted to about as much as the corrected Li_6 intensity, and the peaks were not very sharply defined.

It has been pointed out that a correction was made for the overlapping of scattered rays from Li_7 on the Li_6 bundle. For each source used measurements were made on background intensity between the lithium peaks and on either side, and the intensity at an accelerating voltage corresponding to atomic weight 8 was always deducted from the intensity at atomic weight 6 to determine the corrected Li_6 intensity. It is interesting to consider the magnitude of the corrections and the possible errors introduced by this method of measurement. At low temperatures where the total intensity at atomic weight 6 was very small compared with that at 7, the intensity at 8 amounted in extreme cases to as much as 50 percent of the intensity at 6. Since both were small, neither could be measured with great accuracy, and the error to be expected is large. This is to be seen in the curves in Fig. 2, where most of the large divergences occur with the small intensities. If we consider high temperatures, where ratios Li_7/Li_6 less than 15 were found, the intensity at atomic weight 8 amounted to 5 to 25 percent of the intensity observed at atomic weight 6. Pressure conditions were such in most cases that this intensity was nearer the lower value. From measurements at various temperatures on the smallest intensity between Li_7 and Li_6, and consideration of the intensity-atomic weight curves such as shown in Fig. 1, it is certain that the value at 8 is within 20 percent of the true correction. Then the maximum background error was not more than 5 percent of the Li_6 intensity. To see the influence of this error on the value of the ratio b_6/b_7, let us consider, as an example, the point of greatest intensity on curve (b) of Fig. 2; the measured intensities were $I_7=298$; $I_6'=39.7$; $I_8=6.0$. The corrected ratio is then 8.8. In order for the ratio to be 15, which would be the case if $b_6/b_7=1$ instead of 1.2, the Li_6 intensity should be 20 and the background correction 19.7 or half the observed intensity. This is almost three times as great as the maximum background possible for the measurements made. It is evident from this example that the effects observed cannot be attributed to an overlapping of the bundle as suggested by Morand.

The general effect observed, indicating that the work function of the lighter isotope is greater than that of the heavier one, would not be expected from any previous experiments on the separation of isotopes by evaporation or diffusion. However, in this case the ions are taken out of the solid substance; the temperatures were high, of the order of 900° or 1000°C, although they were in most cases well below the melting points of the substances. It is also significant that the ratio b_6/b_7 is different for different compounds, and that it is large for the very complex molecule of spodumeme. It might be of interest here to refer to articles by Lindemann and Aston on the vapor pressures and chemical affinities of neutral isotopes.[8]

In conclusion the writer wishes to express his thanks to Dr. Dempster, who suggested the problem and gave valuable advice throughout the work.

UNIVERSITY OF CHICAGO,
September 9, 1927

[8] F. A. Lindmann and F. W. Aston, Phil. Mag. **37**, 523 (1919); F. A. Lindemann, Phil. Mag. **38**, 173 (1919).

RECOIL ELECTRONS FROM ALUMINUM

By A. A. Bless

Abstract

The maximum energy of electrons ejected from aluminum by the scattering of x-rays of wave-length 0.48 and 0.712A.—Electrons recoiling from aluminum as a result of the scattering of x-rays were analyzed by a magnetic field and detected by their effect on a photographic film. The filtered radiation from a tungsten tube (effective wave-length 0.48A) and the Mo $K\alpha$ rays (λ0.712A) from a molybdenum tube were used. The maximum energy of the recoil electrons as determined from the position of the high-velocity edge of the blackening on the films is expressed in terms of ν/R (ν, the frequency of a quantum having the same energy; R, Rydberg's constant). The values obtained are 190 for the 0.48A rays and 84.1 for the 0.712 rays.

Test of the Compton and of the Wilson theories of scattering.— According to the Compton theory of scattering based on the assumption that radiant energy travels in the form of quanta having a definite momentum as well as a definite energy associated with them, the electrons scattering the x-ray quanta recoil with a maximum energy $E=2\alpha h\nu/(1+2\alpha)$, where $\alpha=h\nu/mc^2$. On the Wilson postulate that the scattered radiation travels in the form of spherical waves the maximum energy of the recoiling electrons would be about 1/4 that given above. For the two wave-lengths used in the above experiment the values of ν/R computed by the Compton formula are 172.5 and 81.0 respectively while those computed by the Wilson formula are 43.1 and 20.2. The experimental results thus distinctly favor the Compton theory.

Introduction

IN ORDER to explain the change of wave-length of x-rays on scattering Compton[1] assumes that the incident as well as the scattered radiation travels in quanta having a definite momentum and a definite energy associated with them. On the basis of this hypothesis the electrons scattering the incident quanta recoil with an energy

$$E=h\nu\frac{2\alpha\cos^2\theta}{(1+\alpha)^2-\alpha^2\cos^2\theta}$$

where θ is the angle the recoiling electron makes with the direction of the incident radiation, and $\alpha=h\nu/mc^2$, h being Planck's constant, ν the frequency of the incident radiation, c the velocity of light, m the mass of the electron. This energy will be a maximum when θ is zero. In this case

$$E=2\alpha h\nu/(1+2\alpha)$$

On the assumption made by C. T. R. Wilson[2] that the scattered energy proceeds in spherical waves the maximum energy of the recoiling electrons is approximately

[1] A. H. Compton, Phys. Rev. **21**, 483 (1923).
[2] C. T. R. Wilson, Proc. Roy. Soc. **A104**, 1 (1923).

$$E=\alpha h\nu/2(1+2\alpha)$$

i.e., 1/4 of the value given above.

A partial test of the validity of these two equations has been made by Compton and Simon[3] using the Wilson cloud expansion chamber. They obtained a number of photographs of tracks of electrons ejected by x-rays passing through the chamber. From the measured length of these tracks they determined the energy of the electrons by the use of Wilson's empirical formula connecting these two quantities. Because of the very low accuracy with which the length of the tracks could be measured, the doubtful applicability of the Wilson formula for short range tracks and the uncertainty of the length of the wave responsible for the ejection of the electron making the given track the results, while favoring the Compton theory, were not accurate enough to determine the degree of applicability of the theory to recoil electrons.

The aim of the present investigation was to find the energy of the recoil electrons using the magnetic spectrometer method. This method while presenting some difficulties possesses the advantage of higher accuracy.

Apparatus

The apparatus used in this experiment consists of (1) a source of x-rays, (2) a scatterer serving as a source of electrons, (3) a magnetic field to deflect the electrons ejected by the x-rays in the process of scattering and (4) photographic plates properly placed for receiving the impact of these electrons.

In the early experiments a tungsten radiator type of tube was used as the source of radiation. The tube was driven at about 1/4 kilowatt imput. An effective wave-length of about 0.48 angstroms was obtained by filtering the radiation through a piece of aluminum 2 mm thick. Because of the fact that very little radiation was left after filtering, very long exposures were required, and attempts to get results with this tube were abandoned after obtaining one successful exposure. In the later experiments a molybdenum water-cooled tube was used. It was driven at about one kilowatt imput. The voltage across the tube was sufficient to excite the $K\alpha$ lines of molybdenum, and the wave-length of these lines was used in the calculation of the results. A piece of aluminum 0.001 inch thick was used as a scatterer.

The magnetic field was furnished by a pair of Helmholtz coils of average diameter 58.4 cm. Each coil had 780 turns of No. 18 copper wire. The pair of coils when placed 29.2 cm apart gave at the center a field of 24 gauss per ampere of exciting current. The field did not vary by more than one part in a thousand for the whole path of the electrons. For higher fields an auxiliary coil of average diameter 33.7 cm was used. This coil had 1000 turns of wire and was capable of giving 26 gauss per ampere at its center. The arrangement of the apparatus did not permit placing this auxiliary coil so that its center could be near the scatterer, and corrections had to be introduced. These

[3] A. H. Compton and A. W. Simon, Phys. Rev. **25**, 306 (1925).

corrections increased the possible error in the computed value of the field to about 1 percent.

The arrangement of the apparatus is shown in Fig. 1. The x-ray tube T was placed at an angle of about six degrees with the axis of the field coils

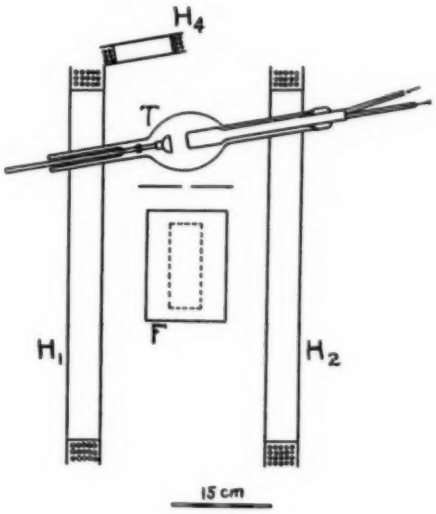

Fig. 1. General arrangement of apparatus.

H_1 and H_2 in order to secure greater intensity of x-rays in the direction of the slit system. This necessitated the use of a compensating coil H_4 in order to

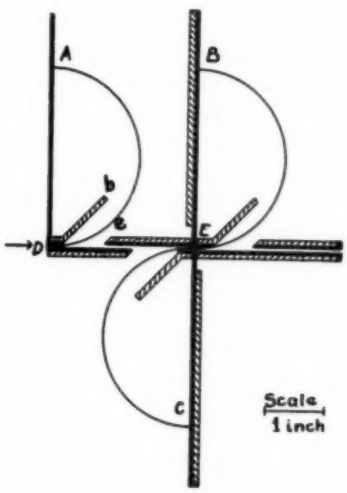

Fig. 2. The slit system and arrangement of the photographic films.

keep the position of the focal spot unchanged when the tube is run with the field on. The size and the number of turns of this coil were calculated and

verified by trial for maximum intensity of x-rays from the tube with the field on. The auxiliary coil H_3 when used was placed between H_2 and the box F. The box contained the scattering material, the slit system and the photographic plates.

The slit system inside the box F is shown in Fig. 2. Pieces of aluminum foil were placed in positions D and E. The scatterer in position D was a little over 8 cm away from the target of the tube. X-rays passing through an aluminum window into the brass box in the direction indicated by the arrow strike the scatterers at D and E. Electrons ejected from the scatterers are deflected by the magnetic field and strike the photographic plates placed in positions A, B, and C. Electrons having a velocity in the forward direction only could fall on A and B, while those having a velocity in the backward direction could strike C. The back of each plate was protected from stray radiation by a piece of lead 1/16 inch thick.

The channel $D \rightarrow E$ through which the x-rays passed was made of brass 1/8 inch thick covered with lead 1/16 inch thick. It was 5/8 inch wide and 1/16 inch high. The channel was in effect a wide slit which limited the electron beam. It was undesirable to have a fine slit in the channel for focusing the electrons because of the increased amount of scattering in the box from the walls of the slit and the disturbing effect of the electrons ejected by the x-rays from these walls. To place a focusing device in the path of the electrons outside the channel would have reduced the electronic beam very appreciably. The absence of a focusing device introduced an error a little over 2 percent in the measurement of the radius of the electronic beam.

The box F containing the scattering material and the photographic films was built of 1/4 inch brass plates and covered with a greased ground brass cover. The box was evacuated by means of a two stage mercury condensation pump backed by a Cenco Hyvac oil pump. The vacuum as measured with a McLeod gauge was kept at about 10^{-5} mm.

Shumann plates and Eastmann Duplitized x-ray films coated with a thin film of oil were used in these experiments. The Shumann plates were not very reliable. Several sets of exposures had to be discarded because of streaks found on the plates. These streaks were later found on the unexposed portions of some plates.

Difficulties were encountered in keeping the field constant because of the changes in the resistance of the coils. Changes in the temperature of the room were sufficient to change the current through the coils appreciably. This was especially true for higher field values when the auxiliary coil was used as it was more closely wound and more sensitive to changes in the temperature of the surroundings.

Many plates were ruined because of sudden failures of the vacuum system. This was attributed to the stop cock grease layer, as the rest of the system had practically no leaks. The exposures lasted three days or longer and the failures of the vacuum usually occurred toward the end of the run. Fractional distillation or some other cause was responsible for the formation of an opening in the grease layer. An hour's run under poor vacuum conditions was sufficient to blacken the plates completely.

The first few exposures showed, together with a band, a great amount of scattered radiation. To reduce the effect of the scattered radiation on the films a lead screen was placed over the opening for the electrons in the

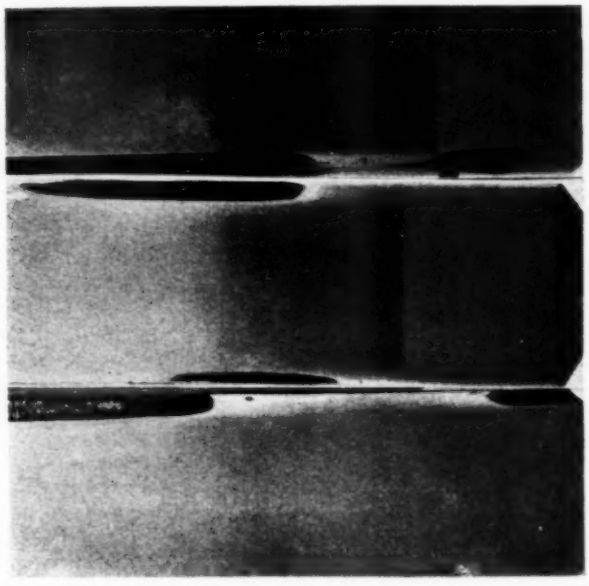

Fig. 3. Electron bands from aluminum which result from the scattering of Mo $K\alpha$ x-rays. The letters indicate the position of the film in the film holder.

channel at about 45 degrees with the direction of the incident x-rays. Its length was such that scattered rays from any portion of the channel could not reach the films directly.

Results and Discussion

Exposure No. 1 of Table I was obtained with the tungsten tube, the effective wave-length of the filtered beam being 0.48 angstroms, as previously mentioned. The spectral width of the band left after filtering was quite great. To make the radiation more nearly monochromatic would require a still greater sacrifice of the intensity of the beam and a consequent increase in the length of exposure. The band on the film has no sharp edge because of the width of the spectral band used. The estimated value of the radius of the path of the electrons having the maximum energy is reliable to not more than 5 percent.

The subsequent exposures were all taken with the unfiltered radiation from the molybdenum tube. The first five successful exposures yielded bands the Hr value of which was nearly the same, H being the value of the magnetic field used to deflect the electrons, and r being the radius of the path of the electrons making the outer, high-velocity edge of the band. To make certain that these electrons are ejected by the encounter of x-rays with the aluminum foil two additional sets of exposures were taken, one with the scatterer in position D only, and another with the scatterer in position E. In both cases

the films above the blank spaces showed no bands, while those above the scatterer gave bands of the same *Hr* value as before.

These experiments show that the blackening on the plates is probably due to corpuscular radiation emitted when x-rays strike the aluminum foil. Electrons may be emitted either in the process of absorption, fluorescence, or scattering of x-rays by aluminum. An examination of the spectra of molybdenum and of aluminum, bearing in mind that the *L* lines of molybdenum are completely absorbed by the walls of the tube and the aluminum window of the box *F* before reaching the scatterer, fails to reveal a probable combination of energy levels which would give photo-electrons having the *Hr* value found on the plates. The conclusion seems probable, therefore, that the bands observed are due to electrons emitted in the process of scattering of x-rays by aluminum. This conclusion is strengthened by the fact that films in position *C* failed to yield bands in all these exposures, showing that these electrons are emitted only in the forward direction.

TABLE I

Comparison of the experimental values of ν/R for the high-velocity edge of the scattered electrons with the values given by the formulas of Compton and of Wilson.

Film	Effective wave-length	Field	Radius	*Hr*	ν/R Exp.	ν/R Calculated (Compton)	ν/R Calculated (Wilson)
1	0.48A	90 g.	1.9 cm.	171	190	172.5	43.1
2	0.712	62.4	1.85	115.	87.	81.	20.2
3	"	40.0	3.01	120.5	94.	"	"
4	"	24.0	4.46	107.5	75.	"	"
5	"	45.0	2.54	114.5	85.5	"	"
6	"	43.0	2.67	114.	85.2	"	"
7	"	28.5	3.93	112.	81.2	"	"
8	"	28.5	3.92	111.5	81.	"	"

Table I shows the results of measuring the energy of the outer, high-velocity edge of these bands and the comparison with the values obtained on the Compton and Wilson hypotheses. As the focusing channel excludes all electrons making an angle with the incident radiation greater than $\tan^{-1} 0.25$ the theoretical values for the energy have been computed for the electrons the direction of which coincides with the direction of the incident radiation. As pointed out before the energy of the electrons is in this case a maximum.

It is convenient to express the energy in terms of ν/R where ν is the frequency of the quantum having the same energy and R is Rydberg's constant. The relation used is

$$Hr = 12.4(\nu/R)^{1/2}.$$

It appears therefore that under the experimental conditions described on the preceding pages the electron band which is attributed to the scattering of x-rays by the aluminum foil has a value for its maximum energy in good agreement with that predicted by Compton on the basis of the quantum

theory. The number of exposures is too small and the conditions have not been varied sufficiently to consider the results conclusive. They are suggestive, however, of the applicability of the Compton theory to recoil electrons.

I wish to thank Professor A. H. Compton for suggesting the problem and Professor F. K. Richtmyer for the advice he has given and the kind interest he has taken in the progress of the work.

ROCKEFELLER HALL,
CORNELL UNIVERSITY,
June 1927.

THE RELATION BETWEEN PLATE CURRENT AND PLATE POTENTIAL IN THE THERMIONIC AMPLIFIER, DEDUCED FROM THE ORBITAL MOTION OF THE ELECTRONS

By L. E. McCarty

Abstract

An expression for the plate current in terms of the grid and plate potentials and geometrical dimensions of a parallel plate type of thermionic amplifier is deduced from the orbital motion of the electrons. The amplifier is assumed to consist of a charged grid of small parallel wires of infinite length situated between two infinite parallel plates at distances from it comparable with the distance between consecutive grid wires, the whole inclosed in a vacuum of such magnitude that the mean free path of the electrons is large in comparison with the distance between the plates. The effect of the space charge is neglected.

Equations giving the force acting on an electron situated at any point in the field due to the charge on the grid and the potential difference between the anode and cathode are derived. These expressions are evaluated and tabulated for various points of the field and the orbits of a number of electrons computed by a process of numerical integration. An empirical relation is found to exist between the distance of the starting points of the electrons, whose orbits turned at a common plane, from the rectilinear projection of a given grid wire on the cathode, and a certain parameter involving the charge per unit length of grid wire, the plate potential, and the geometrical dimensions of the amplifier. Inasmuch as the plate current is determined by the number of electrons reaching the plane where the plate is assumed to be located, before turning back; and since the turning point depends on the starting position of the electron relative to the grid wires, this empirical equation furnishes the required relation between current and plate potential, grid charge, and the geometrical parameters.

Two cases are considered: (a) a negatively charged grid, and (b) a positively charged grid. On account of the greater practical importance of the first case most of the orbits computed are for a negatively charged grid. After substituting for the charge on the grid in terms of the potentials and capacity coefficients, the final equation for this case, assuming the cathode to be at zero potential and at a distance from the grid equal to the distance between consecutive grid wires, is

$$I_P = I_0\{1-2C/[a(kV_P+hV_G)/2(aV_P-SV_G)-\mu_0]\}$$

where I_0 represents the saturation current, V_P and V_G the plate and grid potentials, respectively, the other quantities being constants of the apparatus. A few orbits computed for a positively charged grid seemed to indicate a similar current relation, but no mathematical derivation was attempted for this case.

THE action of the thermionic amplifier has been discussed from the standpoint of the electrostatic problem of a plate and filament separated by a grid, but only in a manner calculated to indicate the general features of the process. The long mean free path of the electrons in the vacuum tube makes the problem one of the orbits of the electrons in a rather complicated field of force, and it is only on this basis that the complete characteristics can be determined. The statical problem of the grid and plane electrode has

been treated by Maxwell,[1] C. Chree,[2] and others, and the relation between current and the constants of the vacuum tube has been investigated, both experimentally and theoretically, without reference to orbital motion, by a number of writers, including J. J. Thomson,[3] C. D. Childs,[4] H. J. Van der Bijl,[5] and W. H. Eccles,[6] and more recently by Irving Langmuir,[7] but nothing has been published to the knowledge of the writer in which the subject is treated from the standpoint of the motion of the electrons about a charged grid. The object of this paper is to deduce a relation, subject to certain restrictions as to the geometry of the tube, the space charge, etc., between plate current and plate potential for two parallel plates separated by a grid, based on the assumption that the electrons move in natural orbits under the action of the charge on the grid and the field between the plates.

The following preliminary assumptions will be made: (a) a charged grid of small parallel wires of infinite length situated between two infinite parallel plates at distances from it comparable with the distance between consecutive wires; (b) a high vacuum so that the distance between the plates is small compared with the mean free path of the electrons; (c) a negligible space charge effect. Other minor assumptions will be introduced later for the purpose of simplifying the calculations.

The general plan of attack followed in the solution of the problem was, briefly stated: first, to derive expressions for the intensity at any point in the field under the specified conditions; second, to integrate the equations of motion in order to obtain the turning points of the electrons; third, to discover, from a number of orbits computed for various values of the constants involved, the relation between the coordinates of the starting points of the electrons which just failed to return to the filament and the plate voltage; and, finally, from this relation, to deduce the relation between plate current and plate voltage. Incidentally, partial orbits were computed and plotted for several electrons, and the relation between plate current and other constants was noted.

Mathematical theory. For a very long charged straight wire the force is radial at all points of the field and is twice the ratio of the charge per unit length to the distance from the point to the center of the wire. The field between the plates may be regarded as being made up of the following parts: (a) a constant field at right angles to the grid due to the charged plates alone; (b) a variable field due to the charged grid superimposed on this constant field; (c) the field due to two infinite series of images of the grid formed in the two plates. It will be shown further on that the forces due to the two series of images are the equivalent of a uniform field. Applying the law of force just stated to the grid wires, neglecting the initial velocities, and

[1] Maxwell, Electricity and Magnetism, Vol. I., pp. 248–253.
[2] C. Chree, Phys. Soc. Proc. **33,** 377 (1921).
[3] J. J. Thomson, Conduction of Electricity Through Gases, 2nd Ed., p. 223.
[4] C. D. Childs, Phys. Rev. **32,** 498 (1911).
[5] H. J. Van der Bijl, Phys. Rev. **12,** 171 (1918).
[6] W. H. Eccles, Radio Review **2,** 31 (1911).
[7] Irving Langmuir, Phys. Rev. **21,** 419 (1923); Phys. Rev. **24,** 49 (1924).

assuming the electron to be a point charge, the x and y components of the force acting on an electron situated at any point (x, y) are (see Fig. 1)

$$F_x = \pm 2e\lambda \sum_{n=-\infty}^{n=+\infty} x[x^2+(na-y)^2]+e(V_P-V_F \pm h\lambda)/S \tag{1}$$

$$F_y = \mp 2e\lambda \sum_{n=-\infty}^{n=+\infty} (na-y)/[x^2+(na-y)^2] \tag{2}$$

where e is the charge on the electron; λ the numerical value of the charge per unit length on the wires; a the distance between consecutive grid wires (from center to center); V_P the potential of the anode (plate); V_G the potential of the cathode (filament); S the distance between anode and

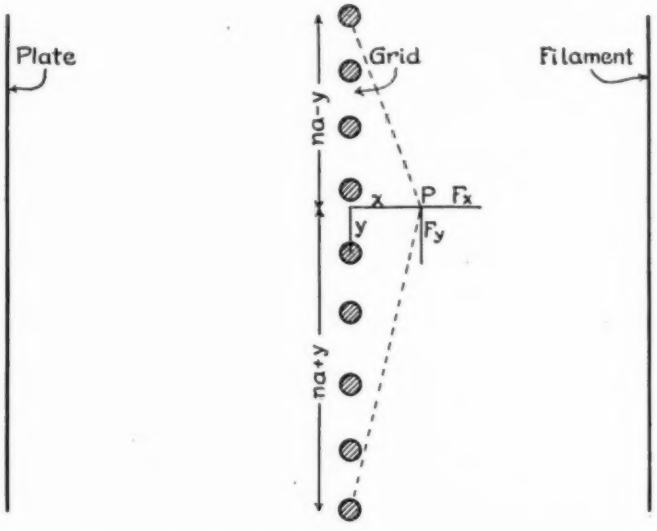

Fig. 1. Cross section of filament, grid and plate with diagrammatic representation of coordinates and force components at any point of the field.

cathode; n the number of wires on each side of the one chosen as origin, and also the number of grid spaces between the origin and the nth wire from origin, the center of the 0'th wire being taken as the origin of (x,y); h a constant depending on the geometry of the apparatus; and $h\lambda$ a correction for the effect of the images of the grid wires in the plates on the potential difference between them (V_P-V_F). This correction will be explained later. The upper one of the double signs is to be used with a positively charged grid.

The summations may be evaluated approximately by integration, by straight summation of a large number of terms, or by summing up a sufficient number of terms to insure the accuracy desired and integrating for the remainder on the assumption that the action of the distant wires is equivalent to that of a uniformly charged plane. The third method was adopted: the

force due to eleven wires was obtained by direct summation and the remainder by integration. The integrations give

$$\pm\int_{5.5a+y}^{\infty}2e\lambda x\,dY/(x^2+Y^2)a\pm\int_{5.5a-y}^{\infty}2e\lambda x\,dY/(x^2+Y^2)a=$$
$$\pm\frac{2e\lambda}{a}\left(\pi-\tan^{-1}\frac{5.5a+y}{x}-\tan^{-1}\frac{5.5a-y}{x}\right) \tag{3}$$

$$\mp\int_{5.5a-y}^{(n+1/2)a-y=\infty}2e\lambda Y\,dY/(x^2+Y^2)a\pm\int_{5.5a+y}^{(n+1/2)a+y=\infty}2e\lambda Y\,dY/(x^2+Y^2)a=$$
$$\mp\frac{e\lambda}{a}\log\frac{x^2+(5.5a+y)^2}{x^2+(5.5a-y)^2} \tag{4}$$

for the x and y components of the force, respectively, where Y represents the ordinate of the wires with the point (x,y) taken as origin. Since

$$\lim_{n=\infty}\{x^2+[(n+1/2)a-y]^2\}/\{x^2+[(n+1/2)a+y]^2\}=1$$

the values of the integrals at the upper limits in Eq. (4) cancel, although they each approach infinity as n approaches infinity.

On substitution of these integrals in (1) and (2) and making a slight rearrangement in form, there results, for the equation of motion of an electron,

$$d^2x/dt^2=-\frac{2e\lambda}{ma}\left\{\mp\sum_{n=-5}^{n=5}ax/[x^2+(na-y)^2]\mp\left(\pi-\tan^{-1}\frac{5.5a+y}{x}\right.\right.$$
$$\left.\left.-\tan^{-1}\frac{5.5a-y}{x}\right)-a(V_P-V_F\pm h\lambda)/2S\lambda\right\}. \tag{5}$$

$$d^2y/dt^2=-\frac{2e\lambda}{ma}\left\{\pm\sum_{n=-5}^{n=5}a(na-y)/[x^2+(na-y)^2]\right.$$
$$\left.\pm\frac{1}{2}\log\frac{x^2+(5.5a+y)^2}{x^2+(5.5a-y)^2}\right\}. \tag{6}$$

Because of the form of Eqs. (5) and (6), if all distances be expressed in terms of a as a unit, and the ratio $(V_P-V_F\pm h\lambda)/\lambda$ maintained constant, the force components remain in constant ratio; and if, in addition, λ and (V_P-V_F) are replaced by λ/a and $(V_P-V_F)/a$, which is the equivalent of measuring charge per unit length and potential in terms of the same unit of length, then the forces are constant at corresponding points for all values of a. This generality of the formulas will be of great practical importance in experimental work for it means that certain results derived from the formulas are independent of the dimensions of the apparatus so long as all dimensions are varied in the same proportion.

In order to obtain the equation of path for the electrons it was necessary to find first and second integrals for these force equations. It is apparently

impossible to obtain analytical solutions, but by using the method of numerical integration they were integrated for a number of values of the constants involved. This is a numerical method[8] by means of which the integral of any function, such as usually occurs in the differential equations met with in physical problems, may be found to any desired degree of approximation provided it possesses derivatives, and is continuous over the range of integration, and has given a set of initial numerical values for the function and its integrals. These criteria are fulfilled in the equations of motion to be integrated in this problem. Neither a complete description of the general method nor a detailed account of the solutions can be given here because of their length, but the principal steps in the application of the method to these equations may be stated briefly as follows: (a) choice of a suitable starting point and of a convenient time interval; (b) evaluation of the functions from the assumed initial values of the integrals by means of formulas given in the article referred to in the footnote, or a table of values computed from them; (c) extrapolation of a value for the functions; (d) calculation of new integrals from formulas given for this purpose; (e) correction of the extrapolated values of the functions and of the first and second integrals by means of other formulas. The complete solutions were in the main a repetition of the above steps. As just stated, the adoption of this method made it necessary to start with a definite set of values for the function and its integrals. Since the grid-filament distance in some commercial tubes is approximately the same as the distance between consecutive grid wires, and because preliminary calculations showed the field to be fairly constant at this distance it was decided to select the point (a,y_0) as the starting point, y_0 being a parameter for which a definite value was assigned for each orbit. The relation to be derived from these orbits will necessarily be restricted to the extent of this choice. In all the orbits computed, then, the initial conditions were those for the starting point (a,y_0) where $dy/dt=0$, $dx/dt=0$ (neglecting thermal velocity), d^2y/dt^2 and d^2x/dt^2 being determined by the value of the field at the point (a,y_0). The time interval was selected by trial and from the estimated velocity of an electron under the given conditions, and was varied considerably depending on the intensity of the field along the orbit. For better convenience in computation, the formulas comprising the integrands were replaced by isolated values calculated for a number of points in the field. By expressing x and y and the time interval in terms of a and dividing by the factor $-2e\lambda/ma$, the only constants remaining to be evaluated are those contained in the ratio $a(V_P-V_F\pm h\lambda)/2S\lambda$. This term contains a number of important parameters, viz., the grid spacing constant, the difference of potential between the plate and filament, and the charge per unit length on the grid wires, and will be retained as a single arbitrary constant to be evaluated later subject to certain limitations. It will be referred to as μ throughout the discussion of results. We shall presently determine h and

[8] An account of this method is given by Prof. F. R. Moulton of the University of Chicago, in an article appearing in Smithsonian Miscellaneous Collection, Vol. 74, No. 1, under the title "Numerical Solution of Differential Equations."

so λ and μ in terms of V_P, V_G, and the geometrical constants on which they depend. For the moment, however, it will be sufficient to make the discussion in terms of assigned values of μ.

The resultant values of the x and y components of the acceleration, each divided by $-2e\lambda/ma$, reveal several interesting features of the field (see Table I). As was to be expected, both the x and y components are very large

TABLE I

Numerical values of d^2x/dt^2 and d^2y/dt^2 (each divided by $-2e\lambda/ma$) near a charged grid composed of an infinite number of fine parallel wires situated between two infinite parallel planes, for the first quadrant only. (See Figs. 2 and 3). The upper value in each pair of values in the table is the value of d^2x/dt^2. The lower is the value of d^2y/dt^2.

y	$x=0$	$0.01a$	$0.02a$	$0.03a$	$0.04a$	$0.05a$	$0.1a$	$0.2a$	$0.5a$	a
$0.5a$	μ	.095-μ	.117-μ	.175-μ	.236-μ	.291-μ	.987-μ	1.75-μ	2.88-μ	3.13-μ
	0	0	0	0	0	0	.001	.001	.002	.001
$0.4a$	μ	.106-μ	.217-μ	.326-μ	.436-μ	.539-μ	1.11-μ	1.87-μ	2.93-μ	3.13-μ
	1.02	1.02	1.02	1.01	.893	.993	.870	.996	.147	.006
$0.3a$	μ	.147-μ	.300-μ	.449-μ	.598-μ	.738-μ	1.39-μ	2.30-μ	3.05-μ	3.14-μ
	2.28	2.33	2.27	2.25	2.33	2.29	1.85	1.35	.253	.015
$0.2a$	μ	.282-μ	.567-μ	.840-μ	1.11-μ	1.35-μ	2.35-μ	2.91-μ	3.22-μ	3.15-μ
	4.32	4.32	4.30	4.21	4.13	4.04	3.33	1.59	.258	.013
$0.1a$	μ	1.03-μ	2.06-μ	2.95-μ	3.58-μ	4.67-μ	5.33-μ	4.65-μ	3.67-μ	3.15-μ
	9.67	9.67	9.36	8.85	8.26	7.68	4.66	1.70	.152	.004
$0.07a$	μ	2.03-μ	3.84-μ	5.27-μ	5.54-μ	6.92-μ	7.04-μ	5.10-μ	3.40-μ	3.15-μ
	14.0	13.8	13.0	11.8	9.10	9.23	3.82	1.34	.122	.003
$0.05a$	μ	3.88-μ	6.97-μ	8.03-μ	8.13-μ	10.2-μ	8.33-μ	5.35-μ	3.41-μ	3.15-μ
	19.8	19.1	17.1	13.4	9.80	9.83	3.46	1.02	.096	.004
$0.03a$	μ	10.0-μ	15.5-μ	16.8-μ	16.1-μ	14.9-μ	9.50-μ	5.53-μ	3.42-μ	3.15-μ
	33.2	29.9	23.0	15.6	11.9	8.74	2.65	.651	.059	.008
$0.02a$	μ	20.0-μ	25.1-μ	23.2-μ	20.1-μ	17.4-μ	9.94-μ	5.59-μ	3.42-μ	3.15-μ
	50.9	39.9	24.9	15.3	9.93	6.83	1.85	.430	.036	.007
$0.01a$	μ	50.0-μ	49.1-μ	30.1-μ	23.7-μ	19.4-μ	10.2-μ	5.59-μ	3.43-μ	3.15-μ
	100	50.0	20.0	9.97	5.85	3.82	.962	.222	.016	.002
0	∞	100-μ	50.1-μ	33.4-μ	25.1-μ	20.2-μ	10.3-μ	5.64-μ	3.33-μ	3.15-μ
	∞	0	0	0	0	0	0	0	0	0

NOTE: The quantities in the table are proportional to the force components acting on the electron at various points in the field, and equivalent to the components when $2e\lambda/a=-1$. The algebraic sign used with the numerical parts of the quantities was chosen according to the sign of the charge on the grid, and the quadrant in which they were used, both x and y-components being negative in the first quadrant when the grid has a positive charge, and positive for a negatively charged grid. The same numbers with appropriate signs will represent the components of the field due to the grid in the other three quadrants.

near the wires, and at a distance from the grid equal to the distance between its consecutive wires, all the x-components approach a constant value (approximately π) and the y-components approach zero, thus showing that the action of the grid becomes equivalent to that of a uniformly charged plane at about this distance, a fact which will afford considerable simplification in the subsequent calculation of h and λ. On account of the periodic

recurrence of values in the direction of the grid plane and the symmetry of the forces with respect to the grid plane, the points calculated were confined to the first quadrant only and between $y=0$ and $y=a/2$. Any results derived from orbits starting between these limits will be duplicated in other regions. An examination of the equation of motion shows that μ represents a force tending to pull an electron in the negative direction, and that it must be greater than the term representing the contribution of the grid in a direction perpendicular to the grid, at the distance of the filament from it, in order

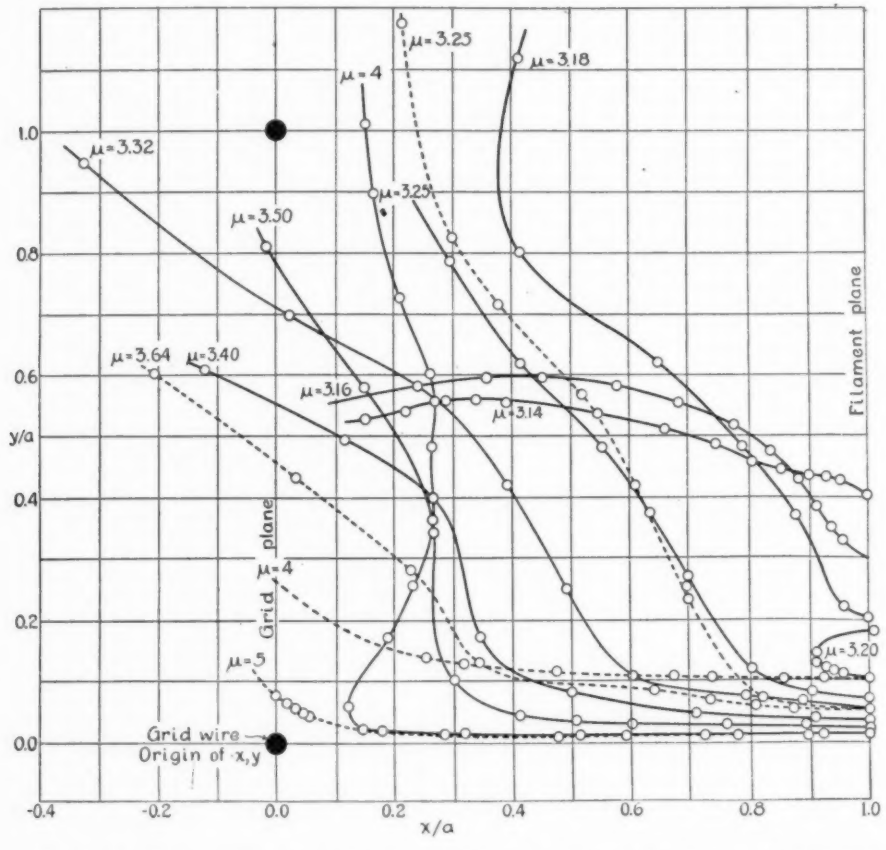

Fig. 2. Orbits of electrons starting from different points of the filaments calculated (a), from critical values of μ (full lines), and (b) from values of μ near the critical values (dotted lines) with negatively charged grid.

for the electron to move from the filament toward the grid. The x-components of the force due to a positively charged grid are negative to the right of the grid in the drawings, and positive for all points to the left; and the y-components are negative in the first and second quadrants and positive in the third and fourth quadrants. The reverse is true when the grid is negatively charged. In the interpretation of some of the results it should be borne in mind that the values shown in the tables are not the forces themselves, but functions of the forces obtained by dividing by the common factor $-2e\lambda/a$.

This will not alter the form of the orbits nor the final relation deduced from them.

The chief purpose of the investigation, as has been stated, was to discover the relation between the plate current and the plate potential. The plan of attack from this point on was to find, by computing a number of the orbits with various values of the parameter μ and y_0 (ordinate of the starting point of the electrons), that fraction of the total number of electrons emitted which fell short of a common plane (the plate) parallel to the grid, and from this fraction to determine the relation sought. In the absence of any definite

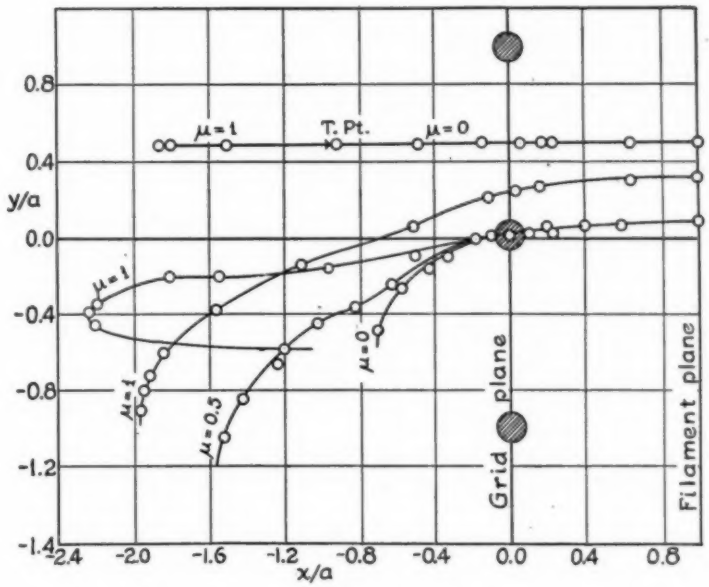

Fig. 3. Orbits of electrons when the grid has a positive charge. Large shaded circles represent wires.

hypothesis to serve as a guide, it was necessary to perform a number of integrations, in order to draw reliable conclusions. Nineteen of the orbits computed are shown in Figs. 2 and 3.

Discussion of the Orbits

The analysis of the orbits falls naturally under two main heads: (a) those computed for a negatively charged grid, and (b) those computed for a positively charged grid.

Case (a). Grid negatively charged. When the charge on the grid is negative the electrons will be retarded and deflected upward to the right of the grid between $y=0$ and $y=a/2$, in the drawings (Fig. 2), while to the left of the grid they will be accelerated toward the plate. Hence, in order to determine whether or not an electron reaches the plate it will be sufficient to plot its path as far as the grid plane only. By inspection of the data and by making a number of preliminary trials using different values of μ, especially at and

near the limiting values of y (i.e., $y=0$ and $y=a/2$) several pairs of values of y_0 and μ were found for which the electron either barely passed the grid or was deflected off parallel to the grid. These critical values of μ and the corresponding values of y_0 are listed in Table II and the orbits shown in Fig. 2 (heavy lines). The $-$ and $+$ signs attached to some of the numbers in the μ-column of Table II indicate, respectively, that the electron either barely passed the grid or that it was turned back too easily. In Fig. 2 the orbits ($\mu=3.50$, $y_0=0.02a$), ($\mu=3.40$, $y_0=0.03a$) and ($\mu=3.32$, $y_0=0.05a$) represent the former of these two classes, and ($\mu=3.20$, $y_0=0.1a$) represents the other. The orbit ($\mu=3.25$, $y_0=0.07a$) goes so far upward that its final destination is uncertain. Although the orbits ($\mu=4$, $y_0=0.01a$), and ($\mu=3.18$, $y^7=0.2a$) went so far away that they were abandoned for the present, yet

TABLE II

Critical values of μ, with corresponding values of y_0, and products $y_0(\mu-\mu_0)$.

y_0	μ	$\frac{\mu-\mu_0}{\mu_0=3.13}$	$y_0(\mu-\mu_0)$ (observed)	$y_0(\mu-\mu_0)$ (calculated)
0.00				
.01a	4.00	0.87	0.0087a	0.0084a
.02a	3.50−	.37	.0074a	"
.03a	3.40−	.27	.0081a	"
.05a	3.32−	.19	.0095a	"
.07a	3.25	.12	.0084a	"
.10a	3.20+	.07	.0070a	"
.20a	3.18	.05	.0100a	"
.30a	3.16	.03	.0090a	"
.40a	3.15	.02	.0080a	"

it seems highly probable from their course and general behavior, that they will not pass the grid; or, at least, if they do pass, they must be very near the border line between the two systems containing those which do and those which do not reach the plate. While the orbits starting at $y_0=0.3a$, and $y_0=0.4a$, passed quite readily across the grid plane, yet their wavering course near the filament, together with the fact that decreases of only 0.7 and 0.3 percent, respectively, in the value of μ would have prevented these electrons from leaving the filament at all, places their orbits also within a small percent of the true critical orbits.

From a superficial examination of Fig. 2, it may appear that too great a difference exists between the form of these orbits to include them all in the same class as forming boundaries between the two systems, as is done in the results that follow; but the very fact that minute differences in the constants causes such large fluctuations in the orbits is evidence of the correctness of the selections which have been made in Table II, and serves accurately to locate the starting point of the critical orbit. The accurate location of the boundary is so essential in the solution of the problem that other orbits were computed with identical starting points but slightly different values of μ from that used in those orbits selected as the critical ones, in order to illustrate further the inconstancy of the orbits when μ is near the critical value.

Some of these orbits are plotted in Fig. 2 (dotted lines). A comparison of a few of these orbits with those drawn in full lines shows that an enormous change in the form and direction of the orbit results from a relatively small change in μ, in the neighborhood of its critical values. For example, the two orbits ($\mu=5$, $y_0=0.01a$) and ($\mu=4$, $y_0=0.01a$) start from the same point and their paths almost coincide until within a very short distance of the origin, but one crossed easily against a strong repulsion near the wire, while the other was forced backward and upward, possibly back onto the filament. Three orbits were computed for the same initial ordinate $y_0=0.05a$ with $\mu=3.25$, $\mu=3.32$, and $\mu=3.64$, respectively. The electron in the first orbit was deflected to some extent but crossed the grid between $y=0.40a$ and $y=0.50a$ and the second crossed at $y=0.71a$, just escaping the strong field about the next wire, which might have reversed it had it passed a little nearer the wire; and the third, with a difference of only two percent in the value of its μ, was stopped near the filament and finally deflected off parallel to the grid. The same contrast is exhibited in the orbits ($\mu=4$, $y_0=0.1a$), in which the electron crossed the grid with very little disturbance to its orbit, and ($\mu=3.20$, $y_0=0.1a$) in which it was completely reversed and driven back to the filament. While the small number of data available, due to the enormous amount of time required for computing orbits, together with the great difficulty of interpolation in the neighborhood of the grid wires where the field is rapidly changing and is large in comparison with the values of μ, must necessarily introduce a considerable probable error which it is impossible to calculate accurately; yet the above comparisons, together with the observed behavior of the electron—its direction, velocity, etc., indicate that these values of μ are not far from the true critical values.

Discussion of Table II

It is obvious from a comparison of the values of μ and of y_0 in the first two columns of Table II that some sort of inverse relation exists between them. Any function expressing this relation must be such that $\mu=\infty$ when $y_0=0$ and approaches a constant minimum value (about 3.13 for the position of filament chosen) in a sort of asymptotic fashion, as y_0 approaches $a/2$. An exponential function, with properly chosen constants might be made to satisfy these conditions and fit the observed values approximately, but the simplest relation which appeared to satisfy such requirements is the equation of the rectangular hyperbola. In order to test this suspected relation the three columns in Table II, headed $(\mu-\mu_0)$, $(\mu-\mu_0)y_0$ (observed), and $(\mu-\mu_0)y_0$ (calculated) were added, where μ_0 is the lower limiting value of μ which is just sufficient to start the electron situated at $y=K(a/2)$, ($K=1$, 3, 5, etc.) on the filament and draw it toward the plate. It is numerically equal to the x-component of the force which the grid exerts at this point when $-2e\lambda/a$ equals unity. It is about 3.13 for the position of the filament chosen, but approaches π as the distance from the grid increases, making the grid field approximate that of a uniformly charged plane whose intensity is constant, perpendicular to the plane, and proportional to π. There are some rather

wide discrepancies in the table, the difference in one or two cases between individual values and their mean being as high as 20 percent, but the general agreement between most of the individual values and their mean is close enough to suggest the equation of the rectangular hyperbola as a good approximation to the correct relation between the true values of μ and y_0. Most of the orbits were computed before this relation was tried, but in order to test its correctness still further, one of the orbits ($\mu=3.25$, $y_0=0.07a$) was computed for the theoretical value of μ calculated from the equation

$$0.07a(\mu-3.13)=0.0084a \tag{7}$$

with the result shown in the diagram of orbits (Fig. 2) where it is seen that this curve bears a fairly close resemblance to other critlcal orbits.

If these values of μ be accepted as the true critical values and if their relation to y_0 is correctly expressed, for grid-filament distance equal to a, by the equation

$$(\mu-\mu_0)y_0=Ca\doteq 0.0084a \tag{8}$$

then the relation between plate current and plate voltage follows directly.

Denoting the plate current by I_P and the total saturation current by I_0, we have

$$I_P/I_0=\frac{\text{No. of electrons reaching plate}}{\text{Total electron emission}}=\frac{(a/2)-y_0}{a/2}=(a-2y_0)/a \tag{9}$$

from which

$$y_0=a(I_0-I_P)/2I_0 \tag{10}$$

Substitution of this expression for y_0 in (8) yields

$$I_P=I_0[1-2C/(\mu-\mu_0)]=I_0\left[1-2C/\left\{\frac{a(V_P-V_F\pm h\lambda)}{2\lambda S}-\mu_0\right\}\right] \tag{11}$$

As was stated in the beginning, the constant h is a geometrical constant arising from the effect of the images on the constant field due to the potential difference between the plate and the filament. Taking into account the inductive effect of the charged grid wires, it follows from the definition of an electrical image that these wires, together with their series of images will impose no difference of potential between the plates, since the image of a charge in a plane is equal and opposite in sign to the charge, and at an equal distance from the plane. Hence the wires and their images each induce a potential difference which is equal but of opposite sign, and which is proportional to the charge. Let this potential difference be $h\lambda$. Then a potential difference of $-h\lambda$ is produced by the images alone; and, since they are so far away that this drop is very nearly uniform, it may be added algebraically to the uniform field (V_P-V_F) already existing between the plate and filament, giving $(V-V_F\pm h\lambda)$ for the corrected value of this potential difference.

In order to determine h it will be necessary to sum up the effect of the separate wires. If p and q are the distances from the grid to filament and

from grid to plate, respectively, the potential difference produced by the nth wire will be (see Fig. 1)

$$2\lambda \log [q^2+n^2a^2]^{1/2}-2\lambda \log (p^2+n^2a^2)^{1/2}=2\lambda \log [(q^2+n^2a^2)^{1/2}/(p^2+n^2a^2)^{1/2}]$$

and summing up for all the wires gives for the total

$$2\lambda \log (q/p)[(q^2+a^2)/(p^2+a^2)][(q^2+4a^2)/(p^2+4a^2)][(q^2+9a^2)/(p^2+9a^2)] \quad (12)$$

This is also equal to $h\lambda$. Therefore,

$$h=2 \log (q/p)[(q^2+a^2)/(p^2+a^2)][(q^2+4a^2)/(p^2+4a^2)][q^2+9a^2)/(p^2+9a^2)] \quad (13)$$

(When $p=q$, $h=0$, and the correction $h\lambda$ is zero.)

The quantity λ may be expressed in terms of the potentials and dimensions of the apparatus as follows: the total potential drop (V_G-V_F) is composed of $p(V_P-V_F \pm h\lambda)/S$ due to the field between the filament and plate, and the drop contributed directly by the charge on the wires. The latter drop is proportional to the charge, or equal to $k\lambda$, where k is a constant of the tube dimensions, similar to h, and expressible in terms of a, p, q, and the radius of the grid wire r. By another summation of the effects of the separate grid wires, similar to that used in getting h, there results, for the total contribution of the grid to (V_G-V_F)

$$k\lambda=2\lambda \log (p/r)[(p^2+a^2)/a^2][(p^2+4a^2)/4a^2][(p^2+9a^2)/9a^2] \cdots \quad (14)$$

(neglecting r in comparison with a in the denominators), from which k is obtained by dividing both members by λ.

Then the required relation between λ and the potentials and dimension constants becomes, solved for λ,

$$\lambda=\frac{(V_G-V_F)-p(V_P-V_F)/S}{\pm k \pm ph/S} \quad (15)$$

with h and k defined by Eqs. (13) and (14). In the numerical calculation of these constants the effect of outlying wires may be neglected, since the terms representing their contribution approach unity and the logarithms approach zero.

Substitution for the negative value of λ in Eq. (11), with V_F set equal to zero for simplicity in writing, and $p=a$ gives, after reduction,

$$I_P/I_0=1-2C/[a(kV_P+hV_G)/2(aV_P-SV_G)-\mu_0] \quad (16)$$

Since $x=a$ was chosen as the starting point of all the orbits used in the derivation of the above equation it cannot be assumed to hold for grid-filament distances differing sensibly from this value. A complete solution would require the calculation and analysis of independent sets of orbits for each of a large number of positions of the filament, but the computation is such a slow process that only the one set has so far been worked out.

In order for the Eqs. (11) and (16) to have any meaning it is evident that the range of values for each of the factors must be restricted by the

condition that the denominator $\mu-\mu_0$ of the fraction shall be positive and equal to or greater than $2C(\doteq 0.0168)$. This may be interpreted physically as meaning that a certain minimum gradient is required to overcome the repulsion of the negatively charged grid before any electrons can leave the filament. As a consequence of the assumption of static conditions with no space charge in the derivation of Eq. (15), V_P cancels out in μ when $V_G=0$, and we arrive at a result entirely inconsistent with all observation and experiment under conditions existing in ordinary tubes, viz., that the current is independent of the plate voltage for zero grid voltage. For the same reason V_G cancels when V_P is set equal to zero. But aside from the special values excluded by the physical limitations and by the assumptions made, the effects of individual factors on I_P appear to be in general what we should expect from elementary considerations. The current I_P is increased by an increase in V_P, V_G, and a and is decreased by an increase in S and r. h and

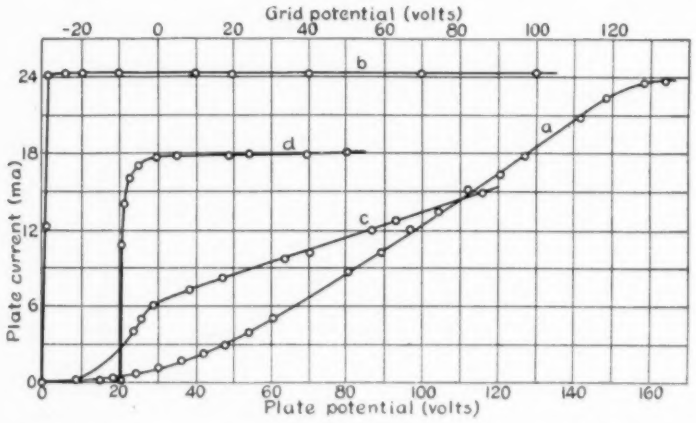

Fig. 4. (a) and (c), experimental characteristics for a W. E. 101-D amplifying tube; (b) and (c) theoretical characteristics obtained by substituting dimensions of the tube in Eq. (11). (a) and (b) represent the variation of plate potential with current; (c) and (d) the variation of grid potential with current.

k are functions of the construction parameters. Quantitative relations were deduced for the two most important factors V_P and V_G. Their characteristics were computed by substituting in Eqs. (13), (14), and (16) the measured constants of a common parallel plate type of amplifying tube, with grid-filament distance about $.6a$, and compared with experimental characteristics taken for the same tube. These curves are shown in Fig. 4. The precipitous rise to maximum current in the theoretical curves as contrasted with the gradual rise in the experimental curves may be attributed to the neglect of the effects of space charge, potential drop along the filament, and the magnetic field about the filament—factors which all operate against attainment of saturation in the vacuum tube. This conclusion is borne out by some experiments of Schottky[9] and Schlichter[10] in which it was found that the

[9] W. Schottky, Ann. d. Physik **44**, 1011 (1914).
[10] W. Schlickter, Ann. d. Physik **47**, 573 (1915).

elimination of these retarding factors permitted the attainment of saturation at very low plate potentials. Neither this equation nor a general equation valid for all grid-filament distances should be expected to conform to the 3/2 power law or to results derived experimentally under ordinary conditions, because it merely represents the isolated effect of one of the several current controlling factors. It should rather be regarded as a correction to be applied together with other effects which may be independently determined, to the experimental characteristic, in order to discover the effect of other factors which have not been isolated and measured.

Case (b). Positively charged grid. In order to study this case a value of μ (i.e., $\mu=1$) was chosen which was found by trial to cause the electron situated at $y_0=a/2$ to turn back at about $S=3a$, since this is approximately the distance beween filament and plate in some tubes. It was found that the same value of μ allowed the electrons to turn at the same distance, within the limits of accuracy warranted by the calculations, regardless of the starting position on the filament (Fig. 3). This means that the current may be made to change from zero to a maximum by placing the plate at a distance of about $2a$ from the grid and by changing V_P very slightly, at the same time making a compensating change in some other factor so as to leave $\mu=1$. It does not necessarily mean that the same thing will be true for other values of μ and, consequently, smaller and greater values of S. To test this point further, especially for positions of the plate nearer the grid where variations seemed most likely to occur, the plate was next assumed to be located at $S=2a$. This would be the turning point with $\mu=0$ of the orbit of the electron situated at $y_0=a/2$. The orbit ($\mu=0$, $y_0=0.05a$) was then computed to its turning point, which occurred at approximately $0.7a$ (see Fig. 3). Again, making allowance for possible error due to following this electron through the rapidly changing field in the region of the wire, it apparently comes very close to the plate. Another orbit was computed with $\mu=0.5$ and $y_0=0.05a$, and found to have a turning point at about $1.5a$. Interpolating between these two turning points to find an approximate critical value of μ needed to cause this electron to turn at the plate ($S=2a$) gave $\mu=0.2$. We have then for the filament and plate each located at a distance from the grid equal to the distance between its wires a variation from zero to about ninety percent in the current, produced by a change from zero to .2 in the value of μ. For such grid potentials as are used in all practical work this change in μ corresponds to a small change in voltage, roughly one quarter of the corresponding change when λ was negative. Two or three other orbits were partially computed for a positive λ, but the difficulty of working with such small differences in μ was so great that no quantitative relation has been derived for this case. However, the results so far obtained indicate a slight inverse relation, probably similar in form to that derived for the negatively charged grid. As in the case of the negatively charged grid, the current is extremely sensitive (at least for grid-filament and grid-plate distances comparable to the grid spacing) to small changes in either plate or grid potential, provided the other is small. This

critical relation, in both cases, should give a very high degree of amplification were it possible to eliminate the other current controlling factors involved. But because of the small magnitude of this effect, it would be very difficult in experimental work to minimize the other factors, especially the space charge, to the point where their effects will not obscure this one, unless the filament is placed quite near the grid.

The incompleteness of most of the orbits leaves the final destination of the deflected electrons undetermined. It is barely possible that some may eventually reach the plate after they have once turned back toward the filament. In the case of the positively charged grid one of the orbits ($\mu=1$, $y_0=a/2$) was continued and found to have successive turning points, indicating that the electron continued to oscillate across the grid plane with gradually decreasing amplitude, until it probably came to rest on the grid. This shows that a further study of the orbits might in itself yield some interesting results, but inasmuch as the chief aim in this problem was to derive a relation between the current and the plate potential, no attempt was made in most cases to trace the electron beyond the point where it could be assumed with a reasonable degree of certainty that it could not reach the plate. For similar reasons, the effect of the construction constants on the current has not been treated except in a general qualitative way, and very little attempt has been made to connect the results up with experiment. In fact the ideal conditions here assumed are so different from those actually existing in the practical operation of amplifiers that a detailed comparison could not have much meaning. However, the relations between the current and the various parameters, as expressed by the equation, appear to be in general agreement with experiment, after making proper allowances for the restrictions imposed by the ideal assumptions made. Unfortunately, it is not a general equation applicable to all positions of the electrodes and to both signs of grid charge, and it is based on too many approximations and too few orbits to warrant its being used for making accurate quantitative deductions. It may be impossible to solve the problem completely by any reasonable expenditure of time and labor. The work may be pursued further, however, for the purpose of learning more concerning the nature of the complete orbits, deriving a more general expression for the current, based on a larger number of orbits, and applying the method under less restricted conditions and to certain types of commercial tubes.

In conclusion, the author wishes to express appreciation for the valuable suggestions and criticisms of Professor W. F. G. Swann, of Yale University, who suggested the problem and under whose supervision the work was carried out; and to thank the Department of Physics of the University of California for the use of apparatus and the facilities necessary for the completion of the problem.

May 15, 1927.

THE PHOTOELECTRIC CONDUCTIVITY OF SULPHUR

By Bernhard Kurrelmeyer*

Abstract

Variation with electric field of the photoconductivity of sulphur.—The primary current is proportional to the electric field from 20 to beyond 15,000 volts per cm. If there is a saturation voltage it is probably higher than 50,000 volts per cm. Light produces charges with and without the aid of the field. No evidences of secondary current were found.

Variation with intensity of illumination.—Current is proportional to intensity of illumination over the range investigated, about 100 to 1, and for all kinds of light.

Variation with time of illumination.—The variation of current with time is investigated in detail, and is explained quantitatively in terms of the charges remaining in the crystal. The positive part of the primary current flows without the help of infrared illumination, under the influence of the original illumination. Without illumination charges disappear very slowly.

Variation with wave-length.—The photocurrent referred to unit incident energy is measured from 420 to 650 mμ; its maximum lies at 470 mμ. The **optical absorption** is measured over the same range; it is large below 500mμ, and complete in the violet. In the region between 500 and 650 mμ it has some unusual features. From the measured absorption values the photocurrents referred to unit absorbed energy are calculated. Formally at least, the quantum-equivalent law is not obeyed. A possible explanation is offered in terms of the peculiarities of the absorption curve. The absolute current yield based on a rough estimate is only about 0.005 times the theoretical value. This together with the absence of a saturation current differentiates sulphur from the other crystals of its class; in fact its behavior resembles that of crystals of the rock-salt type in many respects; but the resemblance is probably only formal.

Variation with crystal orientation.—Currents in different directions in the crystal are equal in absolute magnitude, but exhibit a curious unipolarity along one direction, that of the acute bisector of the optic axes, with components along other directions. The reverse currents exhibit parallel differences. The results suggest that sulphur has a polar axis due to atomic asymmetries, and should show the piezo- and pyro-electric effects.

Introduction

SELENIUM is the most familiar example of a substance whose resistance decreases under the influence of light. The mechanism of this photoconductivity, in the case of selenium and many other substances, is very complicated because the resistance of these substances is comparatively low even in the absence of light. Little information concerning the mechanism of the effect was obtained until Gudden and Pohl, beginning in 1920, investigated crystals which were very good insulators in the dark. They soon found that photoconductivity in these crystals is due primarily to the liberation of electrons inside the crystal by absorbed light; secondary effects are caused by the positive charges, which are in general left behind in the crystal. They distinguished two kinds of crystals possessing photoconductivity, those in which the primary ionization takes place in the pure crystal material, and those in which the ionization is located in impurities or ir-

regularities in the crystal structure. Examples of the second class are all the naturally and artificially colored quartzes and alkali halides; while to the first class belong selenium, cinnabar, zincblende, diamond, sulphur, and numerous others.

It was noticed by Gudden and Pohl that all crystals of the first class possessed a refractive index greater than two, and conversely, that all crystals with $n>2$ which they investigated had photoconductivity. Since the value 2 has no known theoretical significance, it became of interest to investigate sulphur, which has three indices, of which $n_\alpha>2$, while n_β and $n_\gamma<2$, in order to see whether differences in the photoconductivity could be observed in specimens of different orientation.

The photoconductivity of sulphur has long been known[1,2,3]; but observations have hitherto been made on polycrystalline material, and have been purely qualitative. Several difficulties are involved in a quantitative investigation of single sulphur crystals. The currents are small, and the mechanical properties of the material are unfavorable. Rhombic sulphur has a hardness of only about 2; it is very brittle, and extremely sensitive to temperature changes; for example, it may crack when held in the fingers, or when laid, for polishing purposes, on a moist cloth cooled by evaporating water or alcohol. Furthermore, there are no good cleavage planes. On the other hand, sulphur offers certain advantages: large crystals are available, though not plentiful; the specific resistance in the dark is very high ($\rho_{20}>10^{18}$), and surface leakage is low. The smallness of the primary currents means that space charge complications are largely avoided; and hence the current-time relations can be studied in detail.

II. Methods and Apparatus

The technique of the measurements was that developed by Gudden and Pohl. Currents were measured by observing the charging rate of a string electrometer. The electrodes were generally small cells filled with tap water and applied to the crystal with soft wax. The back face of these cells was of very thin glass. The insulation to ground was of amber or cast sulphur throughout, so that the leakage to ground was negligible. The light entered the crystal either parallel to the electric field, i.e., through the electrodes, or transversely. Monochromatic light was furnished by a two-prism constant-deviation monochromator. For some measurements the full radiation of an ordinary tungsten lamp or that of the mercury arc was used.

Between measurements, both electrodes were grounded and illuminated long enough to destroy the space charges left in the crystal during the measurement. In most cases the further precaution of keeping the crystal in the dark for several minutes before each measurement was adopted, cf. Section 1 of Results.

* National Research Fellow.

[1] Monckman, Proc. Roy. Soc. **A46,** 143 (1889).

[2] A. Goldman & S. Kalandyk, Ann. d. Physik [4] **36,** 589 (1911).

[3] F. Kaempf, Phys. Zeits. **23,** 420 (1922).

III. Results

The following relations were investigated: the variations of the photocurrent (1) with the applied electric field; (2) with the intensity of illumination; (3) with the time of illumination; (4) with wave-length, (a) referred to incident energy, (b) referred to absorbed energy (the latter involving measurement of the optical absorption); and (5) with the orientation of the crystal specimen. The results of these measurements will be taken up in order.

1. *Variation with electric field.* The current produced in sulphur by a given illumination, all other conditions being constant, is directly proportional to

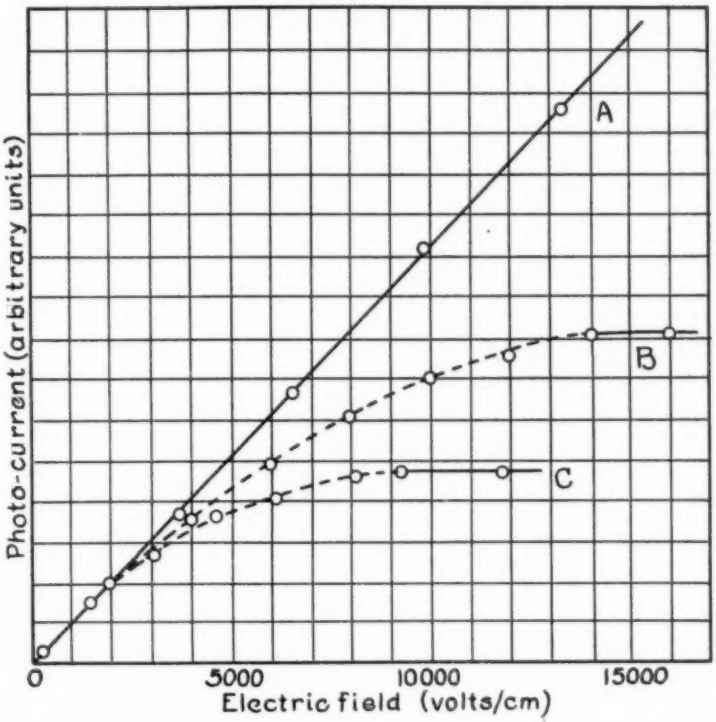

Fig. 1. Variation of photocurrent with electric field.

the applied field throughout the range investigated, or from 20 to 15,000 volts per cm. This is true for all light intensities. In Fig. 1 the current-voltage curves for diamond (*B*) and zincblende (*C*), taken from the papers of Gudden and Pohl,[4] are replotted to coincide in their initial portion with the sulphur curve (*A*). It will be seen that curves *B* and *C* depart from linearity at electric fields far below those required for saturation. Since no departures from linearity were found in sulphur, it is probable that the saturation value of the field strength, if there is one, is above 50,000 volts per cm. This is also found to be the case in the crystals of the rock salt group.

[4] Gudden and Pohl, Zeits. f. Physik **17**, 331 (1923).

No evidences of secondary current[5] were ever found in sulphur, though a systematic search was made at high fields and light intensities.

It has long been doubtful whether the number of charges produced by light increases with the applied voltage, or whether the speed of migration alone increases. The question was answered, at least in part, by the observation[6] that illumination under zero field produces, in the case of rock salt, an excitation ("Erregung") in the crystal, which may last for hours in the dark and at room temperatures, but appears as a current when the crystal is subsequently heated or illuminated with strong infrared light. The original illumination produced charges without the help of the field, which were not free to move at room temperature. It was found that the amount of the excitation is the same whether it is produced with or without the field; furthermore, the excitation has a limiting value independent of the light intensity.

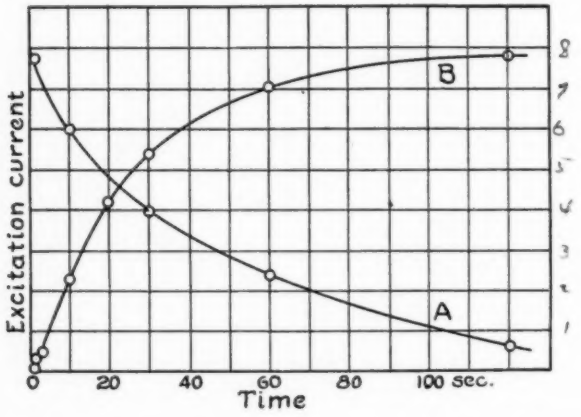

Fig. 2. Variation of excitation with time. (A) decay, (B) growth.

The same effect was found in sulphur, with the difference that here the charges are absolutely free to move. Thus a current flows in the dark as soon as a field is applied. This current will be called the excitation current. Fig. 2, *A* and *B*, records two series of excitation current measurements. In 2*A* the crystal is illuminated a very long time before each observation, with both electrodes grounded. Next follows a varying interval of darkness, after which the field is applied and the current flowing (still in the dark) is measured. This series shows the rate of decay of the excitation. In exactly similar manner the rate of growth of the excitation is recorded in 2*B*. The decay curve is approximately exponential; the growth curve is linear at first, and then approaches the maximum value asymptotically. The maximum value evidently represents equilibrium between the rate of formation and the rate of recombination. From the similarity of the growth and decay curves it follows that the rate of recombination is uninfluenced by the illumination, in spite of the fact that this was intense white light from a

[5] Gudden and Pohl, reference 4, p. 333, and references given there.

[6] B. Gudden & R. Pohl, Zeits. f. Phys. **31**, 651 (1925).

100-watt tungsten lamp. Cutting off the wave-lengths above 500 mμ with a blue filter did not change the results.

Using the rate of formation given by the tangent to the formation curve at the origin, it was found that in sulphur also the charges are produced without the field at the same rate as in the field. The calculation involves the assumption that there has been no recombination in the primary current; but there are several justifications for this. The shape of the current-voltage curve for any crystal is independent of the light intensity even when there is a saturation current.[7] The recombination which takes place without the field doubtless takes place only between the original pairs of ions, for the average ion density in the excitation was only one pair in 10^{15} neutral atoms; such recombination is scarcely possible when the ions of each pair are being separated by the field as soon as they are formed.

The "ions" which constitute the excitation may, however, be nothing but atoms in a metastable excited state, from which they may return to the normal state after a thermal impact in zero field, or may be ionized by a thermal impact in the field. Hence the number of pairs of ions formed and measured may still be influenced by the field. In order to decide the question, the dependence of the excitation on the field used to measure it must be ascertained. This has not yet been done.

Field-free excitation has also been observed in diamond and zincblende[6]; but here it is said to be much smaller than the charges produced in the field.

2. *Variation with intensity of illumination.* In other crystals, strict proportionality between intensity of illumination and photocurrent has always been observed, provided that sufficient precaution was taken to avoid the effects of space charge. In sulphur, measurements over several different ranges of 10 to 1 confirmed the proportionality relation. The shapes of the current-voltage and current-wave-length curves are independent of the light intensities used. These observations are, in fact, the test for absence of secondary current.

3. *Variation with time of illumination.* When the crystal is brought to its normal state, the field applied, and the crystal illuminated, the current reaches its full value in less than the period of the electrometer string (1/10 to 1/100 sec.). This interval has actually been shown to be less than 10^{-4} sec. in the diamond and in other crystals,[8] and it is probably of the same order in sulphur. When the illumination ends, the current falls almost to zero immediately; a small current continues to flow, which is due to the motion of positive ions.

The initial value, as well as the subsequent shape, of the current-time curve depends on the previous history of the crystal. The various possibilities are shown in Table I. Each horizontal line represents one way of making the current measurement; the operations are performed in order from left to right; and the initial value of the current measured is given in the fifth column. The current is measured in the stage whose length is given as *t*.

[7] B. Gudden, Ergebnisse der exakten Naturwissenschaften Vol. III, p. 151.

[8] W. Flechsig, Zeits. f. Physik **33**, 372 (1925).

The field and the light intensity were kept constant throughout these measurements.

I_0 is simply the leakage current over the crystal surfaces. I_1 is the excitation current, which has already been studied in detail. I_2 is the true

TABLE I

Various methods of making current measurements and the initial values of the currents in each case.

No field		Field on			
Time of Illumination	Time dark	Time dark	Time of Illumination	Value of current	Designation of current
∞	∞	t		$0.3\times4\times10^{-14}$	I_0
∞	0	t		8	I_1
∞	∞	0	t	20	I_2
∞	0	0	t	28	I_3
∞	0	∞	t	16	I_4
∞	∞	∞	t	20	I_5

photocurrent, taken by giving the crystal a long period of darkness just before the current measurement. I_3, in which this precaution was omitted, is the sum of I_1 and I_2. I_4 resembles I_3, except that the voltage was applied for a time while the crystal was still in the dark, so that the free charges are swept out; but in doing so a polarization is produced, so that the effective

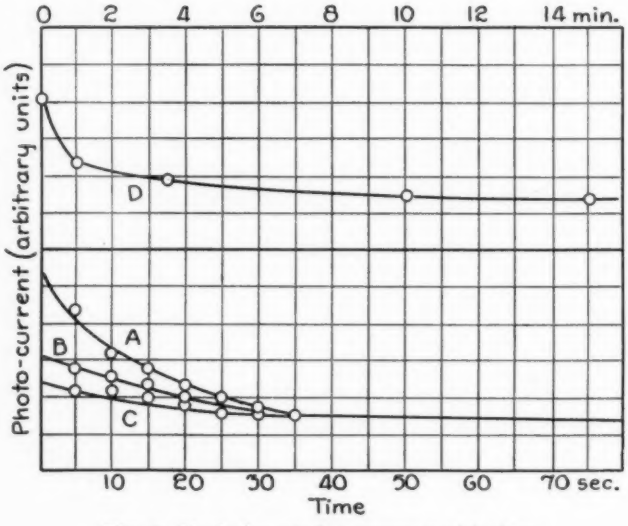

Fig. 3. Variation of photocurrent with time.

field is reduced; hence the initial value of the current is less than the true value. I_5 resembles I_4, except that now there are no more ions left to sweep out; so that the true current is observed. It is evident from these curves that in order to get comparable results a carefully defined procedure of measurements must be adopted.

The differences between these various currents are due in one way or another to the excitation current. It should be said that the value obtained for the excitation current directly agrees well with that obtained by sub-

tracting I_2 from I_3. As the excitation current decreases with time these differences grow less and less and finally disappear. The complete time-current curves are shown in Fig. 3, *A*, *B*, *C*, *D*, of which *B* and *D* show the true photocurrent.

As soon as the current flows, some of the positive ions begin to accumulate in the crystal, and these gradually reduce the effective field, so that the current decreases with time during the illumination. Fig. 3A, which represents the sum of the true photocurrent and the excitation current, has an abnormally steep initial drop due to the rapid decay of the excitation current; whereas Fig. 3C, which represents the true current already reduced by a certain amount of space charge, has a very flat initial portion—it has had a slight lead over the true current.

The question arises whether charges pass through the surface of the crystal. In general the answer is, they do. Continuous photocurrents can be made to pass for indefinite periods of time, and the total charge flowing through the crystal would, if retained within the crystal boundaries, produce an opposing electric field many times higher than the applied field. Gudden and Pohl,[9] have shown, however, that up to a certain limit charges remain inside a crystal, by measuring the charges flowing in the reverse current. This is the current due to the recombination of the charges, after the external field is removed and the crystal short-circuited. The charges flowing in the reverse current were found equal to those which had flowed in the direct current, up to a critical value of the charge which, if considered concentrated at the electrodes, would produce there a surface charge density of about 2×10^{-8} coulombs per sq. cm.

This result was obtained on a zincblende crystal. In sulphur the charge flowing in the reverse current was always considerably less than the charge which had previously flowed in the direct current. The smallest total charge which was observed in a reverse current, 8.5×10^{-12} coul., was only 30 percent of the charge in the corresponding direct current, so that if there is a critical density below which no charges leave the crystal, it is less than 4×10^{-12} coulombs per sq. cm, or over 4000 times smaller than in zincblende. Considering the high specific resistance and the other properties of sulphur, this is rather surprising. While the assumption made in this calculation concerning the distribution of charges is rather questionable, it is certain that the quantities measured are independent of the actual distribution of the charges in the crystal, and give the true value for the fraction of charge which has left the crystal, except for the small losses due to leakage. Nor does recombination affect the result; for, aside from the improbability of recombination, discussed above, the changes produced by its occurrence would be in exactly the same ratio in the direct and in the reverse currents.

Gudden and Pohl found, in the case of the diamond, that under illumination with short wave-lengths the positive-ion half of the primary current was not observed until after an illumination with longer wave-lengths. They were able to separate the positive and negative parts of the primary current

[9] B. Gudden and R. Pohl, Zeits. f. Physik **16**, 176 (1923).

entirely and show that they are equal, thus proving that the positive charges are stationary until set free by long wave-lengths or heat motion. Attempts to separate the two halves of the primary current in sulphur failed; a subsequent illumination with long wave-lengths gave no current. Qualitative attempts to change the ratio of reverse to direct current by the use of filters, infrared radiation from an arc, etc., also gave negative results. A quantitative test with monochromatic light was impossible because of the smallness of the reverse currents. However, the full light of the mercury arc, passing through a water cell, produced exactly the same ratio of direct and reverse currents as the full light of the tungsten lamp. Since the migration of positive ions in the field alone is very slow, the conclusion is that the rate of migration* is increased by the same wave-lengths which produce the primary current. Similar behavior is observed in zincblende.

As time goes on, the current decreases more and more slowly (Fig. 3D), and finally becomes constant at about one-third of its initial value. If the light intensity was changed, the initial and steady values of the current were changed in the same proportion, as was also the initial value of the reverse current. These relations are immediately explained by the relation between the value of the direct current and the ratio of the total charges flowing in the direct and reverse currents. Table II gives the data. At the beginning,

TABLE II

Time of flow of direct current (sec)	Mean value of direct current (amp)	Charge flowing in direct current, Q_d (coulombs)	Charge flowing in reverse current, Q_r (coulombs)	Ratio Q_r/Q_d	Initial value of reverse current (amp)
20	1.04×10^{-12}	22×10^{-12}	6.5×10^{-12}	0.30	$.80\times10^{-12}$
40	.96	40	12	.30	.92
80	.86	73	22	.30	1.08
180	.76	142	38	.27	1.32
710	.54	418	77	.19	1.52
26 min.	.44 (constant value)	770	95	.12	1.52

for about three minutes, the fraction of the charges which remains in the crystal is constant. During this time the direct current is decreasing, and the initial value of the reverse current is increasing. Thereafter the fraction of charge accumulating decreases more and more; the space charge builds up to its limit, and the direct and reverse currents reach a constant value. The action of the space charge is to reduce the effective field causing the direct current, and to build up a proportionate field for the reverse current.

If the light intensity is changed, the initial and final values of the currents are changed in proportion, because the initial and final potential distributions in the crystal are the same as before; and for the same reason the initial value of the reverse current changes in proportion, the total charge remaining the same.

* Migration is probably not an actual motion of the positively charged atom, but the process of handing an electron along from atom to atom in the opposite direction.

The initial value of the reverse current may, in fact, be higher than the initial value of the direct current. Since both are produced by the same illumination, the effective field of the residual charges must be higher than the applied external field. This seeming paradox is explained when we consider that while the external field is applied, the crystal, with its two electrodes, and two layers of charges inside, cannot be considered as a single condenser having the dimensions of the electrodes, but is equivalent to two condensers in series, each having much smaller plate separations. The capacity of this system is larger than that of the electrodes, since the distance between each electrode and its corresponding space charge layer inside the crystal is always less than one-half the electrode separation. On grounding both electrodes, however, the capacity is reduced to that of the single condenser, and the effective difference of potential rises accordingly.

A word should be said about the shape of the reverse current-time curves (not shown). The reverse current, of course, decreases with time. The curve corresponding to the lowest value (Table II) is accurately exponential; the other curves are increasingly bad approximations to exponentials, the decay being slower, especially after the first few seconds. This is reflected in the fact that the total charge flowing in the reverse current increases much more rapidly than the initial value (Table II, columns 4 and 6); and it means that as the total quantity of space charge left in the crystal increases, its geometrical distribution changes.

The experiments described in this section were performed for the most part on a very perfect crystal, having a volume of about 8 ccm and no less than eight pairs of parallel natural faces, among them four pairs of (111), two pairs of (011), and two pairs of (113) faces. Most of these were too small to work on. The measurements were made on a pair of (111) faces of area about one sq. cm, 27 mm apart. All the relations discussed have been found to hold for every other crystal examined. The electric field strength was for the most part about 100 volts per cm. Nothing is gained in using higher fields, because the leakage current increases in the same ratio as the photocurrent. The illumination was the full light of a tungsten 100-watt lamp (run on a battery at a considerable overload) at one meter.

4. *Variation with wave-length.* For these measurements, since the energy of the light was very low, high fields had to be used. The crystals, about $1\times4\times6$ mm, were cemented into an amber plate,[10] and water-cell electrodes were attached to the amber with soft wax. If this is done properly, the surface leakage over the crystal faces is eliminated, and the volume leakage through the cement substituted for it. The only cement found suitable for mounting the crystal was a mixture of thick canada balsam solution and pure paraffine, which melted at about 30°C. No other cement was found having a melting point sufficiently low to prevent cracking the crystal, and an electrical resistance sufficiently high to keep the dark current below 10^{-13} amperes and fairly constant. Even using this cement, only about one attempt in ten was successful.

[10] Gudden and Pohl, Reference 4.

Monochromatic light was obtained from the usual monochromator, in which only the central slit is moved to vary the wave-length. The spectral width of the light varied from 5 mμ at 430 mμ to 30 mμ at 700 mμ for the absorption measurements, and from 15 to 80 mμ between narrower limits for the current measurements. In each case the relative energies were measured with a thermopile and galvanometer. The spectral sensitivity curves of the photocells used in the absorption measurements were not steep enough to introduce an appreciable error into the absorptions with the slit-widths used. The large slit-widths used in the current measurements were necessary to secure measurable currents at the ends of the range; even so the maximum currents observed at 10,000 volts per cm were only of the order of 5×10^{-12} amperes.

Fig. 4 shows the variation of current with wave-length, referred to unit incident energy. The curve has a maximum at 470 mμ, and drops more

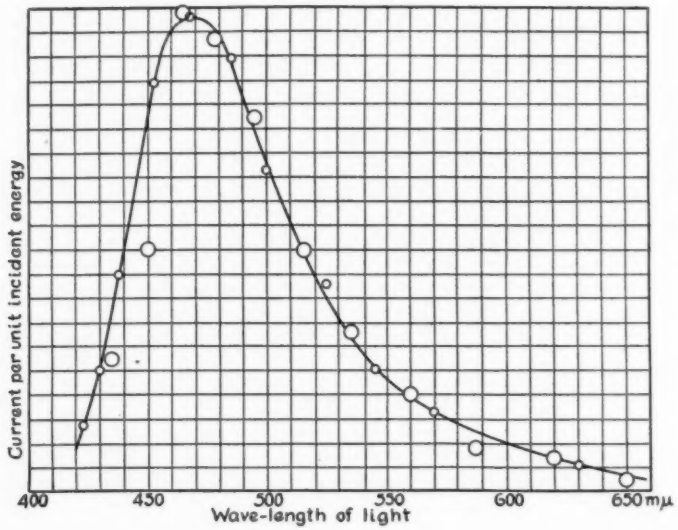

Fig. 4. Photocurrents at different wave-lengths, referred to incident energy.

slowly toward the red than toward the violet. The maximum is blunter than the corresponding curve for the diamond, even when the spectral slit-width is taken into account. The curve is based on measurements on two crystals, the set represented by the large circles being somewhat less accurate. Within the limits of error the curves for the two crystals coincide. The measurements were made at 8,000 and at 12,000 volts per cm.

The optical absorption was determined by measuring the ratio of incident to transmitted energies for a crystal of known thickness. Several different potassium hydride photoelectric cells were used to measure the energies, one in particular which was sufficiently sensitive out to 700 mμ. The string electrometer again served to measure the currents.

Since it was found impossible to obtain perfect optical polish on the faces of the crystal, the corrections for reflection and scattering had to be deter-

mined in a lump sum, empirically. This was done by finding the transmission in a region where it was constant, i.e., the absorption presumably zero (in the extreme red at 700 mμ), and placing this equal to 100. The absorption coefficient for the other wave-lengths was then determined from the fractions transmitted at those wave-lengths. This procedure assumes that the fraction scattered and reflected is the same for all wave-lengths, which is true within the limit of the other errors involved.

It was found impossible to determine exactly the absorption of the same crystals upon which the electrical measurements were made, since the absorption coefficient is low in the region of greatest interest, and the thickness of those crystals was only about 1 mm. Measurements were made upon several crystals of thickness 9 to 12 mm, kindly furnished by Professor Bridgman, and the mean of three sets is given in Fig. 5*A*. The three large circles represent the average of many earlier measurements made on three 1 mm crystals; the agreement is very good.

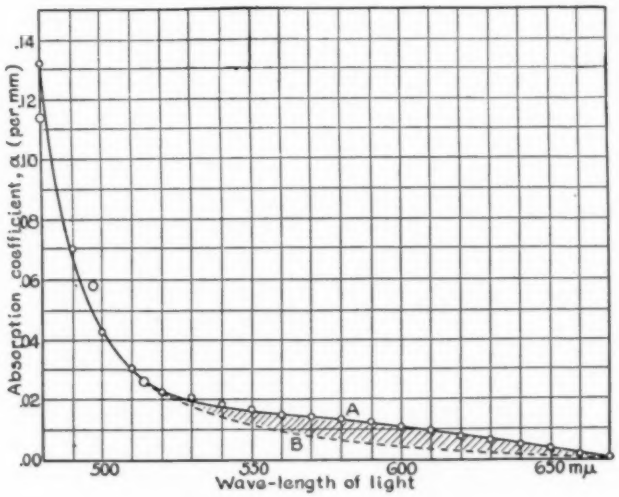

Fig. 5. Optical absorption.

Some of the smaller crystals were grown from CS_2 solution; the larger ones were all natural crystals from Sicily. The errors of the method of determining the scattering correction are rather large; and another cause of error is that sulphur is strongy doubly refracting. Nevertheless, the values of the absorption coefficient given in Fig. 5*A* are probably correct to 10 percent or better, while the ratio of the absorptions at any two not too distant wave-lengths is probably correct to 5 percent or better.

It will be noticed that in the yellow and red region the curve does not resemble the ordinary asymptotic absorption curve, but has a point of inflection near 570 mμ, and becomes concave downward until 650 mμ, where it becomes asymptotic. The curve looks as if a small flat maximum were superposed on the usual smooth absorption curve; and the individual sets of observations show this characteristic just as clearly.

Using the data of Figs. 4 and 5*A*, the photocurrents referred to unit absorbed energy were calculated, and are shown in Fig. 6*A*, while Fig. 6*B* shows the distribution which would be expected on the assumption that each absorbed quantum liberates a definite charge. The slope of the line 6*B* is so chosen that it passes through the maximum of the curve, and, of course, through the origin.

Experimentally it seems certain that the deviations from the quantum equivalent law are genuine. The values for the absorption and for the current referred to unit incident energy are each good to within 10 percent at least, while the deviations to be explained are as large as 100 percent and more. The wave-length scales are good to 1 mμ, and even if one of them

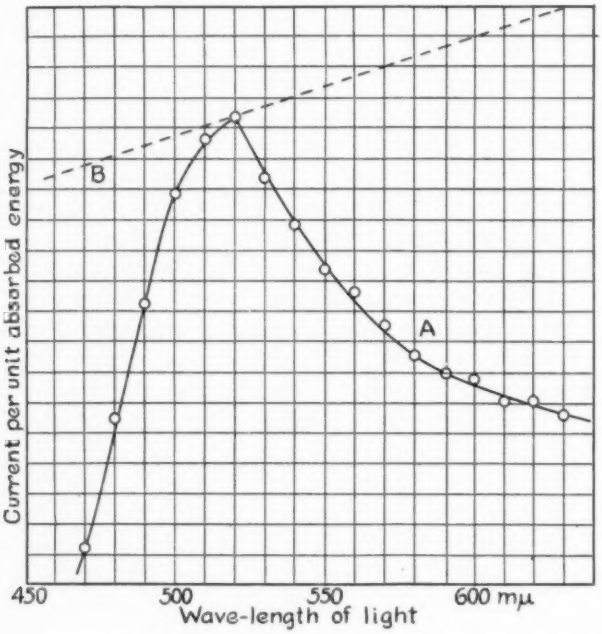

Fig. 6. Photocurrent at different wave-lengths, referred to absorbed energy.

were out by as much as 20 mμ in either direction, the shape of Fig. 6*A* would not be altered materially. It is true that the electrical measurements and the absorption measurements were not made on the same crystal. Still the various crystals examined gave identical results in all cases, so that individual peculiarities are probably not the cause of the deviations.

The curve obtained may still be interpreted in two different ways. One is that the quantum equivalent law actually does not hold for sulphur, so that the yield is truly selective. This does not seem very probable, in the first place because of the similarity in behavior in all other respects between sulphur and the crystals for which the quantum equivalent law is known to hold; and in the second place because the curve obtained does not look like a genuine selective maximum, but more like a composite effect.

The alternate interpretation involves two considerations. The abnormal decrease in yield on the violet side of the maximum is found in the other crystals of the same class also.[4] The drop begins in all cases near the sharp upward bend of the absorption curve. There is as yet no satisfactory theoretical explanation of this drop; but it has been suggested that as the absorption processes increase in density in the crystal, they begin to interfere with each other in some way. On this simple theory, however, it is hard to understand the independence of the shape of the current curves and the light intensities (Section 2). The decrease in the yellow and red which remains to be accounted for is not found in any other crystal, and is entirely unexpected. It is possible that the explanation lies in the peculiar shape of the absorption curve, with its point of inflection at 570 mμ. Fig. 5*B* shows the values of the absorption constant which would be necessary to give the quantum equivalent yield, assuming the values at 520 mμ to hold. While these calculated values are far outside the limit of the experimental values, they lie on a smooth curve which forms the normal continuation of the steeper part of the absorption curve. This gives additional probability to the existence of an electrically inactive absorption, represented by the shaded region in Fig. 5. Such absorption has been observed in other cases, though not superposed on active absorption. In particular, Coblentz[11] has found that sulphur has considerable absorption in the near infrared, down to 1μ, which is doubtless inactive electrically.

Whether the above explanation is the true one or not, it is certain that formally at least the quantum equivalent law does not hold for sulphur. The absolute magnitude of the current yield was not determined accurately; but it is certainly smaller than in crystals where a saturation current is found. A rough estimate based on the spectral distribution curve of an incandescent lamp gives a yield of 0.002 to 0.01 electrons per absorbed quantum, at 15,000 volts per cm. A similar result has been found for rock salt. The explanation, in the case of rock salt, is that while each absorbed quantum produces a pair of ions, the charges move only a small fraction of the crystal thickness.[6] This is well confirmed by the measurements of Flechsig[8] on the time required for the reversal of the current when the applied field is reversed. To adopt this explanation for sulphur is impossible until confirmation by experiments similar to those of Flechsig is obtained; for difficulties are encountered in explaining the experimental facts that seventy percent of the charges flowing leave the crystal, that the positive-ion half of the current flows without the help of long-wave-length light, and that the charges produced in field-free excitation are free to move. Moreover, the differences between sulphur and the other crystals of its own class, namely, lack of saturation current and low current yield, can be understood when we remember the role of the refractive index. The value $n>2$ is the criterion of photoconductivity; and in sulphur n is so much nearer the limiting value than in either the diamond or zincblende, that the saturation field strength ought to be much higher in sulphur than in either of these

[11] W. W. Coblentz, Phys. Rev [1] **19**, 94 (1904).

crystals, for the rule is found to hold that the order of the saturation fields is the reverse of the order of the refractive indices.[12]

5. *Variation with crystal orientation.* The variation of current with orientation in the crystal was one of the principal points of interest when the research was undertaken. Sulphur is an orthorhombic crystal, with the axial ratios $a:b:c=0.813:1:1.900$, and the refractive indices (for the red K-line 768 mμ) $n_\alpha=1.93$, $n_\beta=2.00$, and $n_\gamma=2.19$. The plane of the optic axes is that of the a and c-axes, the a-axis being the acute bisector. Most of the crystals examined were very one-sidedly developed; but one, a natural crystal from Sicily, had two large natural faces perpendicular to the c-axis, and was about a centimeter thick. It had been used for the absorption measurements. It is shown in plan view in Fig. 7, in two-thirds natural size, the dotted lines

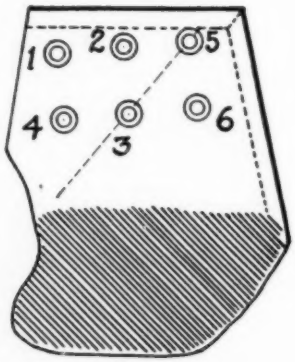

Fig. 7. Crystal used to measure variation of photocurrent with orientation.

indicating the size of the lower face, the heavy lines natural edges. The diagonal dotted line indicates the direction of the bisector of the optic axes. The illumination was the full light of a tungsten lamp, or that of the mercury arc, at various distances. The electrodes were small water-cells placed on the upper (horizontal) surface of the crystal with soft wax, and numbered as shown. The lines connecting the electrodes lay along previously determined directions in the crystal. With each pair of electrodes pairs of current readings were taken, the conditions being the same for each reading of any pair except that the direction of the current was reversed. The value of the reverse current was also observed with each pair of primary current readings. The results are shown in Table III, where the readings for parallel directions are grouped together. The various currents are all for the same light intensity, assuming the illumination to be homogeneous over the whole surface.

Comparing the values up and down the columns, i.e., between different pairs of electrodes, we see that the currents are of the same order of magnitude in all directions; beyond this the readings are not comparable; nor are the differences in any way systematic. This is to be expected, because the various electrodes were not strictly equidistant, having been spaced only by eye; and because some of them are situated over the overhanging edge

[12] B. Gudden, Reference 7, p. 147.

TABLE III

Electrodes 1st	2nd	Direct Current First Elect. neg.	Second Elect. neg.	Reverse Current First Elect. neg.	Second Elect. neg.	Angle with Plane of Opt. Axes	Difference in Direct Currents (percent)
1	3	1.54	1.54	0.11	0.10	90°	0
2	6	1.47	1.52	.01 (?)	.06	"	3
2	4	1.59	1.25	.23	.03	0°	25
5	3	1.30	1.07	.15	.02	"	19
1	2	1.36	1.47	.10	.12	45°	8
4	3	2.04	2.23	.08	.16	"	9
2	5	1.56	1.73	.06	.14	"	10
3	6	1.88	2.02	.05	.18	"	7
1	4	1.66	1.51	.21	.11	45°	9
2	3	2.01	1.86	.12	.05	"	8
5	6	1.75	1.68	.08	.06	"	5

of the crystal (the lower face being smaller), some electrode pairs draw charges from a larger volume of crystal than others. If these things are taken into account, the absolute values of the various currents are as closely equal as could be expected.

The two values in each horizontal row are much more comparable, for they were taken under identical conditions except for the reversal of the applied field. Here the differences become perfectly systematic. In directions perpendicular to the plane of the optic axes, i.e., parallel to the *b*-axis, the two currents are the same within experimental error. Along the *a*-axis, the bisector of the optic axes, the two readings of each set differ by 20 to 25 percent of their mean value. Along any intermediate direction, say at 45° to the *a*- and *b*-axes, an intermediate difference of 8 to 10 percent is observed. Furthermore, the differences in the intermediate directions always have the same sense that they would have as components of the vector representing the largest difference in direction and amount. Thus the current 2−4 is larger than the current 4−2 by 25 percent, and we find that the currents 2−1 and 2−3 are larger than 1−2 or 3−2 by 8 percent each; but 2−5 is smaller than 5−2, showing that the sense and amount of the difference are functions not of the particular electrodes, but of the crystal directions. The initial values of the reverse currents show a similar consistency, considering their greater inaccuracy, except that the percentage differences are much larger; in fact in one direction, that of the bisector, one of the reverse currents is practically zero. Just why the reverse current should be larger where the direct current is larger is not at all obvious, especially as the percentage differences are out of all proportion. The total charges flowing in the various reverse currents have not yet been investigated, but it is quite possible that they are more nearly proportional to the corresponding direct currents.

These effects are so novel that it is worth discussing the possibility of their being caused by unsuspected experimental errors. Local impurities and cracks in the crystal may be eliminated as causes, because the differences were found to be distributed in the same fashion all over the crystal. There

is no reason to suppose that such impurities existed, the crystal being clear and flawless except for a few small cracks in the lower face of the crystal, and except for the large portion shaded in Fig. 7, where no measurements were made. Invisible cracks, even if oriented along the optic axes or perpendicular to them, should produce currents of different magnitudes but without unipolarity; whereas the reverse is actually found. The order in which the measurements were taken was found not to influence the result; and besides the crystal was restored to its normal condition after each reading by a carefully defined procedure which included darkening the crystal to eliminate the excitation current. The differences were reproducible from day to day. The electrodes used were all of the same material (water), and of the same size. The fact that the electric field was inhomogeneous is harmless, because the inhomogeneity is the same for all the measurements.

The reality of the differences is further confirmed by the observation that each of the direct currents recorded in the table is directly proportional to the field between 20 and 200 volts per cm.

The currents along the c-axis show no differences when the voltage is reversed. It is, therefore, not the plane of the optic axes, but the direction of their bisector that is unique.

No explanation of these curious partial unipolarities is offered at this time. The results strongly suggest, however, that sulphur has a polar axis, if not crystallographically, then at least due to atomic asymmetries. If this is so, then sulphur might show the piezo- and pyroelectric effects. While searching for the latter effect, an interesting electrostatic demonstration of the photoconductivity was noticed. A small, thin rod-like fragment of sulphur and a similar rod of glass were suspended side by side, from single fibers of silk, in an electric field of several hundred volts per cm. When the field was applied, both rods set themselves along the lines of force. With a strong light in the room, if the direction of the field was reversed after ten seconds, the sulphur rod turned through 180° as if its ends were permanently charged, the glass rod remaining stationary, though its natural conductivity was higher. If the light in the room was weak, the sulphur would not turn through 180° until the field had been on at least fifty seconds. Evidently the light had caused charges to flow in the crystal; they could be destroyed by illumination after the field was removed.

IV. Summary

As the phenomena of photoconductivity are unfamiliar to a large number of readers, an attempt will be made, in summarizing, to state briefly the present conceptions of the nature of photoelectric conduction.

This type of conductivity is found only in certain crystals. A crystal has photoconductivity if it is a pure crystal of refractive index $n>2$, or, regardless of its refractive index, if it has dispersed throughout its volume certain types of impurities such as metallic colloids. The light produces in the crystal equal numbers of positive and negative charges; the seat of the ionization is, in the first case, the material of the crystal lattice, in the second, the particles of the impurities.

The crystal may or may not be a good insulator in the absence of light. In either case the primary mechanism of photoconductivity is the same; but if the crystal in question is already a poor insulator, secondary processes affect the currents, and the relation between the current and the other variables of the system becomes very complicated. The complications may be traced to a general loosening of the crystal structure due to the accumulation of charges inside the crystal.

If the crystal is a good insulator, certain simple relations may be expected. These have been comfirmed experimentally whenever precautions were taken to avoid the secondary phenomena due to the accumulation of charges. The photocurrents observed depend on three main factors, the light, the crystal, and the field. We shall consider these factors in order.

The current is strictly proportional to the intensity of the incident light. Different wave-lengths are active in different degree, only because they are absorbed differently by the crystal. Every quantum of light absorbed results in an ionization process. Where apparent exceptions to this rule are found, an explanation is always possible in terms of one of the other factors: thus in colored rock-salt, the charges produced move through only a small fraction of the crystal thickness, hence the number of charges observed appears too small. In sulphur both the actual current yield and the wave-length distribution of the yield depart from the rule; the one departure may be explained by the absence of a saturation voltage, the other by the existence of peculiarities in the absorption of the crystal. Both explanations, however, require further confirmation.

The charges produced by light are of two kinds, electrons, and positive ions. The former are free to move in the field through the whole thickness of the crystal. They are not materially impeded by the atoms of the space-lattice, but are caught or slowed down by all kinds of cracks, irregularities, or impurities. In fact, if these are sufficiently numerous the photocurrent may disappear altogether. Positive ions have a much lower mobility, which varies with the specific resistance of the crystal. Under the influence of light, however, the positive charges may also "move" with large velocities. In this case, the "motion" consists of a handing along of electrons toward the cathode. Such currents may occur simultaneously with the electron current under the influence of the original illumination, (sulphur, zinc-blende), or they may occur subsequently, under the influence of light of longer wave-lengths (diamond, rock-salt), or of thermal agitation even at room temperatures (cinnabar). The electronic part of the current flows within 10^{-4} sec. of the beginning of illumination, and ceases in a corresponding interval. The positive part of the current may flow almost as rapidly, or it may require any longer interval up to several hours, depending on the conditions.

When charges flow, they do not always leave the crystal. In order that they be observed as a current, it is sufficient that they move through a part or the whole of the potential difference applied to the crystal. Those that are left inside the crystal produce distortion of the homogeneous field, and cause a diminution of the current. When the external field is removed they

produce a field in the opposite direction, and a reverse current if there is illumination. The total charge flowing in the reverse current measures the charge left in the crystal during the flow of the primary current. The relations between the time of flow and the values of the primary and reverse currents may be followed quantitatively in terms of the total charge left behind.

The field enables the charges produced by the light to flow and be measured. The number of charges observed varies with the field; for low fields it is proportional to the voltage; but for high fields, in most cases, it becomes independent of the voltage. The current and field for which this condition is first reached are called the saturation current and field respectively. The saturation current is determined by the light intensity. The increase of current with field at the lower values may be due either to an increase in the number of charges, or to an increase in their mobility, or to both causes. Currents may be observed when the illumination precedes the application of the field, of the same amount as when the two factors appear simultaneously. This observation offers a means of deciding what part the field plays in the production and motion of charges. This is one of the fundamental questions connected with the phenomenon. Another fundamental question is that of the resistance of the crystal material to the motion of electrons, and the conditions under which an electron may cross the boundary. Why may electrons once liberated inside the crystal cross the boundary freely, whereas electrons cannot penetrate from the outside under any ordinary experimental conditions? In this connection the observation of unipolar photocurrents, in sulphur, with definite orientations in the crystal, promises to be of importance.

This investigation was suggested by Professors Pohl and Gudden; it was begun in their laboratory at the University of Göttingen, and later continued at Harvard University. I wish to thank Professors Pohl and Lyman, who placed the resources of their respective laboratories at my disposal, as well as Professor Bridgman, who furnished the large sulphur crystals and took a constant interest in the work.

JEFFERSON PHYSICAL LABORATORY,
HARVARD UNIVERSITY,
June, 1927.

THERMO-ELECTRIC EFFECT IN SINGLE-CRYSTAL BISMUTH

By R. W. Boydston

Abstract

Thermal e.m.f., thermo-electric power, Peltier heat of single-crystal Bi against constantan as functions of crystal orientation.—Data are presented on the thermal e.m.f. against constantan of nine single-crystal wires of bismuth, of which the inclinations of the vertical axis, with respect to the wire axis, range from 23° to 83.5°. The temperature interval is from −182° to about 300°C. Some of the observed results are also referred to copper for the sake of comparison with results of previous workers. Data are also given on the thermal e.m.f. of liquid bismuth against various crystal orientations. The thermo-electric power, and Peltier heat, computed from the e.m.f.-temperature curves in the usual fashion, agree well with the Voigt-Thomson symmetry relation for temperatures above 0°C, but depart somewhat, though in no consistent fashion, from this relation for temperatures below 0°C.

Thermo-electric power, Peltier heat and difference of Thomson coefficients for $Bi_{\perp}$ against $Bi_{\parallel}$.—From the data are computed the Peltier heat and difference in Thomson coefficients for $Bi_{\perp}$ against $Bi_{\parallel}$. The location of certain maxima and minima in these curves are found not to occur in the region of rapid decline of atomic heat, though Grüneisen and Goens have found such a coincidence for Zn and Cd.

Thermal e.m.f. of polycrystalline specimens.—The thermal e.m.f. of polycrystalline specimens of both bismuth and zinc when determined experimentally agree surprisingly well with the result predicted by Linder's formula.

Introduction

SEVERAL papers have been published on various thermo-electric effects in single-crystal bismuth. Early work in this field, such as that of Perrot,[1] Lownds,[2] Jordan,[3] Borelius and Lindh,[4] seems to be confined to investigations of small single-crystal "slabs" which have been sawed or split from large single crystals. The angle between the longer dimension of the specimen and the principal crystallographic (vertical) axis has usually been either 0° or 90°. The properties of crystals prepared in the above way doubtless are affected by inevitable strains. Besides, on investigating strain-free crystals it seems desirable to investigate crystals of more than two orientations.[5] The only recent work done on bismuth, as far as the author is aware, is that done by Bridgman[6] who prepared single crystal rods of circular cross-section and presumably free from strain. He investigated the thermal e.m.f. against copper over the temperature interval between 20°C and 100°C of ten such

[1] F. L. Perrot, Arch. des Science Phys. et Nat. **6**, 105, 229 (1898). **7**, 149 (1899).

[2] Louis Lownds, Ann. d. Physik **6**, 146 (1901).

[3] F. W. Jordan, Phil. Mag. **21**, 454 (1911).

[4] Borelius and Lindh, Ann. d. Physik **63**, 97 (1917).

[5] The term orientation is used to define the angle between the vertical axis of the crystal and the axis of the wire.

[6] P. W. Bridgman, (a) Proc. Nat. Acad. Sci. **11**, 608 (1925); (b) Proc. Amer. Acad. of Arts and Sci. **61**, 101 (1926).

specimens the orientations of which ranged from 68.5° to 90°. The present report covers an investigation of thermo-electric effects in single crystals of bismuth through temperatures ranging from −182°C to beyond the melting point. The crystal orientations are from 23° to 83.5°, inclusive. From data taken on these orientations, which are shown to follow the Voigt-Thomson law, the author has calculated the properties of crystals of both 0° and 90° orientation. Thus, the work covers the entire range of orientation from 0° to 90° for the above stated temperature interval.

Method and Apparatus

The general method and apparatus previously described by E. G. Linder[7] were used with only some slight changes. The first of these changes consisted in the substitution of carbon dioxide for air in the cooling blast in the crystal-growing apparatus. Thus the crystal-growing process took place entirely in an atmosphere of carbon dioxide and practically no oxidation occurred. In the second place, for orientations above 50° the growing crystal could be started on another single crystal which was bent near the end so that its basal plane was inclined at the desired angle with the surface of the melt. For lower orientations the temperature of the electric furnace had to be much higher, the cooling had to be considerably faster, and the crystal was grown at a more rapid rate. Thirdly, the thermal e.m.f.'s were measured against constantan instead of copper, the temperature of one junction of the bismuth-constantan couple being kept at 0°C while that of the other was varied from −182°C to 300°C, or slightly higher. Constantan was used because its thermoelectric power curve is much closer to that of bismuth (polycrystalline) than copper is. Thus, when the e.m.f. of the crystals is measured against constantan the effect for all orientations is much less than when measured against copper, but the differences between the different orientations are relatively much greater. This results in a better separation between the e.m.f. curves for the various orientations than is possible when copper is used as the reference metal. The thermal e.m.f. curve for the constantan wire was obtained against the same kind of copper wire used by Linder,[7] so that, where necessary, the results for bismuth are referred to copper. In the fourth place, the convention of the positive e.m.f. was changed. In this work e.m.f. is considered positive in the bismuth-constantan circuit if it is directed from the bismuth to the constantan at the junction of variable temperature. Lastly, the author found that for the purpose of splitting the crystal readily along the basal plane, immersing the crystal in liquid oxygen was better than amalgamation.

The bismuth used in this work was Mallinckrodt "C. P. Quality." According to their analysis the maximum impurities present were: Pb 0.00%, Cu 0.00%, Zn 0.01%, As 0.000%, and Fe 0.00%.

Results

I. *Thermo-electromotive force, thermo-electric power, and Peltier heat as functions of crystal orientation.* In Figs. 1 and 2 are found the observed values

[7] E. G. Linder, (a) Phys. Rev. **26**, 486 (1925); (b) Phys. Rev. **29**, 554 (1927).

of the thermal e.m.f. against constantan plotted against the temperature difference of the two junctions for each of nine single crystal specimens. The curves of Figs. 1 and 2 are continuous curves but are plotted separately for convenience in presentation. The curves cannot be represented by a second degree equation in t. Consequently, the thermo-electric power curves are not straight lines. The author did not try to find empirical equations to fit the above mentioned observed curves. Whenever derived quantities, such as the thermo-electric power, $e=de/dt$, appear their values have been

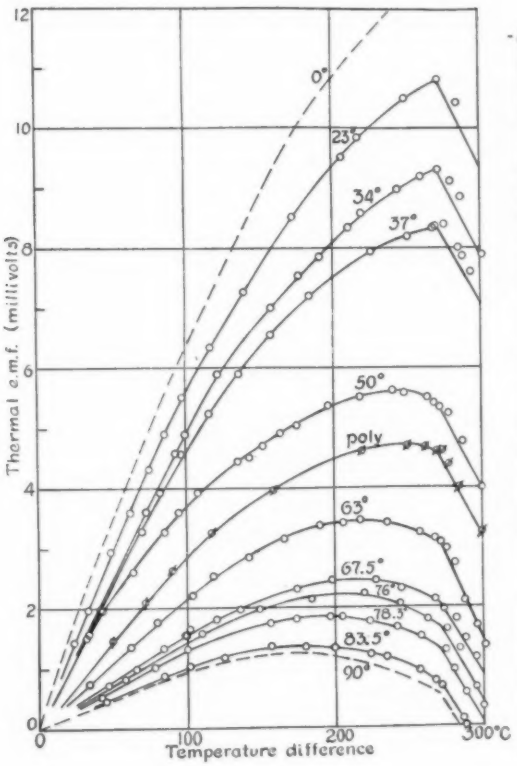

Fig. 1.

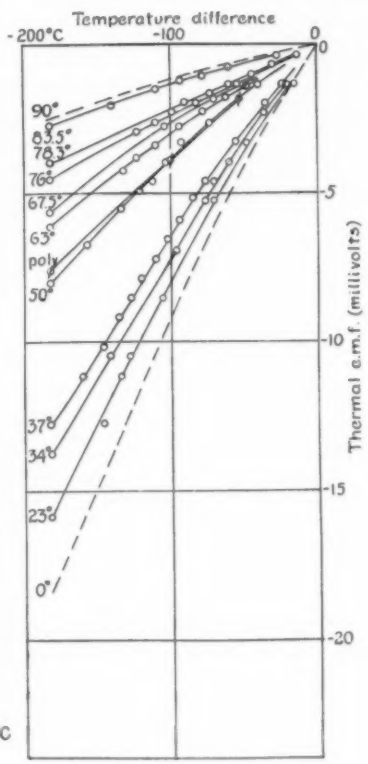

Fig. 2

Fig. 1. E.m.f. against temperature, for various crystal orientations, above zero degrees Centigrade. The orientation angle is shown above each curve.

Fig. 2. Same as Fig. 1, except that temperatures are below zero degrees Centigrade.

obtained by the graphical method of drawing tangents and measuring the slopes. The dotted curves of those figures are calculated e.m.f. vs t curves for crystals of 0° and 90° orientations against constantan. These were obtained by extrapolation, making use of the Voigt-Thomson symmetry relation. The exact procedure is described in II, below.

So far, the only theory proposed to explain the thermo-electric properties of crystals is the thermodynamical theory of Voigt[8] and Thomson[9] according to which

[8] Voigt, Lehrbuch der Kristallphysik.

[9] W. Thomson, Math. and Phys. Papers, I, 232.

$$e_\theta = e_\parallel \cos^2\theta + e_\perp \sin^2\theta = e_\perp + (e_\parallel - e_\perp)\cos^2\theta \qquad (1)$$

where θ stands for the angle between the vertical axis and the axis of the wire, $e_\parallel$ and $e_\perp$ are the thermo-electric powers parallel and perpendicular to the vertical axis, respectively.

Authors disagree as to the validity of Eq. (1) as derived by Voigt and Thomson. Bridgman[6] considers that they have taken no account in their analyses of either the internal or surface Peltier heat and their results, therefore, can not be expected to hold for an actual thermocouple. His experimental work with zinc, bismuth, cadmium and tin tends to substantiate this view. On the other hand Linder,[7(b)] considering the equation as purely empirical, finds it valid for zinc crystals for the temperature range −150°C through 200°C, when tested experimentally. For bismuth

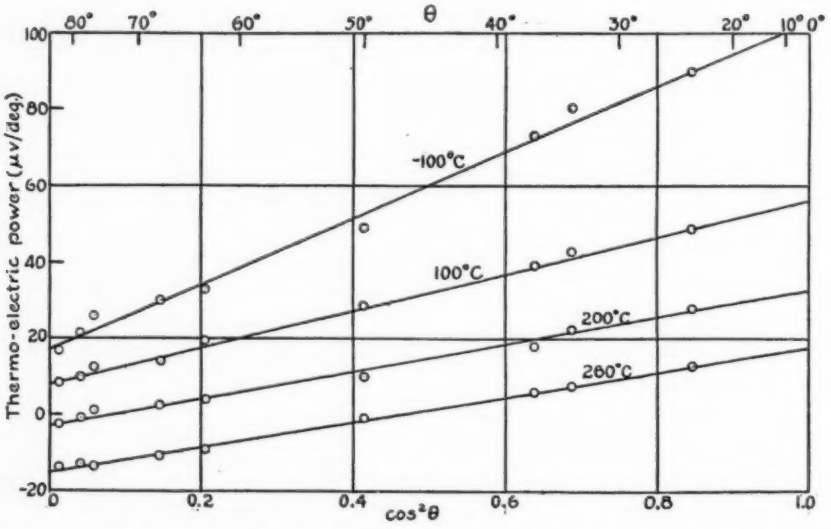

Fig. 3. Test of Voigt-Thomson Law. Thermo-electric power as a function of $\cos^2\theta$, for various temperatures of variable junction.

Bridgman[10] obtains a nearly linear relation between a certain constant, a' (a' is proportional to Peltier heat and to the thermo-electric power at 0°C) and specific resistance. The latter obeys the Voigt-Thomson law so that a' should be a linear function of specific resistance if Eq. (1) is valid. Bridgman considers the departure from linearity real. The writer has tested Eq. (1) in the fashion described by Linder. In Fig. 3 are shown graphs for various temperatures of thermo-electric power against $\cos^2\theta$, where θ stands for the orientation. The points, except for the −100° curve, do not deviate from the expected straight line more than might be due to experimental errors. At −100°C the deviations are somewhat greater but the experimental errors are also thought to be slightly larger in this region. These deviations are not systematic and no smooth curve seems to fit better than the straight line which has been drawn through these points. Points for orientations measured

[10] See Reference 6(b) Figure 7, page 119.

by Bridgman, if plotted in Fig. 3, would lie entirely in the interval between 0 and 0.15 for $\cos^2\theta$. The curved part of his line would lie perhaps between 0 and 0.02. The writer has only one point in that region, but owing to its coincidence with the straight line determined by all the other points, it seems unlikely that there is any considerable deviation from the Voigt-Thomson law.

For the sake of comparing the writer's results with the results of other investigators, Tables I and II are given. Table I includes abstracted results from the earlier writers (above mentioned). The mean temperature is indicated by t_m. The thermo-electric power, e, is given in microvolts per degree (μv/deg). Table II compares the present results with Bridgman's.

TABLE I

Comparison of author's values for the thermo-electric power of single-crystal Bi with those of others.

Observer	t_m	e(μv/deg.)	Boydston e (μv/deg.)
	$\theta=0°$		
Lownds	56.4°C	118.35	109.
Borelius and Lindh	50.	92.	108.
Lownds	−35.	108.	119.
Lownds	−50.	94.	128.
	$\theta=90°$		
Jordan	20°C	53.1	52.
Perrot	55.	54.6	57.2
Lownds	50.6	61.94	55.3
Borelius and Lindh	50.	55.	55.3
Borelius and Lindh	100.	55.	50.5
Lownds	−33.5	28.3	48.
Lownds	−57.3	13.9	48.5

TABLE II

Comparison of present results with those of Bridgman.

θ	Bridgman Total e.m.f. (20° to 100°)	Ave. θ	Average total e.m.f. (20° to 100°)	θ	Boydston total e.m.f. (20° to 100°)
90°	4460μv				
90°	4540	90°	4500μv	90°	4200μv
85.5°	4610				
84.5°	4610	85°	4610	83.5°	4470
80°	5040	80°	5040	78.3°	4600
73.5°	5080			76°	4708
72°	5150	72.7°	5110	67.5°	4900
69.7°	5200				
68.5°	4900				
68.5°	5420	68.9°	5170	67.5°	4900

In both tables the reference metal is copper, the writer's values having been computed from the observed values by making use of the previously mentioned determination of the thermal e.m.f. curve of constantan against copper. The agreement in both tables is probably as good as can be expected in view of the great possible differences in both the material tested and the copper used as reference. The poorest agreement is with Lownds' data for

temperatures below zero degrees. For the parallel orientation his values decrease with decreasing temperature, while the writer's increase.

If the usual thermodynamical relation, $\pi = TdE/dt$, for Peltier heat, π, is valid, Fig. 3 also shows how far Eq. (1) is capable of expressing the nature of variation of the Peltier heat with orientation.

II. *Thermo-electric properties of $Bi_\perp$ and $Bi_\parallel$.* The thermo-electric properties of bismuth may be obtained without reference to another metal by expressing the constants of one principal orientation, $Bi_\perp$ ($\theta = 90°$), against the other, $Bi_\parallel$ ($\theta = 0°$). Assuming the Voigt-Thomson law, which was shown at least to be very nearly true, one obtains, by integration,

$$E_\theta = E_\parallel \cos^2\theta + E_\perp \sin^2\theta \qquad (2)$$

where E_θ represents e.m.f., providing θ is independent of the temperature difference, t, of the junctions. $E_\perp$ and $E_\parallel$ may be calculated for any value of temperature difference, t, by substituting in Eq. (2) values for E_θ and θ from

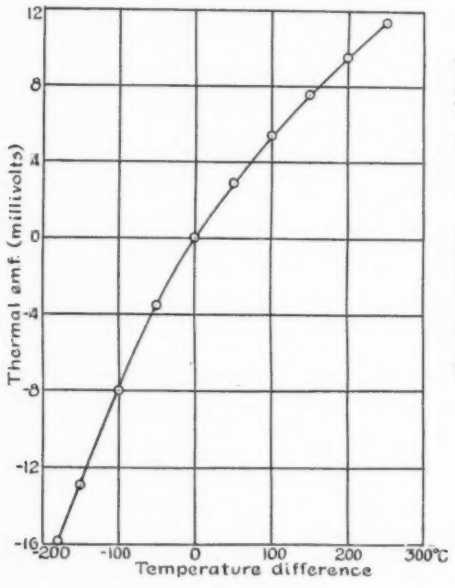

Fig. 4.

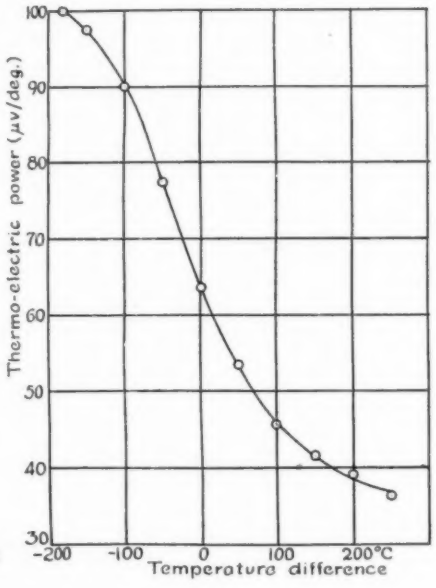

Fig. 5.

Fig. 4. Thermal e.m.f. for $Bi_\perp$ against $Bi_\parallel$.
Fig. 5. Thermo-electric power for $Bi_\perp$ against $Bi_\parallel$.

any two of the experimental curves of Fig. 1, preferably from curves lying far apart. Solving simultaneous sets of such equations yields $E_\perp$ and $E_\parallel$ against constantan for any desired value of t. Subtraction yields the value of the thermo-electromotive force of $Bi_\perp$ against $Bi_\parallel$. Fig. 4 and Table III contain values of this e.m.f. for various temperature differences.

The thermo-electric power, $e = dE/dt$, can be obtained from Fig. 4 by measuring the slope of the tangents at various values of temperature, t. Fig. 5 and Table III contain the values obtained in this way.

TABLE III

Thermal e.m.f., thermo-electric power, Peltier heat, and difference between Thomson coefficients for $Bi_\perp$ against $Bi_\parallel$.

T	e.m.f. (μv)	e (μv/deg.)	π (μv)	$\sigma_\perp - \sigma_\parallel$ (μv/deg.)
−180°C	−15,876	100.	9,300	− 6.7
−150	−12,903	97.5	11,992	−13.3
−100	− 7,982	90	15,570	−32.7
− 50	− 3,537	77.5	17,282	−58.9
0	0	63.6	17,363	−66.6
50	2,910	53.5	17,280	−57.5
100	5,453	45.7	17,046	−38.4
150	7,593	41.7	17,639	−27.9
200	9,581	39.2	18,542	−25.7
250	11,402	36.4	19,037	−24.3

By Thomson's thermodynamical theory the Peltier coefficient is given by $\pi = TdE/dt = Te$, where T stands for the absolute temperature of the variable-temperature junction. Fig. 6 and Table III show the variation of the Peltier coefficient with temperature difference as calculated from this equation.

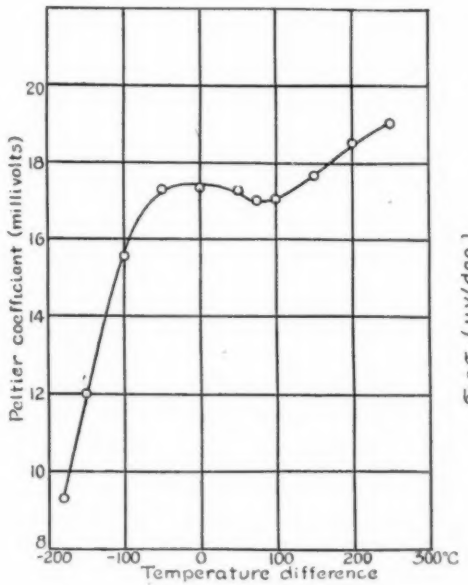

Fig. 6.

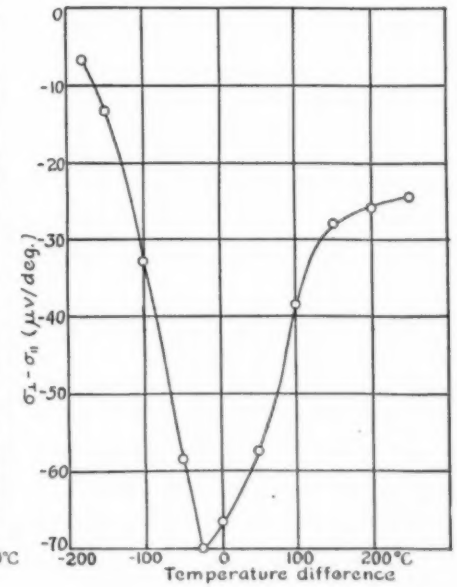

Fig. 7.

Fig. 6. Peltier coefficient for $Bi_\perp$ against $Bi_\parallel$.
Fig. 7. Difference in the Thomson coefficients for $Bi_\perp$ against $Bi_\parallel$.

According to the same theory the differences of the Thomson coefficients are given by $\sigma_\perp - \sigma_\parallel = Tde/dt$. By measuring slopes in Fig. 5, de/dt may be obtained. In Fig. 7 and Table III are given data on the relation between $(\sigma_\perp - \sigma_\parallel)$ and temperature t.

It will be noticed from Figs. 6 and 7 that a distinct maximum in the Peltier coefficient and a maximum in the difference of the Thomson coefficients occur at a temperature slightly below 0°C. These curves are apparently of the same character as similar curves for zinc and cadmium, reported by Grüneisen and Goens.[11] These writers call attention to the fact that a maximum in the thermo-electric power, a maximum in the Peltier coefficient, and a minimum in the difference of Thomson coefficients, for perpendicular against parallel orientations, occur at the same temperature. For zinc this critical temperature is −225°C and for cadmium −255°C. They show further that this temperature in each case lies in a region in which the atomic heat falls off rapidly with decreasing temperature, thus showing a close connection between variation of atomic heat and thermo-electric constants.

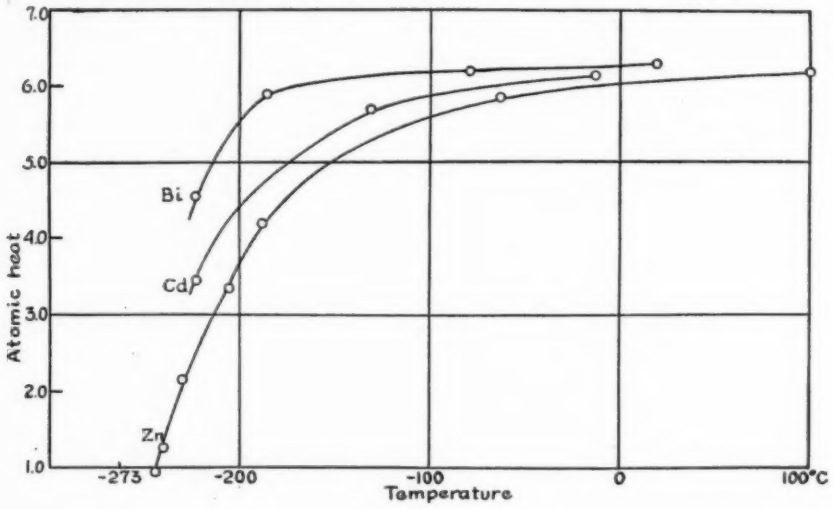

Fig. 8. Atomic heats of Bi, Cd, and Zn.

The facts for bismuth, unfortunately, do not support this supposition very well. No maximum of the thermo-electric power occurs in the region investigated, though it seems likely that a maximum lies about −200°C. The other maximum and minimum to be expected do occur but at a much higher temperature, as has been stated. They do not appear to coincide with a region of rapid decline in atomic heat, as may be seen from Fig. 8 which shows graphs of the atomic heats[12] of zinc, cadmium and bismuth. Perhaps the lack of agreement for bismuth is only another instance of its anomalous behavior.

III. *Behavior at the melting point.* Authors disagree as to whether there is a break in the thermo-electric properties of the various metals at the melting point. Darling and Grace[13] report no discontinuity for the thermo-

[11] Grüneisen and Goens, Zeits. f. Phys. **37**, 378 (1926).

[12] Values used in plotting these curves were taken from Landolt-Börnstein Physikalisch-Chemische Tabellen (5th Ed.) and from Dewar, referred to in these Tables.

[13] Darling and Grace, Proc. Phys. Soc. London, **29**, 82 (1916).

electric power curves of lead, tin, cadmium, zinc, and aluminum. The curve for bismuth is quite generally conceded to have an abrupt break in it. Such writers as Koenigsberger,[14] Darling and Grace,[13] Pélabon,[15] call attention to this break. As may be seen from Fig. 1 the author finds a break at the melting point. It should be pointed out, however, that the change in slope is not so well defined and abrupt as that reported by Linder[7(b)] for zinc. The points immediately beyond the melting point lie above the straight line determined by the later points. It appears, in fact, as if some crystalline arrangement still persists in the molten metal, as shown by a transition region between thermal e.m.f. of solid and liquid. The effect is believed to be real as it occurs in every curve. To avoid confusion, not all of the points obtained beyond the melting point are plotted in Fig. 1, but the straight line portions of the graphs have been drawn to fit all of the observed points. These lines are practically parallel.

The experimental values obtained for the thermo-electric power of solid Bi, e_s, and of $e_l - e_s$, where e_l is the thermo-electric power of liquid Bi, are found, for the various orientations and for polycrystalline bismuth, in Table IV.

TABLE IV

Thermo-electric power of solid and liquid bismuth at the melting point. $e_l = -49.8$ μv/deg.

θ	e_s (μv/deg.)	$e_l - e_s$ (μv/deg.)
23°	12.3	−62.1
34	8.25	−58.1
37	3.38	−53.2
50	− 5.8	−44.0
63	−13.7	−35.3
67.5	−15.5	−34.3
76	−16.6	−33.2
78.3	−17.7	−32.1
83.5	−20.6	−29.2
Poly.	− 6.17	−43.6

An attempt was made to calculate from Bernoulli's and Lorentz's formulas the value for $e_l - e_s$ of the polycrystalline specimen. No agreement could be obtained, however, between the theoretical values and the observed.

IV. *Verification of Linder's formula.* Linder[7(b)] has derived an expression for the thermo-electric properties of a metal specimen, composed of randomly oriented crystal grains. For metals, such as zinc and bismuth, the crystals of which contain a vertical axis of rotational symmetry, he computes 54.5° as the "equivalent orientation," that is to say, the polycrystalline specimen should give the same thermal e.m.f. temperature curve as a single crystal of the stated orientation. Linder's deduction is based on an assumption of the validity of the Voigt-Thomson symmetry relation for thermal e.m.f.

[14] J. Koenigsberger, Ann. d. Physik **47**, 563 (1915).
[15] H. Pélabon, Ann. d. physique **13**, 169 (1920).

The electrical conductivities perpendicular and parallel to the vertical axis are moreover assumed equal, though they are actually slightly different. The only test, so far, of this law is Linder's own test of it in zinc. He found an experimental value of 65–70° for the equivalent orientation of the polycrystalline wire. The present writer has applied this law to bismuth and also again to zinc after preparing polycrystals by what he believes to be a better method than was used by Linder. Linder's preparation of his polycrystals consisted in melting unused single crystals in a Pyrex tube of small circular cross-section, and then cooling them, as rapidly as possible, by directing an air blast against the tube. It seems rather doubtful that random orientation can be produced by this method. A specimen of more nearly random orientation should be obtained if the specimen is cooled at a greater rate, and from all sides simultaneously. The author is indebted to Dr. Taylor, of the Chemistry Department, for providing a mold (of high conductivity) in which polycrystalline specimens could be prepared utilizing the above desired features. The specimens prepared in this mold showed a fine grained structure. Thermal e.m.f. data were then taken for two such polycrystalline specimens of bismuth and two of zinc. The thermo-electromotive force against temperature for one of the polycrystals of bismuth is plotted (ϕ) in Figs. 1 and 2. The data on the other specimen were nearly identical. The results for one specimen of each metal are summarized in Table V, in which

TABLE V

Values of the equivalent orientations, θ_{eq}, of single-crystal Bi and Zn for which the thermal e.m.f is the same as for polycrystalline specimens.
θ(theoretical) = 54.5° for both Bi and Zn.

t		Bismuth θ_{eq}.	Zinc θ_{eq}.
−100°C		56.5°	52.6°
100		54.8	53.0
200		54.2	53.4
260		55.0	53.8
	Ave.	55.1°	53.2°

may be found values of equivalent orientation (θ_{eq}), the thermal e.m.f.'s of which are, for the temperatures shown, identical with those of the polycrystalline specimens. The agreement of the average values with the theoretical value of 54.5° is exceedingly good in both cases.

CONCLUSION

The results show that the thermo-electric properties of single crystal bismuth resemble very much similar properties found in zinc. The Voigt-Thomson symmetry relation for the thermo-electromotive force, Peltier heat, and thermo-electric power, as functions of orientation, appears to hold for both metals. Bismuth is found not to substantiate a connection between thermo-electric properties and variation of atomic heat with temperature which is reported for zinc and cadmium by Grüneisen and Goens.

In conclusion the writer wishes to express his appreciation to the members of the staff of the Physics Department for their friendly interest and cooperation. Mr. E. G. Linder deserves special mention in connection with the above statement. The writer wishes especially to express his thanks to Professor E. P. T. Tyndall for the assignment of the problem and for his criticisms, suggestions, and encouragement during the course of the investigation.

LABORATORY OF PHYSICS,
UNIVERSITY OF IOWA,
July, 1927.

AN ARRANGEMENT OF THE ELECTROMETER METHOD FOR MEASURING THE DIELECTRIC CONSTANTS OF ELECTROLYTES

By A. P. Carman and C. C. Schmidt

Abstract

The electrometer method described by A. P. Carman (Phys. Rev. **24,** 396, 1924), has been modified to meet difficulties of heating effects, of buoyance, of electrolytic polarization, and of exact measurement of potential differences between the fixed plates and the needle plates. The method is particularly adapted to the measurement of relative dielectric constants of water and aqueous electrolytes, even where the concentrations and resulting conductivity of the electrolytes are considerable.

THE electrometer method, described by A. P. Carman in 1924,[1] has been changed in order to overcome some difficulties that appeared in practice, particularly in its application to measuring the dielectric constants of electrolytes. The new arrangement is shown in Fig. 1. The vertical plates A and B, and the corresponding needle plates C_1 and C_2, are charged as in the original arrangement by sliding contacts with the potentiometer wire,

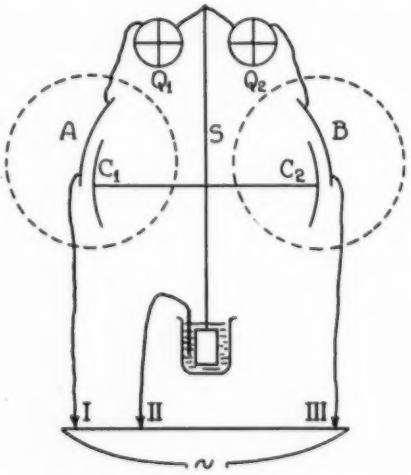

Fig. 1. Schematic diagram of apparatus.

but the connection with the needle is now made through a wire dropped from the center of the needle into a beaker of sulphuric acid. This wire ends in a fairly heavy metal bob which serves to lower the center of gravity of the needle and also acts as a damper. The potential differences between the two pairs of condenser plates are measured by two electrostatic voltmeters Q_1 and Q_2, connection for these voltmeters with the needle being made through

[1] A. P. Carman, Phys. Rev. **24,** 396 (1924).

the phosphor bronze suspension ribbon S. When the plates A and C_1 are immersed in a fluid of dielectric constant k_1, and the plates C_2 and B in a fluid of dielectric constant k_2, and the opposing torques on the needle are balanced by adjusting the potential differences $V_1 - V_2 (= E_1)$, and $V_2 - V_3$ $(= E_2)$, we get $A_1 k E^2 = A_2 k_2 E^2$, where A_1 and A_2 are factors depending upon the sizes and the positions of the attracted pairs of plates. If the dielectric on the right side is changed to one of dielectric constant k_3, and the new balance is for potential differences E_3 and E_4, we get $A_1 k_1 E_3^2 = A_2 k_3 E_4^2$. It follows directly that

$$k_3/k_2 = E_2^2 E_3^2 / E_1^2 E_4^2$$

This assumes that A_1 and A_2 remain constant. For non-conducting liquids, the potential differences may be taken as directly proportional to the resistances of the segments of the potentiometer wire (assuming no inductance), but for conducting liquids, the calculations are not simple, and particularly where the conductivities are different, as in the comparison of "pure" water and a fairly concentrated electrolyte. In such cases, the currents on the two sides of the potentiometer wire may be very unequal. In one case we had practically zero current on one side, and nearly an ampere on the other side. It became necessary then to measure the differences of potentials directly across the plates. With these larger currents, the fine ribbon suspension changed its elastic properties because of heating, and so it was necessary to have the connection with the needle through an independent wire dropped into a conducting liquid.

For the electrostatic voltmeters, we used at first two Kelvin multicellular voltmeters, each of range 30–150 volts, and got only fair results, since the instruments are sluggish and, being pointer instruments, do not indicate very small changes of potential. We then improvised electrostatic voltmeters from Dolezalek electrometers, using them idiostatically and attaching large paper dampers to the stems of the needles. These voltmeters were used ballistically for rapidity of reading. A calibration curve was made before each run of readings, and then check readings were taken at frequent intervals. The potential source for the calibration was a set of small storage cells, the e.m.f.'s of which were known by means of a potentiometer and a standard cell. Potential readings could be repeated with these voltmeters to within a half of one percent.

Another factor that was troublesome with the original instrument was the difference of buoyancy on the two immersed plates of the needle. This difference tilted the plates very slightly, but apparently enough to alter relative positions and distances, so that the factors A_1 and A_2 in the equation of equilibrium could no longer be considered as constant. In the original arrangement, this buoyancy change was compensated by shifting small weights along the horizontal arms of the needle, but this required an auxiliary observation to verify the compensation. When a heavy bob was attached to the wire dropping into the sulphuric acid, it was found that there were no buoyancy shifts for any liquids that were tried. This would of course be

expected, where the density differences were very small, as in the case of water, and an aqueous solution.

Our experience has been that with an electromotive force of the ordinary frequency of 60 cycles per second, there are electrolytic polarization effects. We have recently used a motor generator set giving 500 cycles per second, and have had no disturbing polarization effects for the voltages used and with the electrolytes that we have tested. A difficulty in the force method for electrolytes lies in the rapidly changing temperatures due to heating by the considerable currents through the dielectric. This requires very rapid and simultaneous observations of force and potentials, but this difficulty is not peculiar to the force method. It has been overcome by interpolating from a curve of dielectric constants and temperatures.

The method was tested with a series of non-conducting liquids and the values obtained for the dielectric constants show good agreement with each other and with the generally accepted values for these liquids. These values are shown in Table I at 24°C with a 60 cycle alternating electromotive force with 110 volts total. The balance was against water except for the dielectric constant of water, and that was against air. This last is, of course, an extreme test, owing to the great difference between the dielectric constants of air and water.

TABLE I

Dielectric constants k of various non-conducting liquids.

Liquid	k	Liquid	k
Water (conductivity about 10^{-6})	81.5	Methyl Alcohol	35.0
	79.8		35.7
	81.0		35.8
	79.5		
Mean	80.4	Acetone	24.0
			24.7
Turpentine	2.46		
	2.45	Chloroform	5.6
	2.47		
		Xylol	2.46
			2.47

While the electrometer method is capable of good results for non-conducting liquids, and may have advantages in some cases, its most valuable application at present is likely to be found in the comparison of the dielectric constant of an aqueous electrolyte with that of water. It will be shown later, that with the arrangement described above, it has been possible to obtain the relative dielectric constants of water and aqueous electrolytes of equivalent concentrations of 0.02 and beyond—a result apparently only possible at present with a force method.

LABORATORY OF PHYSICS,
UNIVERSITY OF ILLINOIS,
June, 1927.

THE DIELECTRIC CONSTANTS OF FOUR ELECTROLYTES AS GIVEN BY THE CARMAN ELECTROMETER METHOD

By Clarence C. Schmidt

Abstract

The electrometer method devised by Professor A. P. Carman is used to measure the dielectric constants of aqueous solutions of NaCl, KCl, $BaCl_2$ and $CuSO_4$. Curves showing the relation between dielectric constant and concentration of the solution are obtained for each of these four substances, up to an equivalent normal concentration of 0.018 for NaCl, of 0.01 for KCl, of 0.024 for $BaCl_2$, and of 0.028 for $CuSO_4$. These curves each show first a decrease of the dielectric constant with increasing concentration. After passing through a minimum the dielectric constant increases with the concentration, rising in each case to a value greater than that of water. For solutions of $BaCl_2$ and $CuSO_4$, there is in each case a second minimum in the rising branch of the curve. These experimental results for the dielectric constants of aqueous electrolytes can be explained by an hypothesis in accordance with the general dipole theory of Debeye, as interpreted by Walden, Ulich and Werner.

IN 1897, J. F. Smale,[1] working in Nernst's laboratory by a Nernst force method, got values of the dielectric constants of several electrolytes which showed an increase of the dielectric constant with the concentration of the solution, these values being greater than that of water. Lattey[2] and Walden,[3] on the other hand, find that for aqueous electrolytes the dielectric constants of the solution is less than that of water, and further that the dielectric constant decreases as the concentration increases. Lattey and Walden used resonance methods and could get results only for dilute solutions. Recently Fürth[4] has given results on solutions of NaCl, by a force method, in which he gets first a decrease and then an increase of the dielectric constant of the solution as the concentration increases, but his curves do not show a value of the dielectric constant of the solution greater than that of water. His measurements are peculiar in showing higher values in an electric field of 30 volts than in a field of 15 volts. The following investigation of this interesting subject of the dielectric constants of aqueous electrolytes was carried out by an electrometer method devised by Professor A. P. Carman. This method has proved to be especially adapted for obtaining the relative values of the dielectric constant of two liquids, and in the new arrangement described elsewhere[5] has given consistent and satisfactory results for electrolytes as well as for non-electrolytes.

[1] J. F. Smale, Ann. d. Physik **60**, 625 (1897).

[2] R. T. Lattey, Phil. Mag. **41**, 829 (1921).

[3] P. Walden and Assistants, Zeits. d. Phys. Chem., vols. **110, 111, 115**. Otto Blüh, in Physik. Zeits. (April, 1926) discusses the recent results on the dielectric constants and gives an extended bibliography. L. F. Gilbert in Sc. Progress (July, 1926) discusses the dielectric constants of liquids.

[4] R. Fürth, Physik. Zeits. **25**, 676 (1924).

[5] A. P. Carman and C. C. Schmidt, Phys. Rev. **30**, 922 (1927).

Aqueous solutions of NaCl, KCl, $BaCl_2$ and $CuSO_4$ were used. The materials were marked "c.p." and were probably very nearly pure. In preparing the solutions "conductivity" water obtained from the Department of Chemistry of the University of Illinois was used. This was prepared by redistilling the distilled water from the regular supply in the following manner. After filling the still with distilled water, a solution of $KMnO_4$ dissolved in an alkali, was added. The treated water was then heated and left for six hours or more. This was to insure complete oxidation of organic matter. The solution was prepared by adding twelve grams of $KMnO_4$ to a solution of 120 grams of NaOH in one liter of water. While distilling, the flow of cooling water and steam for heating were so regulated that some steam passed out with the water. This was to prevent CO_2 from going into the bottle. Water obtained by this process was found to have a conductivity of 0.6 to 0.92×10^{-6} mhos by Hovorka.[6] The water was used as soon as possible after it was obtained so as to give less chance for absorption of impurities. Before making up solutions, the water was kept in Jena glass bottles reserved for that one use. The water was usually used within a few hours, although measurements made on water two or three days old showed no apparent differences. Solutions of normal concentration were prepared by weighing the salt to within a milligram and the water to within a gram, giving an accuracy within other experimental errors. The plates used on each side of the electrometer were of gold 2.5 cm square and 0.055 cm thick. There was no sign of any chemical action on the plates by any of the liquids used. The distances between the wires themselves and between the wires and the sides of the vessel were great enough to eliminate capillary attractions. The separation of the needle plates from the fixed plates could be varied, and was usually made as small as possible to get sensitivity. The needle plate and its fixed plate on the left side were immersed in pure water, and the plates on the right side in the solution. As the densities of the liquids on the two sides were very nearly the same, there was no disturbing effects from buoyancy.

The electric current between the plates through the electrolyte amounted in some cases to nearly an ampere, and the rise of temperature was often considerable. While measurements could be made upon non-conducting liquids at room temperatures without temperature disturbances, this could not be done for conducting solutions. It was necessary to measure the temperatures of the solution between the plates where the heat was generated. This was done by a small glass-sheathed thermocouple of copper-constantan. The thermocouple was placed between the plates against the fixed plate, and as the thermocouple was very small and fixed in position for all measurements, it was assumed to have no effect on the results. The e.m.f. of the thermocouple was found by means of a potentiometer and a standard Weston cell, and the temperatures determined from a calibration curve. The temperature could be determined to a tenth of a degree Centigrade, which was considered sufficiently accurate. Because of the heating of the conducting

[6] F. Havorka, Master's thesis in Phys. Chem., University of Illinois Library, 1925.

solutions, it was not practical to get a balance of the electrometer at the exact temperature desired. It is, however, necessary that the values of the dielectric constant should be reduced to the same temperature. By obtaining several electrometer balances and observing the corresponding temperature for each balance reading, it was possible to obtain the ratio of the potential differences for several temperatures; then from a curve with potential ratios as ordinates and temperatures as abscissas, the value of the potential ratio for the derived temperature was obtained. The use of such a curve had also the advantage of averaging the determinations. It is very important in getting a comparison of the dielectric constants of water and of a solution, that the balancing water remain at a constant temperature. It was found possible to maintain the water temperature practically constant for several hours. By making a checking determination with water on both sides in connection with measurements on each sample of the solution, the variations were reduced still further.

The measure of the ratio of the potential differences for the two pairs of evidently all-important for accuracy in the dielectric constants by a force method. These potential differences were measured by two electrostatic

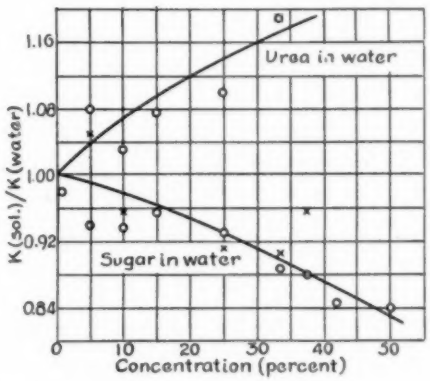

Fig. 1. Variation with concentration of the dielectric constants of solutions of urea and of sugar in water.

voltmeters, using for this purpose two Dolezalek electrometers connected idiostatically. These were used ballistically and calibrated before and after each run of readings. An accuracy within one-half of one percent was reached. An assistant was used in making these potential observations so as to get the readings rapidly and simultaneously with the readings of the electrometer balance. Our first measurements were made on two non-electrolytic aqueous solutions, the solutions chosen being two for which we have measurements made by Fürth,[7] by a resonance method. For these measurements, we used two Kelvin multicellular voltmeters for the potential differences between the plates. Alternating potentials of 60 cycles and about 50 volts on each side were used. The results are shown in the curves on Fig. 1. These

[7] Fürth, Ann. d. Physik **70**, 63 (1923).

show good general agreement with the values obtained by Fürth. The individual observations did not fall as close to the curve as desired, because of the difficulty of estimating fractions of a volt with the pointer instrument. These curves show that the dielectric constants of sugar solutions decrease with the concentration, while for urea the dielectric constants increase with the concentration. Fürth found this also. For the measurements of the dielectric constants of the aqueous solutions, the specially adapted quadrant electrometers were used as voltmeters, and a Crocker-Wheeler motor-generator producing an alternating e.m.f. of 500 cycles was the potential source. Earlier trials with an e.m.f. of 60 cycles had showed irregularities

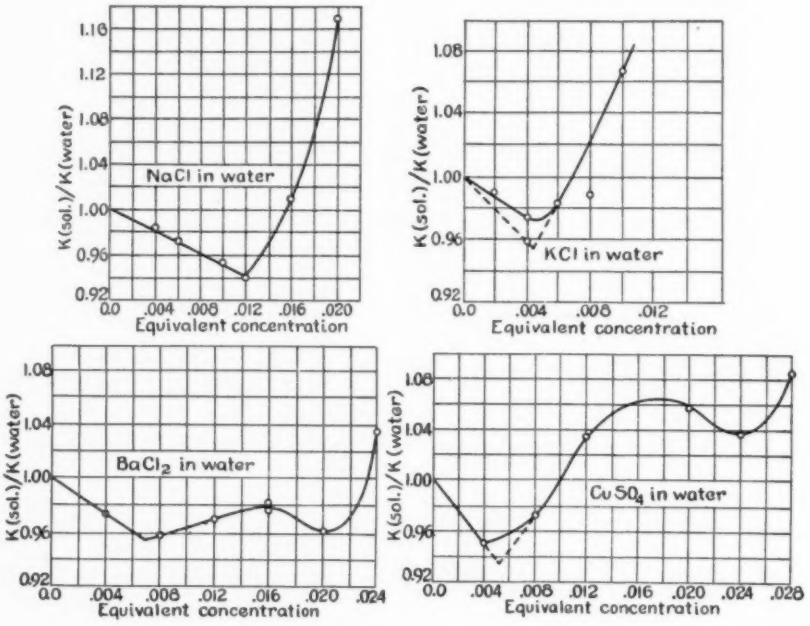

Figs. 2-5. Variation with concentration of the dielectric constants of solutions of NaCl, KCl, $BaCl_2$ and $CuSO_4$ in water.

which we believed due to electrolytic polarization. These irregularities disappeared with the 500 cycle potential source. The results of measurements of the dielectric constants of the four electrolytes are given in the curves Figs. 2–5. These curves show the relation between the dielectric constant and the normal concentration of the solution for each of the four substances. All values are given for 20°C. The alternating e.m.f. used on each side was about 25 volts at 500 cycles. The values of the dielectric constants are given in terms of the dielectric constant of water as unity.

A sample set of observations for a single point is given in Table I for a solution of NaCl of normal concentration 0.006. Curves showing the variation of dielectric constant with concentration in aqueous solutions of NaCl, KCl, $BaCl_2$ and $CuSO_4$ are presented in Figs. 2, 3, 4, and 5. It is seen that the curves for NaCl and KCl are similar. Both show a decrease of the di-

electric constant with increase of concentration until a minimum is reached, after which the curve rises rapidly. The change of slope is apparently more abrupt in the case of NaCl than it is for KCl, though the number of observations is as yet insufficient to warrant definite conclusions. In NaCl the minimum is found at a concentration 0.012 normal while in KCl it is between 0.004 and 0.006 normal. The existence of these sharp minima for aqueous solutions is here shown definitely for the first time, as far as we

TABLE I

Sample set of observations. NaCl solution, concentration 0.006 normal.

Solution on right, water on left				Water on both sides			
Temp.	Potential differences E_1'(left)	E_2'(right)	$(E_1/E_2')^2$	Temp.	E_1(left)	E_2(right)	$(E_1/E_2)^2$
10.7°C	23.1 v	26.6 v	0.755	19.9°C	23.2 v	27.2 v	0.728
12.1	22.8	26.7	.73	19.9	23.2	27.3	.724
14.1	22.8	26.8	.723			(mean)	0.726
16.3	22.6	26.7	.712				
20.1	22.5	26.8	.705	$k_{sol}/k_{water}=0.706/0.726=0.972$			
20.0		(from curve)	0.706				

know, though such minima had been predicted by Walden, Ulich and Werner[7] from similar curves which they obtained with chloroform, pyradin, dichlorbenzol, etc., as solvents. Fürth[8] found for aqueous solutions of NaCl a bend in the dielectric constant—concentration curves, but the bend was very gradual and small. Fürth used a nickel ellipsoid suspended in the liquid at an angle with the impressed alternating electric field. The frequency was only 50 cycles per sec. and hence his results are almost certainly complicated by electrolytic polarization. The fact that he obtains different curves for different impressed electromotive forces also suggests that electrolytic polarization is a factor in his results.

Walden, Ulich and Werner, with their resonance method, were not able to make measurements on aqueous solutions as far as the minimum points indicated on our curves, but they state that such a minimum point should be found for a solution of NaCl at an equivalent concentration of about 0.25. The beginning of the upward bend in Fürth's curve is in the region of 0.003 to 0.006 concentrations, while our curve for NaCl starts up at 0.012, somewhere between Fürth's values and Walden, Ulich and Werner's estimated value.

Our curves for $BaCl_2$ and $CuSO_4$ both show the existence of a second minimum point. In the case of $BaCl_2$ the value of the dielectric constant at the intervening maximum is less than the value for water while in the case of $CuSO_4$ it is greater. It is reasonable to suppose that the presence of the double minima in the case of these solutions is to be associated with the bivalent nature of the metal ion. Walden, Ulich and Werner found such a second minimum point for tetra-prophylammonium iodide in acetylene tetrachloride, but gave no explanation of it.

[7] Walden, Ulich and Werner, Zeits. f. Phys. Chem. **115**, 177 (1925); **116**, 261 (1925).

[8] Fürth, Phys. Zeits. **25**, 676 (1924).

Walden, Ulich and Werner's general explanation of the decreasing and increasing branches of the curve for concentration and dielectric constant is as follows. For the pure solvent the dielectric constant is determined by the dipoles present. When the liquid is placed in an electric field the dipoles arrange themselves in the general direction of the external field. If a substance which is ionized is added to the solvent, then for weak solutions, the ions are widely separated, and each ion has its own electric field. The dipoles of the solvent are attracted by these charged ions, and the directive action of the external electric field is consequently decreased. With the addition of more ions, that is, for more concentrated solutions, the number of ions becomes such that complex formations or groups of ions are formed and these groups direct themselves with the external field and thus tend to increase the dielectric constant again. Our present knowledge of the dielectric constants of electrolytes is too meager to give more than this general explanation. There is evidently need of extended data on the dielectric constants of a considerable number of electrolytes through a wide range of concentrations before a more complete explanation of the phenomena described in this paper is assured. Plans are being made to continue in this laboratory this investigation.

The writer thanks Professor A. P. Carman, who suggested the problem and directed the work, for his suggestions and encouragement during this investigation.

LABORATORY OF PHYSICS,
UNIVERSITY OF ILLINOIS,
June, 1927.

[9] Walden, Ulich, Werner. Zeits. f. Phys. Chem. **116**, 288 (1925).

EXPERIMENTAL TEST OF MAXWELL'S DISTRIBUTION LAW*

By John A. Eldridge

Abstract

A method is described for obtaining a velocity spectrum of a metallic vapor. The apparatus consists of a number of coaxial discs with radial slots which rotate at high speed and serve as a velocity filter for the molecules. The velocity can be measured directly somewhat as in the Fizeau experiment. The apparatus has been used to measure the distribution law of molecular velocities in cadmium vapor and it is found to agree with that of Maxwell within experimental error.

ONE of the most famous achievements of the mathematical physicist is the law of distribution of molecular velocities in a gas. Originally derived by Maxwell, the proof has been varied and presumably rendered more precise by Boltzmann, Lorentz, and Jeans; yet no proof has been above criticism. More recently the newer quantum mechanics has led to a different law but, characteristically, this degenerates with close approximation into the classical law of Maxwell except at low temperatures and high pressures.

Strangely enough, no rigorous experimental test of the law has ever been made. In general such tests as have been made have agreed with the predictions of the law within the precision of the experiment. The older methods were indirect. Richardson has shown that the Maxwellian distribution held for electrons emitted from a hot wire and the measurement of the Doppler broadening in the spectrum from a discharge tube has been found to be in accord with that expected from the law. The first direct measurement of molecular velocities of silver vapor was made by Stern and quite recently Costa, Smyth and Compton[1] have used a method rather similar to that which is to be described to determine the velocity in several permanent gases. The precision of these experiments was quite low and can hardly be said to constitute a verification of the law.

The present experiment aimed to find the distribution of velocities in cadmium vapor. The apparatus used is shown diagramatically in Fig. 1. In a large glass tube was mounted the system of discs shown. The lowest heavier disc acts as the rotor of an induction motor—the other thinner discs have in each a hundred radial slots cut in their periphery and serve as a velocity filter. Leading off from the main tube the bent side tube contains the cadmium metal and projecting from it into the main tube a closely fitting aluminum tube. The protruding end of this tube is closed except for a fine slit (one or two tenths of a millimeter wide) cut in aluminum foil and placed as close as practicable below the lowest of the filter discs. This side tube is

* A report on the earlier results of this work was given before the Iowa Academy of Science in May, 1927.

[1] Stern, Zeits. f. Physik **2**, 49 (1920); Tykocinski-Tykosiner, Journ. Opt. Soc. Am. **14**, 423 (1927); Costa, Smyth and Compton, Phys. Rev. **30**, 347 (1927).

heated by suitable furnaces. Above the filter a glass tube with a flattened end is shown—this contains a little liquid air and acts as collector for the filtered molecules. The success of the experiment depends upon the prompt condensation of all scattered molecules. To accomplish this the walls of the large tube and the disc system were coated with cadmium and surrounded so far as practicable with liquid air. To eliminate more perfectly the collection of these scattered molecules a stationary plate (not shown) was used as as a baffle to keep the scattered molecules from reaching the upper part of the tube.

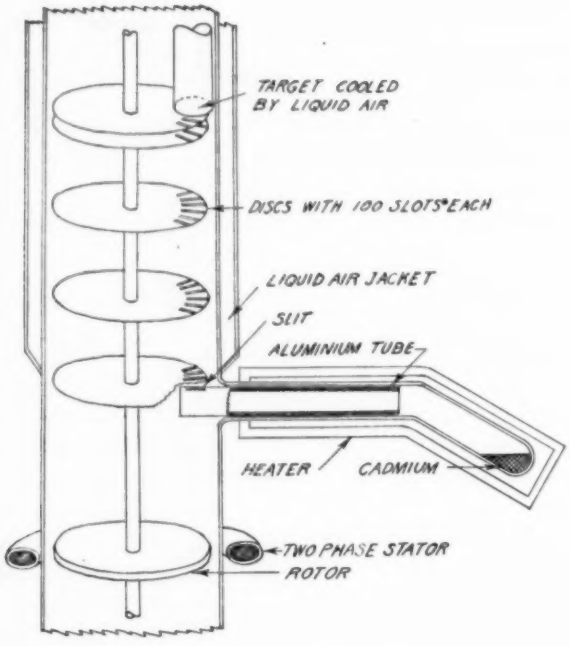

Fig. 1. Diagram of apparatus.

The disc system had hardened steel pivots which were seated in fiber and lubricated. The system could be rotated more or less synchronously up to 7200 R.P.M. Its rate of rotation was measured with a stroboscope.

The theory of the filter is almost self-evident. Consider at first only the two extreme filter discs and suppose each to have but a single slit, the one above the other. The discs are first rotated very slowly and a deposit is obtained marking the "unshifted line." When the discs rotate rapidly the upper disc travels a small distance while the molecule travels the filter length, giving a band of deposit with the fastest molecules registering most closely to the unshifted line. When more slits are used as is desirable to shorten the experiment we get into trouble from "cross fire"; this can be eliminated by using intermediate discs, lined up so as to block all but the desired ray path. As a matter of fact the slots through which a molecular beam travels are not exactly parallel (because of the rotation of the disc during the transit) and

the intermediate discs tend to diminish the effective aperture for the molecules with the larger deflections; this difficulty is easily remedied by making the slots of the intermediate discs somewhat wider than those of the two end discs and by introducing a partially compensating twist in lining up the discs.

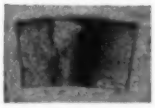

Fig. 2. Photograph of film obtained in a typical run.

Fig. 2 shows the film obtained in a typical run[2] and the points in Fig. 3 give the measured densities as read with a microphotometer by measuring films of known density ratios. The abscissas of the curve and the distances from the base line to a point in the velocity spectrum are proportional to $1/v$ instead of to v.

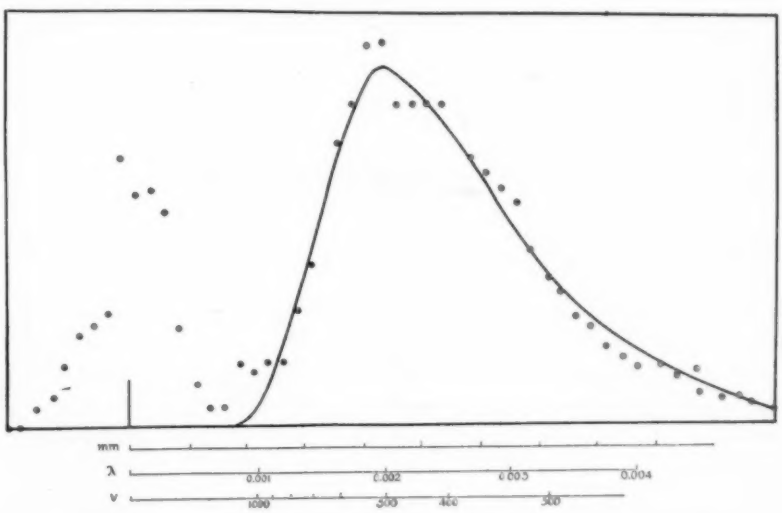

Fig. 3. Densities of the film as measured with a microphotometer.

There are two reasons why the blackening of the film or the ordinate of the curve do not correspond to the ordinate of the Maxwell curve. (1) The densities for low velocities are reduced because these slowly moving molecules are spread out between the center of density and infinity, and the faster molecules, concentrated between the center of density and the origin, have

[2] The photograph (Fig. 2) of the cadmium deposit was taken several months after deposition. It shows the peculiar evaporation or absorption which takes place locally in such films. The dark spots are air bubbles in the glass but the prominent white spot and the smaller white spots in the deposit as well as the disappearance of the central portion of the undisplaced line are phenomena which took place gradually during the course of several months. The "evaporation" seems to be entirely local; a remeasurement of the density of deposit agreed within experimental error with those taken at the time of deposit except in those places where the metal had very obviously and almost completely disappeared.

much greater densities than corresponds to the usual Maxwell probability. (2) What is measured is not the number of molecules of a particular velocity *present* at any instant (as given by the distribution law) but the number *passing through* the slit and landing upon the collecting plate in a certain time which further emphasizes the faster molecules. We may consider the case is more detail.

According to Maxwell the proportionate number of molecules with velocities between v and $v+dv$ which are present at any time in a definite volume is

$$\frac{dN}{N} = \frac{4}{\pi^{1/2}} \frac{v^2}{\alpha^3} e^{-v^2/\alpha^2} dv$$

or combining the constants, $dN = C_1 v^2 e^{-v^2/\alpha^2} dv$, where α is the "most probable velocity." If we confine our attention to the molecules within the aluminum tube which are moving in such a direction as to pass through the slit, we select from the totality a certain small group of molecules whose velocities have certain definite orientations but the distribution law has the above form. However the number of these which pass through a given boundary (the slit) in a given time is proportional to the speed as well as the number present.

$$dN = C_2 v^3 e^{-v^2/\alpha^2} dv \qquad (2)$$

where the meaning of dN has been changed to represent the number of molecules *passing through the slit* in a given time with velocities between v and $v+dv$. But the number of molecules which strike the collector at a distance between x and $x+dx$ and produce the blackening is equal to the number having reciprocal velocities ($\lambda = 1/v$) between λ and $\lambda+d\lambda$. Changing the independent variable then we get

$$dN = (\partial N/\partial v)(dv/d\lambda)d\lambda = C_2 v^5 e^{-v^2/\alpha^2} d\lambda$$

The number of molecules then passing through a slit with "slowness" between λ and $\lambda+d\lambda$ is according to the Maxwell law given by an expression of this form and the blackening of the film should correspond. It is well known that α, the velocity corresponding to the maximum of the Maxwell curve, is the root mean square velocity ($\bar{v}$) times the factor $(2/3)^{1/2}$. The "most probable slowness" the value of λ for which our curve has a maximum can readily be found to be

$$\lambda_m = \frac{1}{\alpha}\left(\frac{2}{5}\right)^{1/2} = \frac{1}{\bar{v}}\left(\frac{3}{5}\right)^{1/2}$$

In the present experiment the temperature was approximately 400°C. The corresponding root mean square velocity ($\bar{v}$) is 388 m/sec, "the most probable velocity" α is 317 m/sec and λ_m, the maximum of our slowness curve, is $\lambda_m = 1/500$ sec/m.

With a disc of 3.15 cm radius rotating 85 revolutions per second and length of filter 12.7 cm, 1 mm shift in spectrum corresponds to a reciprocal speed $\lambda = 1/2140$ sec/m.

The curve is seen to be in good agreement with the theory. Perhaps the agreement is somewhat fortuitous and indeed we have taken some liberty in assigning our zero point which has been taken several tenths of a millimeter away from the most probable center of the undisplaced line to make the points superimpose upon the theoretical curve. The resolution is not as high as desired—the undisplaced line is broader than necessary and if this lack of resolution is considered the agreement between the curve and theory is too good. The measurement of temperature was unsatisfactory—the cadmium was heated and the aluminum tube superheated; the temperature of this tube was determined by an earlier heating when a thermometer was inclosed in the aluminum tube—a direct measurement by thermocouple would be better. The results however are such as to encourage the belief that a really critical test of Maxwell's law is possible.

One consideration of which nothing has been said is the necessity of keeping the vapor pressure of cadmium within the source tube so low that the mean free path is long compared with the slit width. If this were not the case the velocity distribution in the neighborhood of the slit would be far from Maxwellian, and the emerging molecules would collide after leaving the slit and further complicates matters. In the experiment the slit width was less than 0.2 mm and the free path (cadmium at 320°C) was probably of the order of 1 mm. It goes without saying that the gas pressure of the tube must be maintained low enough to make collision during the molecular transit unlikely. In an earlier experiment where these conditions were not suitably attained a curve agreeing rather well with the theory for the faster molecules but departing badly for the slower ones was obtained.

UNIVERSITY OF IOWA,
September 28, 1927.

RADIATION FLUCTUATIONS AND THERMAL EQUILIBRIUM

By Samuel Jacobsohn

Abstract

In the definition of the fluctuation of energy of an oscillator with one degree of freedom there exists an ambiguity involving the energy variation during a single vibration. Only by ignoring this variation is it possible to arrive at the correct fluctuations in a Jeans cube. The energy fluctuations can be accounted for if the radiation in an enclosure is regarded as due to the disturbed vibrations of the charges on the walls provided these disturbances follow, for each mode of vibration, the law of phase relations given by Planck. The method used by Einstein and Hopf for the linear oscillator is extended to the case in which such phase relations exist in the fourier analysis, and in this case it is shown that thermal equilibrium can be accounted for even though the radiation formula be that of Planck, and the electromagnetic theory be used throughout.

THE problem of radiation fluctuations goes back to Einstein's earliest paper on the quantum theory. Starting from the Boltzmann relation $S=k \log W$ between entropy and probability, and the Planck entropy, energy-density formula

$$\partial S/\partial \rho = 1/T$$

he showed that the mean-squared fluctuation from the mean of the energy density in an enclosure containing black-body radiation as given by the Planck radiation formula, could be expressed in the form[1]

$$a v(\epsilon^2) = \rho_\nu d\nu \cdot h\nu + c^3\rho^2 d\nu/(8\pi\nu^2) \qquad (1)$$

The second term could be accounted for on the supposition that these fluctuations are to be ascribed to the interference of the constituent wave trains. The first term was that which would be given by a set of concentrated quanta each of energy $h\nu$, and it was because of this that Einstein was led to his famous hypothesis of light quanta.

For the justification of the second term on the basis of interfering wave trains, Einstein presented a dimensional calculation: the more detailed analysis is due to Lorentz.[2] The separation into these two terms is however of an arbitrary character and Bothe[3] has shown that both terms can be accounted for on extreme quantum lines if account is taken of the fact that the induced emission processes of Einstein[4] give rise to quantum molecules containing two or more quanta.

Inasmuch as the form of expression for the fluctuation which comes out of the thermal theory appears to be inconsistent with that which one com-

[1] Einstein, Ann. d. Physik **17**, 132 (1905); Phys. Zeits. **10**, 185 (1909).
[2] Lorentz, Les Theories Statistiques, p. 114.
[3] Bothe, Zeits. f. Physik **20**, 145 (1923).
[4] Einstein, Phys. Zeits. **18**, 121 (1917).

putes from the interference of the wave trains the Eq. (1) has been held to indicate a fundamental inconsistency between the electromagnetic theory on the one hand, and the Planck law on the other. This conclusion has not been accepted by Laue[5] nor by Planck.[6] The fundamental point at issue is the statistical independence of the constituent wave trains in the fourier analysis of natural radiation. A proof of this independence was given by Einstein and Hopf[7] on the hypothesis that the radiation arose from an independent number of point sources: later in response to the objections of Laue a proof was given by Einstein[8] on somewhat different hypotheses. More recently the question has been taken up again by Planck[6] who, starting from a simplified form of Eq. (1) applicable to a system of only one degree of freedom, which has been given by Laue

$$av[(E-E_{av})^2]=h\nu\cdot E_{av}+(E_{av})^2 \tag{2}$$

shows that the required condition is satisfied if there exist phase relations of a certain type between the various harmonics in the fourier analysis of the vibration.

The question is not only of importance as regards Eq. (1) which has heretofore been the main subject of discussion, but because these fluctuations of energy density are intimately connected with the fluctuations of impulse on an atom placed in the radiation, these determining the Brownian movements, or what is the same thing, the thermal equilibrium of the translational motion of the atom.

It must be pointed out that what is to be called the fluctuation is not even in the case of a system of one degree of freedom, a wholly unambiguous quantity.

Let us consider with Planck a system of one degree of freedom whose vibration expanded as a fourier series over the time interval $t=0$ to $t=T$ is

$$A=\Sigma_n C_n\cos(2\pi nt/T-\theta_n) \tag{3}$$

and whose momentary energy is consequently

$$E=(1/2)mA^2=(1/2)m\Sigma_n\Sigma_{n_1}C_nC_{n_1}\cos(2\pi nt/T-\theta_n)\cos(2\pi n_1t/T-\theta_{n_1})$$

where m is a constant.

Transforming by the relation

$$\cos A\cos B=(1/2)\{\cos(A-B)+\cos(A+B)\}$$

we have

$$\begin{aligned}E=(1/4)m\Sigma_n\Sigma_{n_1}C_nC_{n1}\{&\cos[2\pi(n-n_1)t/T-\theta_n+\theta_{n_1}]\}\\&+\cos[2\pi(n+n_1)t/T-\theta_n-\theta_{n_1}]\}\end{aligned} \tag{4}$$

[5] Laue, Ann. d. Physik **47**, 853 (1915); **48**, 668 (1915).
[6] Planck, Ann. d. Physik **73**, 272 (1924).
[7] Einstein and Hopf, Ann. d. Physik **33**, 1105 (1910).
[8] Einstein, Ann. d. Physik **47**, 879 (1915).

On averaging over the time interval $t=0$ to $t=T$, only the terms $n-n_1=0$ contribute and we have, with Planck

$$E_{av}=(1/4)m\Sigma C_n^2$$

a result which shows that the energy distribution in the fourier analysis is quite independent of the question of the existence of phase relations, depending only on the coefficients.

Planck drops the second term in the expression for E on the ground that the energy is to be considered a slowly variable function of the time. It is not obvious however that the quantity

$$av(E^2-E_{av}^2)=E_{av}\cdot h\nu+E_{av}^2,$$

which is properly an average over all possible phases (in the sense of Gibbs), is to be identified with this quantity rather than the complete expression squared; one obtains an entirely different value for the fluctuation in the latter case, although we shall find reasons for believing that Planck's identification is a correct one. Taking the complete expression, we have

$$E^2=(m/4)^2\Sigma_m\Sigma_{m_1}\Sigma_n\Sigma_{n_1}C_nC_{n_1}C_mC_{m_1}\times$$
$$\left[\begin{array}{l}\cos\,[2\pi(n-n_1)t/T-\theta_n+\theta_{n_1}]\cos\,[2\pi(m-m_1)t/T-\theta_m+\theta_{m_1}]^*\\ +\cos\,[2\pi(n-n_1)t/T-\theta_n+\theta_{n_1}]\cos\,[2\pi(m+m_1)t/T-\theta_m-\theta_{m1}]\\ +\cos\,[2\pi(n+n_1)t/T-\theta_n-\theta_{n_1}]\cos\,[2\pi(m-m_1)t/T-\theta_m+\theta_{m_1}]\\ +\cos\,[2\pi(n+n_1)t/T-\theta_n-\theta_{n_1}]\cos\,[2\pi(m+m_1)t/T-\theta_m-\theta_{m_1}]\end{array}\right]$$

where only the starred terms occur in Planck's analysis. Making the same trigonometric transformation as before and noting that the second and third products when summed are alike,

$$E^2=(1/2)(m/4)^2\Sigma_n\Sigma_{n_1}\Sigma_m\Sigma_{m_1}C_nC_{n_1}C_mC_{m_1}\times$$
$$\left[\begin{array}{l}\cos[2\pi(n-n_1+m-m_1)t/T-\theta_n+\theta_{n_1}-\theta_m+\theta_{m_1}]^*\\ \qquad\qquad +\cos\,[2\pi(n-n_1-m+m_1)t/T-\theta_n+\theta_{n_1}+\theta_m-\theta_{m_1}]^*\\ +2\cos\,[2\pi(n-n_1+m+m_1)t/T-\theta_n+\theta_{n_1}-\theta_m-\theta_{m_1}]\\ \qquad\qquad +2\cos[2\pi(n-n_1-m-m_1)t/T-\theta_n+\theta_{n_1}+\theta_m+\theta_{m_1}]\\ +\cos\,[2\pi(n+n_1+m+m_1)t/T-\theta_n-\theta_{n_1}-\theta_m-\theta_{m_1}]\\ \qquad\qquad +\cos\,[2\pi(n+n_1-m-m_1)t/T-\theta_n-\theta_{n_1}+\theta_m+\theta_{m_1}]\end{array}\right]$$

When averaged over the time $t=0$ to $t=T$ each cosine runs through one or more complete cycles unless the coefficient of t is zero. As we are supposing the vibration to be nearly periodic, the integers n, n_1, m, m_1 are nearly equal and the coefficient can only be zero if there occur two positive and two negative signs in the coefficient. Besides the two starred terms which occur in Planck's analysis, we have only the last term contributing to the average of E^2. This represents the part which arises from the fluctuation of the disturbance during a vibration. It will be seen that the three terms which

come into consideration are obtainable from one another by permuting the indices, so that

$$av(E^2) = (3/2)avE^{*2} \tag{5}$$

where E^* is the value obtained by Planck.

If d_{ij} denotes the well known quantity which is unity for $i=j$ and zero for $i \neq j$

$$av(E^2) = (3/2)av(E^{*2}) = (3/2)(m/4)^2\Sigma_n\Sigma_{n_1}\Sigma_m\Sigma_{m_1}C_nC_{n_1}C_mC_{m_1}d_{n-m,n_1-m_1}\cos(\theta_n - \theta_m - \theta_{n_1} + \theta_{m_1}) \tag{6}$$

In the classical case where the phases are completely haphazard, the cosine terms contribute systematically only if $n=m$, $n_1=m_1$, or if $n=n_1$, $m=m_1$, in which cases the cosine is unity. This would give

$$av(E^2) = (3/2)av(E^{*2}) = 3(m/4)^2\Sigma_n\Sigma_m C_n{}^2C_m{}^2 = 3(m/4)^2\Sigma_n C_n{}^2\Sigma_m C_m{}^2 = 3(E_{av})^2$$

so that

$$av(E^2 - E_{av}{}^2) = 2(E_{av})^2 \tag{6a}$$

whereas

$$av(E^{*2} - E_{av}{}^2) = E_{av}{}^2 \tag{6b}$$

If we rely on Laue's formula (2) which reduces to

$$\epsilon^2 = av(E^2) - E_{av}{}^2 = E_{av}{}^2$$

for $h=0$, we shall have to prefer the method of calculation which Planck uses. The following line of argument points in the same direction and gives some additional information.

Consider in a Jeans cube of side unity the $8\pi\nu^2 d\nu/c^3$ standing waves of frequency between ν and $\nu+d\nu$. We shall suppose the different waves entirely independent of one another, and that each of them on account of the disturbance of the charges which maintain the boundary conditions, is not strictly monochromatic but is representable by a fourier series of form (3). The momentary fluctuations of the standing waves must be considered additive, since between them there exist no phase relations. Since positive and negative fluctuations are to be regarded as equally probable, we have $av(E-E_{av})^2 = (8\pi\nu^2 d\nu/c^3)av(E_1 - E_{1av})^2$, where E, E_1 denote the respective values for the whole system and the single waves. If we put with Planck $av(E_1 - E_{1av})^2 = av(E_1{}^2 - E_{1av}{}^2) = h\nu E_{1av} + E_{1av}{}^2$ we obtain

$$av(E - E_{av})^2 = h\nu E_{av} + c^3 E_{av}{}^2/(8\pi\nu^2 d\nu)$$

since the average energy of the composite system is $8\pi\nu^2 d\nu/c^3$ times that of a single system. If we had included also the terms which arise from the fluctuation of energy during a period we should have arrived at a result which in the classical case was twice too large.

It is further seen that the fluctuation Eq. (1) will be satisfied if the various standing waves are completely independent but each of them is

subject to the relation (2). The term E^2 arises as we have remarked from the terms in which the cosine is identically unity, and Planck shows that the rest of the expression is precisely what would be given if the vibration were to consist of a large number of strictly monochromatic vibrations each of energy $h\nu$ which last for a definite time and then disappear. The natural interpretation of this result on the view of a hohlraum as a kind of Jeans cube is that large groups of electrons come into a kind of resonance for a certain time, and the group is then broken up. It hardly seems possible by merely quantizing individual emitting centers to provide for the fluctuations since Einstein and Hopf established the statistical independence of the wave trains precisely on the assumption of truncated processes of emission by *independent* emitting centers. That the hope of reconciling the wave theory with the quantum theory rests in giving up the idea of the independence of different atoms in radiation and absorption processes has been expressed both from the classical theory side[9] and the quantum theory side[10] and the foregoing may be taken as pointing in the same direction.

Not only is the fluctuation equation of Einstein a consequence of the entropy-probability relation and the Planck law, but if the fluctuation equation be correct and we admit a certain relation of statistical mechanics, the Planck law must follow.

According to Gibbs,[11] the canonical distribution requires the relation

$$kT^2(\partial E/\partial T) = a\nu(E - E_{av})^2$$

setting this equal to

$$h\nu E_{av} + c^3 E_{av}^2/(8\pi\nu^2\, d\nu) \tag{7}$$

we have on integrating

$$E = g(\nu)/[e^{h\nu/kT} - c^3 g(\nu)/(8\pi h\nu^3 d\nu)]$$

For this to be infinite when $T = \text{infinity}$, $g(\nu) = 8\pi h\nu^3 d\nu/c^3$, and

$$E = 8\pi h\nu^3\, d\nu/c^3(e^{h\nu/kT} - 1)$$

On the other hand, if we adhere to the relation

$$a\nu(E - E_{av})^2 = c^3 E_{av}^2/(8\pi\nu^2\, d\nu) \tag{7a}$$

and add the condition $E = 0$ for $T = 0$, we shall have the Rayleigh-Jeans law: $8\pi\nu^2 kt/c^3$.

It is therefore pretty clear that whatever mechanism we may discuss for the purpose of introducing the temperature into the argument, whether it be as with Einstein and Hopf the Brownian movements of an oscillator, or with Planck[12] the mean and mean-squared increase in energy of an oscillator, if the wave trains are assumed constituted so as to lead to Eq. (7a)

[9] Lorentz, Atomes et Electrons, Conseil Solvay, 1923, p. 23.

[10] Stoner, Proc. Camb. Phil. Soc. p. 586 (1925).

[11] Gibbs, Elementary Principles, p. 71; cf. Reiche, The Quantum Theory, p. 139.

[12] Planck, Warmestrahlung, 4. auflage, 1921, pp. 145–159.

only the Rayleigh-Jeans law can come out. If we admit the analysis of Einstein and Hopf, this equation is a necessary consequence of the assumption that the emitting centers are independent.

It is not difficult to give up this assumption, since in an enclosure a large part of the emission from any one atom must be due to the absorption and scattering of light from other centers.

We shall now take up the question of the motion of a resonator in the radiation field[13] and seek to show that the Brownian movements required by equipartition between the translation degrees of freedom will be fully accounted for by the classical laws of electromagnetism if phase relations of a kind exactly analogous to those introduced by Planck exist among the different frequencies in the fourier analysis.

The notation and method used by Einstein and Hopf will be followed to facilitate comparison in the classical case of assumed independence of phase, which must serve as a guide in making approximations.

Let the oscillator vibrate parallel to the z-axis, the differential equation for its electric moment f being:

$$16\pi^4\nu_0^3 f+4\pi^2\nu_0 d^2f/dt^2-2\sigma d^3f/dt^3=3\sigma c^3E_z \tag{8}$$

If the oscillator is acted on by the disturbance $E_z=\Sigma B_n\cos(2\pi nt/T-\theta_n)$, and we put $D_n=3c^3T^3B_n/16\pi^3$,

$$\sin\gamma_n=1/(1+[T^3\pi^2(\nu_0^2-n^2/T^2)/\sigma n^3]^2)^{1/2} \tag{8a}$$

the solution for the electric moment is:

$$f=\Sigma D_n(\sin\gamma_n/n^3)\cos(2\pi nt/T-\theta_n-\gamma_n) \tag{8b}$$

it being supposed that the oscillator has been so long in the field that the initial conditions have been damped out.

For the impulse J communicated to the oscillator between the times t_1 and $t_2=t_1+\tau$, one may write[14]:

$$J=\int_{t_1}^{t_2}(\partial E_z/\partial x)\,f\,dt$$

where

$$\partial E_z/\partial x=\Sigma E_m\sin(2\pi mt/T-\eta_m)$$

In the analysis of Einstein and Hopf the quantities C, D, θ, η are supposed completely independent, a hypothesis which we are dropping, although we may suppose it approximately fulfilled at high temperatures and long wavelengths.

We have

$$J=\int_{t_1}^{t_2}dt\Sigma_m\Sigma_n E_mD_n(\sin\gamma_n/n^3)\cos(2\pi nt/T-\theta_n-\gamma_n)\sin(2\pi mt/T-\eta_m) \tag{9}$$

[13] Breit, Phil. Mag. **49**, 537–565, has treated from somewhat the same standpoint the problem of the motion of an electron in a radiation field. His methods are similar to those of Lorentz and his pupils, whereas the present paper uses the earlier ones of Einstein.

[14] Einstein and Hopf, Ann. d. Physik **33**, 1112 (1910).

or since

$$\cos A \sin B = \tfrac{1}{2}[\sin (A+B) - \sin (A-B)]$$

$$J = (1/2)\int_{t_1}^{t_2} dt \Sigma_m \Sigma_n (\sin \gamma_n / n^3) E_m D_n \{\sin [2\pi(m+n)t/T - \theta_n - \eta_m - \gamma_n] - \sin [2\pi(n-m)t/T - \theta_n + \eta_m - \gamma_n]\}$$

On integration of the first term the quantity $2\pi(m+n)/T$ comes down as a divisor. This is of order $4\pi\nu$ and so this term need not be considered in comparison with the much larger quantity arising from the second term, so that

$$J = \Sigma_m \Sigma_n E_m D_n (\sin \gamma_n / n^3)[T/2\pi(n-m)]\{\cos [2\pi(n-m)t_2/T - \theta_n + \eta_m - \gamma_n] - \cos [2\pi(n-m)t_1/T - \theta_n + \eta_m - \gamma_n]\}$$

which may be written, since $t_2 - t_1 = \tau$

$$J = -\tfrac{1}{2}\Sigma_m \Sigma_n E_m D_n (\sin \gamma_n / n^3) \sin [2\pi(n-m)(t_1+t_2)/2T - \theta_n + \eta_m - \gamma_n] [\sin \pi(n-m)\tau/T]/[\pi(n-m)/T] \tag{10}$$

Making use of the relation $\sin A \sin B = (1/2)\{\cos(A-B) - \cos(A+B)\}$ we have on squaring (10)

$$J^2 = (1/8)\Sigma_m \Sigma_n \Sigma_{m_1} \Sigma_{n_1} E_m D_n E_{m_1} D_{n_1} (\sin \gamma_n / n^3)(\sin \gamma_{n_1} / n_1^3) \frac{[\sin \pi(n-m)\tau/T]}{\pi(n-m)/T} \times \frac{[\sin \pi(n_1 - m_1)\tau/T]}{\pi(n_1 - m_1)/T}$$

$$\times \begin{Bmatrix} \cos [2\pi(n-m-n_1+m_1)(t_1+t_2)/2T - \theta_n + \theta_{n_1} + \eta_m - \eta_{m_1} - \gamma_n + \gamma_{n_1}] \\ -\cos [2\pi(n-m+n_1-m_1)(t_1+t_2)/2T - \theta_n - \theta_{n_1} + \eta_m + \eta_{m_1} - \gamma_n - \gamma_{n_1}] \end{Bmatrix}. \tag{11}$$

Here $(t_1+t_2)/2$ is the mean time on the interval under consideration. If J^2 be averaged over all possible intervals each such cosine will run over one or more cycles of values and contribute nothing in the average. This does not apply, however, to those terms in which the coefficient of t_1+t_2 vanishes. The average of J^2 therefore reduces to terms of the latter type. Letting, as before, d_{ij} represent the quantity which is unity for $i=j$ and zero otherwise

$$av J^2 = (1/8)\Sigma_m \Sigma_n \Sigma_{m_1} \Sigma_{n_1} E_m D_n E_{m_1} D_{n_1} (\sin \gamma_n / n^3)(\sin \gamma_{n_1} / n_1^3) [\sin^2 \pi(n-m)t/T]/[\pi(n-m)/T]^2 \times [d_{n-m, n_1-m_1} \cos (\theta_n - \theta_{n_1} - \eta_m + \eta_{m_1} + \gamma_n - \gamma_{n_1}) - d_{n-m, m_1-n_1} \cos (\theta_n + \theta_{n_1} - \eta_m - \eta_{m_1} + \gamma_n + \gamma_{n_1})]$$

The second set of terms must be expected to contribute in the classical case if at all. But we shall find that to arrive at the accepted result in this case these terms may be ignored. No further account will be taken of them, therefore.

We have further in the classical case that only the terms $n=n_1$, $m=m_1$ contribute systematically. As the natural extension it may be supposed that the cosine factors contribute systematically within a band of frequencies which is small compared to the resonance band of an oscillator. This will permit setting $\gamma_n=\gamma_{n_1}$ so that

$$av(J^2)=(1/8)\Sigma_m\Sigma_n\Sigma_{m_1}\Sigma_{n_1}E_mD_nE_{m_1}D_{n_1}(\sin^2\gamma_n/n^6)\,[\sin^2\pi(n-m)\tau/T] \\ /\,[\pi(n-m)/T]^2 d_{m-n,m_1-n_1}\cos(\theta_n-\theta_{n_1}-\eta_m+\eta_{m_1}) \qquad (12)$$

In the case where the terms are restricted to $n=n_1$, $m=m_1$ we have on re-introducing the quantity B_n from (8a)

$$av(J^2)=\tfrac{1}{2}(3c^3T^4/32\pi^4)^2\Sigma_m\Sigma_nE_m{}^2B_n{}^2(\sin{}^2\gamma_n/n^6)\,[\sin^2\pi(n-m)\tau/T]/(n-m)^2 \qquad (12')$$

As this is the expression obtained by Einstein and Hopf by a calculation differing in detail from the present one, it appears that our neglect of the second set of terms in (11) was legitimate.

Referring back to (12), it will be seen that the factor $\sin^2\gamma$ represents the resonance curve which renders values of n remote from ν_0T inoperative. The factor $\sin^2\pi(n-m)/T \div [\pi(n-m)\tau/T]^2$, which is of order $1/\pi^2(\nu-\nu_0)^2$, further restricts the values of m to those near n. We have already postulated a systematic contribution only for $n \doteqdot n_1$ and the factor $d_{n-m\ n_1-m_1}$ finally restricts m_1 to the value n_1-n+m. In spite of the fact that $av(J^2)$ appears as an infinite summation, the values of the integers involved all lie near ν_0T. To actually evaluate this expression would require us to express the C's and η's in terms of the D's and θ's, involving as yet unsolved details in regard to the structure of the radiation. Considering the similarity of this expression to that obtained by Planck for the energy fluctuations, it seems reasonable that the effect is here also to increase the fluctuations of impulse in the ratio

$$(\rho h\nu+c^3\rho^2/8\pi\nu^2)/(c^3\rho^2/8\pi\nu^2)$$

This is all that thermal equilibrium demands.

The writer wishes to express his great indebtedness to Professor W. F. G. Swann for his continual encouragement and many suggestions.

SLOANE PHYSICAL LABORATORY,
YALE UNIVERSITY,
June, 1925.

NOTE ON THE FLUCTUATIONS IN BLACK BODY RADIATION

By Samuel Jacobsohn

Abstract

The method used by Ehrenfest for the calculation of energy fluctuations in a one-dimensional continuum is adopted for a re-examination of Lorentz's calculation in the three dimensional case. It is shown that on the basis of the quantum statistics this goes through and yields the result required by the Planck formula. The difficulty that the fluctuations involve a term depending on the square of volume appears here also, and a suggestion is given as to the source of the difficulty which promises information on the structure of the light-quantum.

IN AN illuminating paper[1] Ehrenfest has re-examined the fluctuation of energy distributed among the various frequencies for the case of the one-dimensional analog of the Jeans-Debye cube and has found, in addition to the term proportional to the square of the energy-density arising from the interference *per se*, another term which takes its origin from the statistics of the system. If the statistics of the system is that required by the Debye system of quantised standing waves this second term is precisely what has been sought for on the basis of the Planck radiation formula, at least if the discussion is limited to the hohlraum in its entirety. In what follows these considerations have been applied to the Lorentzian calculation in the three-dimensional case, with results which seem particularly instructive.

Let us consider a set of plane wave trains whose electric vectors are in the typical case[2]

$$\begin{aligned} &b_1\mathbf{b}_1 \cos(nt-\xi x-\eta y-\zeta z+q_1) \\ &b_2\mathbf{b}_2 \cos(nt-\xi x-\eta y-\zeta z+q_2) \end{aligned} \tag{1}$$

where $\mathbf{b}_1\mathbf{b}_2$ are unit vectors at right angles to each other and to the direction of propagation. As it is necessary to compound the fields of wave trains of nearly the same direction, it is particularly convenient to suppose that the directions $\mathbf{b}_1\mathbf{b}_2$ are continuous functions of the direction of the wave normal. The electric and magnetic components of the field being linear functions of these quantities, the energy appears as a set of terms of form $\cos^2(nt-\xi x-\eta y-\zeta z+q)$ plus a set of product terms of form $\cos(nt-\xi x-\eta y-\zeta z+q)\cos(n't-\xi' x-\eta' y-\zeta' z+q')$. When integrated through a rectangular parallelepiped of sides f, g, h, the energy is found by Lorentz to be $E=fgh\times$

[1] Ehrenfest, Zeits. f. Physik **34**, 363 (1926).

[2] The vector expression has been used by Breit, Phil. Mag. **49**, 537–565 (1925). Otherwise the notation is that of Lorentz, Les Theories Statistiques, Note 7, p. 114.

$$\left[\begin{array}{l} \tfrac{1}{2}\Sigma(b_1^2+b_2^2) \\ +\tfrac{1}{2}\Sigma\Sigma'\dfrac{\sin\frac{1}{2}(\xi-\xi')f}{\frac{1}{2}(\xi-\xi')f}\cdot\dfrac{\sin\frac{1}{2}(\eta-\eta')g}{\frac{1}{2}(\eta-\eta')g}\cdot\dfrac{\sin\frac{1}{2}(\zeta-\zeta')h}{\frac{1}{2}(\zeta-\zeta')h}(\boldsymbol{b}_1\cdot\boldsymbol{b}_1'+\boldsymbol{b}_2\cdot\boldsymbol{b}_2') \\ \times\{b_1b_1'\cos[(n-n')t+(q_1-q_1')]+b_2b_2'\cos[(n-n')t+(q_2-q_2')]\} \end{array}\right] \quad (2)$$

+ terms found to have negligible effect.

It is clear that the time average of E appears here as

$$E_{av}'=(1/2)fgh\cdot\Sigma(b_1^2+b_2^2) \quad (3)$$

and Lorentz proceeds by averaging $(E-E_{av}')^2$. But what the statistical reasoning furnishes as $(E-E_{av})^2$ is not directly the time average of the square of the departure of E from its time average, but rather the grand average of the square of the departure of E from its grand average, where the grand average must be considered as taken over all possible redistributions of the constants b, q. If we may indeed consider this a time average it will only be on the basis of an assumption that the system (and the constants b, q) will in the course of time pass through all possible revaluations.

Confining ourselves then to the grand average, we have to evaluate

$$\text{av. } (E-E_{av})^2=\text{av. } (E^2)-E_{av}^2$$

which we may do by using the form of expression on the right.

Squaring the expression (2), we have first to be averaged

$$E^2=(fgh)^2\times\left[\begin{array}{c} \tfrac{1}{4}\sum\sum'(b_1^2+b_2^2)(b_1'^2+b_2'^2) \\ +\tfrac{1}{8}\sum\sum'\dfrac{\sin^2\frac{1}{2}(\xi-\xi')f}{[\frac{1}{2}(\xi-\xi')f^2]}\dfrac{\sin^2\frac{1}{2}(\eta-\eta')g}{[\frac{1}{2}(\eta-\eta')g]^2}\dfrac{\sin^2\frac{1}{2}(\zeta-\zeta')h}{[\frac{1}{2}(\zeta-\zeta')h]^2} \\ (\boldsymbol{b}_1\cdot\boldsymbol{b}_1'+\boldsymbol{b}_2\cdot\boldsymbol{b}_2')^2\,(b_1^2b_1'^2+b_2b_2'^2 \end{array}\right] \quad (4)$$

+ terms which vanish in the averaging.

Because of the rapid convergence introduced by the factors $\sin^2\frac{1}{2}(\xi-\xi')f/[\frac{1}{2}(\xi-\xi')f]^2$, etc., and the assumed continuity of the vectors $\boldsymbol{b}_1$, $\boldsymbol{b}_2$, $\boldsymbol{b}_1'$, $\boldsymbol{b}_2'$, we have for all relevant terms $\boldsymbol{b}_1\cdot\boldsymbol{b}_1'+\boldsymbol{b}_2\cdot\boldsymbol{b}_2'=2$, very approximately, and since av. $(b_1^2b_1'^2+b_2b_2'^2)=(\text{av. } b_1^2)^2+(\text{av. } b_2^2)^2$, the second term in (4) reduces to

$$\frac{1}{4}\Sigma\Sigma'\frac{\sin^2\frac{1}{2}(\xi-\xi')f}{[\frac{1}{2}(\xi-\xi')f]^2}\frac{\sin^2\frac{1}{2}(\eta-\eta')g}{[\frac{1}{2}(\eta-\eta')g]^2}\frac{\sin^2\frac{1}{2}(\zeta-\zeta')h}{\frac{1}{2}(\zeta-\zeta')h}\{(\text{av.}\,b_1^2)^2+(\text{av.}\,b_2^2)^2\}$$

the summation now allowing each term to recur again as a permutation of (ξ, η, ζ) with (ξ', η', ζ').

It is to be noted that in this second term there are lacking the contributions corresponding to $\xi=\xi'$, $\eta=\eta'$, $\zeta=\zeta'$. Insofar as these need to be taken account of physically, they are present in the first term of (4), which for statistical reasons must be dealt with separately. For the purpose of converting the double summation into an integration, we add and subtract the missing terms[3] and obtain in quite the way outlined by Lorentz the slightly different result.

[3] Lorentz takes no account of these terms in passing to the integration, but we shall find the subtracted terms of use.

$$(fgh)^2\begin{cases}\frac{1}{4}\Sigma\Sigma'(b_1^2+b_2^2)(b_1'^2+b_2'^2)_{av}-\frac{1}{4}\Sigma(\text{av}.b_1^2)^2+(\text{av}.b_2^2)^2\\ +\pi^2c^3\{f(n)\}^2dn\cdot fgh/n^2\end{cases} \tag{5}$$

where $f(n)dn=\Sigma(b_1^2)_{av}$.

We have now to subtract

$$E_{av}^2=\tfrac{1}{4}\Sigma\Sigma'(\text{av}.b_1^2+\text{av}.b_2^2)(\text{av}.b_1'^2+\text{av}.b_2'^2). \tag{6}$$

and besides the last term of (5) which Lorentz finds, there are the terms

$$\begin{aligned}(fgh)^2&\left[\begin{matrix}\frac{1}{4}\Sigma\text{av}.b^4+\frac{1}{4}\Sigma\Sigma'\text{av}.b^2\cdot\text{av}.b'^2-\frac{1}{4}\Sigma(\text{av}.b^2)^2\\ -\frac{1}{4}\Sigma\Sigma'\text{av}.b^2\cdot\text{av}.b'^2-\frac{1}{4}\Sigma(\text{av}.b^2)^2\end{matrix}\right]\\ &=V^2\cdot\tfrac{1}{4}\{\Sigma(\text{av}.b^4)-2\Sigma(\text{av}.b^2)^2\}\quad\text{where}\quad V=fgh\end{aligned} \tag{7}$$

The products of terms by themselves give rise to the single summations, of distinct terms to the double summations.

It will be seen that there remain only single summations to consider, permitting one to speak unambiguously of the summation over a band of frequencies dn. Because of the occurrence of the terms $\frac{1}{4}\Sigma[b^4{}_{av}+2(b^2{}_{av})^2]$, it is not possible to calculate the desired fluctuation independently of a knowledge of the statistics of the system. With Ehrenfest, we therefore apply the Planck-Debye statistics. There being by the Jeans analysis $8\pi\nu^2d\nu\cdot V/c^3$ independent coefficients in the problem, it remains only to compute the value of

$$\text{av}.(\tfrac{1}{2}b^2V)^2-2(\text{av}.\tfrac{1}{2}b^2V)^2 \tag{8}$$

which on the basis of the Planck assumption that the probability of an energy $nh\nu$ is proportional to $e^{-\frac{nh\nu}{kT}}$, is readily found to be $h\nu\cdot\frac{1}{2}(b^2V)_{av}$. The summation of all the terms is thus $8\pi\nu^2d\nu\cdot V\cdot h\nu(\frac{1}{2}b^2V)_{av}/c^3$ or $h\nu\cdot E_{av}$, the remaining term required by the Planck radiation formula.

While the desired result has been arrived at, the argument is nevertheless open to objection. In the final result the fluctuation is proportional to the volume, whereas from formula (7) it is to be expected that if the coefficients b correspond to physical wave trains, they should be independent in magnitude and number of the size of the volume V, and the contribution of the terms (7) therefore proportional to V^2. A similar difficulty turns up in Ehrenfest's analysis and is attributed to the fact that the fluctuation in one volume element is not independent of that in another.

It may be argued with some justice that the whole procedure of computing the energy in a small part of a larger enclosure is at fault[4]; that the Jeans-Debye analysis into standing waves subject to the quantum theory succeeds only because the surface charges necessary to maintain the conditions on the boundary constitute Hertzian oscillators, and it is in reality these which have been quantized, and whose energy has been computed.

[4] Cf. Lorentz, Theory of Electrons, § 18. Swann, Fundamentals of Electrodynamics pp. 36, 37, in Bulletin Nat. Research Council No. 24.

Such a stringent view seems however not to be necessary. If we seek in the analysis why one term comes out proportional to V while the other is proportional to V^2, we shall find that while the former arises from the interference of distinct terms and is thus affected by the factor

$$\frac{\sin^2 \tfrac{1}{2}(\xi-\xi')f}{[\tfrac{1}{2}(\xi-\xi')f]^2} \frac{\sin^2 \tfrac{1}{2}(\eta-\eta')g}{[\tfrac{1}{2}(\eta-\eta')g]^2} \frac{\sin^2 \tfrac{1}{2}(\zeta-\zeta')h}{[\tfrac{1}{2}(\zeta-\zeta')h]^2} \tag{9}$$

which on integration introduces a factor $1/V$, the latter term arises from the interference of each wave train with itself. Yet if we consider that there does not exist in nature a set of infinite, unidirectional and strictly unifrequentic wave trains, we see that a finer analysis would resolve each of the wave trains which we have assumed into a set of coherent wave trains of approximately the same direction and frequency. In the calculation of the mutual interference of these components such a factor (9) may be expected to enter. This brings us back to a standpoint close to that of the preceding paper, and particularly close to that of Breit.[3] A re-analysis of the problem with the object of finding a suitable example of a set of coherent wave trains of the required kind should provide a wave picture of the light-quantum.

THE GAERTNER SCIENTIFIC CORPORATION,
CHICAGO, ILL.
July 12, 1927.

INTERNAL FRICTION IN SOLIDS

By A. L. Kimball and D. E. Lovell

Abstract

It is shown from tests on eighteen different solids, including several metals, glass, celluloid, rubber and maple wood, that the internal friction for strains below the elastic limit does not obey the liquid viscosity law, as is usually assumed, according to which the frictional force depends upon the velocity of strain, but that the internal friction is entirely independent of strain velocity, so far as can be observed. It was found to depend upon the amplitude of strain during the strain cycles and approximately to obey the law: Energy loss per cycle per unit volume equals ξf_m^2. In this expression f_m is the maximum value of the stress during the stress cycle and ξ a proportionality factor, which may be called the internal friction constant. The method used was to measure the transverse deflections of the end of a rod, about a meter long, of the material being studied, which transverse deflections were produced during rotation of the rod when its end was deflected downwards by suitable loads on it. The experiments differ from most previous work in that relatively large masses of material were employed, tending to reduce surface effects, which are likely to enter in the case of vibration decrement experiments on wires and on thin strips. A table of the internal friction constants obtained is given, and also a table of similar internal friction constants calculated from data of previous investigators. A reasonable agreement is found.

FOUR years ago one of the authors of this paper briefly described how internal friction within a revolving shaft supported in bearings produced a disturbing force which should cause the shaft to whirl or whip at its natural vibration period, and demonstrated the phenomenon by a small model.[1] An attempt was subsequently made to evaluate the coefficient of viscosity of a nickel steel shaft, in order to obtain quantitative information about this disturbing force, but it was unexpectedly found that the internal frictional forces were not like those of a viscous fluid where the forces are greater the more rapid the deformation, but that the dissipative forces were the same whatever the speed of deformation. A search of the literature on the subject revealed the fact that internal friction in solids has been and is at the present time treated as a viscous friction by the great majority of writers on this subject.[2] There are a few, however, who appreciate that this law does not hold in the range of ordinary low period vibration frequencies.[3]

[1] A. L. Kimball, Phys. Rev. **21**, 703 (June 1923).

[2] See Honda and Konno, Phil. Mag. **42**, 115 (1921); Iokibe and Sakai, Phil. Mag. **42**, 397 (1921); Lesch, Zeits. angew. Math. und Mech. **4**, 124 (1924); C. E. Guye, Jour. d. Physique 620 (1912). See also Ibbetson, Mathematical Theory of Elasticity, p. 175 (Macmillan, 1887); Prescott, Applied Elasticity, p. 44 (Longmans, 1924).

[3] See, for instance, Hopkinson and Williams, the Elastic Hysteresis of Steel, Roy. Soc. Proc. **A87**, pp. 502–511 (1912); F. E. Rowett, Elastic Hysteresis in Steel, Roy. Soc. Proc. **A89**, 528–543 (1914); K. Bennewitz, Phys. Zeits. **21**, 703 (1920); K. Bennewitz, Phys. Zeits. **25**, 417–431 (1924); H. Jordan, Deutsch. Phys. **18**, 423 (1915). See also results of Lindsay, Phys. Rev. **3**, 397–438 (1914).

In this paper it is shown that over a considerable frequency range and stress amplitude range for a number of solids of very different physical properties the frictional loss per cycle of stress at a point in the solid is independent of the frequency of performance of the stress cycles, like magnetic hysteresis. In fact, this law has not been found to fail thus far for any solids tested by the writers of this paper, except for very low frequencies of the order of one cycle in several minutes, where the frictional loss per cycle is found to *increase*.

Method of Experiment

The method used was a refinement of that used by Wöhler in studies of the fatigue strength of metals made by him many years ago. Recently this method was used by Mason and analyzed by him.[4] An article on this subject by Inglis has also recently appeared.[5] In the experiments described in this paper, however, the internal friction during stress cycles below the elastic limit only was studied.

Figs. 1 and 2 show a photograph and drawings of the apparatus used. The materials tested were made into the form of rods, usually 1.27 cm in

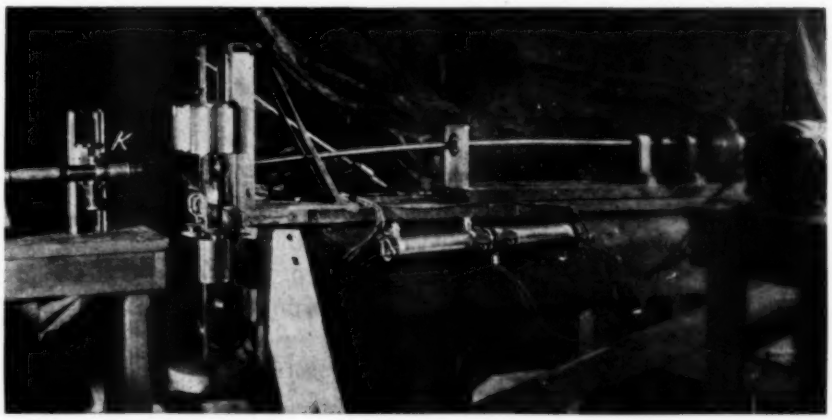

Fig. 1. Photograph of apparatus.

diameter and about 1 meter long. The rod was supported in two ball bearings B_1 and B_2, and revolved by means of an electric motor through the pulley P which was supported in the bearings marked B, the torque being transmitted to the rod by means of a small universal coupling C. The bearing B_2 was located so that more than half of the rod overhung. On the projecting end of the rod was another ball bearing B_3, on which was hung the frame U, which carried a weight W on the pan at its bottom. The rod was thus deflected downwards, as shown in the photograph of Fig. 1, and at the same time it was free to revolve. The frame U carries four plungers which dip into

[4] See article on this subject by Mason, Engineering **15**, 698–9 (1923).

[5] N. P. Inglis, Hysteresis and Fatigue of the Wöhler Rotating Cantilever Specimen, The Metallurgist, Feb. 1927.

four rigidly supported cups containing a suitable damping fluid. This proved an effective means of steadying the end of the rod during revolution, so that the amount of its deflection could be observed.

Fig. 3 shows how the end of the rod was deflected in these experiments. The deflection was not exactly downwards but was displaced by an angle ϕ from the vertical, because of the internal friction in the revolving rod. As

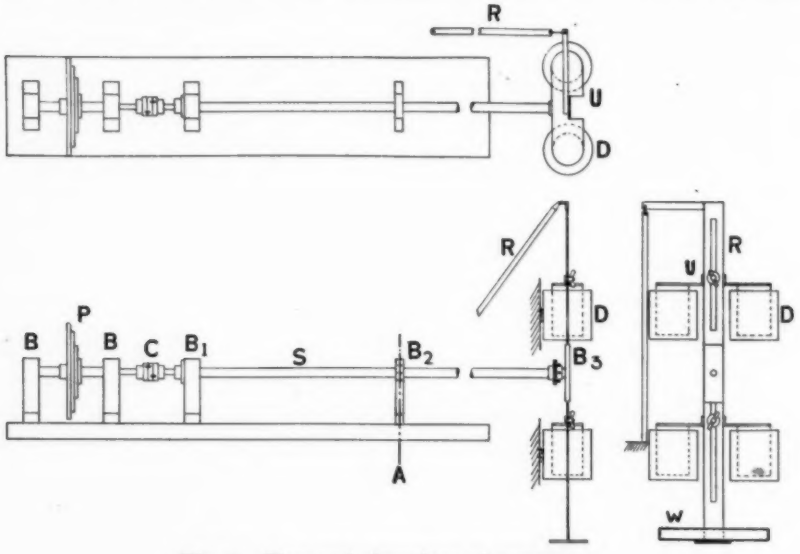

Fig. 2. Plan and elevations of apparatus.

the rod revolves, the fibers parallel to its axis are carried around its axis, alternately up on one side and down on the other. As they move up they stretch, and as they move down they shorten. Any frictional resistance to the process of lengthening results in tension, and frictional resistance to the process of shortening results in compression. Consequently, in this case the upward moving fibers are in frictional tension, T_F, and the downward moving ones are in frictional compression, C_F. For the direction of rotation shown in Fig. 3, the left hand fibers are therefore in tension due to this cause and the right hand ones are in compression. These frictional stresses are superimposed upon the elastic stresses, T_E and C_E, and just as the elastic stresses by themselves produce an upward reaction, R_E, so the frictional stresses by themselves produce a transverse reaction. The forces, R_E and R_F, are components of the force which balances W exerted by the weight on the end of the shaft (Fig. 3). If the weight is removed, R_E and R_F vanish (neglecting the weight of the rod) so that both the elastic and frictional couples must vanish. If $\phi=0$, $R_F=0$, that is, no frictional force is present. This is true when the rod has the weight on its end, but is not revolving. It will be shown later that the transverse deflection produced by R_F gives a means of measuring the amount of internal friction in the rod, and how the internal friction varies with stress amplitude and frequency.

The sideways displacement of the rod was measured by means of a cathetometer (K, Fig. 1). On the end of the shaft was fixed a pin point, the

tip of which was polished and illuminated by means of an arc lamp, giving a small bright spot suitable for observation. Set screws were provided in order to set the point as nearly on the axis of rotation as possible. Observations were taken as follows: a suitable weight was placed upon the pan W, Fig. 2; the speed of revolution of the rod was brought up to some chosen value, say 1,000 r.p.m.; and the position of the pointer noted on the scale of the cathetometer. In most cases oscillations made it impossible to have the pin point centered for all speeds, so that a small bright circle or ellipse was seen in the cathetometer. The position of its center was found by taking settings on its circumference. The direction of rotation of the rod was then *reversed*, and another observation of the position of the pin point taken.

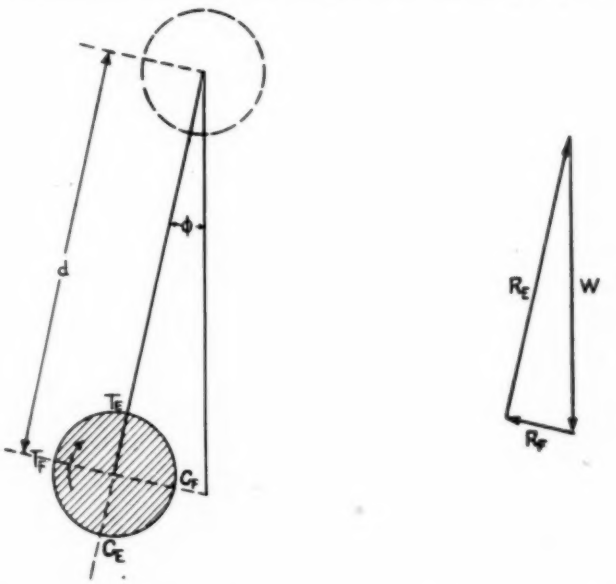

Fig. 3. View of weighted end of shaft showing sideways deflection due to internal friction.

In the design of this apparatus great precaution was required to avoid surface friction effects or reactions of any kind which might produce a false reading, such as might come from the couplngs or the bearings. Friction in the bearing journals does not enter as long as all the bearing axes are parallel. An experiment on an exaggerated case of bearing friction was made and this conclusion verified. No rings of any sort should be fitted on the test rod, otherwise surface contact friction may be produced. This point was kept in mind when using the ball bearings.

Internal Friction Independent of Speed of Performance of Strain Cycle

According to the classical theory of viscosity the transverse deflection of the rod should be proportional to the speed of rotation. The first experiment was made on a rod of 3.5 percent nickel steel in order to observe the increase in the transverse deflection with speed, but no such increase in deflection

was observed over a speed range of from 2 to 3 up to 200 cycles per second. A definite deflection was present, however, as was found by reversing the direction of rotation of the rod. The amount of the transverse deflection could be increased only by increasing the load on the end of the rod, but was

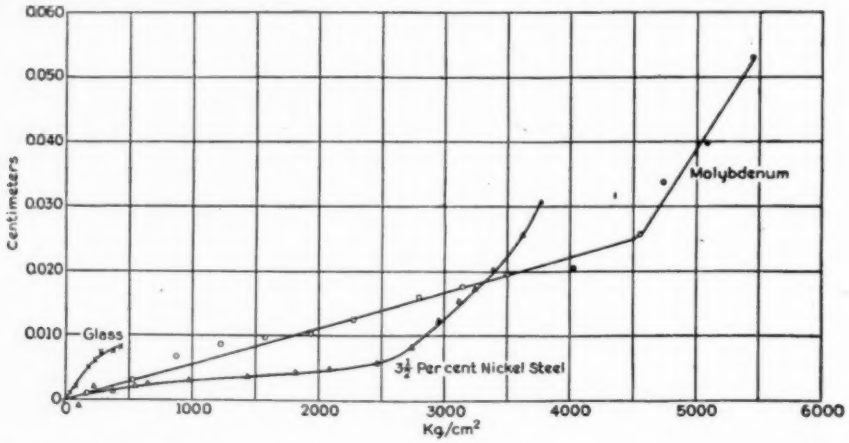

Fig. 4. Curves of sideways deflection at end of shaft plotted against downward deflection and maximum stress intensity.

found for every load to be entirely independent of the rotational speed of the rod. This showed that for nickel steel the forces produced by friction within the rod are independent of the velocity of strain, and that for a given amplitude of strain, the frictional loss per cycle is independent of the speed of performance of the strain cycle.

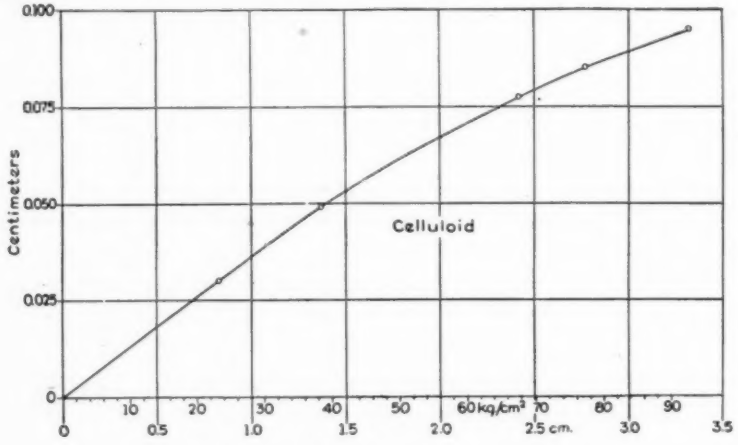

Fig. 5. Same as Fig. 4 for case of celluloid.

A considerable number of metals, alloys and other solids have been tested by the revolving rod method, and every solid thus far examined exhibits an internal friction which is independent of the speed of performance of the strain cycles. This characteristic of internal friction in solids thus appears to be universal.

Figs. 4 and 5 show typical curves of internal friction for molybdenum, 3.5 percent nickel steel, glass and celluloid for varying loads on the rods; that is, for varying bending stresses in the rods, the speed in each case being constant. Figs. 6 and 7 show the same thing but with fixed loads on the rods and varying speed.

Other materials which exhibit a linear relation between internal friction and maximum stress are: swaged quarter-inch-diameter tungsten (up to its

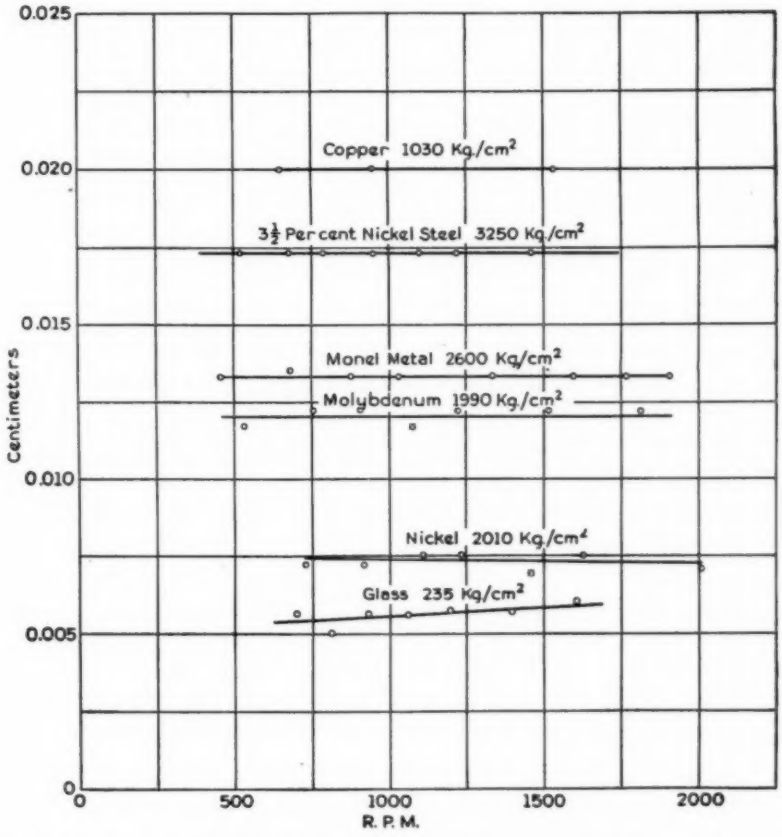

Fig. 6. Curves of sideways deflection at end of shaft plotted against speed of rotation for several different materials.

breaking point), maple wood, zinc, commercial rolled nickel, and copper (up to 7,000 lbs. per sq. in.). In the case of the other materials listed, the linear relation is only an approximation.

Internal friction is known to be a very variable thing, depending upon the past thermal and mechanical history of the specimen. The material often appears to be in an unstable state which is shown by a considerable change in the internal friction, with the first few cycles. After a few hundred cycles a so-called "cyclical state" is reached in which the internal friction remains about constant as long as stress and heat conditions are not changed too much.

The materials whose friction coefficients are compared in Table I were in a cyclical state, and the values of these coefficients afford a fairly good comparison between the internal friction of these various materials.

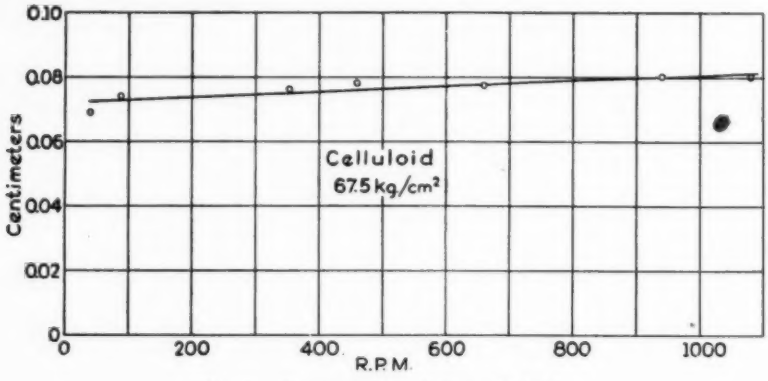

Fig. 7. Same as Fig. 6 for celluloid.

Definition of Coefficient of Internal Friction

A question which arises at this point is how the coefficient of internal friction is best defined. To have a definite meaning the coefficient of internal friction must be based upon a definite law of internal friction. From a study of a large number of curves of the revolving rod experiment in connection with the literature on this subject, the law of internal friction which most generally fits the facts and which at the same time is a simple one, is

$$F = \xi f^2_m \tag{1}$$

where F is the frictional loss per unit volume per cycle at a particular point; f_m the amplitude of the stress cycle above and below zero stress at the point in question; and ξ is the internal friction constant, the internal friction loss per unit volume per cycle per unit stress amplitude.

Table I gives a list of all the materials thus far tested. The internal friction constant is expressed in ergs per cm³ per dyne/cm² stress amplitude. The materials in this table, with four exceptions, are seen to be metals and alloys. Even for the others, celluloid, glass, maple wood and rubber, the frictional loss per stress cycle is independent of frequency. Glass was somewhat erratic, because of the small stresses used and the difficulty of observation, but there is no doubt as to the frictional loss per cycle being practically independent of frequency. In the case of rubber a vibration test was made, using a circular bar of rubber 2.48 cm diameter and 53.3 cm long. Torsional vibrations were produced using a weight whose moment of inerita was so varied that a 4 to 1 variation in frequency was produced. In this case also, as nearly as could be observed, the frictional loss per cycle was a constant for a given stress amplitude. Of the metals and alloys tested, tin and zinc are seen to have much higher coefficients of internal friction than the others. Monel metal and nickel, though very ductile, have little frictional loss.

Discussion of the Law of Internal Friction

It should be clearly understood that the internal friction studied in this paper is for small stress amplitudes, such as those which arise in a vibrating body. If the stress range is so large that the elastic limit of the solid is approached, the internal friction begins to rise rapidly, and the law of Eq. (1) no longer holds. The plastic yielding characteristic of many solids above the yield point belongs to a class of internal friction phenomena completely outside of the range of, and governed by different laws from, the phenomena here studied.

Table I

Internal friction constant for various materials.

Material	Tan ϕ $\times 10^3$	Elastic Modulus in dynes/cm^2 $\times 10^{-11}$	Internal Friction constant (c.g.s. units) $\times 10^{15}$
Rubber 90% pure*			19,000,000.
Celluloid	14.4	0.214	21,000.
Tin, swaged	40.7	3.1	402.
Maple wood	6.69	1.3	172.
Zinc, swaged	6.30	9.4	20.8
Glass	2.05	6.3	10.2
Aluminum, cold-rolled	1.07	5.8	5.7
Brass, cold-rolled	1.54	8.5	5.6
Copper, cold-rolled	1.59	10.	4.95
Tungsten, swaged	5.24	38.7	4.26
Swedish iron, annealed	2.50	18.9	4.16
Phosphor bronze, annealed	1.01	12.	2.67
Mild steel, cold-rolled	1.57	21.	2.33
Molybdenum, swaged	2.19	34.6	1.95
Nickel, cold-rolled	1.02	21.	1.55
Nickel steel, 3½% swaged	0.73	21.	1.10
Monel, cold-rolled	0.454	17.8	0.79
Phosphor bronze, cold-rolled to maximum hardness	0.117	11.6	0.306

* Vibration test.

The first column of Table I gives the value of tan ϕ which is a direct measure of the ratio of the frictional moment which produces the transverse deflection, to the elastic moment, which balances the weight by its upward reaction (see Fig. 3). It follows from Eq. (1) that this moment ratio is equal to

$$\tan \phi = \xi E/\pi \qquad (2)$$

from which it is seen that tan ϕ is independent of the rod dimensions. The derivation of this relation is given in Appendix I. Eq. (2) also shows that tan ϕ is independent of the load W, that is, it requires that the ratio of transverse deflection to downward deflection be constant so that the curves of Figs. 4 and 5 are straight lines.

The values of ξ obtained from Eq. (1), as given in Table I, give a very useful means of comparing internal frictions in solids, whereas constants based on the old idea that the viscosity of a solid is like that of a liquid are completely misleading.

It is to be noted that this law gives a constant logarithmic decrement of vibration amplitudes, because the frictional loss per cycle is proportional to the square of the amplitude.

The theory presented is established only within the range of the experiments outlined in this paper, but the authors are of the opinion that a law of the type represented by Eq. (1) will be found to hold over a very wide

TABLE II

Internal friction constants as calculated from results of previous investigators.

Material	Treatment	Investigator	Youngs modulus $E\times10^{-11}$	Rigidity modulus $G\times10^{-11}$	Logarithmic decrements Normal δ_η	Logarithmic decrements Tangential δ_τ	Internal friction constants $\times10^{15}$ Normal ξ_η	Internal friction constants $\times10^{15}$ Tangential ξ_τ
Tin		Voigt	3.2	*1.6	.0129	.0110	40.3	69.
Zinc		"	9.4	*3.9	.00605	.00581	6.4	14.9
Aluminum		"	5.8	*3.35	.000820	.00603	1.41	1.80
Steel		"	21.	*8.29	.00239	.00193	1.14	2.32
Bronze		"	11.8	*4.4	.001006	.000308	0.85	0.70
Nickel		"	21.	*7.82	.00177	.00109	0.84	1.39
Brass		"	8.5	*3.6	.000674	.000310	0.795	0.86
Copper		"	10.	†5.5	.000715	.000420	.715	0.764
Copper		Thompson		†5.5		.00365		6.63
Aluminum		"		*3.35		.00670		20.0
Copper	Annealed	Honda	10.		.0075		7.5	
Copper	Rolled	"	10.		.00177		1.77	
Aluminum	Rolled	"	5.9		.00055		.93	
Zinc	Rolled	"	9.6		.00501		5.2	
Zinc	Annealed	"	9.6		.0017		1.77	
Nickel	Rolled	"	21.		.00169		.805	
60–40 Brass		"	8.66		.00192		2.2	
Copper		Guye		5.5		.001		1.8
Glass		"		*2.54		.00015		0.59
Zinc		Iokibe & Sakai		3.0		.0587		195.
Aluminum		"		2.5		.0055		22.
Copper		"		5.5		.00076		1.4
Nickel		"		7.2		.000106		0.147
Iron		"		7.8		.00128		1.64
Tungsten		"		13.25		.00035		0.264
.55% C Steel		"		7.65		.00119		1.55
.9% C Steel		"		7.7		.00086		1.1
1.3% C Steel		"		7.6		.00089		1.2
Glass	Plate glass	Quimby					0.205	
Aluminum	Rolled	"					0.605	
Copper	Hard drawn	"					1.08	
Copper	Wire	Lindsay	10.		.00169		1.69	
Steel	"	"	21.		.00072		.342	
Phosphor bronze	"	"	11.8		.00037		.314	

* From Smithsonian Tables (1920).
† From Iokibe & Sakai.

range of frequencies. The only case to the authors' knowledge where measurements have been made for very high frequencies is that of the experiments of Quimby.[6] He uses Stokes liquid-viscosity law in interpreting his results and obtains constants smaller than those of previous investigators in approximately the same ratio as his frequencies are higher than theirs. On the basis of the authors' law, however, Quimby's results and those of previous

[6] S. L. Quimby, Phys. Rev. **25**, 528–573 (1925).

investigators give constants of the same order of magnitude, although Quimby's constants are somewhat smaller. This is perhaps because these constants were obtained from stress cycles of much smaller amplitude than used in this investigation.

Table II gives a list of values of ξ which have been calculated from the results of previous investigators, using their logarithmic decrements as a means to calculate ξ. The value of ξ can be found by the very simple relation

$$\xi=\delta/E \tag{3}$$

where δ is the logarithmic decrement and E Young's modulus. The proof of Eq. (3) is given in Appendix II.

It must be kept in mind, however, that ξ as determined by (1), (2) and (3) may not always mean the same thing. It depends upon the kind of stress in the stress cycle. It is known from the theory of elasticity that the stress at any point in any body, however stressed, may be resolved into a pure dilatation and a pure shear. In bending vibrations, where normal stresses are produced, they are combined dilatations and shears, but for torsional oscillations, the stresses are almost pure shears. When (3) is applied to torsional vibrations, E should be replaced by the rigidity modulus. In the revolving rod experiments, the cyclical stresses are normal in character. Table II contains values of ξ obtained from logarithmic decrements produced both by normal and by tangential stresses, the former being specified by ξ_n and the latter by ξ_τ.

The complete analysis of internal friction phenomena in solids requires a separation of that produced by pure dilatation and that produced by pure shear, and a knowledge of the effect of their combination in various ratios.

Attention should be called to the fact that for frequencies of the order of those in bells and in bodies which respond with a prolonged ring when struck, the law of Eq. (1) shows that such a ring is perfectly possible, whereas on the basis of the old liquid-viscosity law, using the constants of previous investigators for that law (except Quimby's constants), no ring is possible. A bell would be aperiodic, as if made of putty. This is mentioned by Quimby in his paper.

In conclusion we wish again to point out that the law of Eq. (1) is not to be considered as complete or exact, as regards the loss being proportional to the stress amplitude squared. There are divergencies from this in the experiments of others as well as our own. Rowett[3] finds that for annealed iron the cube law fits his results best. Bennewitz[3] uses the square law, however. The static tests of Rowett show a cube law. Some results of static tests on armco iron for eccentric stress cycles by G. H. Keulegan of the Bureau of Standards have recently appeared,[7] which the cube law fits. These latter results were based on stress cycles of quite small amplitude, going up to less than 1/10 the elastic limit of the material.

The thing which we particularly wish to bring out is that for stress cycles of frequency of two to three a minute, up to fifty a second (that is, within

[7] G. H. Keulegan, U. S. Bur. Stds. Tech. paper No. 332, Nov. 1926.

the range of the experiments) the frictional loss per cycle is strictly independent of the frequency of performance of the cycles for every solid thus far tested.

We are unable by the use of the revolving rod method to check results of certain investigators, whose results do not show this independent frictional loss per cycle upon frequency, notably some of Voigt's[8] results and recent results obtained by Subrahmaniam.[9] The discrepancy may lie in the fact that in the present experiments relatively large masses of material were used which would tend to minimize surface effects. Further study is required to settle this point.

RESEARCH LABORATORY,
GENERAL ELECTRIC COMPANY,
SCHENECTADY, NEW YORK.

APPENDIX I

Proof that in the rotating rod experiments the internal friction constant $\xi = \pi\eta/E$ where $\eta = \tan\phi$, Fig. 3, and E = Young's modulus. In Fig. 3 let the downward elastic deflection at the end of the rod from the undeflected position of its axis be d. Then using the symbols of Fig. 3, the potential energy of downward elastic deflection is given by

$$W_E = (1/2)R_E d \; ; \tag{4}$$

and the work per cycle due to internal friction by

$$W_F = 2\pi R_F d \tag{5}$$

From (4) and (5)

$$W_F/W_E = 4\pi R_F/R_E = 4\pi \tan\phi = 4\pi\eta \tag{6}$$

ξ is found by evaluating W_F and W_E and substituting in (6).

W_F, the frictional dissipation per cycle of rotation of the rod is found as follows: First the frictional loss ΔW_F in a slice of the rod of thickness Δx will be found. From the law of equation (1)

$$\Delta W_F = \int_0^{2\pi} \int_0^a \xi f^2{}_m r \; d\theta \; dr \; \Delta x \tag{7}$$

In this expression, f_m, the maximum stress per cycle, is, according elastic theory, a linear function of the radial distance r and may be expressed in terms of F_m, the maximum stress per cycle at the edge of this slice, and the radius a as follows:

$$f_m = F_m r/a \tag{8}$$

Substituting (8) in (7) and integrating,

$$\Delta W_F = (\pi/2)\xi F_m{}^2 a^2 \Delta x \tag{9}$$

The total work per cycle W_F is found by integrating (9) along the entire length of the rod l after expressing F_m in terms of F_M the maximum stress in the entire rod, from the relation $F_M/F_m = l/x$

This gives

$$W_F = (\pi/6)a^2 l \xi F^2{}_M \tag{10}$$

[8] W. Voigt, Ann. d. Physik **47**, 671–693 (1892).
[9] G. Subrahmaniam, Phil. Mag. p. 711 (1925); p. 716 (1925); p. 1074 (1926); p. 854 (1927).

W_E, the total potential energy of elastic deflection of the rod is easily found in terms of the maximum stress F_M to be

$$W_E = \pi a^2 l F^2{}_M / 24E \tag{11}$$

Substituting (10) and (11) in equation (6),

$$W_F / W_E = 4\xi E = 4\pi\eta \; ; \; \xi = \pi\eta / E \tag{12}$$

which is the required relation.

In obtaining (11) the approximate beam theory was used, neglecting shearing stresses which are relatively small. The expression (10) can also be obtained by assuming some form of stress-strain hysteresis loop and summing the work done. The result comes out independent of the form of the hysteresis loop assumed, as of course it must, the only requirement being that the area of the loop conform to the energy requirement of equation (1).

Appendix II

Proof that $\xi = \delta/E$ where δ is the logarithmic decrement and E the elastic modulus. For any unit volume in the vibrating body, the potential energy P_m is given by

$$P_m = \tfrac{1}{2} E \epsilon_m{}^2 \tag{13}$$

where ϵ_m is the maximum value of strain at that point. Now dP_m/dt is equal to the frictional dissipation per sec.* in the unit volume in question. Therefore $E\epsilon_m d\epsilon_m/dt = -\xi f_m{}^2 n$ where n is the number of stress cycles per sec. Solving for ξ, and substituting for f_m its value $E\epsilon_m$,

$$\xi = -\frac{1}{En}\left(\frac{d\epsilon_m/dt}{\epsilon_m}\right) = -\frac{1}{En}\left(\frac{dy/dt}{y}\right) \tag{14}$$

where y is the vibration amplitude of the body at some convenient point. The above substitution of y for ϵ_m follows from the elastic theory, by which strains are proportional to vibration amplitude for *all* points in a body vibrating in a given mode. The exponential decrement curve of vibration amplitude is given by $y = y_0 e^{-\alpha t}$ from which $(dy/dt)/y = -\alpha$. But if T is the vibration period, the logarithmic decrement

$$\delta = \log_e \frac{y_0 e^{-\alpha t}}{y_0 e^{-\alpha(t+T)}} = +\alpha T = \alpha/n = -\frac{1}{n}\left(\frac{dy}{dt}/y\right) \tag{15}$$

Substituting (15) in (14) the required relation $\xi = \delta/E$ is obtained.

*Actually the maximum value of P occurs at one instant only in each cycle, but P_m is here regarded as a continuous function represented by a curve drawn through the successive maxima.

THE OBLIQUE INCIDENCE OF ALPHA-PARTICLES ON MICA

By Haraprasad De

Abstract

The oblique incidence of alpha-particles on mica surfaces has been studied in a Wilson condensation chamber. Bose (Zeits. f. Physik **12**, 207 (1922)) attributed a tail, which appears with the incident alpha-particle track, to ionized adsorbed gases on the surface upon which the alpha-particles are impinging. The new explanation as here offered is that the tail is due to diffusion of ions repelled by the charged sheet upon which the alpha-particles are incident.

IN 1922 D. M. Bose[1] investigated the effect of the oblique incidence of alpha-particles on thin sheets of mica, etc. He placed a source of alpha-particles inside a C. T. R. Wilson expansion chamber in front of a mica sheet which could either be connected directly to the outer vessel, or through a battery of about 220 volts placed between the two. On taking photographs of the alpha-particle tracks it was found that when the mica sheet was electrified the oblique tracks which struck against the mica sheet had continuations ("tails") parallel to the mica sheet. Such continuations were absent when the mica sheet was connected to the outer vessel. Bose explained the observed phenomenon by the assumption that when an alpha-particle struck the mica sheet obliquely it retained its velocity parallel to the sheet and ionized the gas adsorbed thereon. These ions cannot escape out of the adsorbed layer unless an electric field is applied, when they diffuse to a region filled with supersaturated water vapor. Thus with an electric field on, the continuation of the alpha-particle track parallel to the surface of the mica sheet can be seen, while in the absence of the field this continuation remains invisible.

The present paper describes a continuation of the above investigation. For this purpose alpha-particles from mesothorium *C*, range 8.7 cm in air, were taken and such thin mica sheets were selected that alpha-particles could pass through some of them and still retain their ionizing power. Thin tin-foil was also used in place of mica.

The apparatus used consisted of a circular condensation chamber, inside which pieces of mica were attached as shown in Fig. 1. R is the thin mica sheet, S_3 is a thick mica screen, S_2 a slit which allowed a limited number of alpha-particles to go through and S_1 is the source of the alpha-particles. The diameter of the chamber was about 15 cm. The slit S_2 was about 0.5×0.1 cm and the position of the slit could be shifted according to the activity of the source. The screen S_3 was used to keep the region to the left of it free from heavy ionization. R was charged by a lead taken out through an air-tight metal cap. Sunlight was used for illuminating the tracks, the

[1] D. M. Bose, Zeits. f. Physik **12**, 207 (1922).

rays being concentrated and limited so as to traverse only the plane in which the alpha-particles were coming through the slit.

Instantaneous photographs were taken. The shutter *Sh* was released by a system of levers connected to the rod which released the cock of the evacuated chamber. The timing was so regulated as to produce sharp alpha-ray tracks. Ilford extra-rapid plates were used in most of the experiments. Hydrogen and air were the gases usually chosen to fill the chamber.

The principal feature of each photograph was a well defined alpha-particle track with a tail parallel to the charged mica sheet (or metallic foil). This tail appeared on the boundary of the region of no condensation, just in front of the sheet. The existence of this region may be attributed to the thermal conductivity of the sheet and adjacent gas. It was much thicker in the case of hydrogen than in the case of air on account of the higher thermal conductivity of the former.

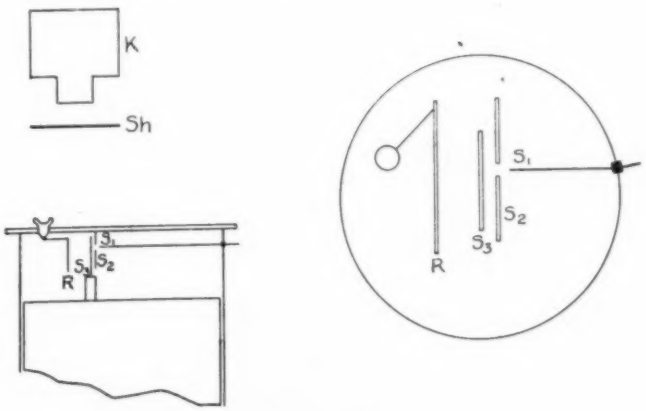

Fig. 1. Diagram of apparatus.

It was noted that the tail was more diffuse than the sharply defined alpha-particle tracks. The tails were longer the greater the angle of incidence of the alpha-particles and the tail appeared always in the plane of incidence. If the angle of incidence be θ then the length of the tail was roughly equal to $d \tan \theta$, where d was the depth of the region of no condensation. In some of the photographs the plane of incidence was not parallel to the focal plane of the camera; in these cases the tails were foreshortened. Some photographs were taken with very thin mica whose stopping power in air was about 1 cm and through which alpha-particles could penetrate, thus making tracks visible on both sides of the sheet. With such sheets, tracks could be seen with tails on both sides of the sheet, the tail on the exit side being inverted. In the case of hydrogen the tracks were much longer than in air, and also, because of the greater thickness of the region of no condensation, the tails were longer.

The explanation of Bose[1] is not found adequate to explain the phenomena occurring in very thin films of mica penetrated by the alpha-particles. The explanation which is now put forward is as follows: By the passage of the

alpha-particle both positive and negative ions are formed but in the absence of sufficient water vapor or at too high a temperature the condensation track cannot be seen. In the region of no condensation the ions are separated by an electric field of about 220 volts, one kind being absorbed by the plate and the other kind being repelled from the plate. The ions repelled by the charged plate form the tail when they reach the region of demarcation between condensation and no condensation. In case the alpha-particles penetrate the mica sheet similar phenomena occur on the exit side. The nearly uniform brightness of the tail indicates that the ions suffer but little resistance to their motion in the region of no condensation.

In conclusion I wish most respectfully to thank Professor D. M. Bose for his kind suggestion of the problem and for the facilities offered me in its solution.

PHYSICS DEPARTMENT,
UNIVERSITY COLLEGE OF SCIENCE,
CALCUTTA, INDIA.
August 11, 1927.

ERRATA

IONIZATION EFFICIENCY OF ULTRA-VIOLET LIGHT IN CAESIUM VAPOR. Edward Milton Little. Vol. 30, pp. 109–118, August, 1927.

The following changes should be made in the headings and data of Table II, p. 115. These changes are made necessary because the cross-section of the beam varied from 0.860 to 1.154 sq cm for various wave-lengths from 2400 to 3660A (1.000 sq cm at 3000A). An additional column has been inserted in which quantum units of energy are used.

TABLE IIA

Ionization of caesium vapor.

Average temperature 166°C; potential of opposite plate = +3.0 volts.

Wave-length (Angstroms)	Ions/cm/erg	Ions/atom per erg/sq cm = B	Ions/atom per quantum/sq cm
2399	1.147×10^{5}	1.924×10^{-10}	1.573×10^{-21}
2525–35–37–39	1.068	1.798	1.388
2804	.703	1.177	.827
2967	1.522	2.485	1.647
3022–28	1.291	2.170	1.407
3126–32–45	2.085	3.520	2.210
3342–52	.111	.187	.110
3650–56–63–80	.072	.120	.064

These changes in the data make necessary a slight correction of Fig. 4, p. 116. The corrected figure is shown below. The units for the ordinate have

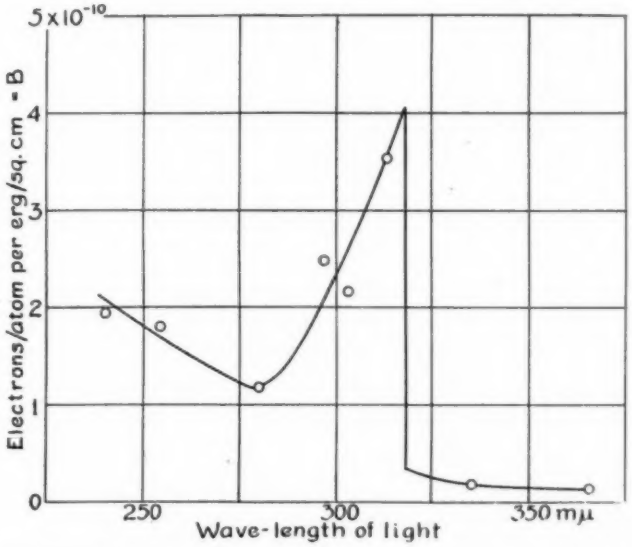

Fig. 4a. Ionization efficiency, B, for caesium vapor at 166°C.

been changed to ions/atom per erg/sq cm. It is to be noted that if the number of ions/atom per quantum/sq cm were used for ordinates the curve would be slightly less steep at the threshold.

EDWARD MILTON LITTLE.

HALL EFFECT IN BISMUTH WITH LOW MAGNETIC FIELDS. Palmer H. Craig. Vol. 27, pp. 772–878, June, 1926.

My attention has been called by Mr. H. Rowe to an error in presenting the data contained in Table I, page 777, of the above paper. On page 775 it is erroneously stated that a longitudinal current through the specimen of 1.5 amp. was used throughout Table I, and that the thickness of the film was 0.012 cm. The following is a corrected form of Table I in which it will be noted that the current through the specimen was 0.150 amp. in some cases and 1.50 in others. The thickness of the film was 0.0012 cm throughout. The values of the Hall coefficient remain unchanged, however, since the correct values of the current and film thickness had been used in the calculations.

CORRECTED FORM OF TABLE I

Hall effect in bismuth for low, intermediate, and high fields.

Field strength (gausses)	Current through specimen (amp.)	"Residual" e.m.f. (μ volts)	Residual+Hall e.m.f. (μ volts)	Net Hall e.m.f. (μ volts)	$-R$
0.07	0.150	14.00	15.50	1.50	171
.08	.150	14.10	15.60	1.50	150
.09	.150	14.20	15.72	1.52	135
.10	.150	14.20	15.86	1.66	133
.13	.150	14.4	16.1	1.7	131
.15	.150	14.3	16.9	2.6	126
.24	.150	14.04	16.30	2.26	75
.29	1.50	14.60	21.10	6.50	18
.30	1.50	14.50	19.80	5.30	14
.32	1.50	14.40	19.60	5.20	13
.35	1.50	14.80	20.50	5.70	13
.50	1.50	14.60	22.70	8.10	13
.80	1.50	14.60	26.60	12.00	12
1.00	1.50	14.60	29.60	15.00	12
15.00	.150	14.30	35.10	20.80	11
28.50	.150	14.40	55.00	40.60	11
1000.	.150	14.00	1889.	1875.	15
2500.	.150	14.00	7514.	7500.	24
4220.	.150	14.00	15324.	15310.	29

PALMER H. CRAIG.

Proceedings of the American Physical Society, Reno, Nevada June 23, 1927, Vol. 30, p. 362, September, 1927.

Through an oversight, the paper by S. J. Barnett on Researches on the Gyromagnetic Anomaly, which appeared on the supplementary program of the above meeting, was omitted from the abstracts published in the September, 1927, issue. The abstract follows.

18. Researches on the gyromagnetic anomaly. S. J. BARNETT, University of California at Los Angeles and California Institute of Technology.—Experiments on (1) magnetization by

rotation, and later experiments on (2) the converse effect, appear to show that the ratio ρ of the angular momentum to the magnetic moment of the magneton is approximately one-half $R(=2m/e)$, the ratio for a Bohr orbit. In all precise work hitherto done on (2) ρ has been determined from the reaction on a magnetized rod to the total magneton momentum produced by magnetization, while it is possible that some of the reaction may have gone to the magnetizing system, thus making the calculated ρ too small. In the precise method developed for the present investigation the total reaction is measured, the magnetizing coil being wound rigidly on the rod. With iron and permalloy this work, together with the earlier work by others, has already proved that at least most of the reaction goes to the rod; nevertheless very concordant values of ρ obtained are several percent greater than one-half R, though not so great as ρ from the experiments on (1), viz. $0.53R$. In the extensive investigation under way further search will be made for systematic errors, which appear now to have been eliminated in the work on permalloy and soft iron.

BOOK REVIEWS

Theorie der Strahlung. H. A. LORENTZ.—In these five lectures the author has sought to trace the steps by which the theory of heat radiation has evolved at the hands of Kirchhoff, Boltzmann, Wien, Jeans and Planck. The subject is taken up in the way in which it grew, and no attempt is made to include the more recent quantum formulations such as Einstein's deduction of Planck's law.

The first chapter on Kirchhoff's law relating the coefficient of absorption to the emissivity is followed by a chapter on Boltzmann's thermodynamic proof that the total energy density of a radiation field is proportional to the fourth power of the absolute temperature of the black body with which it is in equilibrium and Stefan's empirically discovered law for the rate of radiation from a black body. Chapter three takes up Wien's displacement law, carrying the theory as far as it can be developed on purely thermodynamic and electromagnetic grounds. In the next chapter Jeans' aether-box is discussed, and with the aid of the principle of equipartition of energy the false Rayleigh-Jeans law is deduced. The last chapter takes up Planck's formula, which is derived in two ways; first, from the number of degrees of freedom in Jeans' aether-box, and secondly from a consideration of a set of damped linear oscillators.

The exposition is concise and clear, and in the opinion of the reviewer the book forms an even better introduction to the theory of heat radiation for the use of the beginner than Planck's Wärmestrahlung. Pp. 81, 17 figs. Akademische Verlagsgesellschaft m. b. H., Leipzig, 1927. Price 7.80 R. M.

LEIGH PAGE

Wahrheit und Irrtum in der Relativitätstheorie. FRIEDRICH R. LIPSIUS.—This is a critical discussion of the special and general relativity theories from the philosophical rather than the mathematical point of view. The first chapter contains an account of the hypotheses underlying the special theory and some of the consequences flowing from them. The second chapter is concerned mainly with the ether. The author attaches a good deal of credence to the results of Miller's repetition of the Michelson-Morley experiment and discourses on space-ether, field-ether and gravitation-ether. In the third chapter some of the difficulties which have led to the quantum theory are discussed and the significance of Schrödinger's formulation is commented on. The last chapter takes up the general theory of relativity and its philosophical implications. With few exceptions the literature referred to is of German origin. Pp. 154, J. C. B Mohr, Tübingen, 1927. Price 7.50 R. M.

LEIGH PAGE

Lectures on Theoretical Physics. Volume I, Aether Theories and Aether Models—Kinetical Problems. H. A. LORENTZ, translated by L. Silberstein and A. P. H. Trivelli.—This is the first of three volumes of lectures delivered by Professor Lorentz at the University of Leiden. The remaining volumes will contain lectures on Thermodynamics, Entropy and Probability, Theory of Radiation, Theory of Quanta and The Principle of Relativity for Uniform Translations, the three together comprising a fairly comprehensive treatment of the whole field of theoretical physics.

The present volume contains two courses of lectures. In the first of these, dated 1901–1902, Professor Lorentz takes up in his first chapter a theoretical discussion of the aberration of light and of the attempts to explain it satisfactorily on the aether theory, in particular by means of Planck's compressible aether and Fresnel's theory. This is followed by two chapters on mechanical aether theories, in which especial attention is paid to Kelvin's quasi-rigid model of the aether. The final chapter comprises a hydrodynamical investigation of a fluid containing pulsating spheres which leads to the subject of aether sources and sinks and Pearson's theory.

The author concludes by remarking that these aether theories give little satisfaction and become more and more artificial the more they attempt to explain. Nevertheless he emphasizes the values of mechanical analogies in visualizing phenomena and suggesting new ideas for investigation.

The second course of lectures, dated 1911–1912, starts with a hydrodynamical investigation of a viscous fluid, including the deduction of Stokes' formula for the motion of a sphere through a stagnant liquid. This is followed by an account of Knudsen's theoretical and experimental investigations on the flow of rarified gases. Next come short chapters on Le Sage's theory of gravitation and the effect of friction and heat conduction on the propagation of sound through a gaseous medium. The remainder of the book has to do with the kinetics of electrons in a metal or in equilibrium with a metal, including Richardson's investigations and experiments such as those of Nichols in which an attempt was made to drive the free electrons to the periphery of a metal disc by setting it into rapid rotation.

The whole book is characterized by Professor Lorentz's pleasant style and lucid exposition. The translators have put it into excellent English and it seems to be singularly free from misprints. Pp. 195+ix, 39 figs. Macmillan and Company, London, 1927.

LEIGH PAGE

Dielectric Phenomena. S. WHITEHEAD.—In this book of 160 pages the author has succeeded in giving a clear and comprehensive account of our knowledge especially of the spark and corona discharge, the latter form of discharge including dark, glow and brush discharges. The material is divided into three parts; in the first part we find a short review of the ideas of atoms, ions, ionization by radiation, impact of electrons, thermal ionizations and general principles of discharges. In the second part the phenomena of the spark are treated in great detail. The author tries to bring the phenomena under the rule of physical principles, but as these are rare outside Townsend's general principle of discharge, there remains a great deal of purely empirical data, which are given by careful diagrams. The lack of a thorough-going theory makes itself felt through the whole book whose empirical character makes the reading in parts a little tiresome. In the third part the phenomena of the corona discharge have received a masterly treatment. In the rectification of alternating currents by the corona I did not find the difference between hydrogen and the other gases. The complete bibliography is very valuable. The book, in its entirety, is an important contribution to the subject of discharges in gases and is recommended to students of physics and electrical engineering alike. Pp. 176, 42 figs., D. Van Nostrand Company, New York, 1927. Price $4.00.

JAKOB KUNZ

Elastizität und Festigkeit. DR. ERNST KÖNIG.—This is the third of seven projected volumes of the Handbuch der Werkräfte, edited by Professor Paul Krais. The purpose of this book is to present to engineers as much of the subjects of elasticity and strength of materials as is necessary for the practical needs of their profession. The first section of 29 pages deals with the mathematical elements of the theory of elasticity; the second section of 73 pages with special applications and methods of approximate calculation; the third section of 15 pages treats in outline the most important topics in the strength of materials; and finally the fourth section of 19 pages deals with a method of approximately solving certain problems by a cord construction. The second section in which the complete solution of a number of practical problems, particularly on the loading of beams, is carried through in detail, will probably prove to be of most value. In general, the book seems to be well written, and should be of importance to the audience for which it is written. Pp. 140+xii, 90 figs. J. A. Barth, Leipzig, 1927. Price 10 R. M. unbound, 12 R. M. bound.

P. W. BRIDGMAN

General Chemistry, Theoretical and Descriptive. THOMAS P. MCCUTCHEON and HARRY SELTZ.—According to the preface, "This book has been designed for use in a course of General Chemistry based on a series of illustrated lectures and quiz hours, and for a text of reference for the student performing the laboratory work, which usually accompanies such a course. It is believed that the division into two parts, theoretical and descriptive chemistry, offers certain

advantages: Firstly, the student will have at hand a concise and orderly summary of chemical facts, emphasizing the natural groupings and relationships of the elements from the standpoint of the Periodic Law: Secondly, the student will have available chapters on each of the essential topics of theoretical chemistry, each complete in itself, and free from diverting and irrelevant matter. This will be especially valuable in reviewing the subject for examination: Thirdly, the instructor will have the maximum opportunity to inspire and interest his students by injecting his own method and personality into the course." · · · · "In the interests of brevity, it is felt that many matters may be ommitted from a text, which may be properly introduced in lecture or recitation or covered in supplementary reading assignments. For this reason almost no historical material has been used, and references to industrial processes have been made as concise as possible." · · · · "Finally, no effort has been made to popularize the subject. It is believed that the science of chemistry, when properly presented, will appeal to the student as of such surpassing interest and importance, that he will be willing to study a book from which every effort has been made to eliminate the unessential."

A "syllabus of lectures" given in the preface involves an entirely different sequence of subjects and a very pronounced change in grouping of material from those found in the book.

The first fifteen chapters in this book cover a wide range of theoretical material. Mathematical formulations are numerous and the style is essentially that of a text on physcial chemistry. Lists of selected problems are appended to each chapter in this section of the book. Chapters are found on Reaction Velocity, Mass Action, Electrolytic Dissociation, Standard Solutions, Solubility Product, Atomic Structure, Radioactivity and Disperse Systems.

Part two contains twenty six chapters on descriptive chemistry. The first chapters in this section deal with acids, bases and salts. The non-metals are next discussed and finally the metals. There are only nine figures in the 225 pages comprised in this section and no exercises follow the chapters. A short discussion of the Werner Theory is found in Chapter XII.

The reviewer feels that this book would not prove to be a satisfactory text for students in a first college course in chemistry. The scarcity of illustrations, the absence of historical material, and the paucity of applications would, in his opinion, greatly handicap any instructor using this book. As a reference work the book seems undesirable, since it is so fragmentary in its treatment. Pp. 415+x, 33 figs. D. Van Nostrand Company, New York, 1927. Price $3.50.

R. E. KIRK

AUTHOR INDEX TO VOLUME 30

References with (A) are merely to abstracts of papers presented at meetings of the Physical Society.

Allison, Fred. Effect of wave-length on the differences in the lags of the Faraday effect behind the magnetic field for various liquids—66

Allison, Samuel K. Experimental study of the relative intensities of x-ray lines in the *L*-spectrum of thorium—245, 365(A)

Babcock, Harold D. Pressure effect for iron-arc lines—366(A)

——— (see Dieke, G. H.)—366(A)

Balinkin, Isay A. Optical determination of axial stresses in long rectangular plates under torsion—520

Barnett, S. J. Researches on the gyromagnetic anomaly—964(A)

Barton, Henry A. Ionization of HCl by electron impacts—614

———, Francis A. Jenkins and Robert R. Mulliken. The beta bands of nitric oxide. II. Intensity relations and their interpretation—175

——— (See Jenkins, Francis A.)—150

Bateman, H. Modification of Gordon's equations—55

Batho, H. F. (see Dempster, A. J.)—644

Birge, R. T. and **J. J. Hopfield.** The theoretical relation between infra-red and ultra-violet bands—365(A).

Bless, A. A. Recoil electrons from aluminum—871

Boydston, R. W. Thermo-electric effect in single-crystal bismuth—911

Breit, G. Book reviews—225, 359.

Bridgman, P. W. Book review—967

Brinsmade, J. B. Magnetic spectrum of secondary electrons—364(A)

——— Reflected and secondary electrons from an aluminum target—494

Brown, Hugh M. Effect of a magnetic field upon thermal conductivity of iron, copper, silver and gold—364(A)

Cady, W. G. Book reviews—89, 223

Cajori, Florian. Book review—224

Carman, A. P. and **C. C. Schmidt.** An arrangement of the electrometer method for measuring the dielectric constants of electrolytes—922

Caswell, A. E. An electron-quantum theory of galvanomagnetism and thermomagnetism—364(A)

Chamberlain, Katherine and **George A. Lindsay.** Determination of certain outer x-ray energy levels for the elements from antimony (51) to samarium (62)—369

Chase, Carl T. Trouton-Noble ether drift experiment—516

Compton, K. T. (see Costa, J. L.)—349

Compton, K. T. and **P. M. Morse.** Theory of the normal cathode fall in glow discharges—305

Condon, Edward U. Zeeman effect of the symmetrical top—781

Constantinides, Philip A. Electrical properties and nature of active nitrogen—95

Cork, J. M. (see Mack, J. E.)—741

Costa, J. L., H. D. Smyth and **K. T. Compton.** A mechanical Maxwell demon—349

Craig, Palmer H. Correction to paper "Hall effect with low magnetic fields"—964

Crawford, F. H. (see Kemble, E. C.)—438

Crew, W. H. and **E. O. Hulburt.** Pressures in discharge tubes—124

Cummings, N. W. and **Burt Richardson.** Evaporation from lakes—527.

Curtiss, L. F. Half-period of radium E—539.

Darrow, K. K. Book review—224.

Davisson, C. and **L. H. Germer.** Diffraction of electrons by a crystal of Ni—705

——— Note on the thermionic work function of tungsten—634

Dawson, L. H. Motion of striae in discharge tubes—119

Dempster, A. J. and **H. F. Batho.** Light quanta and interference—644

Dewey, Jane M. Intensities in the stark effect in helium II—770

Dieke, G. H. and **Harold D. Babcock.** The structure of the atmospheric absorption bands of oxygen—366(A)

——— and **J. J. Hopfield.** Structure of the ultra-violet spectrum of the hydrogen molecule—400

Durbin, F. M. Absorption of potassium ions in various gases—844
Du Sault, L. (see Loeb, L. B.)—362(A)

Edwards, Hiram W. Total reflection of x-rays and the index of refraction of certain metals—91
Eldridge, John A. Experimental test of Maxwell's distribution law—931
Erikson, Henry A. On the effect of the medium on gas ion mobility—339
Eyring, H. (see Gibson, G. E.)—553

Foote, Paul D. Depolarization of resonance radiation—300
——— Quenching of mercury resonance radiation by foreign gases—288
Frantz, H. W. (see Westwater, W.)—363(A)
Fredrickson, W. R. and **William W. Watson.** Sodium and potassium absorption bands—429

Gardiner, E. W. (see Gibson, G. E.)—543
George E. F., W. M. Young and **Harry Hill.** Remarkable electrical conditions accompanying west Texas sand storms—362(A)
Germer, L. H. (see Davisson, C.)—634, 705
Gibson, G. E. and **H. Eyring.** Ionization and stopping power of various gases for alpha-particles from polonium: II—553
——— and **E. W. Gardiner.** Ionization and stopping power of various gases for alpha-particles from polonium: I—543
——— and **H. C. Ramsperger.** Band spectra and dissociation of iodine monochloride—598, 363(A)
Gortner, Ross Aiken. Book review—88
Green, J. B. and R. A. Loring. Spectra of tin and their Zeeman effects—574
Gronwall, T. H. Longitudinal vibrations of a liquid contained in a tube with elastic walls—71

Hagenow, C. F. and **A. Ll. Hughes.** Intensity ratio of the blue caesium doublet—284
Haraprasad De. On oblique incidence of α particles on mica—960
Heaps, C. W. Hall effect in a bismuth crystal—61
Hildebrand, J. H. (see Westwater, W.)—363(A)
Hill, Harry. (see George, E. F.)—362(A)
Hogness, T. R. and **E. G. Lunn.** Positive ray analysis of nitric oxide and collisions of the second kind—26
Hopfield, J. J. (see Birge, R. T.)—365(A)
——— (see Dieke, G. H.)—400
Houston, William V. Spectroscopic determination of e/m—608
Hughes, A. Ll. (see Hagenow, C. F.)—284
——— and **A. M. Skellett.** Dissociation of hydrogen by electrons—11
——— and **A. R. Thomas.** Absorption of resonance radiation in mercury vapor—466
Hulburt, E. O. (see Crew, W. H.)—124
Hundley, John Leslie. Relative intensities of positive rays from the isotopes of lithium—864
Hunt, Franklin L. X-rays of long wave-length from a ruled grating—227

Ingersoll, L. R. Book review—357
Illingworth, K. K. Repetition of the Michelson-Morley experiment using Kennedy's refinement—692

Jackson, W. J. Secondary emission from Mo due to bombardment by high speed positive ions of the alkali metals—473
Jacobsohn, Samuel. Note on the fluctuations in black body radiation—944
——— Radiation fluctuations and thermal equilibrium—936
Jauncey, G. E. M. Book review—537
Jenkins, Francis A., H. A. Barton and **Robert S. Mulliken.** The beta bands of nitric oxide. I. measurements and quantum analysis—150
——— (see Barton, Henry A.)—175
Jones, Howard A., Irving Langmuir and **G. M. J. Mackay.** Rates of evaporation and vapor pressures of tungsten, molybdenum, platinum, nickel, iron, copper and silver—201

Kaplan, Joseph. Some properties of atomic hydrogen—639
Kellogg, J. M. B. and **E. P. T. Tyndall.** Note on the Barkhausen effect under mechanical stress—354
Kemble, E. C. Rotational distortion of multiplet electronic states in band spectra—387
——— **R. S. Mulliken** and **F. H. Crawford.** Zeeman effect in the Angstrom CO bands—438
Kendall, James. Book review—87
Kent, Norton A., Lucien B. Taylor and **Hazel Pearson.** Doublet separation and fine structure of the Balmer lines of hydrogen—266
Kimball, A. L. and **D. E. Lovell.** Internal friction in solids—948
King, Arthur S. Characteristics of the neutral and of the singly and doubly ionized spectra of cerium—366(A)
Kirk, R. E. Book review—967
Kovarik, Alois F. Book reviews—357, 358
Kunz, Jakob. Book review—967
Kurrelmeyer, Bernhard. Photo-electric conductivity of sulphur—893

Lang, R. J. Spectrum of Ga, Ge and In—762
——— (see Laporte, Otto)—378
Langmuir, Irving. (see Jones, Howard A.)—201
Laporte, Otto, and R. J. Lang. Second spark spectrum of zinc, Zn III—378
Lind, S. C. Book reviews—88, 358
Linder, Ernest G. Photo-electric effect and surface structure in zinc single crystals—649
Lindsay, George A. (see Chamberlain, Katherine) —369
——— (see Van Dyke, George D.)—562
Little, Edward Milton. Ionization efficiency of ultra-violet light in caesium vapor—109; errata—963
Loeb, L. B. and L. Du Sault. Gas ion mobilities in $C_2H_2 - H_2$ mixtures—362(A)
Loring, R. A. (see Green, J. B.)—574
Loughridge, Donald H. Direction of photo-electron emission—488
Lovell, D. E. (see Kimball, A. L.)—948
Lunn, E. G. (see Hogness, T. R.)—26

MacDougall, F. H. Book reviews—225, 357
Mack, J. E. and J. M. Cork. X-ray K absorption in elements W(74) to U(92) and K screening numbers —741
Mackay, G. M. J. (see Jones, Howard A.)—201.
Margenau, Henry. On the Zeeman effect in the cerium spectrum between 3000 and 5000 A-units —458
Masius, Morton. Factorial functions in entropy calculations—84
McCarty, L. E. Relation between plate current and plate potential in the thermionic amplifier—878
Meserve, W. E. Some current-time relations in the aluminum cell—215
Miley, H. A. (see Pietenpol, W. G.)—697
Moore, C. L. E. Book review—89
Morrow, Roger M. (see Stewart, G. W.—232)
Morse, P. M. (see Compton, K. T.)—305
Mulliken, Robert S. Electronic states and band spectrum structure in diatomic molecules. V. Bands of the violet CN ($^2S \rightarrow {}^2S$) type—138; VI. Theory of intensity relations for case *b* doublet states. Interpretation of CH bands λλ 3900, 4300—785
——— Book review—535
——— (see Barton, Henry A.)—175
——— (see Jenkins, Francis A.)—150
——— (see Kemble, E. C.)—438

Osgood, T. H. X-ray spectra of long wave-length —567.

Page, Leigh. Book reviews—89, 966
Parmley, T. J. Photo-electric threshold of single bismuth crystals—656
Payne, Cecelia H. Book review—359
Pearson, Hazel. (see Kent, Norton A.)—266
Perkins, B., Jr. (see Watson, William W.)—592
Pfund, A. F. Book review—223
Piersol, R. J. Photo-electric conduction in selenium —664
——— Book review—87
Pietenpol, W. G. and H. A. Miley. Liquid wires and their surface films—697.
Poetker, A. H. Infra-red radiation of hydrogen—418
——— Infra-red radiation of nitrogen—812
Pool, M. L. Post-arc conductivity and metastable states in mercury—848

Ramsperger, H. C. (see Gibson, G. E.)—598, 363(A)
Richardson, Burt. (see Cummings, N. W.)—527
Richtmyer, F. K. Further experimental tests of theories of absorption of x-rays—755
Rogers, R. A. M series x-ray absorption spectra of osmium, iridiam, and platinum—747
Row, C. K. Venkata. Theory of the gravitational field in the light of Maxwell's theory—189
Ruark, Arthur E. Book review—535

Saunders, F. A. Book reviews—360, 361
Schmidt, Clarence C. Dielectric constants of four electrolytes—925
——— (see Carman, A. P.)—922
Shea, John D. Structure of the swan bands—825
Shenstone, A. G. The spark spectrum of nickel (Ni II)—255
Skellett, A. M. (see Hughes, A. Ll.)—11
Slosson, Edwin E. Book reviews—222
Smyth, H. D. (see Costa, J. L.)—349
Stewart, G. W. and Roger M. Morrow. X-ray diffraction in liquids: primary normal alcohols —232

Taylor, Lucien B. (see Kent, Norton A.)—266
Thomas, A. R. (see Hughes, A. Ll.)—466
Tonks, Lewi. Space charge as a cause of negative resistance in a triode and its bearing on short wave generation—501
Tyndall, E. P. T. Magnetic properties of thin films of electrolytic iron—681
——— and **J. M. B. Kellogg.** Note on the Barkhausen effect under mechanical stress—354
Vaidyanathan, V. I. Magnetic susceptibilities of vapors of organic liquids—512

Valasek, Joseph. Book reviews—360, 537
Van Dyke, George D. and **George A. Lindsay.** *L* x-ray absorption edges of Sn (50), In (49), Cd (48), Ag (47), Pd (46), Rh (45), Ru (44)—562
Van Vleck, J. H. Dielectric constants and magnetic susceptibilities in the new quantum mechanics. Part II. Application to dielectric constants—31
Van Voorhis, C. C. Heats of condensation of electrons and positive ions on molybdenum in gas discharges—318
Vinyard, H. R. (see Weniger, W.)—362(A)

Warburton, F. W. Hall effect and resistance in sputtered tellurium films—673
Watson, E. C. Velocity and number of the photoelectrons ejected by x-rays as a function of the angle of emission—479
Watson, William W. Book review—224
——— (see Fredrickson, W. R.)—429
——— and **B. Perkins, Jr.** Zeeman effect in the band spectra of AgH, AlH, ZnH, MgH—592
Webster, David L. Direct and indirect ejection of K electrons by cathode rays—365(A)
——— Large losses of energy by cathode rays: ratio of the probabilities of the two types—365(A)
Weinland, Clarence E. Intermittent photographic exposure as affected by wave-length and intermittency ratio—363(A)
——— Intermittent photographic exposure in various regions of the plate curve—367(A)
Weniger, W. and **H. R. Vinyard.** A translucent black "board"—362(A).
Westwater, W., H. W. Frantz and **J. H. Hildebrand.** Internal pressures of pure liquids and liquid mixtures—363(A)
Winans, J. G. Impact fluorescence of zinc—1

Young, W. M. (see George, E. F.)—362(A)

ANALYTIC SUBJECT INDEX TO VOLUME 30

References with (A) are merely to abstracts of papers presented at meetings of the Physical Society.

Absorption of light (see also Spectra, X-rays)
In Hg vapor, resonance radiation, A. Ll. Hughes, A. R. Thomas—466.
In S crystals, B. Kurrelmeyer—893

Actino-electric (see Photo-electric).

Activated gases (see also Collisions of second kind)
Active nitrogen, electrical properties and nature, P. A. Constantinides—95
Active nitrogen, temperature, H. A. Barton, F. A. Jenkins, R. S. Mulliken—175
Atomic hydrogen, properties of, J. Kaplan—639

After-glow
Duration of, in active nitrogen, P. A. Constantinides—95

Alpha particles
Ionization and stopping power in varius gases, G. E. Gibson, E. W. Gardiner—543; G. E. Gibson, H. Eyring—553
Oblique incidence on mica, Haraprasad De—960

Amplifier tubes (see Vacuum tubes)

Arcs (see also Discharge of electricity in gases)
Post-arc conductivity, critical restriking potentials, M. L. Pool—848

Atmospheric electricity
Conditions accompanying Texas sand storms, E. F. George, W. M. Young, H. Hill—362(A)

Atomic rays
Test of velocity distribution in, J. L. Costa, H. D. Smyth, K. T. Compton—349; J. A. Eldridge—931

Barkhausen effect
Under mechanical stress, E. P. T. Tyndall, J. M. B. Kellogg—354

Book reviews
Bedford, T. J., Practical Physics—89
Blasdale, W. C., Equilibria in Saturated Salt Solutions—357
Bligh, N. M., Evolution and Development of the Quantum Theory—225
Brüninghaus, L., Donées numérique de spektroscopie—360

Book reviews—cont.
Bulletin of National Research Council, Molecular Spectra in Gases—535
Cohen, Ernst, Physico-chemical Metamorphosis and Some Problems in Piezochemistry—225
Cohn, Emil, Das electromagnetische Feld—359
Doty, Marion Foster, Selenium, a List of References—87
Eddington, A. S., Internal Constitution of the Stars—359
Ergebnisse der exacten Naturwissenschaften, Vol. V—224
Freundlich, Herbert, New Conceptions in Colloidal Chemistry—88
Glauert, H., Elements of Airfoil and Airscrew Theory—89
Haas, Arthur, Atomic Theory—535
Haber, Fritz, Aus Leben and Beruf-Aufsätze. Reden. Vorträge—358
Handbuch der physicalischen Chemie: Spektroskopie und Kolorimetrie, I. Lifschitz—537
Handbuch der physikalischen Optik, Vol. I, second half—360 Vol. II, second half—537
Harrow, Benjamin, Eminent Chemists of our Time—222
Hess, Victor F., Die elektrische Leitfähigkeit der Atmosphäre und ihre Ursache—357
Hevesy, Georg v., Die seltenen Erden vom Standpunkte des Atombaues—87
Houston, R. A., Treatise on Light—224
Howe, Harrison E., Chemistry and the World's Work—222
Kayser, H., Tabelle der Hauptlinien der Linienspektra aller Elemente nach Wellenlänge geordnet—361
Kohlrausch, Fritz, Probleme der Gamma-Strahlung—358
König, Ernst, Elastizität und Festigkeit—967
Lifschitz, I., Spektroskopie und Kolorimetrie—537
Lipsius, Friedrich R., Wahrheit und Irrtum in der Relativitätstheorie—966
Lorentz, H. A., Problems in Modern Physics—89
Lorentz, H. A., Lectures on Theoretical Physics, Vol. I—966
Lorentz, H. A., Theorie der Strahlung—966

Book reviews—cont.
McCutcheon, Thomas P., and Harry Seltz, General Chemistry—967
Mayer, Edgar, Clinical Applications of Sunlight and Artificial Radiation—223
Merkel, Friedrich, Die Grundlagen der Wärmeübertragung—257
Pullin, V. E., and W. J. Wiltshire, X-Rays Past and Present—537
Reymond, Arnold, History of the Sciences in the Greco-Roman Antiquity—224
Rideal, Eric K., Catalysis in Theory and Practice—88
St. Meyer and E. Schweidler, Radioaktivität—358
Sheldon, H. Horton, C. V. Kent, Carl W. Miller and Robert F. Paton, Physics for Colleges—223
Soddy, Frederick, Science and Life—222
Trevor, J. E., General Theory of Thermodynamics—225
Whitehead, S., Dielectric Phenomena—967

Cathode dark space
Length of, variation with pressure, L. H. Dawson—119

Cathode fall
Theory of normal cathode fall, K. T. Compton, P. M. Morse—305

Cathode rays
Ejection of *K* electrons, D. L. Webster—365(A)
Large losses of energy, ratio of loss by collision transfer to loss by radiation, D. L. Webster—365(A)

Charge, fundamental unit
Ratio, to mass of electron, spectroscopic determination, W. V. Houston—608

Collisions of the second kind
In Hg vapor, quenching resonance radiation, P. D. Foote—288
In Hg vapor, depolarization of resonance radiation, P. D. Foote—300
In iodine vapor, with active nitrogen, P. A. Constantinides—95
In NO, with A^+ and He^+, T. R. Hogness, E. G. Lunn—26
In Zn vapor with Hg′, fluorescence, J. G. Winans—1

Compton effect (see X-rays, scattering)

Conductivity (see Electrical conductivity, Thermal conductivity)

Crystals, single
Of Bi, Hall effect, C. W. Heaps—61
Of Bi, photo-electric threshold, T. J. Parmley—656
Of Bi, thermo-electric effects, R. W. Boydston—911
Of Ni, diffraction of electrons by, C. Davisson, L. H. Germer—705
Of S, photo-conductivity, B. Kurrelmeyer—893
Of Zn, photo-electric effect and surface structure, E. G. Linder—649

Cybotactic state
In primary normal alcohols, G. W. Stewart, R. M. Morrow—252

Dielectric constant
Of electrolytes, method of measuring, values for H_2O, turpentine, CH_3OH, $CHCL_3$, zylol, acetone, A. P. Carman, C. C. Schmidt—922
Of gases, influence of magnetic field, theory, J. H. Van Vleck—31
Of solutions of NaCl, KCl, $BaCl_2$, $CuSO_4$, C. C. Schmidt—925

Diffraction
Of x-rays, by ruled grating, F. L. Hunt—227; T. H. Osgood—567
Of x-rays in primary normal alcohols, G. W. Stewart, R. M. Morrow—232

Discharge of electricity through gases
Heats of condensation of electrons and positive ions on Mo, C. C. Van Voorhis—318
In Hg vapor, post-arc conductivity, M. L. Pool—848
Motion of striae with variation of pressure, L. H. Dawson—119
Pressure changes and dissociation in discharge tubes, W. H. Crew, E. O. Hulburt—124
Theory of cathode fall, K. T. Compton, P. M. Morse—305

Dissociation (see also Dissociation, heat of)
Of H_2, O_2, N_2, air, CO, CO_2 as functions of pressure and power input in discharge tubes, W. H. Crew, E. O. Hulburt—124
Of H_2, by electron impact, A. Ll. Hughes, A. M. Skellett—11
Of HCl by electron impact, H. A. Barton—614

Dissociation, Heat of
Of H_2, from ultra-violet band spectra, G. H. Dieke, J. J. Hopfield—400
Of ICl, from band spectra, G. E. Gibson, H. C. Ramsperger—598
Of NO, from critical potentials, T. R. Hogness, E. G. Lunn—26

Doublet separation
In Balmer lines of hydrogen, N. A. Kent, L. B. Taylor, H. Pearson—266
In spectrum of Sn II, J. B. Green, R. A. Loring —574

e/m
Spectroscopic determination, W. V. Houston—608

Elasticity
Longitudinal vibrations of a liquid in a tube with elastic walls, T. H. Gronwall—71
Optical determination of stresses, I. A. Balinkin—520

Electrolytes
Dielectric constants of solutions of NaCl, KCl, $BaCl_2$, $CuSO_4$, C. C. Schmidt—925

Electrolytic cell
Current time relations in aluminum cell, W. E. Meserve—215

Electrical conductivity and resistance (see also Photo-conductivity)
Of active nitrogen, P. A. Constantinides—95
Of Pb, temperature variation through melting point, W. G. Pietenpol and H. A. Miley—697
Of sputtered Te films, effect of heat treatment, F. W. Warburton—673

Electrical oscillations and waves
Short wave generation in triode, relation to space charge, L. Tonks—501
Speed, along wires, F. Allison—66

Electromagnetic theory
Of the gravitational field, Venkata Row—189

Electronic states (see Electrons, energy states)

Electrons
Boundary and charge density of individual electron, theory, H. Bateman—55
Charge on, ratio to mass, W. V. Houston—608
Diffraction of, by Ni crystal, C. Davisson, L. H. Germer—705
Heats of condensation on Mo, C. C. Van Voorhis —318
Loss of energy on impact with metals, D. L. Webster—365(A)
Orbits, calculation, in amplifier tube, L. E. McCarty—878

Electrons, energy states
Of Cu I, Zn II, Ga III, Ge IV, Zn I, Ga II, Ge III, R. J. Lang—762
Of diatomic molecules, from band spectrum structure, R. S. Mulliken, —V, 138; VI, 785

Electrons, energy states—cont.
Of elements from Ru to Su, L, M, N, O levels, G. D. Van Dyke, G. A. Lindsay—562
Of elements from Sb to Sa, N_{IV}, N_V, $O_{II\text{-}III}$ levels, K. Chamberlain, G. A. Lindsay—369
Of NO, from band spectrum structure, F. A. Jenkins, H. A. Barton, R. S. Mulliken—150
Rotational distortion, theory and application to OH bands, E. C. Kemble—387

Electrons, reflected, scattered, secondary (see also Photo-electric emission of electrons)
Direct and indirect ejection of K electrons by cathode rays, D. L. Webster—365(A)
Efficiency of ejection of K electrons by cathode rays, D. L. Webster—365(A)
From electrodes in active nitrogen, P. A. Constantinides—95
Reflected, from Ni crystal, C. Davisson, L. H. Germer—705
Reflected and secondary electrons from Al, magnetic analysis of velocity distribution, J. B. Brinsmade—364(A), 494
Secondary electrons from Mo due to bombardment by high speed positive ions of alkali metals, W. J. Jackson—473

Electrons, impacts in gases (see also Arcs, Discharge of electricity in gases)
Dissociation of H_2, A. L. Hughes, A. M. Skellett —11
Evidence for high speed "secondaries," C. C. Van Voorhis—318

Electrons, thermionic emission (see thermionic emission of electrons)

Energy levels (see Electrons, energy states)

Entropy calculations
Factorial functions in, M. Masius—84

Errata
Hall effect in bismuth with low magnetic fields, P. H. Craig—964
Ionization efficiency of ultra-violet light in caesium vapor, E. M. Little—963

Ether-drift
Trouton-Noble experiment, repetition, C. T. Chase—516
Michelson-Morley experiment, repetition, K. K. Illingworth—692

Evaporation
From lakes, calculation of, N. W. Cummings, B. Richardson—527
Rate, for W, Mo, Pt, Ni, Fe, Cu, Ag, H. A. Jones, I. Langmuir, G. M. J. Mackay—201

Faraday effect
Of liquids, differences in lag behind magnetic field, F. Allison, 66

Fine structure
Of Balmer lines, N. A. Kent, L. B. Taylor, H. Pearson—266
Of Na_2, K_2 bands, analysis, W. R. Fredrickson, W. W. Watson—429

Fluorescence
Of Zn vapor, due to impact with Hg′, J. G. Winans —1

Friction
Internal, in solids, A. L. Kimball, D. E. Lovell— 948

Gordon's equations
Modification of, H. Bateman—55

Gravitation,
Theory, in the light of Maxwell's theory, Venkata Row—189

Galvanomagnetic effects (see also Hall effect)
Electron-quantum theory of, A. E. Caswell—365 (A)

Hall effect
In Bi, low magnetic fields, errata, P. H. Craig—964
In Bi single crystal, C. W. Heaps—61
In sputtered Te films, effect of heat treatment, F. W. Warburton—673

Hydrogen, atomic
Properties of, J. Kaplan—639

Instruments (see also Measurements, methods)
Pressure gauge, discharge tube, L. H. Dawson —119

Intensity in spectra
In absorption spectrum of ICl, variation with temperature, G. E. Gibson, H. C. Ramsperger —363(A), 598
In band spectra of diatomic molecules, R. S. Mulliken—138, 785
In blue Cs doublet, ratio, C. F. Hagenow, A. Ll. Hughes—284
In NO beta bands, measurement and interpretation, H. A. Barton, F. A. Jenkins, R. S. Mulliken—175
In Stark effect in He, J. M. Dewey—770
In x-ray L spectrum of Th, S. K. Allison—365(A), 245

Interference of light
Of individual quanta, A. J. Dempster, H. F. Batho —644

Ionization by collisions of second kind
Of C_2H_2 and NH_3, by positive air ions, H. A. Erikson—339
Of iodine vapor, P. A. Constantinides—95
Of NO, by He^+, A^+ ions, T. R. Hogness, E. G. Lunn—26

Ionization by electron impact
Of HCl, nature of ions produced, H. A. Barton —614
Of NO and mixtures with A and He, nature of ions formed, T. R. Hogness, E. G. Lunn—26

Ionization by alpha-particles
In $(CN)_2$, HCN, CO, CO_2, N_2O, CH_3I, O_2, CH_3N, NO, G. E. Gibson, H. Eyring—553
In H_2, Ne, N_2, O_2, A, CH_3I, G. E. Gibson, E. W. Gardiner—543

Ionization by radiation (see Photo-ionization)

Ionization potentials (see Potentials, critical)

Ions (see also Mobility of Ions)
Absorption of K^+ ions in He, air, A, N_2, O_2, F. M. Durbin—844
Analysis of ions formed by electron impact in NO and mixtures with A and He, T. R. Hogness, E. G. Lunn—26
Analysis of ions formed in HCl by electron impact, H. A. Barton—614
Heat of neutralization of A^+ ion on Mo, C. C. Van Voorhis—318
Residual, in Hg arc, post-arc duration, M. L. Pool—848
Secondary electron emission produced by high speed positive ions of alkali metals, W. J. Jackson—473

Isotopes
Of Li, abundance ratio as function of temperature, J. L. Hundley—864

Magnetic properties (see also Hall effect, Galvanomagnetic effects, Thermomagnetic effects)
Barkhausen effect under mechanical stress, E. P. T. Tyndall, J. M. B. Kellogg—354
Faraday effect, lag behind magnetic field, F. Allison—66
Magnetization and hysteresis curves for thin Fe films, E. P. T. Tyndall—681
Susceptibilities, in the new quantum mechanics, J. H. Van Vleck—31
Susceptibilities of vapors of organic liquids, V. L. Vaidyanathan—512

Magnetization by rotation
Differences between direct and inverse effect, S. J. Barnett—964(A)

Mathematics
Factorial functions in entropy calculations, M. Masius—84

Maxwell's distribution law
Experimental test, J. L. Costa, H. D. Smyth, K. T. Compton—349; J. A. Eldridge—931

Measurements, methods (see also Instruments)
For dielectric constants of electrolytes, electrometer method, A. P. Carman, C. C. Schmidt—922
For magnetic susceptibilities in vapors, V. I. Vaidyanathan—512
For temperature coefficients of resistance, W. B. Pietenpol, H. A. Miley—697

Mechanics, quantum
Application to dielectric constants and magnetic susceptibilities, J. H. Van Vleck—31
Modification of Gordon's equation, H. Bateman—55

Mechano-magnetic effects
Barkhausen effect under mechanical stress, E. P. T. Tyndall, J. M. B. Kellogg—354
Magnetization by rotation, S. J. Barnett—964(A)

Metastable states
In Hg, relation to post-arc conductivity, M. L. Pool—848

Michelson-Morley experiment
Repetition, using Kennedy's refinement, K. K. Illingworth—692

Mobility of Ions
Effect of the medium on mobility of air ions, H. A. Erikson—339
In $C_2H_2-H_2$ mixtures, L. B. Loeb, L. Du Sault—362(A)

Molecular space array
In primary normal alcohols, G. W. Stewart, R. M. Morrow—232

Molecular structure
Of carrier of Swan bands, constants, J. D. Shea—825
Of Na_2, K_2, from band spectra, W. R. Fredrickson, W. W. Watson—429
Of NO, constants, from band spectra, F. A. Jenkins, H. A. Barton, R. S. Mulliken—150
Of O_2, constants, from band spectra, G. H. Dieke, H. D. Babcock—366(A)

Peltier heat (see Thermo-electric effects)

Photo-chemical effects
Intermittent exposure, as affected by wave-length and intermittency ratio, C. E. Weinland—363(A)
Intermittent exposure in various regions of plate curve, C. E. Weinland—367(A)

Photo-electric conduction
Of S crystals, variation with electric field, intensity of illumination, wave-length, crystal orientation, B. Kurrelmeyer—893
Of Se, variation with light intensity and temperature, R. J. Piersol—664

Photo-electric emission of electrons
From Al, by x-rays, energy, A. A. Bless—871
From Bi single crystals, threshold, T. J. Parmley—656
From Cs-Au alloy, efficiency, E. M. Little—109
From electrodes, by active nitrogen, P. A. Constantinides—95
From thin metal films, by x-rays, variation of velocity and number with angle of emission, E. C. Watson—479
From Zn single crystals, effect of orientation, E. G. Linder—649
In air, H_2, A by x-rays, direction of ejection, D. H. Loughridge—488
Indirect ejection of K electrons by cathode rays, D. L. Webster—365(A)

Photographic effects (see Photo-chemical effects)

Photo-ionization of gases
Of Cs vapor, efficiency of ultra-violet light, E. M. Little—109; correction—963

Polarization of radiation
Depolarization of resonance radiation in Hg vapor, P. D. Foote—300

Positive ray analysis
Of ionization products in HCl, H. A. Barton
Of ionization products in NO and mixtures with A and He, T. R. Hogness, E. G. Lunn—26
Of Li isotopes, J. L. Hundley—864

Potentials, critical
For dissociation of H_2, A. L. Hughes, A. M. Skellett—11
Ionization and resonance potentials of Sn I, Sn II, Sn III, from spectrum analysis, J. B. Green, R. A. Loring—574
Ionization potentials of H^+ and $(HCl)^+$, H. A. Barton—614
Ionization potential of N II, from spectrum, A. G. Shenstone—255

Potential, critical—cont.
Ionization potentials in NO, T. R. Hogness, E. G. Lunn—26
Ionization potential of Zn III from spectrum, O. Laporte, R. J. Lang—378
Resonance potential of H_2, G. H. Dieke, J. J. Hopfield—400
Restriking potentials in Hg arc, M. L. Pool—848

Pressure
Internal, in pure liquids and liquid mixtures, W. Westwater, H. W. Frantz, J. H. Hildebrand —363(A)

Pressure effect in spectra
in spectrum of Fe, H. D. Babcock—366(A)

Quanta
Interference of individual quanta, A. J. Dempster, H. F. Batho—644

Quantum mechanics (see Mechanics, quantum)

Radiation, black body
Fluctuations in, and thermal equilibrium, S. Jacobsohn—936 note, S. Jacobsohn—944

Radioactivity
Half-period of Ra E, L. F. Curtiss—539
Ionization and stopping power of gases for alpha-particles from Po, I, G. E. Gibson, E. W. Gardiner—543; II, G. E. Gibson, H. Eyring —553
Oblique incidence of alpha-particles on mica, peculiarities of tracks, Haraprasad De—960

Reflection, total
Of x-rays, by glass, Sn, Ag, Se, Zn, H. W. Edwards —91

Refractive index
Of gases, in the new quantum mechanics, J. H. Van Vleck—31
Of glass, Sn, Ag, Se, Zn, for x-rays, H. W. Edwards—91

Relativity
Michelson-Morley experiment, repetition using Kennedy's refinement, K. K. Illingworth—692
Trouton-Noble ether drift experiment, repetition, C. T. Chase—516

Resonance potential (see Potentials, critical)

Resonance radiation
Absorption in Hg vapor, A. L. Hughes, A. R. Thomas—466
Depolarization of, by foreign gases, P. D. Foote —300
Of Hg, quenching by foreign gases, theory, P. D. Foote—288

Rydberg constant
For H and He, W. V. Houston—608

Shottky effect (see Thermionic emission of electrons)

Space charge
As cause of negative resistance in a triode, bearing on short wave generation, L. Tonks—501

Spectra, atomic
Of Ce, Ce (I), Ce (II), identification, A. S. King —366(A)
Of Ce, Zeeman effect, H. Margenau—458
Of Cs, intensity ratio of blue doublet, C. F. Hagenow, A. L. Hughes—284
Of Fe, pressure effect, H. D. Babcock—366(A)
Of Ga (III), Ge (IV), In (II), wave-lengths and classification, R. J. Lang—762
Of H, extension of Paschen series, A. H. Poetker —418
Of H, doublet separation and fine structure of Balmer lines, N. A. Kent, L. B. Taylor, H. Pearson—266
Of He, intensities in Stark effect, J. M. Dewey —770
Of Ni (II), classification, Zeeman effect, A. G. Shenstone—255
Of O, resolution of 9265 triplet, A. H. Poetker— 812
Of Sn, Sn (I), Sn (II), Sn (III), In (II), Ge (II), classification, J. B. Green, R. A. Loring—574
Of Zn (III), wave-lengths and classification, O. Laporte, R. J. Lang—378

Spectra, fluorescence
Of Zn, due to collisions of second kind with Hg, J. G. Winans—1

Spectra, molecular
Of AgH, AlH, ZnH, MgH. Zeeman effect, W. W. Watson, B. Perkins—592
Of CO, Angstrom bands, Zeeman effect, E. C. Kemble, R. S. Mulliken, F. H. Crawford—438
Of diatomic molecules, electronic states and structure, R. S. Mulliken—V. Bands of violet CN type—138; VI. CH bands, interpretation of bands λλ 3900, 4300—785
Of H_2, in ultra-violet, structure, G. H. Dieke, J. J. Hopfield—400
Of H_2, in infra-red, new lines, A. H. Poetker—418
Of ICl, absorption, analysis and interpretation, G. E. Gibson, H. C. Ramsperger—363(A), 598
Of N_2, in infra-red, extension of first positive group, reassignment of vibration numbers, A. H. Poetker—812
Of Na_2, K_2, absorption, fine structure, W. R. Fredrickson, W. W. Watson—429

Spectra, molecular—cont.
Of NO, beta bands, intensity relations and interpretation, H. A. Barton, F. A. Jenkins, R. S. Mulliken—175
Of NO, band structure and wave numbers, F. A. Jenkins, H. A. Barton, R. S. Mulliken—150
Of O_2, absorption, wave-lengths and quantum interpretation, G. H. Dieke, H. D. Babcock—366(A)
Of OH, rotational distortion of electronic states, E. C. Kemble—387
Rotational distortion in multiplet band spectra theory, E. C. Kemble—387
Swan bands, frequencies, quantum analysis, molecular constants of carrier, J. D. Shea—825
Theoretical relation between infra-red and ultra-violet bands, R. T. Birge, J. J. Hopfield—365(A)

Stark effect
In He, intensities, J. M. Dewey—770

Straggling of alpha-particles
In various gases, G. E. Gibson, H. Eyring—553

Stresses
Optical determination in long rectangular plates under torsion, I. A. Balinkin—520

Striae
Motion of, in discharge tubes, L. H. Dawson—119

Surface films
On wires of Pb, Sn, Zn, Bi, W. G. Pietenpol, H. A. Miley—697

Susceptibility (see Magnetic properties)

Term values, spectroscopic (see electrons, energy states)

Thermal conductivity
Of Fe, Cu, Ag, Au, as effected by magnetic field, H. M. Brown—364(A)

Thermionic emission of electrons
Work function of W, C. Davisson, L. H. Germer—634

Thermo-electric effects
In Bi single crystal, thermal e.m.f., thermo-electric power, Peltier heat, differences in Thomson coefficient for $Bi_\perp$ against $Bi_\parallel$, R. W. Boydston—911
In polycrystalline Bi, Zn, thermal e.m.f., R. W. Boydston—911

Thermo-magnetic effects
Effect of magnetic field on thermal conductivity of Fe, Cu, Ag, Au, H. M. Brown—364(A)

Thermo-magnetic effects—cont.
Electron-quantum theory of, A. E. Caswell—364(A)

Trouton-Noble experiment
Repetition, C. T. Chase—516

Vacuum tubes
Relation between plate current and plate potential in amplifier, L. E. McCarty—878
Space charge as a cause of negative resistance in triode, relation to short wave generation, L. Tonks—501

Vaporization (see Evaporation)

Vapor pressures
Of W, Mo, Pt, Ni, Fe, Cu, Ag, H. A. Jones, I. Langmuir, G. M. J. Mackay—201

Velocity distribution in gases
Experimental test of Maxwell's distribution law, J. L. Costa, H. D. Smyth, K. T. Compton—349; J. A. Eldridge—931

Vibrations, elastic
Longitudinal, of a liquid in tube with elastic walls, T. H. Gronwall—71

Wave mechanics (see Mechanics, quantum)

Work function
Heats of condensation of electrons and positive ions on Mo in gas discharges, C. C. Van Voorhis—318
Of Li_6 and Li_7, ratio, J. L. Hundley—864
Of W, correction for Shottky effect, C. Davisson, L. H. Germer—634

X-rays, absorption
Further test of theories, mass absorption of Sn, F. K. Richtmyer—755
K absorption in elements W to U, J. E. Mack, J. M. Cork—741
L absorption edges of Sn, In, Cd, Ag, Pd, Rh, Ru, G. D. Van Dyke, G. A. Lindsay—562
L absorption edges of elements Sb to Sa, K. Chamberlain, G. A. Lindsay—369
M absorption spectra of As, Ir, Pt, R. A. Rogers—747

X-rays, continuous
Efficiency of production, D. L. Webster—365(A)

X-rays, diffraction
By ruled grating, F. L. Hunt—227; T. H. Osgood—567
In primary normal alcohols, G. W. Stewart, R. M. Morrow—232

X-rays, reflection and refraction
Total reflection and index of refraction in glass, Sn, Ag, Se, and Zn, H. W. Edwards—91

X-rays, photo-electric effect
Angular distribution of photo-electrons from thin metal films, E. C. Watson—479
Efficiency of ejection of *K* electrons, D. L. Webster—365(A)
From Al, energy of recoil electrons, A. A Bless—871
In air, H_2, A, direction of emission of photoelectrons, D. H. Loughridge—488

X-rays, scattering
Test of theories, A. A. Bless—871

X-ray, spectra
L spectrum of Th, relative intensities of lines, S. K. Allison—245; 365(A)

Zeeman effect
In AgH, AlH, ZnH, MgH bands, W. W. Watson, B. Perkins—592
In Angstrom CO bands, E. C. Kemble, R. S. Mulliken, F. H. Crawford—438
In Ce spectrum, H. Margenau—458
In Ni (II) spectrum, *g* values, A. G. Shenstone—255
In Sn, Sn (I), Sn (II), Sn (III), *g* values, J. B. Green, R. A. Loring—574

Physics Lib

Annual Subscription, Ten Dollars, New Rate, Effective January 1, 1928

VOLUME 30 SECOND SERIES NUMBER 6

DEC 12 1927

THE PHYSICAL REVIEW

A JOURNAL OF EXPERIMENTAL AND THEORETICAL PHYSICS

CONDUCTED BY

THE AMERICAN PHYSICAL SOCIETY

BOARD OF EDITORS

Managing Editor: JOHN T. TATE, University of Minnesota, Minneapolis

K. K. DARROW, E. C. KEMBLE, F. L. MOSHER, J. A. GRAY, G. E. M. JAUNCEY, J. H. VAN VLECK, G. BREIT, P. W. BRIDGMAN, L. W. MCKEEHAN

DECEMBER, 1927

Diffraction of Electrons by a Crystal of Nickel — C. DAVISSON AND L. H. GERMER 705

X-Ray K Absorption in Elements W(74) to Ag(47) and K Screening Numbers — J. E. MACK AND J. M. CORK 741

M-Series X-Ray Absorption Spectra of Osmium, Iridium and Platinum — R. A. ROBERTS 747

Further Experimental Tests of Theories of the Absorption of X-Rays — F. K. RICHTMYER 751

The Spectra of Gallium, Germanium and Indium — R. J. LANG 762

Anomalies in the Stark Effect of Helium: II — JANE M. DEWEY 770

Zeeman Effect of the Symmetrical Top according to the Wave Mechanics — EDWARD U. CONDON 781

Electronic States and Band Spectrum Structure in Diatomic Molecules: VI. Theory of Intensity Relations for case b Doublet States. Interpretation of CH Bands at 3900, 4300 — ROBERT S. MULLIKEN 785

Infra-Red Emission of Nitrogen — A. H. PFUND 812

Structure of Carbon Bands — JOHN D. HERTZ 835

Absorption Spectra of Cerium Ions in Various Crystals — F. M. DUFFIEUX 844

Post-arc Conductivity and Metastable States of Mercury — M. L. POOL 848

Relative Intensities of Positive Rays from the Isotopes of Lithium — JOHN LESLIE HOBBLEY 864

Band Electron Gas, Aluminum — A. A. BERGE 871

Relation between Plate Current and Plate Supplied in the Thermionic Amplifier, deduced from the Orbital Motion of Electrons — L. E. MCCARTY 879

Photoelectric Sensitivity of Sulphur — NEBENHARD KURRELMEYER 892

Thermo-electric Effect in Single Crystal Bismuth — R. W. BOYDSTON 911

Arrangement for the Electrometer Method for Measuring the Dielectric Constants of Electrolytes — A. P. CARMAN AND C. C. SCHMITT 922

Dielectric Constants of four Electrolytes in Water by the Cermak Electrometer Method — CLARENCE C. SCHMITT 933

Experimental Proof of Maxwell's Distribution — JOHN A. ELDRIDGE 971

Radiation Pressures and Thermal Equilibrium — SAMUEL JACOBSOHN 976

Notes on the Illumination in Black Bodies — SAMUEL JACOBSOHN 984

Thermal Emission of Solids — A. L. KIMBALL AND D. E. LOVELL 948

Critical Potentials of Alpha-Particles and Electrons — HARAPRASAD DAS 960

[illegible] 963

[illegible] 964

[illegible] 969

PUBLISHED BY THE AMERICAN PHYSICAL SOCIETY

MINNEAPOLIS, MINN.

THE AMERICAN PHYSICAL SOCIETY

OFFICERS OF THE SOCIETY

President:	K. T. Compton	Princeton University, Princeton, N.J.
Vice-President:	Henry G. Gale	University of Chicago, Chicago, Ill.
Secretary:	H. W. Webb	Columbia University, New York City.
Treasurer:	G. B. Pegram	Columbia University, New York City.
Editor:	John T. Tate	University of Minnesota, Minneapolis, Minn.
Local Secretary for the Pacific Coast:	D. L. Webster	Stanford University, Calif.

THE PHYSICAL REVIEW

Published monthly

Two volumes annually

First series. From July 1, 1893 to January 1, 1913, the Review was conducted by Edward L. Nichols, Ernest Merritt and Frederick Bedell, with the financial support of Cornell University. The first four volumes were issued annually; subsequent volumes, semi-annually; thirty-five volumes in all.

Second series. On January 1, 1913, the Review was transferred to the American Physical Society as announced on the first page of the new series which was then begun. Since then it has been conducted by a Board of Editors elected by the Society. Semi-annual volumes begin in January and July.

Contributors are referred to page 2 of the advertisements for further information.

Annual Subscription, throughout the Postal Union, $10.00 in advance.

Single Copies, $1.00.

General Index, 1893-1920, $4.00, in advance.

Back Volumes, $6.00 per volume; Back Numbers, $1.00 per copy. Postage is free if remittance accompanies order; otherwise postage is extra. No bound volumes can be supplied. The Review offers to purchase a limited number of First Series, Vol. 1, No. 1 (at $2.00 each); Second Series, Vol. 7, No. 1, January 1916; Vol. 7, No. 2, February 1916; Vol. 7, No. 4, April 1916; and Vol. 7, No. 5, May 1916 (at $2.00 each).

Advertisements. Rates will be supplied by the Editor on request. Copy for each number must be received at Minneapolis before the 1st of the preceding month; old copy is used until new copy is received. Send electrotypes direct to the printers, George Banta Publishing Co., Menasha, Wisconsin.

Discount of ten per cent is allowed subscription agencies and members of the American Physical Society.

Changes of address and Complaints of failure to receive the Review, in the case of members of the Physical Society, should be addressed to the Treasurer; otherwise, to the Editor. *New copies will be sent free if complaint is received within three months of date of issue.*

Correspondence should be addressed to the Physical Review, University of Minnesota, Minneapolis, Minn.

Entered at the postoffice at Menasha, Wis., as second class matter.
Acceptance for mailing at special rate of postage provided for in section 1103, Act of October 3, 1917, authorized September 6, 1926

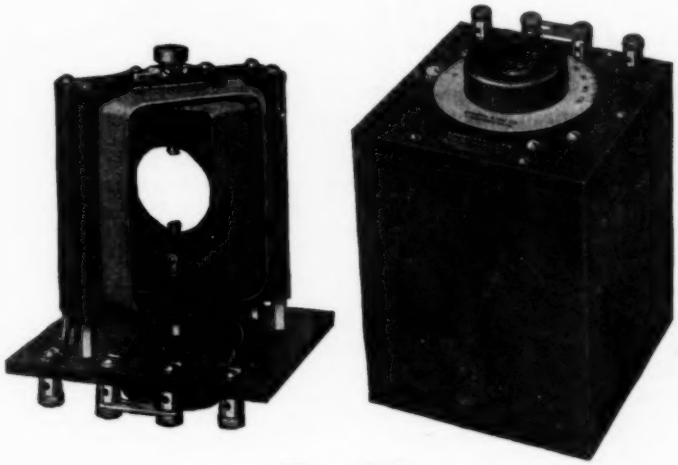

Type 107

Laboratory Variometer

A variable inductance for general laboratory use. The coils are designed to have a low high frequency resistance and high current-carrying capacity.

Three types cover the range from 0.02 to 18 MH.

Described in Bulletin 3050P.

Type 107 Variometer.....$25.00

Mounted calibration curve $5.00 extra.

Manufactured by

General Radio Company

Manufacturers of Electrical and Radio Laboratory Apparatus for Over a Decade.

30 STATE ST. **CAMBRIDGE, MASS.**

INFORMATION FOR CONTRIBUTORS TO THE PHYSICAL REVIEW

Purpose of the Review is to publish articles that add to our knowledge of experimental or theoretical physics.

Articles which have not previously been published may be submitted by any physicist whether American or not. Each manuscript will be acknowledged by the Managing Editor as soon as received. An article to be considered must be in English and in a form ready for publication; it must be provided with a preliminary abstract prepared in accordance with the directions given on a following page. Carelessly written articles and figures not carefully drawn will be returned for revision. All manuscripts should be typed double space and symbols written in with great care so as to be quite clear to the printer.

Suggestions as to Contents. On account of the high cost of printing, brevity is of great practical importance. Historical summaries of previous results and also discussions which consider various possible explanations without leading to definite conclusions should be made very brief, except in special cases. The greater part of the paper should be devoted to the actual new results and to a concise presentation of the conclusions to which they lead. Attention should be directed to the more accurate and more conclusive experiments, omitting any which add nothing. The amount of detail included should be governed somewhat by the importance of the results and their interest to physicists.

Suggestions as to form. Clearness is of great importance. Pains should be taken to insure that the order and form of presentation are such as to enable the reader to grasp the new information as easily and quickly as possible. In general the order should be: Statement of the problem and of the purpose, scope and general method of the investigation, followed by a description of the apparatus, experiments and results in such order as to bring out clearly the evidence for the main conclusions, the paper ending with perhaps a brief discussion of the significance and bearing of the results on other problems. Avoid the historical or laboratory note-book style; use rather the text-book or lecture style. Footnotes should be numbered consecutively and each reference should contain author's name.

Abbreviations. Omit periods after such symbols for units as the following: cm, mm, kv, lb, A, °C; also after I, II, . . . and percent, and after headings in columns in Tables. Write a.c., e.m.f., abscissas, disk, in vacuum, wave-length, x-rays, percent. Refer to figures as Fig. 1, Figs. 3 and 4; and to equations as: Eq. (5); Eqs. (7) and (8). Number equations on the right.

Mathematics. Indicate division by a slant line where possible. Avoid unusual symbols, symbols with rules over them, cumbersome fractions.

Figures or illustrations. Use only jet black ink, on white or on blue-lined cloth or paper. Tracing cloth is especially suitable. Curves plotted or traced on such cloth or paper may have co-ordinates ruled in black at desired intervals, say every centimeter or inch, as blue lines are not reproduced photographically. *Colors other than blue and black should be avoided.* Indicate observed points on all plots. Arrange material in each figure compactly. It is well when possible, to make the longer dimension horizontal, as larger reproduction can then be permitted; if vertical figures are necessary space may be saved by making two of the same height, and putting them side by side. *All lettering should be at least* $\frac{3}{16}$″ *high* for an 8″×10″ figure, so as to be legible after reduction. Lettering left in pencil will be inked in by a draftsman in this office. In general each figure and table should have a caption, describing it briefly. Reduce the number of tables and figures to the necessary minimum.

Proofs. Galley proof of each article is sent directly from the publishers to the author and should be corrected with great care so as to eliminate all errors, as page proof cannot always be submitted. Only necessary changes should be made; extensive additions will mean the delay of a month in publication. All corrected proof should be sent promptly with the manuscript to THE PHYSICAL REVIEW, 1500 University Ave., S.E., University of Minnesota, Minneapolis.

Permission to republish any article is given, if proper acknowledgment is made.

Reprints ordered on the proper form with the return of the galley proof, will be furnished by the printer according to the prices given on the form.

CAMBRIDGE INSTRUMENTS

Type "B" String Galvanometer

Einthoven String Galvanometer

THIS well known instrument possesses the advantages of extreme sensitivity, short period and negligible self-induction or capacity. It is largely used for physical and physiological investigations. Several types are furnished.

TYPE "A" incorporates the greatest sensitivity obtainable in this type galvanometer with proportionality of string deflections over wide range. String length 13 cms.—weight 200 lbs.

TYPE "B" has a readily interchangeable suspension which makes possible Quick replacement of strings of different characteristics. String length 7 cm.—weight 45 lbs.

TYPE "C" is conspicuous for its small size and weight. The string suspension is interchangeable. The stray field set up by this galvanometer is extremely small. String length 6 cm.—weight 10 lbs.

Salomonson Type—this instrument provides an interchangeable suspension with two low resistance metal strings. It has relatively low current sensitivity and extremely short period.

The following accessories used with String Galvanometers can be furnished—Incandescent, Pointolite and Automatic Arc Lamp Sources; Photographic Recorders to take 4.5 cm., 6 cm., or 12 cm. bromide paper or film, Tuning Fork-driven Synchronous Time Markers and Standardizing Resistance Boxes for calibrating galvanometer deflections.

Full particulars furnished on request.

Temperature Measuring & Controlling Instruments
Engineering Instruments
D. C. Electrical Instruments

CAMBRIDGE
INSTRUMENT Co INC
FACTORY OSSINING-ON-HUDSON NEW YORK
SALES OFFICE & SHOWROOM GRAND CENTRAL TERMINAL NEW YORK CITY

A. C. Electrical Instruments
Physiological Instruments
Special Instruments

The New Form of

NON-INDUCTIVE TUBULAR RHEOSTATS

with sliding contact

No. 2748

Costs Less ***Added Usefulness***

We offer, at exceptionally low prices, a complete range of Rheostats in this durable, heavy duty type, wound on non-inductive tube.

Inductive effect reduced more than 90% by non-magnetic core.
Wire is of high specific resistance and negligible temperature coefficient.
Laminated brush contacts are made of brass.
Heavy oxidation provides ample insulation.
Nickel-plated, brass slide-rod gives rapid and smooth adjustment.

These rheostats are all wound on tubes 30 cm long and 4 cm diameter. The end supports are substantial, aluminum castings, not stamped sheet metal such as is usually provided in this type of rheostat. The tube is of insulating material throughout, thus eliminating the danger of short-circuiting found in the iron-core type, due to chipping of the enamel coating. This rheostat can be used in conjunction with galvanometers and meters with negligible induction effects, which is not true of iron-core rheostats. Comparative tests show that this inductive effect is less than 1/15th that produced by an iron-core rheostat.

Approx. Resistance, ohms	6	12	20	50	70	100	190	600	2,800
Current Capacity, amperes	7.3	5.6	4.2	3.3	2.5	2.	1.7	1.5	.8
Price each.....	$6.00	$6.00	$6.00	$6.00	$6.00	$6.00	$6.00	$6.00	$6.00

Price in lots of six or more, any selection of ranges, each $5.40.

PACIFIC COAST REPRESENTATIVES

Braun-Knecht-Heimann Company
576-584 Mission Street
San Francisco, California

Braun Corporation
363 New High Street
Los Angeles, California

A Sign of Quality QUALITY WELCH SERVICE *A Mark of Service*

W. M. Welch Scientific Company

1516 Orleans Street — Manufacturers, Importers and Exporters of Scientific Apparatus and School Supplies — Chicago, Ill., U. S. A.

PHYSICAL REVIEW

PREPARATION OF PRELIMINARY ABSTRACTS

An article will not be accepted for publication in THE PHYSICAL REVIEW unless the manuscript is accompanied by an adequate abstract for publication at the beginning of the article. This abstract is intended to aid the reader by furnishing an index and a brief summary of the contents of the article. Besides serving these purposes it should also be suitable for reproduction in abstract journals so as to make it unnecessary for the editors of these journals to have another abstract prepared.

As an index it should be complete; all the subjects, major and minor, concerning which new information is presented, should each be given, with sufficient precision so that any reader can tell from the abstract whether the article contains anything of interest to him. The subject indexes of abstract journals are fundamental in reference work. These indexes are prepared exclusively from the abstracts and whatever is omitted from the abstracts cannot be included in the index and may thus be lost. The writer of an abstract should therefore feel himself under an important obligation to his scientific colleagues to make sure that the abstract is accurate and complete, at least as an index.

As a summary the abstract should give briefly the conclusions of the article, important advances in experimental technique and theory, and all numerical results of general interest that may be conveniently given including all that might belong in a hand book and table of constants. It should give all the information that readers who are not specialists in the particular field involved might desire to know about the article thus saving them the time and trouble in referring to the article itself. Experience has shown that in general the length of the abstract should be from four to eight percent of the length of the article.

THE PHYSICAL REVIEW 1923-1925 contains many examples of adequate abstracts. Most of these contain paragraph titles and subtitles which indicate the subjects concerning which new information is given and it is requested that authors include such subtitles when all the information contained in the article does not refer to the subject indicated by the title of the article. Such subtitles may be frequently avoided by rewording the title so as to make it more precise.

NUMERICAL DOCUMENTATION

Biologists, Chemists, Physical Chemists, Physicists, Engineers, etc., etc.

WHY WASTE YOUR TIME

in searching the Literature to find the Constant or the numerical data that you require?

Since 1910 the Collaborators of the Committee have done this work for you in publications that have appeared all over the world.

The results of this work have been classified and published in

Annual Tables of Constants and Numerical Data

published under the patronage of the International Research Council and of the International Union of Pure and Applied Chemistry.

IF YOU ALREADY KNOW the Annual Tables, make them known to your friends; you will render them a great service.

IF YOU DO NOT KNOW THEM, write at once to **M. C. MARIE**, General Secretary of the International Committee, 9 rue de Bagneux, PARIS (6ᵉ).

VOLUMES PUBLISHED

Volume I (data for 1910)
Volume II (data for 1911)
Volume III (data for 1912)

Volumes I, II, III, are sold only with volumes IV and V.

Cloth Bound

Volume IV (data for 1913-1916).....$25
Volume V (data for 1927-1922).....$25
Price of a complete set
(Volume I, II, III, IV, V).....$71

IN THE PRESS:

(Volume VI (data for 1923-1924))

Closing date of the subscription June 30, 1927

Subscription Price: (Bound copies)
Ordinary subscribers.....$20
Members of Scientific Societies and Subscribers to The International Critical Tables.....$15

From July 1, 1927, onwards, the price of Volume VI will be increased to.....$30

Subscriptions Should Be Sent with the Remittance

To McGRAW HILL BOOK CO., Inc., 370 Seventh Avenue, New York, U. S. A.

The Secrétariat of the Committee (9 rue de Bagneux, Paris) sends free of charge specimen pages taken from the following chapters: *Spectroscopy, Electricity, Magnetism, Electrochemistry, Radioactivity, Crystallography, Mineralogy, Biology, Engineering, Metallurgy, Colloids.*

Samples are Convincing

We have found it so. Very seldom, in reply to an inquiry, do we fail to get an order after submitting samples or the sample book of cross section papers. You are interested in accurate cross section and we print on a high grade paper. Write for the sample book.

CORNELL CO-OPERATIVE SOCIETY

BARNES HALL **ITHACA, N. Y.**

Western Electric

No. 4-A

Audiometer

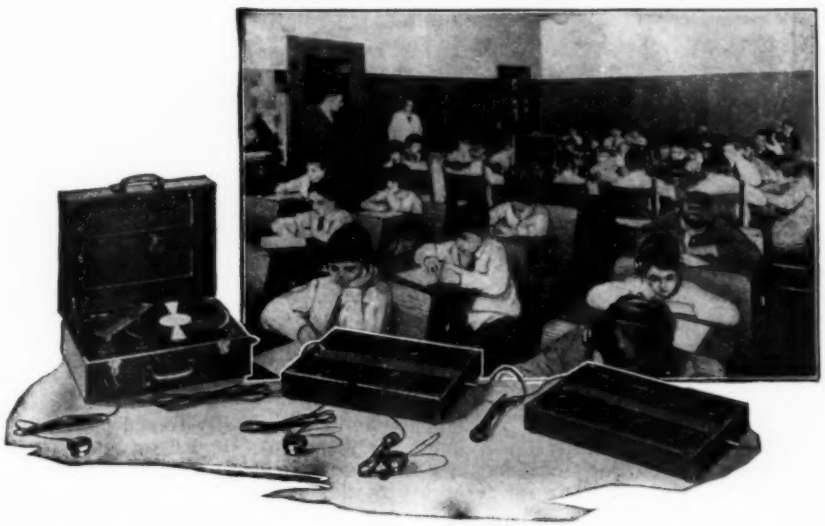

This Audiometer measures acuity of hearing quickly and accurately. It is particularly adapted for school and industrial use.

Essentially the instrument is a phonograph to which telephonic apparatus has been added so the sounds produced in the phonograph can be transmitted to the ears of those under examination.

From one to forty persons can be tested simultaneously according to a standard of measurement which is the same for all and is also unvarying when tests are made at different times. With this Audiometer the errors possible when a hasty whisper or watch tick test is used are avoided.

The No. 4-A Audiometer is as simple to operate as a phonograph and is equally rugged and free from complicated adjustments. No batteries or other outside sources of electrical energy are needed. The necessary electrical energy is developed in the magnetic reproducer which takes the place of the acoustic reproducer usually used in phonographs.

Write for a copy of descriptive bulletin T-791-A

GraybaR

ELECTRIC COMPANY

SUCCESSOR TO Western Electric SUPPLY DEPARTMENT

Scientific Equipment Division

420 Lexington Avenue - - NEW YORK, N.Y.
30 North Michigan Boulevard, CHICAGO, ILL.
1700 Walnut Street - - PHILADELPHIA, PA.

The New

Students' Potentiometer

With Two Ranges

THE lower range, 0 to 16 millivolts, is suitable for instruction in the measurement of temperature with a thermocouple. The higher range, 0 to 1.6 volts, is for general purposes.

The instrument is ruggedly built, with easily-traced circuits. Its accuracy interests students. In design, it follows the Standard Type K Potentiometer, so that work with this instrument is excellent training for later use of the Type K.

The Physics Department uses Students' Potentiometers for most potential measurements made by undergraduates.

The Electrical Engineering Department uses Students' Potentiometers for calibrating instruments.

The Chemistry Department uses Students' Potentiometers for pH and electrolytic conductivity measurements.

The Mechanical and Metallurgical Engineering Department uses the lower of the two ranges of Students' Potentiometers for teaching the principles of potentiometer pyrometry.

Specifications: Two ranges, 0 to 1.6 volts and 0 to 16 millivolts. 15 coils 10 ohms each and slide-wire having a resistance of 10 ohms; slide-wire has 100 divisions. Guaranteed accuracy of coil adjustment, 0.04 per cent; of slide-wire calibration, 0.5 division. Separate connections to the slide-wire, and end-coils which may be cut out of circuit. Potentiometer current required, 0.01 ampere. Grained bakelite top-plate. Polished mahogany case with cover.

Send for Bulletin P-765

LEEDS & NORTHRUP COMPANY
4901 STENTON AVENUE, PHILADELPHIA

LEEDS & NORTHRUP

Galvanometers
Potentiometers
Bridges and Resistances
Condensers and Inductances
Testing Sets
Recording and Controlling Pyrometers
Hump and Home Electric Heat Treating Furnaces
Instruments for Measuring and Controlling Conductivity of Electrolytes and Hydrogen Ion Concentrations

G-66-b

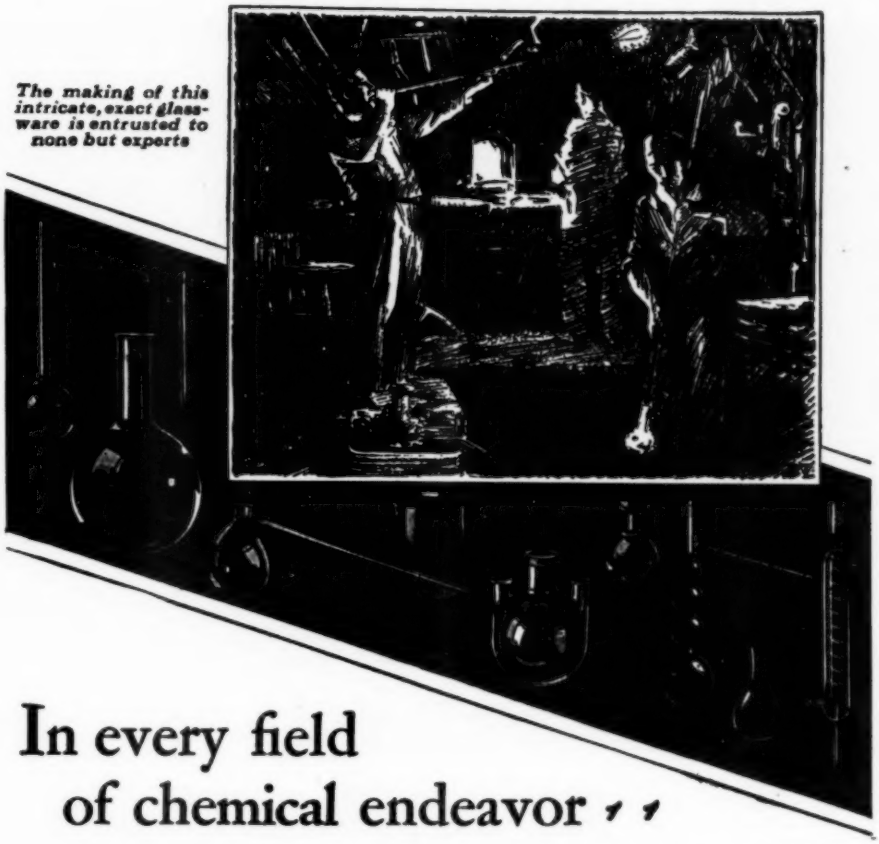

The making of this intricate, exact glassware is entrusted to none but experts

In every field of chemical endeavor

this trade-mark is the recognized standard

EXPERIENCED chemists all over the world specify *PYREX laboratory glassware. They know that back of the PYREX trade-mark stand years of research, highly specialized experience, carefully trained craftsmen, and rigid inspection. They know that each piece of PYREX equipment is uniformly dependable—and durable to the highest possible degree.

CORNING GLASS WORKS
Laboratory Glassware Division, Corning, New York
New York Office: 501 Fifth Avenue
Largest Makers of Technical Glassware in the World

*Trade-mark Reg. U. S. Pat. Off.

The trade-mark PYREX designates a product of Corning Glass Works. It is synonymous with highest quality in materials and workmanship.

The Stabilized Oscilloscope

A Visual Oscillograph

SIMPLE TO OPERATE: An instrument no more difficult to operate than a high grade radio receiving set.

PORTABLE: Weighing but 40 pounds in its beautiful walnut cabinet, it is easily taken from research room to lecture room or to a distant substation.

LINEAR TIME AXIS: By the use of a unique scheme, a linear time axis is obtained which is synchronized with the circuit under study, so that a perfectly stationary visual wave is obtained which may be examined with great care, traced or photographed.

HIGH FREQUENCIES: As there is no damping and the inertia of the electron beam is only 10^{-18} grams, the response to all frequencies and harmonics is true and accurate.

SMALL CURRENT: One micro-ampere is sufficient to accuate this small moving element.

IMMEDIATE RESULTS: Because it is visual, a class in Electrical Engineering or Radio can watch the effect of changing the constants in any circuit **while it is happening.** A power engineer can observe the effect on wave form of various loads, field excitations, etc., making a photographic record of the results which it is deemed should be permanent.

POWERFUL RESEARCH TOOL: Wherever vibrational phenomena are involved.

THE PRICE IS REASONABLE.

Described by Prof. F. Bedell, A.I.E.E. Journal, June, 1927.

Write for Reprint and Circular No. 273.

THE BURT-CELL: A Photo-electric cell without fatigue, previously advertised is described in Bulletin No. 271. Write for a copy. We also manufacture quartz photo-cells of remarkable constancy.

Scientific Instruments

DR. R. C. BURT
327 South Michigan Ave.
PASADENA, CALIFORNIA
Cable address: *"Burt Pasadena"*

Research Fellow California Institute of Technology

BECBRO
Laboratory Rheostats

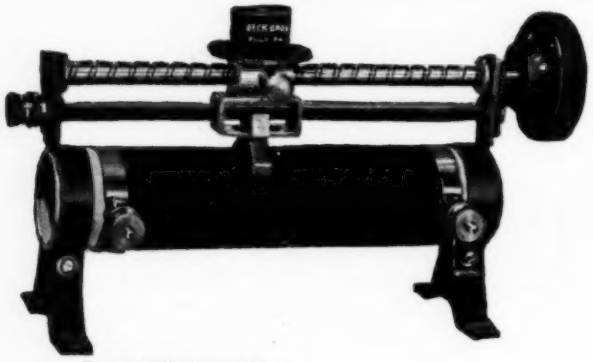

Screw Adjustment Type

"BECBRO" Rheostats carried in stock include numerous ratings.

Included in the stock sizes are tubular types of length 20"; 16"; 8"; the resistance element being Wire or Ribbon.

Each tube has a slider adjustment which varies the resistance by very small steps from Zero to total value of the unit.

The approximate total resistance of these stock rheostats vary from 0.3 ohm to 30,000 ohms per unit, and have corresponding current capacities of 25 amperes down to 0.1 ampere.

Rheostats of more or less special construction include the Single Tube equipped with two rods and two sliders; Single and Double Tube equipped with Screw Adjustment (see cut); Double and Triple Tubes mounted as a Unit; Non-Inductive Wound Tubular and Stone Types.

"BECBRO" Carbon Compression Rheostats with corresponding Normal Ratings of 250; 1000; 1500; 3000 Watts.

Write for Catalog P-20

BECK BROS.

3640-42 North Second Street **Philadelphia, Pa.**

UTILITY

G-E portable instruments are designed to operate with the same high accuracy in the field as in the laboratory.

Every instrument is thoroughly shielded from the effects of adjacent electric circuits. The windings are of special alloy to provide unchanging resistance values and consequent freedom from errors caused by thermal and parasitical voltages or temperature changes.

These instruments combine accuracy and utility. They are the product of a generation's experience in the manufacture of testing equipment.

GENERAL ELECTRIC

GENERAL ELECTRIC COMPANY, SCHENECTADY, NEW YORK

G-E Portable Instruments

A-c. (*Type P-3*)

Voltmeters
Ammeters
Milliammeters
Wattmeters
Power Factor Meters
Frequency Meters

D-c. (*Type DP-2*)

Voltmeters
Ammeters
Millivoltmeters
Milliammeters
Microammeters
Thermal-Ammeters
Ohmmeters

The above instruments can be furnished with standard or special ratings to conform with every requirement. All scales are hand calibrated and marked to fit the characteristics of the individual instrument—a final operation of extreme importance in coördination of electrical and mechanical design.

Special Instruments

General Electric engineers are constantly in search of new methods for the indication of electrical measurements. Among the most recent developments is a thermionic microammeter that will indicate a current change so small as one ten-billionth of an ampere.

There are also thermal and suspended-armature types, of high sensitivity, which have proved to be invaluable for laboratory use.

Whatever your problems of electrical measurement, G-E engineers welcome the opportunity to be of assistance in their solution. Detailed information will be gladly supplied from the nearest G-E Sales Office.

GENERAL ELECTRIC

GENERAL ELECTRIC COMPANY, SCHENECTADY, NEW YORK

Siemens & Halske

Precision Millivolt— *and* Voltmeter

is used largely by Physicists, Electrical and Electrochemical Engineers in Research Laboratories. It is different in design, construction and characteristics from any other d.c. measuring instrument made.

As a Millivoltmeter the range is 0 to 45 mv., with resistance of 10 ohms; and as a Voltmeter the range is 0 to 3 volts, with a resistance of 1000 ohms. **All ranges are compensated for temperature changes; the instrument is accurate and it holds its calibration.**

Illustrated Catalog 1015-R will be sent on request.

Write for copy.

JAMES G. BIDDLE
Scientific Instruments
1211-13 Arch Street, PHILADELPHIA

Cat. No.	*Description*	*Price*
560001	Precision Millivolt and Voltmeter for 45 millivolts and 3 volts, 150 scale divisions. Complete with carrying case	$74.25
560006	Precision Combined Manganin Shunt for .015, .03 and .075 amperes	$20.25
560007	Ditto, for .15, .3 and .75 amperes	$13.50
560008	Ditto, for 1.5, .3 and 7.5 amperes	$14.40
560009	Ditto, for 15 and 30 amperes	$15.30
560010	Precision Manganin Shunt for 75 amperes	$ 9.00
560024	Combined Multiplier for 15, 150, 300 and 750 volts	$36.00

The above prices are net f.o.b. Philadelphia

Baker Wollaston Wires Are Strong and Uniform

OUR Wollaston wires exhibit maximum strength, uniformity of diameter and have a good smooth surface. We usually ship them in the jacket which is to be removed by the user. Full details for doing this are sent with each order.

We have in stock: Au Wollaston Wire .0005″, .0004″, .0003″, .0002″, .0001″, .00005″, .00002″, .00001″; Pt. .0005″, .0004″, .0003″, .0002″, .0001″, .00005″ (and somewhat smaller, if required only in very short lengths), Ag, Al, Pd, 60 Au 40Pt and 90Pt 10Rh .0005″, .0004″, .0003″, .0002″ and .0001″.

We make fine wires, too, by the Taylor Process, by Extrusion and Bare Drawing. Whenever you need fine wires in unusual sizes or of unusual materials, write to us. It is very likely we can give you what you want.

BAKER & CO., INC.
54 Austin St., NEWARK, N. J.
New York **San Francisco** **Chicago**

Back Numbers Wanted of the PHYSICAL REVIEW

We will pay $1.50 each for copies of the January, February, April and May issues of Volume 7, 1916; also $0.75 for copies of the January, 1927, issue.

Send to the Physical Review, 1500 University Ave. S. E., Minneapolis, Minnesota.

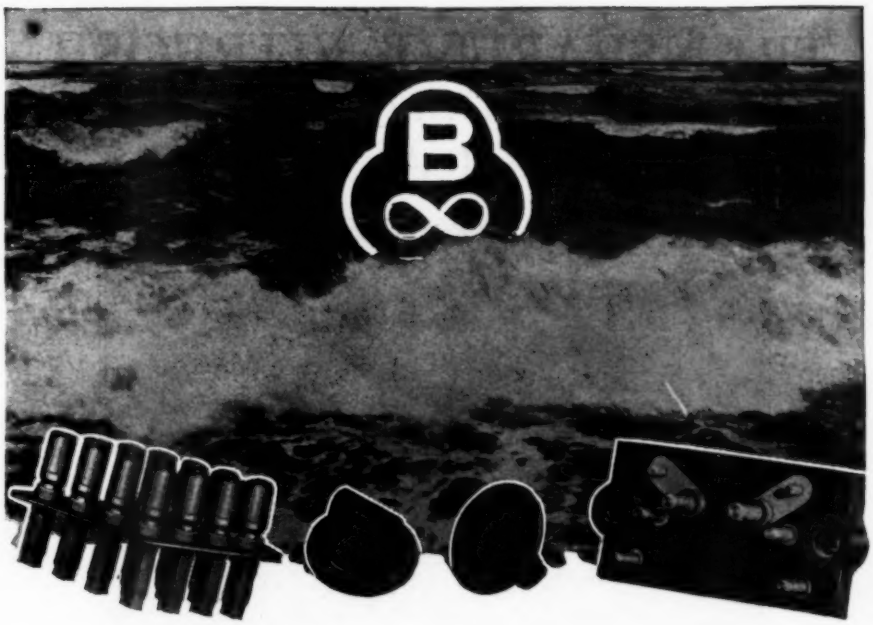

The Rising Tide *of* Simplification

In production processes, "Simplification" means shortening the period between inception and completion. It means producing a dozen units in the time formerly required for one; or making in one operation some part that once was a tedious assembly job. One reason why Bakelite Molded has found such wide acceptance among manufacturers in almost every line, is that it helps to simplify production.

The production of the contact buttons shown at the left has been simplified by the use of Bakelite Molded. In a multiple cavity mold, sixteen of these buttons are formed in two operations, the round ends of red and the square ends of green Bakelite Molded.

The dials shown in the center are also produced in Bakelite Molded. Three operations are eliminated, improved design is made possible and the manufacturing cost is reduced 25%. The third illustration shows a molded terminal block for a subway door control. It is formed in one operation with ten metal inserts securely embedded, finished holes for mounting screws, and sharply defined relief lettering.

❖ ❖ ❖

These are but three among hundreds of instances in which the use of Bakelite Molded has proved to be the key to simplification. Our engineers and research laboratories welcome opportunities to co-operate with manufacturers in adapting Bakelite Molded to their own needs. Write for Booklet No. 12, "Bakelite Molded."

BAKELITE CORPORATION

247 Park Ave., New York, N. Y., Chicago Office: 635 W. 22nd St.

BAKELITE CORP. OF CANADA, LTD., 163 Dufferin Street, Toronto, Ont.

BAKELITE

REGISTERED U. S. PAT. OFF.

THE MATERIAL OF A THOUSAND USES

"The registered Trade Mark and Symbol shown above may be used only on products made from materials manufactured by Bakelite Corporation. Under the symbol "B" is the commercial sign for infinity, or unlimited quantity. It symbolizes the infinite number of present and future uses of Bakelite Corporation's products."

TRANSPARENT VITREOSIL

(Fused Pure Quartz)

for OPTICAL USES

The above illustration shows a pair of penta prism blanks which can be supplied at a cost remarkably low, considering the decided advantages which vitreosil possesses over glass in being free from temperature distortion because of its extremely low coefficient of expansion (.00000054 per degree C.).

Other properties of transparent vitreosil such as its ability to transmit ultra-violet light, infra-red rays and the intermediate spectrum, resistance to corrosive liquids and gases, as well as to withstand high and abrupt changes of temperatures, have made it particularly suited for the following and kindred applications.

Vacuum-Tight Seals for Electrical Fused Quartz Equipment
Details for Interferometer Expansion Apparatus
Plates for Ultra-Violet Light Transmission
Apparatus for Photo-Chemical Reactions
Lenses for Optical Systems
Photo-Electric Cells
Spectrum Tubes
Liquid Cells
Applicators
Etc.

Quotations cheerfully given on equipment suited to your particular needs.

THE THERMAL SYNDICATE LTD.

1726 Atlantic Avenue **Brooklyn, New York**

Announcing

THE NEW-IMPROVED GAERTNER

L101 Students' Spectrometers

Design 1927

Our new Students' Spectrometer embodies a number of decided improvements over our former model L101 spectrometer which has given so general satisfaction and of which many hundreds have been supplied to the best laboratories throughout the world.

The instrument in its new form is very much more substantial and more convenient in use. A delicate focusing device for the telescope and a magnifier for reading the Verniers have been added without increasing the price.

The outstanding feature of this new spectrometer is the construction of the circle and verniers. The graduations lay in the same plane as in our precision spectrometer, allowing very much easier reading. The lines and figures appear white on a black background. They are filled in with permanent white by our special recently developed process. The circle and the verniers are covered by a dust-tight cap with glass windows over the verniers. An adjustable, rotatable magnifier is provided for convenience in reading.

The centers for circle and vernier are made of high grade steel and the bearing of hard bronze, assuring accurate concentricity and free rotation with least friction.

The collimator is firmly mounted in a double cradle, fitted with screws for adjustment in vertical and horizontal planes. The slit is of improved design; the jaws are of nickel-silver with carefully ground and polished edges. The jaws are 4mm long, operated by a fine adjusting screw and spring.

The telescope is fitted with Gauss eyepiece and a spiral delicate focusing arrangement and is likewise mounted in a substantial double cradle fitted with adjusting screws. It is provided with a clamp and tangent screw for delicate motion. The objectives for telescope and collimator are achromatic, 25mm aperture, 160mm focal length.

The prism table is of brass, 80mm in diameter, with provisions for all necessary conveniences such as, height adjustment, tilt, clamping arrangement, delicate rotation screw, etc. It is fitted with a spring prism clamp of adjustable height.

Height from table to optical axis about 200mm.....$90.00

IMMEDIATE DELIVERY FROM STOCK—(For accessories see our catalog M-L—pages 48-49)

The

GAERTNER SCIENTIFIC CORPORATION

SUCCESSOR TO WM. GAERTNER & CO.

ESTABLISHED 1900 INCORPORATED 1920

1201 WRIGHTWOOD AVENUE, CHICAGO

Our catalogs listing High Grade Scientific Instruments sent on request

Please Mention the PHYSICAL REVIEW when Writing to Advertisers

TWO SIMPLE DEMONSTRATION PIECES

for Making Clearer some of the Theories of

ATOMIC AND MOLECULAR STRUCTURE

SHIPP ALPHA RAY TRACK APPARATUS

A Simplified Modification of C. T. R. Wilson's Apparatus for Rendering Visible the Path of Alpha Particles

This piece makes visible to the naked eye the path of a single atom from *Radium* emanation, which is probably the nearest we shall ever come to seeing an atom. This concrete demonstration has proved very helpful in giving the elementary student a proper conception of the atom, a difficult proposition even with the brightest.

The apparatus as shown consists essentially of a glass chamber in the shape of an inverted [illegible] cone, with the upper end constituting a [illegible] closed cylinder with the end plane. Above the water, which should nearly fill the cylinder, is an air space into which projects a glass tip [illegible] a small amount of radium salt.

When an electrostatic field of 100 to 200 volts is established across this space and the air is compressed by means of the rubber bulb and the pressure suddenly released, the paths of the alpha particles from the radium becomes visible as a result of the condensation of moisture upon the ions produced by their passage through the air. Suitable illumination is provided by means of a lamp enclosed in a lamp house with a slit [illegible] opposite the air space.

No. 11200. Knipp Alpha Ray Apparatus..... $35.00

...ENCO BROWNIAN MOVEMENTS APPARATUS

No. 11205

The apparatus is noteworthy for the [illegible] manner in which it shows [illegible] the irregular, and apparently [illegible] movement of minute particles in air. Essentially [illegible] for [illegible], with [illegible] a small [illegible] in which there are no [illegible] currents; means for [illegible] dark field illumination [illegible] and [illegible] with a compound [illegible] of 50 or 100 diameters, a small section of the illuminated region. Each [illegible] appears like a pure source of light, and their excursions are most fascinating to observe. Designed for clamping on the microscope stage. Almost any source of light will serve for the illumination. As described, but not including microscope or source of light.....$4.10

Central Scientific Company

LABORATORY APPARATUS AND SUPPLIES

Chicago U.S.A.